TECHNISCHE UNIVERSITÄT MÜNCHEN
Ingenieurfakultät Bau Geo Umwelt
Lehrstuhl für Siedlungswasserwirtschaft

H_2/CO_2 biomethanation in anaerobic thermophilic trickle bed reactors - Development of a flexible and efficient energy conversion technology

Dietmar Strübing

Vollständiger Abdruck der von der Ingenieurfakultät Bau Geo Umwelt der Technischen Universität München zur Erlangung des akademischen Grades eines

Doktors der Ingenieurswissenschaften
-Dr.-Ing.-

genehmigten Dissertation.

Vorsitzender:	Priv.-Doz. Dr.-Ing. habil. Konrad Koch
Prüfer der Dissertation:	1. Prof. Dr.-Ing. Jörg E. Drewes
	2. Prof. Dr. Largus T. Angenent
	3. Prof. Dr. Lars D. M. Ottosen

Die Dissertation wurde am 10.10.2019 bei der Technischen Universität München eingereicht und durch die Ingenieurfakultät Bau Geo Umwelt am 11.02.2020 angenommen.

Abstract

By flexible conversion of excess variable renewable energy source into a storable form, Power-to-Gas technologies provide a promising approach to stabilize the electricity grid and balance electrical power production and demand. The application of biomethanation (BM) with hydrogenotrophic methanogenic archaea can become such a flexible Power-to-Gas technology that generates high-quality substitute natural gas (a long-term energy storage compound without injection restrictions) and uses the huge capacity of the existing natural gas grid infrastructure. Still, BM systems face H_2 gas-liquid mass transfer as the main rate limiting step. While various reactor concepts have been studied with the purpose of overcoming these limitations, the highest methane production rates were achieved with H_2 introduction by energy-intensive stirring in continuous stirred tank reactors.

For this reason, the core objective of this dissertation was to develop an efficient alternative reactor concept with low H_2 gas-liquid mass transfer restrictions and simultaneously low parasitic energy consumption (i.e., for mixing), suitable for flexible on-demand operation. In this respect, anaerobic thermophilic trickle bed reactors (ATTBR) were identified as a promising reactor concept and several experiments with ATTBR systems at laboratory and technical-scale have been carried out. Implementing the BM process within an ATTBR, providing a high surface-area per reactor volume, is expected to enhance gas-liquid mass transfer. Furthermore, BM within trickle bed reactors has been investigated only in a few studies and only under mesophilic conditions, although substantially higher methane generation rates were generally found for reactors operated at thermophilic temperatures due to enhanced microbial growth and conversion rates.

Within the first research objective, the possible mass-transfer advantages of trickle bed systems were combined with the potential enhancement of biological conversion of CO_2 and H_2 to CH_4 under thermophilic conditions. In order to evaluate the potential to establish an efficient BM process minimizing H_2 gas-liquid mass transfer restrictions and simultaneously low parasitic energy consumption, an ATTBR with a trickle bed volume of 58 L was set up, inoculated with sewage sludge from a local wastewater treatment plant digester and operated at 55°C at ambient pressure for more than 300 days. This long-term experiment demonstrated the potential of ATTBR as a very efficient energy conversion and storage technology, achieving grid injection qualities ($> 96\%$ CH_4) at comparably high methane production rates (up to 15.4 $m^3_{CH_4}/(m^3_{\text{trickle bed}} \cdot d)$ and could thus prove the desired reactor concept at technical-scale. The ATTBR required no mixing energy or introduction of pressurized gas and can easily compete with the performance of other mixed culture BM

reactors. Moreover, inoculation with digested sludge showed high adaptive capacity due to intrinsic biological diversity being a potential benefit for practical applications. However, control of pH and nutrient supply turned out to be crucial for stable operation, and was affected significantly by dilution due to metabolic water production.

The capability to deal with fluctuating gas loads is crucial for the future application of ATTBR as a flexible and efficient energy conversion and long-term storage technology. Depending on the renewable energy scenario studied, the extent of required storage capacities, required respond times and duration of surplus energy peaks, and hence operation periods, are being controversially discussed. In order to apply ATTBR in any of those energy conversion and storage scenarios, different combinations of standby and restart strategies were evaluated. In this context, the focus of the second research objective was to elucidate the capability of the ATTBR concept for flexible and demand-oriented H_2/CO_2 BM as well as to identify operational constraints and suitable strategies to manage standby periods and rapid restart and load change scenarios.

The impact of standby period settings on the restart performance was investigated within the established ATTBR technical-scale set-up. Critical operational parameters during various reactor standby settings were identified and the applicability of an ATTBR as a robust system with very good restart performance even after long standby periods, which is inevitable for demand-oriented operation within a dynamic energy system, has been demonstrated. Different combinations of standby period duration and temperature have revealed that the influence of the standby period temperature on the restart performance greatly outweighs the standby period duration in the settings studied. A higher remaining biological gas conversion capacity was observed after standby periods at 25°C compared to 55°C, which can be attributed to the impact of significantly higher inactivation rates for thermophilic hydrogenotrophic methanogens at 55°C. Moreover, especially repetitive standby periods at 55°C affected the restart performance.

In addition to a suitable standby management, the ability to re-attain full methanation capacity after restart is critical. Currently, the time period to respond to available excess power cannot be determined with certainty from existing studies. Thus, limitations of various restart strategies have been studied, expecting the restart performance to be influenced by standby effects as well as by the restart strategy. The resulting study demonstrated the load change capability of an ATTBR while maintaining a high methane content. The application of full load (62.1 $m^3_{H_2}/(m^3_{\text{trickle bed}} \cdot d)$) after 30-minutes operational breaks was possible almost immediately, while 24-hour interruptions required a 60-minutes stepwise load increase to reactivate the microbial community in the entire trickle bed. The actual gas conversion can be monitored and controlled using the ratio of substrate and product gas, allowing suitable load increase strategies that ensure reactivation, avoid short-circuiting and guarantee a suitable gas quality. In addition, the trickle bed gas phase provides a high quality gas buffer during the initial load increase phase.

The investigations performed within the framework of this thesis demonstrated the

capability of the developed ATTBR set-up for efficient and dynamic BM. The ATTBR concept demonstrated its competitiveness with other mixed microbial culture systems, although it could be applied to pure cultures as well, which can achieve an even higher performance as indicated in the literature. However, in order to prove and improve the general feasibility for ATTBR scale-up and implementation into the changing energy sector, several research question require further investigations, particularly the following aspects: i) reactor design optimization, ii) identification of an optimum biomass state (immobilized vs. planktonic), iii) integration of membrane systems to remove metabolically produced water, and iv) evaluation of the economic feasibility of various ATTBR integration approaches.

Zusammenfassung

Durch die flexible Umwandlung überschüssiger, variabler erneuerbarer Energien in ein speicherbares Produkt bieten Power-to-Gas-Technologien einen vielversprechenden Ansatz zur Stabilisierung des Stromnetzes durch Ausgleich von Stromerzeugung und -nachfrage. Biomethanisierung (BM) mit hydrogenotrophen methanogenen Archaeen kann eine solch flexible Power-to-Gas-Technologie werden, die hochwertiges Biomethan (als langfristig speicherbarer Energieträger ohne Einspeisebeschränkungen) erzeugt und damit die enorme Kapazität der bestehenden Erdgasnetzinfrastruktur nutzt. Derzeit sind BM-Technologien häufig durch den H_2-Stoffübergang von der Gas- in die Flüssigphase limitiert. Während verschiedene Reaktorkonzepte zur Überwindung dieser Limitierungen untersucht wurden, wurden die höchsten Methanproduktionsraten bei der H_2-Zufuhr mittels energieintensiver Durchmischung in kontinuierlichen Rührkesselreaktoren erreicht.

Aus diesem Grund lag der Fokus dieser Dissertation auf der Entwicklung eines effizienten, alternativen Reaktorkonzeptes zur Optimierung des H_2-Stoffübergangs, mit gleichzeitig niedrigem Eigenenergieverbrauch und hoher Flexibilität für einen bedarfsgerechten Betrieb. In diesem Zusammenhang wurden anaerobe thermophile Rieselbettreaktoren (ATTBR) als vielversprechendes Reaktorkonzept identifiziert und verschiedene Experimente mit ATTBR- und Biofilmreaktoren im Labor- und technischen Maßstab durchgeführt. Es wird erwartet, dass durch Implementierung des BM-Prozesses in einem ATTBR mit hoher spezifischer Oberfläche pro Reaktorvolumen der H_2-Stoffübergang verbessert wird. Bis dato wurde der BM-Prozess in Rieselbettreaktoren nur in wenigen Studien und nur unter mesophilen Bedingungen untersucht, obwohl thermophilen Reaktoren aufgrund beschleunigter mikrobieller Wachstums- und Umsatzsraten im Allgemeinen wesentlich höhere Methanbildungsraten zulassen.

Das erste Forschungsziel bestand in der Kombination der möglichen Stoffübergangsvorteile von Rieselbettsystemen mit der potentiell beschleunigten biologischen Umwandlung von CO_2 und H_2 zu CH_4 unter thermophilen Bedingungen. Um das Potenzial für einen effizienten BM-Prozess zur Minimierung von H_2-Stoffübergangslimitierungen bei gleichzeitig niedrigem Eigenenergieverbrauch zu bewerten, wurde ein ATTBR mit einem Rieselbettvolumen von 58 L errichtet, mit Klärschlamm aus einem lokalen Kläranlage angeimpft und mehr als 300 Tage bei 55°C und Umgebungsdruck betrieben. In diesem Langzeitexperiment konnte das Potenzial des ATTBR als effiziente Energieumwandlungs- und Speichertechnologie aufgezeigt werden. Es wurden Einspeisequalitäten ($> 96\%$ CH_4) bei vergleichsweise hohen Methanproduktionsraten (bis zu 15,4 $m^3_{CH_4}/(m^3_{Rieselbett} \cdot d)$) erreicht und damit die

Funktionalität des untersuchten Reaktorkonzeptes im technischen Maßstab unter Beweis gestellt. Der ATTBR benötigt keine Energie für Durchmischung oder Gaszufuhr unter Überdruck und erreicht mindestens die Umsatzleistung vergleichbarer BM-Reaktoren mit Mischkultur. Darüber hinaus zeigte die Animpfung mit Faulschlamm durch die intrinsische biologische Vielfalt eine hohe Anpassungsfähigkeit an veränderte Prozessbedingungen. Die Stabilität des pH-Wertes sowie der Nährstoffversorgung erwies sich als entscheidend für einen effizienten Prozess, wurde durch die Verdünnung der Prozessflüssigkeit aufgrund metabolischer Wasserproduktion jedoch erheblich beeinträchtigt.

Die Fähigkeit, mit schwankender Gaszufuhr umzugehen, ist entscheidend für den zukünftigen Einsatz des ATTBR als flexible und effiziente Energieumwandlungs- und Langzeitspeichertechnologie. Abhängig vom untersuchten Ausbauszenario erneuerbarer Energien werden der Umfang der benötigten Speicherkapazitäten, die erforderlichen Reaktionszeiten, die Dauer von Überschussenergiespitzen und damit die ATTBR-Betriebszeiten kontrovers diskutiert. Um ATTBR in einem dieser Energieumwandlungs- und Speicherszenarien einzusetzen, wurden verschiedene Kombinationen von Stillstands- und Schwarzstartstrategien bewertet. Vor diesem Hintergrund lag der Schwerpunkt des zweiten Forschungsziels auf der Untersuchung der Leistungsfähigkeit des ATTBR-Konzeptes für flexible und bedarfsorientierte H_2/CO_2 BM. Betriebliche Limitierungen wurden identifiziert und geeignete Strategien zur Steuerung von Stillstandsphasen und schnellen Wiederanlauf- und Lastwechselszenarien entwickelt.

Der Einfluss der Stillstandsdauer auf die Schwarzstartleistungsfähigkeit wurde in einem etablierten ATTBR-System im Technikumsmaßstab untersucht. Kritische Betriebsparameter bei verschiedenen Stillstandseinstellungen wurden identifiziert und die Anwendbarkeit des ATTBR als robustes System mit sehr gutem Schwarzstartverhalten auch nach langen Stillständen wurde nachgewiesen. Verschiedene Kombinationen von Stillstandsdauer und Stillstandstemperatur haben ergeben, dass der Einfluss der Stillstandstemperatur auf die Schwarzstartleistungsfähigkeit die Stillstandsdauer unter den betrachteten Bedingungen bei weitem übertrifft. Eine höhere verbleibende biologische Gasumsatzkapazität wurde nach Stillständen bei 25°C im Vergleich zu 55°C beobachtet, was auf den Einfluss deutlich höherer Inaktivierungsraten für thermophile hydrogenotrophe Methanogene bei 55°C zurückzuführen ist. Darüber hinaus beeinträchtigten besonders wiederholte Stillstände bei 55°C die Wiederanlaufleistung.

Neben einem geeigneten Stillstandsstrategie ist die Fähigkeit, nach dem Schwarzstart wieder die volle Leistungsfähig zu erreichen, von entscheidender Bedeutung. Derzeit kann der Zeitraum, in dem auf verfügbare Überschussenergiespitzen reagiert werden muss, aus bestehenden Studien nicht mit Sicherheit bestimmt werden. So wurden die Grenzen verschiedener Schwarzstartstrategien untersucht, wobei erwartet wurde, dass die Schwarzstartleistungsfähigkeit sowohl durch Stillstandseffekte als auch durch die Schwarzstartstrategie beeinflusst wird. Die resultierende Studie zeigte die Lastwechselfähigkeit des ATTBR unter Beibehaltung eines hohen Methangehalts. Der Betrieb bei Volllast (62,1

$m^3_{H_2}/(m^3_{Rieselbett} \cdot d)$) nach 30-minütigen Betriebspausen war nahezu sofort möglich, während 24-stündige Unterbrechungen eine schrittweise Lastzunahme über 60 Minuten erforderten, um die mikrobielle Gemeinschaft im gesamten Rieselbett zu reaktivieren. Der ATTBR-interne Gasumsatz kann dabei über das Verhältnis von Substrat- und Produktgas überwacht und gesteuert werden. Dies ermöglicht geeignete Lastwechselstrategien, welche eine ausreichende Reaktivierung sicherstellen, Kurzschlussströmungen vermeiden und eine geeignete Gasqualität gewährleisten. Darüber hinaus bietet die Gasphase im Rieselbett einen hochwertigen Gasspeicher zu Beginn des Lastwechsels.

Die im Rahmen dieser Arbeit durchgeführten Untersuchungen zeigten die Leistungsfähigkeit des entwickelten ATTBR- Konzeptes für effiziente und dynamische BM. Der ATTBR bewies seine Wettbewerbsfähigkeit als Mischkultursystem, kann aber auch für Reinkultur-Konzepte angewendet werden. Für den Nachweise der allgemeinen Eignung des ATTBR zur Implementierung in einen sich wandelnden Energiesektor, bedürfen mehrere Forschungsfragen weiterer Untersuchungen, insbesondere die folgenden Aspekte: i) Optimierung des Reaktordesigns, ii) Identifizierung eines optimalen Biomassezustands (immobilisiert vs. planktonisch), iii) Integration von Membransystemen zur Entfernung von metabolisch generiertem Wasser und iv) Bewertung der wirtschaftlichen Machbarkeit verschiedener ATTBR-Integrationsansätze.

Acknowledgements

To perform my PhD studies at the Technical University of Munich was a wonderful, creative, intense and outstanding experience, at the same time it was also hard work, sometimes even with frustration. During my time at the Chair of Urban Water Systems Engineering plenty of people contributed directly or indirectly to the completion of this dissertation. Here is a tribute to them.

First of all, I wish to thank my supervisor Prof. Dr. Jörg E. Drewes for providing me a wonderful and great scientific environment at his chair to carry out this research, allowing me to develop scientifically as well as personally. Thank you for the valuable advice and support.

My co-supervisor and mentor PD Dr. Konrad Koch deserves my deepest gratitude for his trust and the great degree of freedom he gave me to develop the direction of this research. He always provided excellent and instant support and shared experiences during the reflection of research results and questions. I absolutely enjoyed this working atmosphere.

I would also like to thank Prof. Dr. Lars T. Angenent and Prof. Dr. Lars D. M. Ottosen for joining my PhD committee and supporting me with valuable advice during my research proposal as well as during research visits.

I would like to show my appreciation to the Bavarian Ministry of Economic Affairs, Regional Development and Energy (Bayerisches Staatsministerium für Wirtschaft, Landesentwicklung und Energie) for their financial support of this research project and to TUM Graduate School for international conference scholarships.

Special thanks to our project partners and my co-authors Dr. Michael Lebuhn and Dr. Bettina Mößnang from the Bavarian State Research Center for Agriculture (Bayerische Landesanstalt für Landwirtschaft), for performing the entire molecular biological analysis for this research project as well as for very valuable, critical and constructive discussion of our common publications.

It is an honor for me to thank Dr. Mads B. Jensen, visiting PhD student from Aarhus University, for a great international exchange experience, inspiring discussion of research ideas and results as well as for a productive collaboration, during his time in Munich up to now.

I am grateful for the irreplaceable technical support from Hubert Moosrainer and Jürgen Ederer during the countless enjoyable hands-on hours we spend together for the preparation of the research-container, the set-up of the reactors and their never-ending optimization. I also wish to thank Wolfgang Schröder, Myriam Reif and Nicole Zollbrecht for their lab

support and sample analysis.

I am deeply thankful to the team and colleagues at the Chair of Urban Water Systems Engineering Dr. Therese Burkhardt, Dr. Johann Müller, Dr. David Miklos, Thomas Lippert, Meriam Muntau, Sema Karakurt-Fischer, Veronika Zhiteneva, Philipp Michel, Dr. Max Weißbach, Dr. Nils Horstmeyer and Dr. Carmen Leix and all the other colleagues from the institute, for a great not-only-working atmosphere that made my PhD an unforgettable experience.

Additionally, I owe my students a great debt of gratitude for their interest in the research topic and personal commitment during their master theses and study projects and I would like to thank Andreas Möller, Carolina Feickert-Fenske, Franz Weiß, Felix Wiese, Mounia Lahmouri, Hazal Sahanoglu, Stéphanie Andrianjafidago, Luis Guilherme Sampaio de Oliveira, Mariana Serrao, Frank Herb, Marius Rupp and Dara Dahabreh.

I would like to thank my family and friends for their encouragement and support during my entire way up to now and for unforgettable hours in the Freising climbing gym and the alps.

And finally: Thank you, Lisa, for your endless positive energy, understanding, support and love over the last four years, which have made life outside the PhD so much more worth living.

Contents

List of Figures

List of Tables

Abbreviations

AAS	Atomic absorption spectrometry
AEL	Alkaline electrolysis
A_s	Specific reactor wall surface area
ATBR	Anaerobic trickle bed reactor
ATTBR	Anaerobic thermophilic trickle bed reactor
BEM	Biocatalytic electromethanogenesis
BM	Biomethanation
c_{Ac}	Acetate concentration
CAPEX	Capital expenditures
$c_{H_2,L}$	H_2 liquid phase concentration
$c_{H_2,SG}$	H_2 substrate gas content
COD	Chemical oxygen demand
CSTR	Continuous stirred tank reactor
DNA	Deoxyribonucleic acid
F_1	Liquid flow rate
$\Delta G^{0´}$	Standard Gibbs free energy
GWh	Gigawatt hour
GRT	Gas retention time
$H_{H_2,cp}$	Henry's law constant for H_2
HRT	Hydraulic retention time
HSB	Hot standby
$k_L\alpha$	Volumetric mass transfer coefficient
kWh	Kilowatt hour
LCE	Load change experiment
LCOE	Levelized cost of energy
LHV	Lower heating value
MWh	Megawatt hour
NDIR	Non-dispersive infrared
OPEX	Operational expenditures
OTU	Operational taxonomic units
PEM	Proton exchange membrane electrolyzer
$p_{H_2,G}$	H_2 partial pressure in the gas phase
PG	Product gas
P_{st}	Standard pressure (1 bar)

PtG	Power-to-gas
PVC	Polyvinylchlorid
ΔP_X	Difference in partial pressure
Q_{PG}	Product gas flow rate
Q_{SG}	Substrate gas flow rate
q_s	Specific heat loss by conduction
R_{H_2}	Overall H_2 volumetric mass transfer rate
r_{H_2}	H_2 consumption rate
r_{CH_4}	CH_4 production rate
r_{n,H_2}	Molar H_2 consumption rate
RO	Reverse osmosis
SAOB	Syntrophic acetate oxidizing bacteria
SG	Subtrate gas
SGF	Syngas fermentation
SNG	Substitute natural gas
SOEC	Solid oxide electrolysis
SP	Standby period
SRT	Solid retention time
STP	Standard temperature and pressure
ΔT	Temperature difference
Δt	Duration
TCD	Thermal conductivity sensor
T_{exp}	Headspace temperature
TS	Total solids
T_{sp}	Standard temperature (273.15 K)
TWh	Terrawatt hour
U	Heat transfer coefficient
UASB	Upstream anaerobic sludge blanket
UF	Ultrafiltration
V	Total reactor volume
VFA	Volatile fatty acids
V_{hs}	Reactor head space volume
V_{Liquid}	Process liquid volume in a trickle bed reactor
VRE	Variable renewable energies
$V_{Reaction}$	Reaction volume in any BM reactor
V_{Remain}	Remaining reaction volume at a defined conversion state within the trickle bed
VS	Volatile solids
$V_{Trickle\ bed}$	Reaction volume in a trickle bed reactor
WWTP	Wastewater treatment plant
X_{SG}	Substrate gas conversion rate
Y_{CH_4}	CH_4 yield from H_2
$Y_{H_2,Ac}$	Acetate yield from H_2

1. Introduction

Within the Energy Roadmap 2050, the European Commission has set the target to reduce greenhouse gas emissions by 80-95% below 1990 levels[1]. Besides increasing the energy efficiency of buildings and new technologies, renewable energies will play a significant role for electric power generation in order to achieve these targets. The Energy Roadmap 2050 envisions substantially high shares of renewable energies, covering 75% of the gross final energy consumption and up to 97% of electricity consumption in the European Union. The current progress towards these goals presents an average share of energy from renewable sources in gross final energy consumption of 17% (data from 2016) in the EU-28[2], however, varying strongly among different countries (Figure 1.1). Out of 28 countries, 11 have already achieved their targets for 2020, with Sweden (53.8%) and Finland (38.7%) on the first ranks and Germany at the 18th position (14.0%).

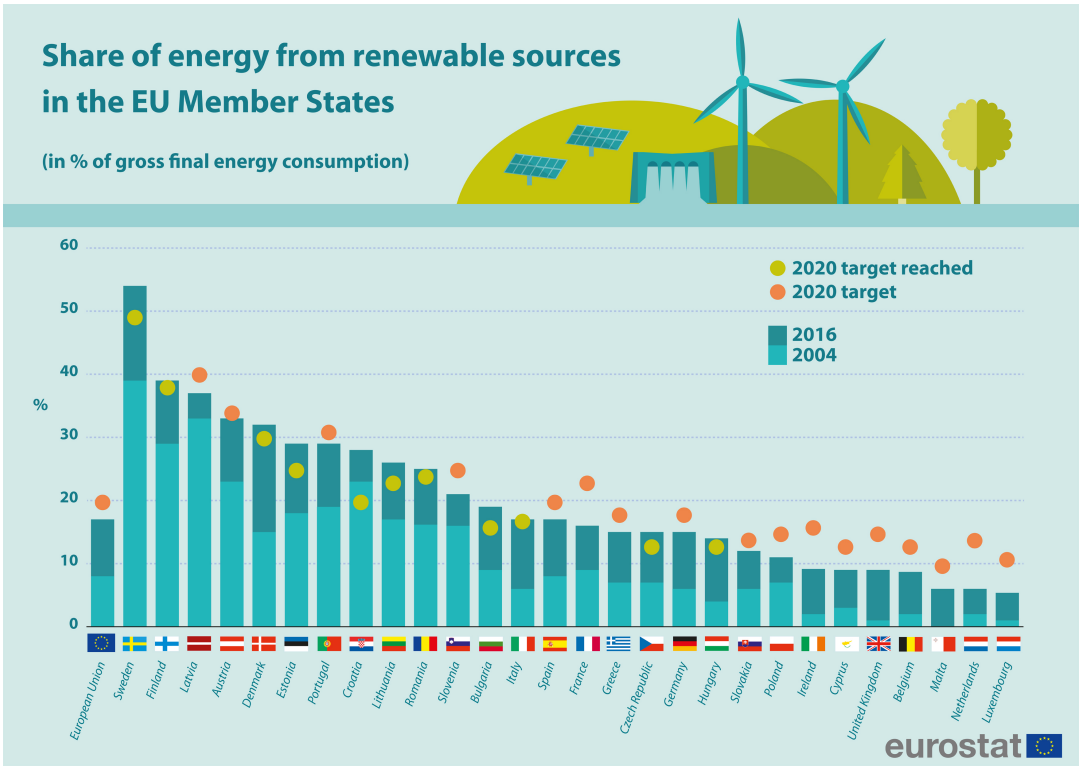

Figure 1.1: Share of energy from renewable sourcesin % gross final consumption of energy, 2004 and 2016 (in % of gross final energy Consumption) Source: Eurostat (t202031)[2]

In 2016, the gross electricity generation from renewable resources in the EU-28 is dominated by hydro power (36.9%), followed by wind (31.8%) and solar power (11.6%)[2]. While, hydro power

remained nearly constant between 2006 and 2016 (Figure 1.2), the highest development rates were observed for solar (+4,440%) and wind power generation (+370%). Along with this trend, also the challenges originating from of these variable renewable energy sources (VRE) are growing. VRE show strong seasonal variations and even higher fluctuations on a shorter timescale (hours to days)[3–5] The resulting imbalances between supply and electrical demand will affect the security and stability of the electricity grid[3], and the development of flexible energy conversion and long-term storage technologies is required in order to maintain grid stability[6,7].

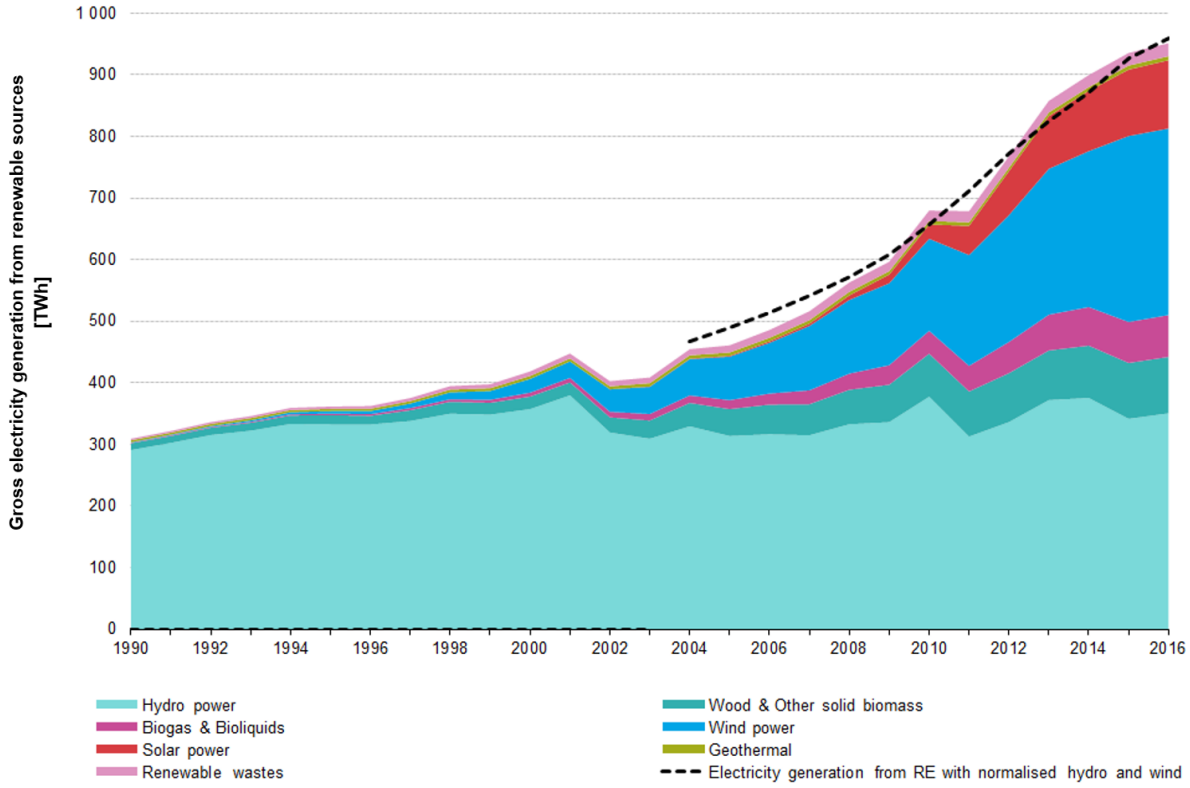

Figure 1.2: Gross electricity generation from renewable sources , EU-28, 1990-2016 Source: Eurostat (nrg105a)[2]

The relation between storage capacity and discharge time of current and potential future storage technologies is illustrated in Figure 1.3. The highest storage capacity, run time and lifetime cycles are currently provided by pumped hydropower storage systems, whereas their energy density is very low and their implementation faces geographical and ecological restrictions[8]. Systems with a higher energy density (e.g. batteries, thermal storage) can only offer limited storage capacity, run time and lifetime cycles (batteries). For the reliability of smooth and uninterrupted power supply, short and long-term storage systems and capacities need to be combined. This requires power quality management (rapid reponse within nano- to milliseconds), load shifting capability (dynamic uptake of excess energy) and standby reserve capability (hold charge for long periods and operate for days without interruption)[8].

Considering these requirements, power-to-gas (PtG) presents a promising storage technology. Although response within nanoseconds may not be achieveable[9], PtG combines huge storage

capacities with high energy density and long discharge times. However, only within the last ten years PtG is gaining increasing interest and many technologies are still at demonstration or even at development stage[9].

For this reason, the core objective of this dissertation was the development of an efficient biological PtG process with low parasitic energy consumption in order to contribute to the establishment of PtG as a flexible energy conversion and long-term storage technology. Due to very local/regional VRE overproduction and curtailment, the envisioned application of the studied system is designed to serve mainly decentralized and at smaller scale at wastewater treatment facilities or biogas plants.

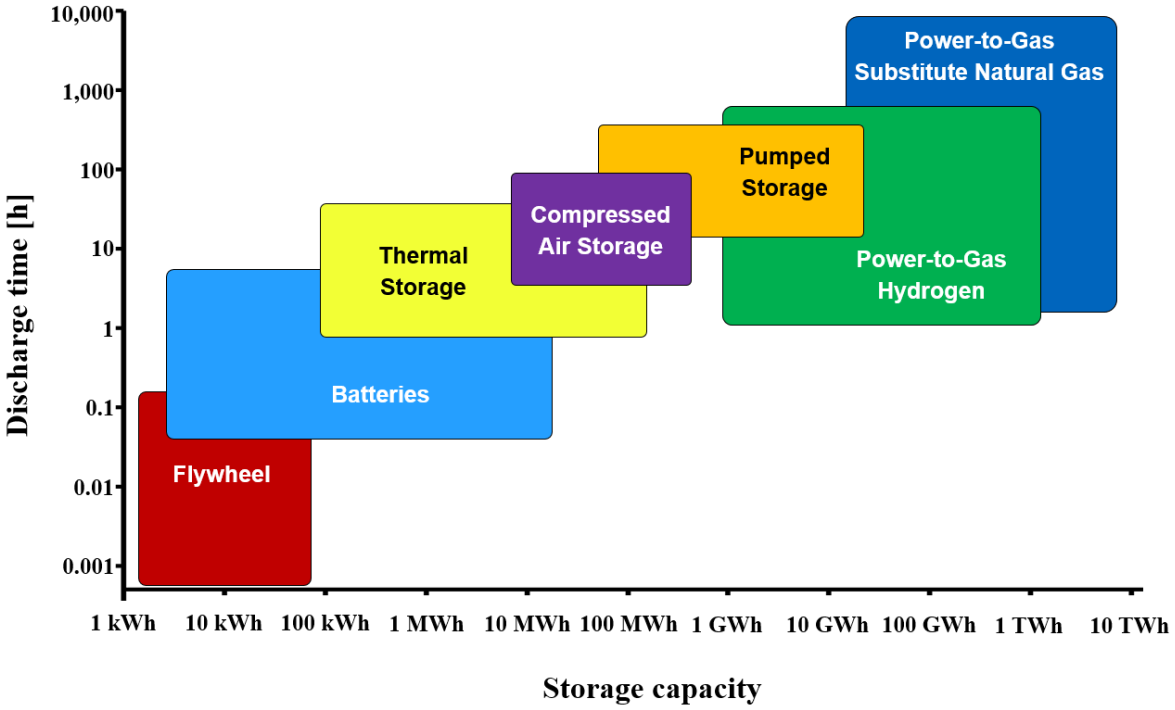

Figure 1.3: Relation between storage capacity and discharge time for current and potential future storage technologies (adapted from Newton[10])

2. Background

The growing proportion of VRE, especially wind and solar photovoltaic, increases the challenges of balancing power production and demand and affect the security and stability of the electricity grid[11]. In order to maintain the stability of the electricity grid, flexible energy conversion and long-term storage technologies are required[6,7]. One promising approach to tackle this challenge is the use of PtG technologies, enhancing grid integration and reducing curtailment of excess VRE. PtG provides a flexible VRE conversion into storable gaseous or liquid fuels for a subsequent on-demand utilization[12,13]. The PtG process chain consists of two steps (Figure 2.1).

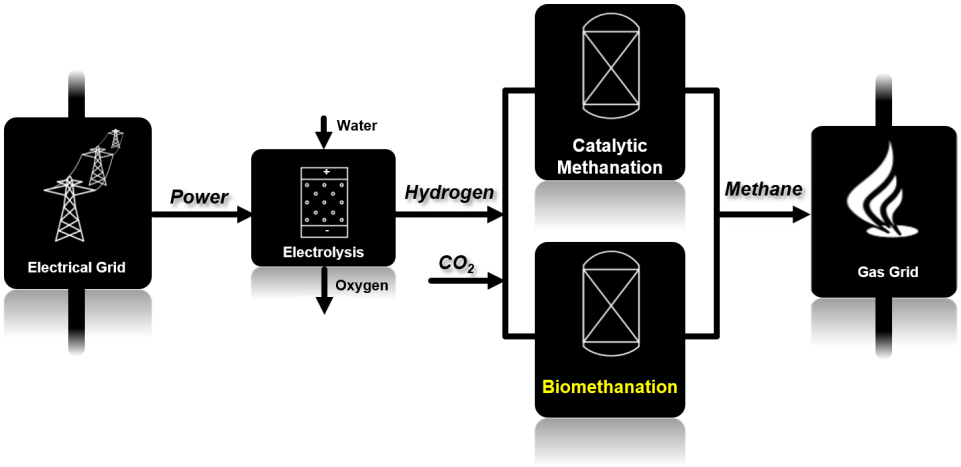

Figure 2.1: Simplified PtG process chain, coupling electrical and natural gas grids.

In a first step, water electrolysis uses power (from VRE) to generate H_2[14], which can then be used as a fuel for transportation[15], as a feedstock for chemicals (e.g. acetate, polyhydroxybutyrate)[16], or can be stored in existing natural gas grids. However, the direct H_2 injection into the gas grid is limited between $\leq$ 0.5 Vol.% (Sweden, The Netherlands) and $\leq$ 6.0 Vol.% (France)[15,17,18]. This is due to narrow H_2 tolerances of various devices in the natural gas infrastructure, as the addition of hydrogen to natural gas changes the combustion properties (increases combustion temperature and laminar flame speed, reduces ignition delay times)[15]. Due to the outlined H_2 grid injection restrictions, a further conversion step (methanation) is necessary. The methanation step, converting H_2 together with CO_2 into high-quality substitute natural gas (SNG) according to Eq. 2.1, can generate a long-term energy storage compound without injection restrictions, using the huge capacity of the existing natural gas grid infrastructure[9] (cf. Figure 2.2).

$$4\ H_2 + CO_2 \rightarrow CH_4 + 2\ H_2O \tag{2.1}$$

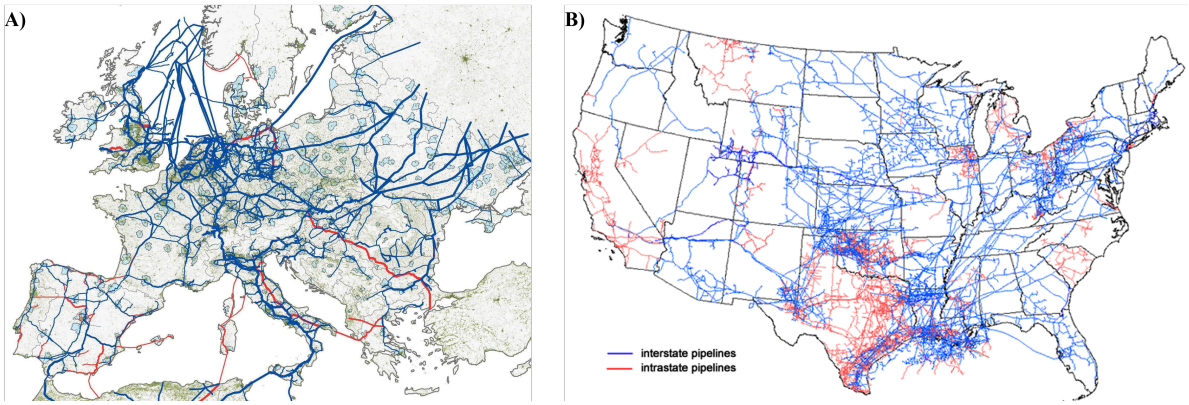

Figure 2.2: Maps of A) European interstate natural gas pipelines (Source: https://british businessenergy.co.uk/ europe-natural-gas-network/) and B. U.S interstate and intrastate natural gas pipelines (Source: U.S. Energy Information Administration, https://www.eia.gov/)

SNG can then be utilized in all natural gas facilities on demand, or as a fuel in the form of compressed and liquefied natural gas[18,19]. Methane concentrations required for injection into the natural gas grid are in the range of $> 80\%$ (Netherlands) to $> 96\%$ (Austria, Switzerland)[18,20]. According to Eq. 2.1, this requires H_2/CO_2 conversion efficiencies of 95% to 99% within the methanation process (Figure 2.3), resulting in a challenging reactor design and operation of methanation technologies. This conversion can either be performed by means of the chemical-catalytic Sabatier process or via H_2/CO_2 biomethanation (BM) by hydrogenotrophic methanogenic archaea (Figure 2.1).

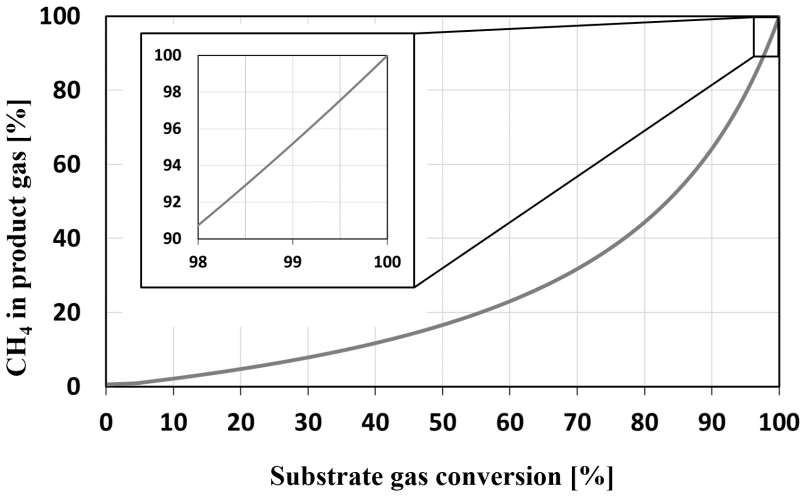

Figure 2.3: Substrate gas conversion and CH_4 concentrations in the product gas. Substrate gas: H_2 / CO_2 = 80% / 20%. (adapted from Götz et al.[9])

2.1 Water electrolysis

Water electrolysis, the first step of the PtG chain, is an electro-chemical process, using an electrical current passing to two electrodes and splitting water into H_2 and O_2 (Eq. 2.2)[9].

$$2\ H_2O + 4\ e^- \rightarrow 2\ H_2 + O_2 \tag{2.2}$$

The process is usually integrated within an electrochemical cell. An electrolyzer typically contains up to hundreds of electrochemical cells (cell-stack). Each cell consists of two porous electrodes (anode and cathode), which are connected electrically by an external circuit and an ionic-conductive electrolyte. O_2 is generated via oxidation at the anode, while H_2 is formed at the cathode via reduction. A membrane gas barrier avoids recombination of the two product gases[21]. In order to ensure process stability, high purity water is required, which makes a pretreatment to remove minerals and ions mandatory[21,22]. There are currently three technologies for water electrolysis: alkaline electrolysis (AEL), solid oxide electrolysis cells (SOEC) and proton exchange membrane (PEM) electrolysis[9].

AEL is the most mature and durable electrolysis technology and commercially available for decades. AEL uses an alkaline solution (KOH or NaOH) as electrolyte and can be operated between 1 bar and 200 bars with an electrical efficiency of 62-82%[17,22]. Dynamic AEL operation is possible between 20% and 150% of the design load, however, restart after shutdown requires 30 to 60 minutes[9]. Furthermore, the alkaline electrolyte is highly corrosive and thus, causes high maintenance cost. Still, AEL has currently the lowest capital cost of the available three available electrolysis technologies[9,15].

SOEC, or high temperature electrolysis, is still at the laboratory stage. ZrO_2 doped with 8 mol% Y_2O_3 is used as the electrolyte in SOEC.[9] This electrolyte is highly conductive for oxygen ions, which are used as charge carrier. While SOEC electrolysis has the highest reported electrical efficiencies (90-95%), the operational temperature of 700°C to 1,000°C results in a total energy efficiency of 50%-90%. Furthermore, due to high temperature operation the product gas is a mixture of H_2 and steam, which requires a further separation step, and SOEC systems face challenges like fast material degradation and limited long term stability[9]. Moreover, the high temperature does not allow flexible operation, which would be required for VRE conversion[23].

PEM electrolysis uses solid polymer membranes with high proton conductivity as electrolyte[22]. The electrical efficiency range of PEM electrolysis is similar to AEL (67-82%)[22] and improved PEM efficiency is expected in the future (87-93%)[9,15]. Still, the applied noble metal catalysts (Pt, Ir, Ru) and expensive membranes cause high capital cost for PEM electrolysis[15,17]. Regarding VRE fluctuations, PEM electrolysis is the most flexible electrolysis technology available and allows load reduction down to 5% as well as cold start within seconds[15].

2.2 Catalytic methanation

For catalytic methanation systems, operational pressure and temperature can range from 1 to 100 bar and 200°C to 550°C, respectively[9,24]. These high process temperatures correlate with high reaction rates, and catalytic methanation reactors typically operate at substantially higher gas

feed rates (10 - 100 times higher) than BM systems[9]. However, due to the highly exothermic methanation reaction (cf. Eq. 1.1), high reaction rates also correspond to a substantial heat release[9], which can thermodynamically limit the conversion efficiency due to too high process temperatures. Figure 2.4 illustrates the theoretical thermodynamic equilibrium of the methanation reaction for two operational pressures, indicating that comparably low temperature levels or higher operational pressures are required for full substrate gas conversion. Heat removal and temperature control is thus the major engineering challenge for catalytic methanation systems in order to achieve thermodynamically suitable conditions for full conversion.

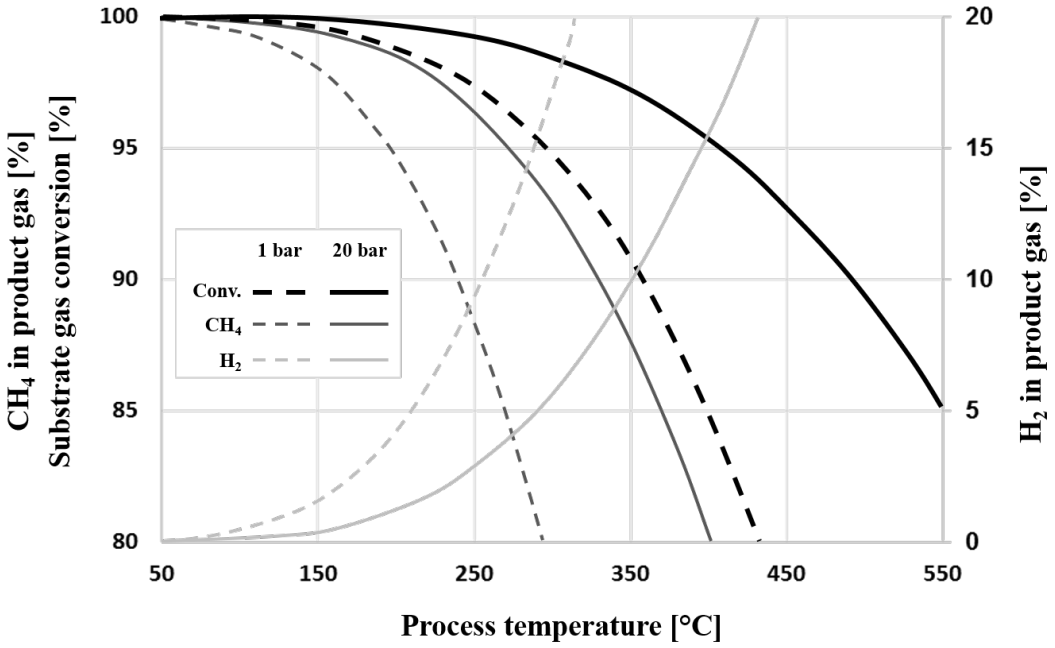

Figure 2.4: Theoretical thermodynamic equilibrium of substrate gas conversion and CH_4 and H_2 concentrations in the product gas at operational pressures of 1 bar and 20 bar. Substrate gas: H_2 / CO_2 = 80% / 20%. (adapted from Götz et al.[9] and Ghaib et al.[24])

Several reactor concepts were developed to optimize temperature management, with a main research focus on fixed-bed (most matured technology[9,24,25]), fluidized bed, three-phase, microchannel and structured monolith reactors[9,24–27]. Within all reactor types, the catalytic methanation reaction typically takes places on a Ni catalyst. Ni is applied due to its high selectivity for CH_4[24,25,28], while Ru, Rh and Co are also used less frequently. A major drawback of these catalysts is their sensitivity for impurities in the feed gas (sulphur, siloxane, NH_3)[9,24,29]. Especially sulphurous compounds are considered a catalyst poison[24,30]. This limits the direct utilization of potential CO_2 sources (e.g. emission streams from wastewater treatment facilities, biogas plants or other industrial processes) without intensive pretreatment, as their sulphur content (50 to 10,000 ppmv H_2S)[20] exceeds the allowed concentrations for catalysts (below 1 ppm_v)[9].

With respect to the required flexible operation, load changes during catalytic methanation can cause severe temperature variations (cooling down or exceeding desired operational temperature), particularly in fixed-bed reactors, and thus sensitive temperature control is necessary. During full shut down a CO_2-free gas phase is required to avoid catalyst sintering and a temperature above

200°C needs to be maintained for a subsequent fast restart[9,24].

While catalytic methanation can be considered as suitable technology for large-scale industrial applications[9,24,25], operational challenges such as i) temperature management (particularly during dynamic operation) as well as ii) pretreatment requirements for a high purity feed gas, limit the applicability for small-scale systems, e.g. as an add-on upgrading technology for wastewater treatment or biogas plants[31]. In contrast, BM has a great potential for the latter applications[9,31] and is thus, discussed in detail in the following section.

2.3 Biomethanation (BM)

The biological reduction of CO_2 with H_2 to CH_4 according to Eq. 2.1, performed by hydrogenotrophic methanogenic archaea (hydrogenotrophic methanogenesis)[32,33] is an important sub-process during the complex degradation of organic substances that is present within every anaerobic digester[34,35] (Figure 2.5 - process 6). In contrast to the catalytic methanation process, hydrogenotrophic methanogenic archaea can operate at ambient pressure and at temperatures between 5°C and 122°C[36]. Thermodynamically, this allows full substrate gas conversion already at ambient pressure (Figure 2.4). Furthermore, hydrogenotrophic methanogenic archaea have a higher tolerance for impurities in the feed gas (e.g. H_2S)[29]. Thus, they can use H_2 directly together with CO_2 emission streams (e.g. from wastewater treatment facilities, biogas plants or other industrial processes) to generate CH_4, reducing the requirements for upstream gas treatment. Generation of high-quality SNG via BM by hydrogenotrophic methanogenic archaea has thus a great potential to become a flexible VRE conversion technology[31,36–38].

In order to improve methane production rates at grid injection qualities, PtG BM technologies aim for the enhancement of hydrogenotrophic methanogenesis or even isolation of hydrogenotrophic methanogenic archaea. This has been investigated in various reactor systems in *in-situ* and *ex-situ* BM configurations[31,38,39].

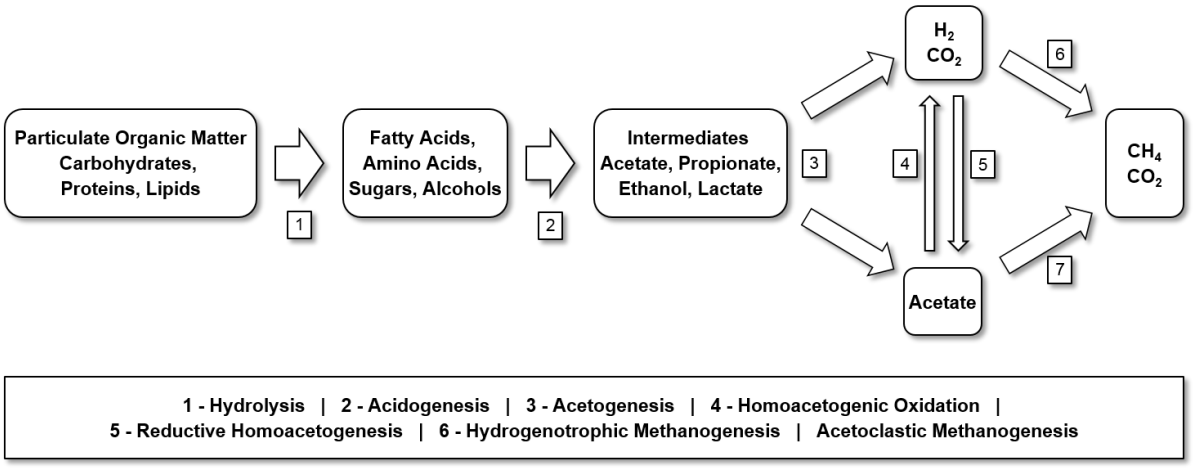

Figure 2.5: Process scheme of the degradation of organic substances during anaerobic digestion (modified from Demirel and Scherer[40] and Angelidaki et al.[41]).

2.3.1 *In-situ* BM

In-situ BM systems apply direct H_2 injection into anaerobic digesters, to upgrade the produced biogas by converting a portion of the CO_2 into CH_4[32,42–49]. This approach uses the existing microbial community and allows to increase the volumetric methane production of the existing digester volume[50]. According to Zabranska and Pokorna, two main restrictions exist for H_2 injection into anaerobic digesters: i) mass transfer and ii) metabolic limitations[38].

H_2 gas-liquid mass transfer can be limiting for *in-situ* BM within anaerobic digesters. Hydrogenotrophic methanogenic archaea are typically either suspended (planktonic) or immobilized in anaerobic granules or other biofilms structures[31,44,51]. As they can only utilize dissolved H_2 and CO_2[51], the surrounding liquid creates an additional barrier for gas-liquid mass transfer, mainly due to the very low H_2 solubility in water (0.67 $mmol_{H_2}/(L \cdot bar)$ at ambient temperature compared to 16.28 $mmol_{CO_2}/(L \cdot bar)$ at 55°C)[52]. Several technologies to enhance H_2 introduction were investigated in *in-situ* BM reactors, e.g. hollow-fiber membranes[49], ceramic sponges[44], ceramic membranes[53] or intense stirring[48], achieving methane concentrations of up to 96% in the upgraded biogas[49]. Jensen et al.[46] showed that H_2 gas-liquid mass transfer could be increased with increasing injection rates with a venturi-type device, however, also the H_2 content in the final biogas increased due to incomplete mass transfer.

Furthermore, metabolic limitations can result from increasing pH values that were observed during *in-situ* BM. This effect is mainly attributed to bicarbonate consumption from the fermentation broth through hydrogenotrophic methanogenesis[32,49,54]. While O'Flaherty et al. found that already pH levels above 7.5 affect the performance particularly of methanogenic archaea[55], Bassani et al. observed a substantial drop of reactor performance during *in-situ* methanation only above pH 8.0[56]. Also results from Luo and Angelidaki indicate an adaption of the microbial community to elevated pH levels between 7.7 and 7.9 after H_2 injection[32]. Additionally, increasing pH (as well as increasing temperature) shift the NH_4^+/NH_3-equilibrium towards NH_3, and *in-situ* BM systems may face inhibitory effects induced by NH_3, which are well known from anaerobic digestion processes[57]. A thorough pH control is thus essential for *in-situ* BM systems.

Although gas-liquid mass transfer is critical and can be enhanced by increasing H_2 partial pressures[38], sensitive H_2 injection is required for *in-situ* BM. Too high H_2 partial pressure can thermodynamically limit H_2 releasing processes[58], particularly propionate oxidation (Eq. 2.5)[59], n- and iso-butyrate β-oxidation (Eq. 2.6 and Eq. 2.7)[60,61] as well as n- and iso-valerate β-oxidation (Eq. 2.8 and Eq. 2.9)[62] (Table 2.1). The resulting accumulation of volatile fatty acids (VFA) can deteriorate the overall performance of anaerobic digestion and further inhibit upstream conversion processes (mainly acidogenesis and acetogenesis)[63–65]. Due to their very low tolerances for H_2 partial pressures, H_2 releasing processes strongly rely on a syntrophic relation with a H_2 consuming microbial community[34,66]. In anaerobic digestion, H_2 is typically kept low by hydrogenotrophic methanogenic archaea and is therefore frequently used for process control. Still, a number of studies showed that homoacetogenic acetate formation (Eq. 2.10, Figure 8 - process 5) by homoacetogens can become the dominating H_2 uptake pathway when excess H_2 was available after in situ H_2 injections[42,43,67]. However, Agneessens et al. also found that after several H_2 injection cycles hydrogenotrophic methanogens dominated again[42,43], showing that the microbial community can adapt to *in-situ* BM conditions.

Table 2.1: Selected biochemical pathways during anaerobic digestion and their respective change in Gibbs free energy at 25°C and pH 7. Values obtained from Schink[34] and Batstone et al.[68]

Process	Reaction	$\Delta G^{0\prime}$ [kJ/mol]	#
Homoacetogenic oxidation	$CH_3COOH + 2\ H_2O \rightarrow 2\ CO_2 + 4\ H_2$	-94.9	(2.3)
Acetoclastic methanogenesis	$CH_3COOH + 2\ H_2O \rightarrow CO_2 + CH_4$	-31.0	(2.4)
Propionate oxidation	$CH_3CH_2COOH + 2\ H_2O \rightarrow 2\ CH_3COOH + CO_2 + 3\ H_2$	76.2	(2.5)
n-butyrate β oxidation	$CH_3CH_2CH_2COOH + H_2O \rightarrow 2\ CH_3COOH + 2\ H_2$	48.4	(2.6)
iso-butyrate β oxidation	$CH_3(CHCH_3)COOH + H_2O \rightarrow 2\ CH_3COOH + 2\ H_2$	48.4	(2.7)
n-valerate β oxidation	$CH_3(CH_2)_3COOH + 2\ H_2O \rightarrow CH_3COOH + CH_3CH_2COOH + 2\ H_2$	48.4	(2.8)
iso-valerate β oxidation	$CH_3(CHCH_3)CH_2COOH + CO_2 \rightarrow 3\ CH_3COOH + H_2$	25.2	(2.9)
Reductive homoacetogenesis	$2\ CO_2 + 4\ H_2 \rightarrow CH_3COOH + 2\ H_2O$	94.9	(2.10)

Approaches to reduce thermodynamic restrictions thus focus on i) injection techniques to allow optimized H_2 distribution for immediate consumption (e.g. membrane approaches) as well as on ii) separation of the process steps into several stages (e.g. hydrolysis+acidogenesis and acetogenesis+methanogenesis), to uncouple upstream processes from the effect of H_2 addition into the final (methanogenesis) stage[53,56]. The concluding development of the latter approach would be the entire isolation of hydrogenotrophic methanogenesis in separate reactors, which is known as *ex-situ* BM.

2.3.2 *Ex-situ* BM

An isolated hydrogenotrophic methanogenesis in *ex-situ* BM systems allows the application of optimal operational conditions (e.g. pH, temperature, H_2 partial pressure, process design)[36] that are unfavorable for the upstream processes as described above. Several *ex-situ* BM studies have shown that the isolated process achieves substantially higher gas conversion rates compared to the *in-situ* approach, and thus requires smaller reactor volumes[50]. Table 2.2 shows a compilation only of *ex-situ* BM studies that achieved methane concentrations above 75%, while a comprehensive overview of *ex-situ* BM studies can be found elsewhere[36,50]. Both, pure methanogenic strains[29,33,69–77] as well as mixed microbial cultures[54,78–87] were used in *ex-situ* BM systems. While pure culture based systems generally achieved higher methane production rates (Table 2.2), potential advantages of mixed microbial cultures are no sterilization requirements as well as their microbial diversity and adaptive capacity resulting in an increased process resilience[88].

Also *ex-situ* BM reactors face limitations in methane productivity most commonly found as a result of limited H_2 gas-liquid mass transfer between the introduced gases and the methanogenic archaea in the liquid phase[36]. Eq. 2.11 is a simplified description of the gas-liquid mass transfer:

$$R_{H_2} = k_L\alpha \ \cdot \ (H_{H_2,cp} \ \cdot \ p_{H_2,G} - c_{H_2,L}) \tag{2.11}$$

where R_{H_2} [mol/(L · h)] and $k_L\alpha$ [1/h] are the overall volumetric hydrogen mass transfer rate and the volumetric mass transfer coefficient, respectively. The driving force for the hydrogen gas-liquid mass transfer is the gradient between $H_{H_2,cp} \cdot p_{H_2,G}$ and $c_{H_2,L}$, where $H_{H_2,cp}$ [mol/(L · bar)], $p_{H_2,G}$ [bar] and $c_{H_2,L}$ [mol/L] are the Henry's law constant, the partial pressure in the gas phase and the liquid phase concentration of hydrogen, respectively.

Table 2.2: Comparison of reactor type, process temperature and methane production rates from experimental studies achieving methane concentrations above 75% (adapted from Lecker et al.[50]).(Sorted by methane production rates.)

Reactor type	Microbial culture	Methane production rate $[m^3_{CH_4}/(m^3 \cdot d)]$	Methane concentration [%]	Temp. [°C]	Ref.
CSTR	pure	288	96	65	Peillex et al., 1990[74]
CSTR	pure	137.2	85	65	Seifert et al., 2014[77]
Biofilm plug-flow	mixed	30.0	93	37	Savvas et al., 2017[89]
Trickle bed	mixed	15.4	98	55	Strübing et al., 2017[90]
Loop reactor	mixed	12.1	100	37	Savvas et al., 2017b[86]
CSTR	pure	9.9	85	60	Martin et al., 2013[72]
HFM	mixed	9.6	79	55	Díaz et al., 2015[91]
Fixed bed	mixed	6.4	75	54	Alitalo et al., 2015[92]
CSTR	mixed	5.3	95	55	Luo and Angelidaki, 2012[32]
HFM	mixed	4.6	80	37	Ju et al., 2008[93]
CSTR	mixed	4.1	92	38	Kim et al., 2013[94]
Trickle bed	mixed	3.1	96	38	Burkhardt et al., 2017[95]
Trickle bed	mixed	1.9	96	38	Rachbauer et al., 2016[84]
Trickle bed	mixed	1.7	96	55	Porté et al. 2018[54]
Fixed bed	mixed	1.3	100	35	Lee et al., 2012[96]
Granular UASB	mixed	1.1	82	55	Bassani et al., 2016[44]
HFM	mixed	0.65	99	37	Wang et al., 2013[97]
Bubble-column	mixed	0.5	98	52	Kougias et al., 2017[82]
CSTR	mixed	0.5	92	65	Guneratnam et al., 2017[98]
Serial upflow columns	mixed	0.2	98	52	Kougias et al., 2017[82]

CSTR: Continuous Stirred Tank Reactor; HFM: Hollow-Fiber-Membrane UASB: Upstream Anaerobic Sludge Blanket

Operating a reactor at elevated pressure increases the gas solubility (via $p_{H_2,G}$), Seifert et al. observed a 25% higher methane production rate along with an increase from ambient pressure to 1.5 barg[77]. Furthermore, elevated pressure reduces the gas bubble size and thus increases the gas-liquid phase boundary interface[99] as well as the gas retention time due to a reduced bubble rise velocity[100]. An improved reactor design may also allow for locally elevated $p_{H_2,G}$ (e.g. by plug flow conditions)[99]. The phase boundary interface can also be influenced and optimized by the reactor design, which strongly enhances the volumetric mass transfer coefficient $k_L\alpha$as shown in different studies[99,101–103].

Reactor concepts for *ex-situ* BM

All reactor concepts for *ex-situ* BM thus aim at maximizing the gas-liquid phase boundary interface, occasionally combined with elevated operational pressure. Continuous stirred tank reactors (CSTR) were the most frequently studied *ex-situ* BM system[29,72,77,82,94,98,104–110]. In CSTR, high agitator-power-per-volume ratio and improved reactor and impeller design enhance gas-liquid mass transfer due to decreased gas bubble size and optimized gas distribution. The highest methane production rate in CSTR was achieved by Peillex et al.[74] (288 $m^3/(m^3 \cdot d)$, c_{CH_4} = 96%, 1,200 rpm, Table 2.2). With stirring speed typically ranging from 100 rpm up to 1,500 rpm[107], the amount of energy that is required for mixing corresponds to up to 10% of the produced CH_4 and increases with increasing reactor size[89]. For a constant stirring speed, also mechanical constraints limit the reactor size, which might be a potential drawback regarding reactor upscaling[103]. Due to these CSTR constrictions, several alternative reactor concepts have been investigated.

Hollow-fiber membrane reactors enhance H_2 gas-liquid transfer by gas diffusion through a membrane[78,91,93,111]. Typical materials for these membranes are polysulfone[93], polyvinylidene difluoride[91], polyurethane or polyethylene[49]. These reactors are based on planktonic microorganism and require only minor mixing of the process liquid to ensure even distribution of microorganism and nutrients. Still, due to their substrate gas affinity, the microbial community tends to form biofilms on the hollow-fiber membrane (membrane fouling). Luo and Angelidaki[49] found mass transfer resistance due to biofilm formation, which led to increased energy consumption for gas supply and reduced applicability. The highest methane production rate ($c_{CH_4} > 75\%$) in hollow-fiber membrane reactors was achieved by Díaz et al.[91] (9.9 $m^3/(m^3 \cdot d)$, $c_{CH_4} = 85\%$, Table 2.2).

Increased gas retention time and enlarged phase boundary interface is the key to enhance gas-liquid mass transfer in bubble-column reactors with planktonic microorganism[79,82]. The energy input required for the gas supply depends on the gas introduction system (aiming for small bubble size), but typically, no additional mixing is needed. Savvas et al. developed a mesophilic loop reactor[85,86] by integrating a highly mixed gas introduction (centrifugal pump) into a circulated up-flow column achieving 12.1 $m^3/(m^3 \cdot d)$ at $c_{CH_4} = 100\%$ (Table 2.2).

Fixed bed reactors aim for biomass immobilization on a carrier material[92,96,112]. Gas introduction system with small bubble sizes increase the gas distribution and due to its flow resistance the carrier material increases gas retention time. Alitalo et al.[92] reported the highest methane production rates ($c_{CH_4} > 75\%$) for fixed bed reactors with 6.4 $m^3/(m^3 \cdot d)$ at $c_{CH_4} = 75\%$ (Table 2.2).

Recently, anaerobic trickle bed reactors are gaining increasing interest for *ex-situ* BM, resulting in several studies[54,80,81,83,84,90,113–119]. The previous application of trickle bed systems for other biological processes with gaseous substrates, e.g. syngas fermentation (SGF)[99,102,103,114,115] or biological gas treatment applications[101,120], already showed an improved gas-liquid mass transfer. Trickle bed reactors use packing/carrier material that provides a high surface-area per reactor volume to increase the phase boundary interface for mass transfer. Contrary to fixed bed reactors, this carrier material is not covered with process liquid, but only by a thin liquid layer that is surrounded by a gas phase[80,113]. This reduces the diffusion limitation and makes optimal use of the large phase boundary interface to enhance gas-liquid mass transfer. Furthermore, the gas phase allows controlling the superficial gas velocity independently, in contrast to several other reactor systems with rising gas bubble in the process liquid (CSTR, fixed bed, bubble column). The energy input for these systems is comparably low, as no mixing and pressurized gas introduction is required[117]. Furthermore, a high length-to-diameter-ratio allows for approaching plug-flow conditions and therefore locally elevated $p_{H_2,G}$, especially close to the substrate gas introduction (Figure 2.6). Typical length to diameter ratios for trickle bed reactors are in the range of 5:1[113,119] to 19:1[84]. Trickle bed reactors can further benefit from their capability for biomass immobilization, to avoid washout of the desired hydrogenotrophic methanogenic archaea[81].

In a biofilm tube reactor consisting of a PVC tube filled with carrier material (length: 7 m; inner diameter: 13 mm) Savvas et al.[86] reached 30.0 $m^3/(m^3 \cdot d)$ at $c_{CH_4} = 93\%$ (Table 2.2). This shows the importance and potential of almost ideal plug-flow conditions in biofilm based reactors without mixing. Still, maintaining the plug-flow properties at a length-to-diameter-ratio of 538:1 may limit the upscaling capability of such a reactor type.

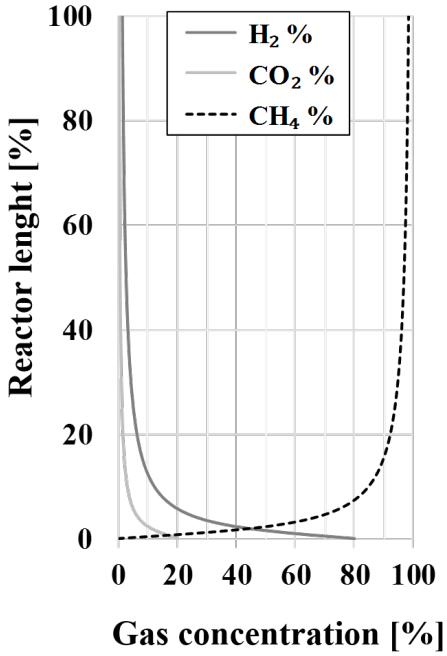

Figure 2.6: Simplified relation between gas concentration and reactor length for ideal plug-flow conditions. Substrate gas: H_2 / CO_2 = 80% / 20%.

Biofilm based processes

A wide range of biological processes uses immobilization of a desired microbial community to increase process efficiency through decoupling hydraulic retention time (HRT) and solid retention time (SRT)[121]. By providing large surface areas in trickle bed reactors, the benefits of a potential biofilm establishment can be combined with enhanced gas-liquid mass transfer[101,120]. As previous studies of trickle bed reactors for BM already observed biofilm formation at mesophilic conditions[80,81,86], it is assumed that an immobilized microbial community can be beneficial with regard to process performance and resilience during demand-oriented operation. Still, the actual contribution of immobilized and planktonic biomass to the total gas conversion as well as mechanism for a rapid reactor start-up have not been identified for thermophilic systems. While biofilm formation at thermophilic conditions has been studied for various anaerobic applications, the desired immobilization of thermophilic hydrogenotrophic methanogenic archaea has rarely been examined[92].

Generally, biofilm formation can be achieved by application of various driving forces, such as low HRT and/or high hydrodynamic shear forces[122–126]. At these selective conditions, immobilized microorganism have a competitive advantage compared to planktonic biomass. While high hydrodynamic shear forces can be easily applied in upflow biofilm systems (e.g., fixed bed reactor, UASB reactor, moving bed biofilm reactor), trickle bed system only allow HRT as a driving force, as high trickling rates (inducing high hydrodynamic shear forces) would negatively impact the gas-liquid mass transfer[113]. In hyper-thermophilic upflow biofilm reactors for mixed culture biohydrogen production, Zheng et al.[127] reported that low HRT was essential for biofilm formation. Still, although low HRT led to faster biofilm formation, they observed lower production rates at too

low HRT due to increased washout of high yielding biomass. Thus, a careful selection of HRT is required to derive the optimum operating point for start-up of biofilm based systems.

Influence of temperature on *ex-situ* BM processes

Process temperature has been proven to play a significant role for *ex-situ* BM systems[36,50,98]. Increasing temperature results in a lower solubility of substrate gases in the process liquid, whereas the parallel increase of diffusion rates can almost compensate this effect[51]. Gas-liquid mass transfer is thus not limited by higher process temperatures. With regard to microbial activity, substantially higher volumetric methane production was found for reactors operated at thermophilic conditions due to enhanced microbial growth and conversion rates compared to mesophilic operation (cf. Table 2)[32,51,56]. Although increasing temperature furthermore shift the NH_4^+/NH_3-equilibrium[57], inhibitory effects from NH_3 in *ex-situ* BM systems can be avoided as the nitrogen supply can be controlled individually (typically via NH_4^+ dosage[108,128]).

Considering the growth and conversion rates of hydrogenotrophic methanogenic archaea, thermophilic temperature is a favorable process conditions for *ex-situ* BM systems, especially for pure cultures. With regard to the overall diversity of the microbial community (in an anaerobic digesters treating household biowaste), Levén et al.[129] observed a higher diversity at mesophilic temperature, compared to the microbial community at thermophilic temperature. Whether a lower diversity is particularly critical for an mixed culture *ex-situ* BM process remains open. Considering the stability of anaerobic microbial processes, research clearly shows that changing temperature in anaerobic digestion systems cause disturbance of the microbial community and might affect VFA conversion (especially propionate)[130–134]. However, van Lier et al.[133] also found a decreasing sensitivity to temperature fluctuations over time, suggesting an adaption of microbial community and conversion pathways. This may be a potential advantage for dynamic operation of *ex-situ* BM systems with long-lasting standby periods (SPs) that needs to be proven.

Operational constrains for *ex-situ* BM systems through VRE

Van Dael et al. emphasized the importance of the demand-oriented operation of microbial PtG systems for conversion of excess energy peaks from fluctuating VRE generation[23]. The duration of these peaks will depend strongly on future VRE penetration scenarios as well as on the VRE mix, but specifying statements are controversial[135,136]. A study of German meteorological data revealed that maximum duration of periods without sufficient wind velocities and solar radiation for renewable power generation occurring between 2006 and 2016 was only about two weeks, which can be considered as meteorological worst case[137]. However, the duration of periods without excess VRE resulting in BM standby as well as the required response times are presently not well defined. Moreover, electricity pricing can influence the economic feasibility of PtG technologies[23,138–140] and thus, also effects potential standby durations. Electricity pricing can be impacted by future VRE curtailment due to too high excess VRE generation[141,142]. For 2016, Joos and Staffell[143] found that curtailment of wind VRE in Germany (3.35 TWh) resulted in cost for compensation of €325.89 million (average price of €92.32/MWh). Converting this amount of curtailed energy via PtG and avoiding compensation would clearly enhance the feasibility of PtG technologies. For restart or ramping scenarios, the gradients of excess power production from VRE sources, as presented in

Huber et al.[144], must also be considered. These gradients will increase with the increasing proportion of wind and photovoltaic power in total power generation (α) as well as with the proportion of photovoltaic power in VRE generation (β). Depending on these parameters, maximum negative gradients (= excess energy) in 2014 for the EU28 were found to be 9.9% (1-hour gradient) and 33.4% (8-hour gradient) of the system peak load[3], but ranged from 10% (1-hour gradient, α=0.1, β=0.2) up to 200% (12-hour gradient, α=0.7, β=0.6) in a modelled scenario[144].

With regard to the stability of anaerobic microbial processes, research clearly shows that dynamic operation as well as changing substrate availability/starvation in anaerobic digestion systems cause disturbance of microbial processes and/or shifts from established towards more suitable conversion pathways[132,145,146].

Regarding the restart performance of the BM process, it is hypothesized that standby settings influence the restart performance and the time required to re-attain a stable CH_4 production rate similar to previous levels. Savvas et al.[85] observed 80% recovery of substrate gas conversion (according to Eq. 2.1), within 17 and 24 hours subsequent to SPs of 13 and 45 days, respectively. Graf et al.[147] reported that restart after a 23-day SP was possible without problems using BM lab-scale reactors. However, the authors did not report operational or process performance parameters. Hence, *ex-situ* BM systems require suitable standby strategies that also maintain the ability to re-attain full methanation performance as quickly as possible after restart.

CO_2 sources for *ex-situ* BM

Emissions from energy-intensive manufacturing industries, such as iron and steel or cement production as well as crude oil cracking, are among the largest available CO_2 sources worldwide[148]. Still, to use these CO_2 sources for BM would require prior gas upgrading to capture CO_2 and remove various trace compounds originating from the production processes, which could substantially reduce the energy efficiency and economic feasibility of these sources[9]. The most considered CO_2 source for *ex-situ* BM is biogas[9,19,84,140,149], with a typically composition of CH_4 (50-70%), CO_2 (30-50%) and traces of H_2S, NH_3, water vapor and siloxanes[9]. Considering the european biogas production of 181,565 GWh (energy equivalent) in 2015[150], conversion of the remaining 30 to 50% of CO_2 to CH_4 according to Eq. 2.1 can provide an additional energy equivalent of approximately 108,000 to approximately 181,000 GWh. Biogas can be directly injected into *ex-situ* BM reactors and the omission of gas cleaning is the major advantages of this CO_2 source. Contrary, the CH_4 content in the biogas reduces the gas retention time of the actual substrate gases as well as their partial pressure in the reactor, resulting in reduced gas-liquid mass transfer and conversion efficiency[151]. Alternatively, CO_2 from membrane based biogas upgrading plants can be used[140]. Still, the economic feasibility of these CO_2 source has to be evaluated for each case. In addition, high-purity CO_2 sources are available in several processes in industry and fuel production. Due to their partial dependency on fossil fuels (e.g. natural gas processing, coal-to-gas, coal-to-liquids, ethanol production, ethylene oxide production)[9], they were not further considered in this thesis.

3. Research significance and hypotheses

By flexible conversion of excess VRE into a storable gas, PtG technologies provide a promising approach to stabilize the electricity grid and balance electrical power production and demand[12,13]. The application of BM with hydrogenotrophic methanogenic archaea can become such a flexible PtG technology that generates high-quality SNG (a long-term energy storage compound without injection restrictions) and uses the huge capacity of the existing natural gas grid infrastructure[31,36–38]. Still, BM systems face H_2 gas-liquid mass transfer as the main rate limiting step. While various reactor concepts have been studied with the purpose of overcoming these limitations[31,36,38], the highest methane production rates were achieved with H_2 introduction by energy-intensive stirring in CSTR[50]. For this reason, the core objective of this dissertation was to develop an alternative and efficient reactor concept with low H_2 gas-liquid mass transfer restrictions and simultaneously low parasitic energy consumption, suitable for flexible on-demand operation. In this respect, anaerobic thermophilic trickle bed reactors (ATTBR) were identified as a potentially suitable reactor concept and several experiments with ATTBR systems at laboratory and technical-scale have been carried out. The investigation of ATTBR's capability for efficient BM focused on two key research objectives, which are elucidated along with their respective hypothesis in detail as follows. Moreover, Figure 3.1 provides an overview of this dissertation's structure.

Chapter		Research objectives	Hypothesis	Publications
4	Pilot scale	Evaluating the potential to establish an efficient BM process with low H_2 gas-liquid mass transfer restrictions and simultaneously low parasitic energy consumption within an ATTBR (Proof of concept).	**Hypothesis #1** An ATTBR, operated at ambient pressure with a mixed microbial culture, can achieve at least 12.3 $m^3_{CH4}/(m^3 \cdot d)$ at $c_{CH4} > 96\%$.	**Paper I** **Strübing, D.**; Huber, B.; Lebuhn, M.; Drewes, J.E.; Koch, K. (2017), *Bioresource Technology*, 245, 1176-1183.
5		Elucidating the capability of the ATTBR concept for flexible and demand-oriented H_2/CO_2 biomethanation within a dynamic energy system. Identifying operational constraints and suitable strategies to manage standby periods as well as rapid restart and load change scenarios.	**Hypothesis #2** The standby strategy (temperature and duration) influences the time required to re-attain a stable CH_4 production rate (similar to previous levels) after standby periods.	**Paper II** **Strübing, D.**; Moeller, A.B.; Mößnang, B.; Lebuhn, M.; Drewes, J.E.; Koch, K. (2018), *Applied Energy*, 232, 543-554.
6			**Hypothesis #3** An ATTBR has the capability for a rapid response, re-attaining full CH_4 production rate (at $c_{CH4} > 96\%$) within 60 minutes after standby periods.	**Paper III** **Strübing, D.**; Moeller, A.B.; Mößnang, B.; Lebuhn, M.; Drewes, J.E.; Koch, K. (2017), *Bioresource Technology*, 289, 121735.

Figure 3.1: Dissertation structure summarizing research objectives, hypothesis and corresponding publications

3.1 Research objective #1

Evaluating the potential to establish an efficient BM process with low H_2 gas-liquid mass transfer restrictions and simultaneously low parasitic energy consumption within an ATTBR (Proof of concept).

In order to achieve the core objective of this dissertation, the first research objective aimed at proofing the ATTBR concept. Implementing the BM process within an ATTBR, providing a high surface-area per reactor volume[120], is expected to enhance gas-liquid mass transfer (section 2.3.2). Furthermore, BM within trickle bed reactors has been investigated only in a few studies and only under mesophilic conditions[80,81,84,95,113–115], although substantially higher methane generation rates were generally found for reactors operated at thermophilic temperatures due to enhanced microbial growth rates[32,56]. Thus, within the first research objective, the possible mass-transfer advantages of trickle bed systems were combined with the potential enhancement of biological conversion of CO_2 and H_2 to CH_4 under thermophilic conditions. The potential to establish an efficient BM process with low H_2 gas-liquid mass transfer restrictions and simultaneously low parasitic energy consumption within an ATTBR was evaluated by testing hypothesis #1:

***Hypothesis #1**: An ATTBR, operated at ambient pressure with a mixed microbial culture, can achieve at least methane production rates of 12.3 $m^3_{CH_4}/(m^3 \cdot d)$ at $c_{CH_4} > 96\%$.*

The performance comparison level considered in hypothesis #1 was derived from the highest previously published methane production rate of a mesophilic trickle bed reactor system (3.1 $m^3_{CH_4}/(m^3 \cdot d)$ at $c_{CH_4} > 96\%$)[95]. This level was adapted to the potential thermophilic methane production rate by applying a factor of $e^{0.069 \cdot (55°C\text{-}35°C)}$ to account for the enhanced growth rate of hydrogenotrophic methanogens under thermophilic conditions[152].

In order to test hypothesis #1, an ATTBR at technical-scale was set up, inoculated with sewage sludge from a local wastewater treatment plant digester and operated at 55°C at ambient pressure for more than 300 days. These investigations resulted in **Paper I**.

Paper I: D. Strübing, B. Huber, M. Lebuhn, J. E. Drewes, and K. Koch, "High performance biological methanation in a thermophilic anaerobic trickle bed reactor", *Bioresource Technology*, vol. 245, pp. 1176–1183, 2017.

3.2 Research objective #2

Elucidating the capability of the ATTBR concept for flexible and demand-oriented H_2/CO_2 biomethanation within a dynamic energy system. Identifying operational constraints and suitable strategies to manage standby periods as well as rapid restart and load change scenarios.

The capability to deal with fluctuating gas loads is crucial for the future application of ATTBR as a flexible and efficient energy conversion and long-term storage technology[153]. Depending on the

renewable energy scenario studied, the extent of required storage capacities, required respond times and duration of surplus energy peaks are being controversially discussed[135,136,153,154]. In order to apply ATTBR in any of those energy conversion and storage scenarios, different combinations of standby and restart strategies need to be evaluated. In this context, the focus of the second research objective is to elucidate the capability of the ATTBR concept for flexible and demand-oriented H_2/CO_2 BM as well as to identify operational constraints and suitable strategies to manage SPs as well as rapid restart and load change scenarios.

Extended ATTBR SPs could affect gas conversion performance, and thus have to be considered for demand-orientated operation. A decreased gas conversion capacity due to a loss of activity or even severe decay of the microbial community[155], can be expected as the most severe effect of these SPs. Thus, particularly temperature can become a critical standby parameter, as significantly higher decay rates prevail at thermophilic conditions compared to mesophilic systems (decay rates: 55°C: 0.48 d^{-1}, 38°C: 0.034 d^{-1})[152,155,156]. To test hypothesis #2, the impact of SP settings on the restart performance was investigated within the established ATTBR technical-scale set-up, resulting in **Paper II**.

***Hypothesis #2**: The standby strategy (temperature and duration) influences the time required to re-attain a stable CH_4 production rate (similar to previous levels) after standby periods.*

Paper II: D. Strübing, A.B. Moeller, B. Mößnang, M. Lebuhn, J. E. Drewes, and K. Koch, "Anaerobic thermophilic trickle bed reactor as a promising technology for flexible and demand-oriented H_2/CO_2 biomethanation", *Applied Energy*, vol. 232, pp. 543–554, 2018.

In addition to a suitable standby management, the ability to re-attain full methanation capacity after restart is critical[153]. Currently, the time period to respond to available excess power cannot be determined with certainty from existing studies. In addition, potential delays due to hydrogen availability strongly depend on the electrolysis technology applied[9,157]. Thus, limitations of various restart strategies need to be studied. It is expected that restart performance will be influenced by standby effects as well as by the restart strategy applied. The impact of restart strategies was investigated by testing hypothesis #3 within the ATTBR technical-scale set-up, resulting in **Paper III**.

***Hypothesis #3**:: ATTBRs have the capability for fast response, re-attaining full CH_4 production rate (at $c_{CH_4} > 96\%$) within 60 minutes after standby periods.*

Paper III: D. Strübing, A.B. Moeller, B. Mößnang, M. Lebuhn, J. E. Drewes, and K. Koch, "Load change capability of anaerobic thermophilic trickle bed reactors for dynamic H_2/CO_2 biomethanation", *Bioresource Technology*, vol. 289, Article No. 121735, 2019.

3.3 Additional publication

Identifying the key parameters that allow a rapid start-up of biofilm based biomethanation systems.

This dissertation additionally yielded another peer-reviewed publication (**Paper IV**) that aimed at studying a key parameter that allows a rapid start-up of a biofilm-based system for H_2/CO_2 BM. A wide range of biological processes uses immobilization of a desired microbial community to increase process efficiency through decoupling HRT and SRT[121]. By providing large surface areas in trickle bed reactors, the benefits of a potential biofilm establishment can be combined with enhanced gas-liquid mass transfer[101,120]. As previous studies of trickle bed systems for BM already observed biofilm formation at mesophilic conditions[80,81,89], it is assumed that an immobilized microbial community can be beneficial with regard to process performance and resilience.

Biofilm formation requires application of driving forces, such as high dilution rates and/or high hydrodynamic shear forces[123–126]. At these selective conditions, immobilized microorganism have a competitive advantage compared to microorganism growing in suspension. Trickle bed systems only allow HRT as a driving force, as high trickling rates (inducing high hydrodynamic shear forces) would negatively impact the gas-liquid mass transfer[113]. In order to elucidate the effect of HRT on methanogenic biofilm activity and composition during reactor start-up, a lab scale set-up was established at the Aarhus University (DK) and investigated in a joint study.

Paper IV: M. B. Jensen, D. Strübing, N. de Jonge, J. L. Nielsen, L. D. M. Ottosen, K. Koch, M. V. W. Kofoed, "Stick or leave – pushing methanogens to biofilm formation for *ex-situ* biomethanation", *Bioresource Technology*, vol. 291, Article No. 121784, 2019.

4. High performance biological methanation in a thermophilic anaerobic trickle bed reactor

With the aim of developing an efficient reactor concept with low H_2 gas-liquid mass transfer restrictions and simultaneously low parasitic energy consumption, this study tested **hypothesis #1**:

An ATTBR, operated at ambient pressure with a mixed microbial culture, can achieve at least methane production rates of 12.3 $m^3_{CH_4}/(m^3 \cdot d)$ at cCH4 > 96%.

An ATTBR system at technical-scale has been set up in order to combine the possible mass transfer advantages of trickle bed reactors with the potential enhancement of BM rates at thermophilic conditions and test hypothesis #1. The corresponding long-term experiment resulted in **Paper I**, were we demonstrated the potential of ATTBR as a very efficient energy conversion and storage technology, achieving grid injection qualities (> 96% CH_4) at comparably high methane production rates (15.4 $m^3_{CH_4}/(m^3 \cdot d)$) and could thus proof the desired reactor concept at pilot scale. Thus, the tested **hypothesis #1 can be accepted**.

The ATTBR required no mixing energy or introduction of pressurized gas and can easily compete with the performance of other mixed culture BM reactors. Moreover, inoculation with digested sludge showed high adaptive capacity due to intrinsic biological diversity being a potential benefit for practical applications. However, control of pH and nutrient supply turned out to be crucial for stable operation, and was affected significantly by dilution due to metabolic water production, especially during demand-orientated operation.

This chapter was published in a similar form with editorial changes as:

D. Strübing, B. Huber, M. Lebuhn, J. E. Drewes, and K. Koch, "High performance biological methanation in a thermophilic anaerobic trickle bed reactor", *Bioresource Technology*, vol. 245, pp. 1176–1183, 2017.

Author contribution: D. Strübing (80%); B. Huber (5%); M. Lebuhn (5%); J. E. Drewes (5%); K. Koch (5%)

Abstract

In order to enhance energy efficiency of biological methanation of CO_2 and H_2, this study investigated the performance of a thermophilic (55°C) anaerobic trickle bed reactor (ATBR) (58 L) at ambient pressure. With a methane production rate of up to 15.4 $m^3_{CH_4}/(m^3_{\text{trickle bed}} \cdot d)$ at methane concentrations above 98%, the ATBR can easily compete with the performance of other mixed culture methanation reactors. Control of pH and nutrient supply turned out to be crucial for stable operation and was affected significantly by dilution due to metabolic water production, especially during demand-orientated operation. Considering practical applications, inoculation with digested sludge, containing a diverse biocenosis, showed high adaptive capacity due to intrinsic biological diversity. However, no macroscopic biofilm formation was observed at thermophilic conditions even after 313 days of operation. The applied approach illustrates the high potential of thermophilic ATBRs as a very efficient energy conversion and storage technology.

4.1 Introduction

In order to keep up with an increasing amount of power generated discontinuously from renewable resources, the need for flexible and efficient energy conversion and long-term storage technologies is clearly growing. Considering the huge storage capacity of existing natural gas grids, generation of storable methane from H_2 and CO_2 can become a suitable conversion and storage approach, e.g. by using H_2 generated with excess electricity via electrolysis and CO_2 emission streams (e.g. at biogas or wastewater treatment plants)[9,37,50,158]. However, methane concentrations required for injection into the natural gas grid are in the range of $> 80\%$ (Netherlands) to $> 96\%$ (Austria, Switzerland)[20].

$$4\ H_2 + CO_2 \rightarrow CH_4 + 2\ H_2O \tag{4.1}$$

According to Eq. 4.1, this requires conversion efficiencies of 95% to 99% of the educt gases within the methanation process, which can be performed by means of the chemical catalytic Sabatier process or in a biological process by hydrogenotrophic methanogenic archaea. Compared to the Sabatier process, the biological methanation is very resistant to impurities in the feed gas, such as H_2S[29], which significantly reduces pre-treatment requirements for the usage of raw biogas as a potential CO_2 source. Furthermore, the biological process can already be operated at ambient pressure and temperatures between 5°C and 122°C[158], instead of pressures of up to 100 bar and temperatures between 250°C and 700°C required for the Sabatier process[9].

Still, many studies of the biological process in different reactor systems revealed limitations in volumetric methane productivity, most commonly found as a result of limited gas-liquid mass transfer between the introduced gases and the methanogenic archaea in the liquid phase[158]. Due to its very low solubility in water with 0.67 $mmol_{H_2}/(L \cdot bar)$ compared to 16.28 $mmol_{CO_2}/(L \cdot bar)$ at 55°C for CO_2, hydrogen gas-liquid mass transfer is usually the limiting process. It can be described by Eq. 4.2:

$$R_{\mathrm{H2}} = k_{\mathrm{L}}\alpha \ \cdot \ (H_{\mathrm{H_2,cp}} \ \cdot \ p_{\mathrm{H_2,G}} - c_{\mathrm{H2,L}}) \tag{4.2}$$

where R_{H2} [mol/(L · h)] and $k_L\alpha$ [1/h] are the overall volumetric hydrogen mass transfer rate and the volumetric mass transfer coefficient, respectively. The driving force for the hydrogen gas-liquid mass transfer is the gradient between $H_{H_2,cp} \cdot p_{H_2,G}$ and $c_{H2,L}$, where $H_{H_2,cp}$ [mol/(L · bar)], $p_{H_2,G}$ [bar] and $c_{H2,L}$ [mol/L] are the Henry's law constant, the partial pressure in the gas phase and the liquid phase concentration of hydrogen, respectively. To enhance this driving force, $p_{H_2,G}$ can be increased, either by a reactor design allowing locally elevated $p_{H_2,G}$ (e.g. by plug flow conditions)[99] or by operating a reactor at elevated pressure[77]. Furthermore, an improved reactor design, providing optimal phase boundary interface, can strongly enhance the volumetric mass transfer coefficient k as shown in different studies[99,101–103].

Continuously stirred tank reactors (CSTR)[29,72,77,82,94,98,104,108] were the most frequently studied system. In CSTR, optimized agitator-power-per-volume ratio and improved reactor and impeller design led to enhanced gas-liquid mass transfer due to decreased gas bubble size and improved gas distribution. However, upscaling is limited due to the increasing amount of energy that will be required for mixing[86,103]. In hollow-fiber membrane reactors, gas diffusion through a membrane material enhances H_2 gas-liquid transfer[91,93,111]. Still, Luo and Angelidaki[48] found mass transfer resistance due to biofilm formation on the hollow-fiber membrane, leading to increased energy consumption for gas supply. Increased gas retention time and enlarged phase boundary interface is the key to enhance gas-liquid mass transfer in bubble-column reactors[82] as well as in fixed bed reactors[92,96,112]. The energy input required for the gas supply depends on the gas introduction system, but typically no additional mixing is needed in neither bubble-column reactors nor fixed bed reactors.

An improved gas-liquid mass transfer can also be expected by implementing the biological methanation process within an anaerobic trickle bed reactor, as it was already found for syngas fermentation processes[99,102,103,115] as well as for biological gas treatment applications[101,120]. Trickle bed reactors use packing/carrier material that provides a high surface-area per reactor volume to increase the phase boundary interface for mass transfer. This carrier material is only surrounded by a gas phase, which allows controlling the superficial gas velocity independently, in contrast to several other reactor systems (CSTR, fixed bed, bubble column). The energy input for these systems is comparably low, as no mixing and no compressed gas introduction is required. Furthermore, a high height-to-diameter-ratio allows for plug flow conditions and therefore locally elevated $p_{H_2,G}$. However, biological methanation within trickle bed reactors has been investigated only in a few studies and only under mesophilic conditions[80,84,113–115], although substantially higher methane generation rates were found for reactors operated at thermophilic temperatures due to enhanced microbial growth rates[32,56].

Therefore, the aim of the present study was to evaluate process performance and stability of an anaerobic trickle bed system, converting CO_2 and H_2 to CH_4 under thermophilic conditions. The achieved conversion efficiency was compared with previous studies of different reactor systems and different process temperatures. Since little prior knowledge exists regarding the start-up of thermophilic biological methanation reactors[91,92], this study is focusing on i) the performance of a mixed mesophilic inoculum (containing a diverse biocenosis) adapting to thermophilic conditions

and ii) the challenges during start-up without pH control and additional nutrient and trace element supply. Finally, this study aimed at evaluating process stability and performance during dynamic operation, including the potential influence of process by-products, and identifying potential limitations of the technical-scale trickle bed system with regard to opportunities of upscaling this technology.

4.2 Material and methods

4.2.1 Trickle bed reactor setup

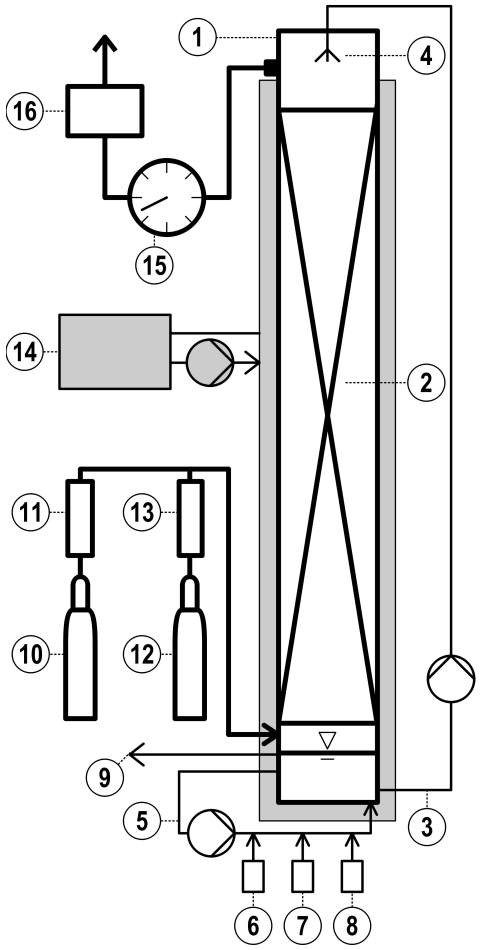

Figure 4.1: Simplified scheme of the studied trickle bed system. (1) trickle bed reactor, (2) packed trickle bed, (3) trickling liquid circuit, (4) spraying nozzle, (5) liquid recirculation, (6) pH buffer solution, (7) sulfide solution, (8) trace element solution, (9) excess liquid withdrawal, (10) H_2 gas bottle, (11) H_2 mass flow controller, (12) CO_2 gas bottle, (13) CO_2 mass flow controller, (14) thermostat, (15) drum gas counter, (16) gas analyzer.

The experiments were performed in a gastight and thermally insulated trickle bed reactor at technical-scale. A simplified process scheme of the trickle bed reactor is shown in Figure 4.1.

The trickle bed was installed in a stainless steel column with a height of 2000 mm and an inner diameter of 215 mm. Two different carrier materials were used for the trickle bed, and placed in four polypropylene net bags, each with a height and diameter of 400 mm and 215 mm, respectively. The two carrier material bags, positioned at the bottom of the trickle bed, contained RFK 25L type carrier with a specific surface area of 313 m^2/m^2 (RVT Process Equipment, Germany). The two upper bags contained Hel-X bio carrier HXF12KLL with a specific surface area of 859 m^2/m^3 (Christian Stöhr GmbH & Co.KG, Germany). The reactor had a packed bed volume of 58.1 L (0.827 $m^3_{\text{gas volume}}/m^3_{\text{trickle bed}}$) at a height-to-diameter ratio of 7.4. The top of the trickle bed column was sealed gastight with a plastic lid containing the connections for off-gas and trickling liquid. Underneath the trickle bed column, a double walled stainless steel column with height and inner diameter of 500 mm and 164 mm, respectively, was flange-mounted and used as trickling liquid reservoir (10.6 L). The trickling liquid was circulated at an average rate of 10 L/h by a membrane pump (ProMinent GmbH, Germany). The trickling liquid was taken from the bottom of the trickling liquid reservoir and distributed on top of the trickle bed by a spraying nozzle (Bete Deutschland GmbH, Germany). The distance of the nozzle above the trickle bed was set in order to achieve a homogeneous distribution of the spraying cone over the entire cross section of the trickle bed. Underneath the flange connection of trickle column and liquid reservoir, an overflow valve was installed to withdraw excess trickling liquid. In order to avoid settlement of solids in the trickling liquid reservoir, trickling liquid was continuously recirculated by a centrifugal pump from the bottom to the top of the trickling liquid reservoir. During the entire experiment, a temperature of 55±1°C was maintained in the trickle column and liquid reservoir. Therefore, tubing, wrapped around the trickle column, as well as the double walled trickling liquid reservoir were connected to a temperature controlled thermostat (Julabo GmbH, Germany). Furthermore, all tubing as well as the reactor were thermally insulated.

H_2 (> 99.9 Vol.%) and CO_2 (> 99.7 Vol.%) were obtained in gas bottles (Air Liquide Deutschland GmbH, Germany) and were provided continuously underneath the trickle bed in countercurrent to the liquid trickling flow at a H_2/CO_2 ratio ranging from 3.75 to 4.00, except for short periods as indicated in sections 3.1 and 3.2. Gas flow rates were controlled for each gas individually by means of mass flow controllers (Brooks Instruments GmbH, Germany).

4.2.2 Inoculation and operating conditions

In order to provide the required anaerobic conditions, the reactor was flushed with a mixture of H_2/CO_2 (80%/20%) for 15 min prior to inoculation. Since there were no suitable thermophilic anaerobic digesters in the vicinity, an anaerobic sludge originating from a mesophilic full-scale wastewater treatment plant (WWTP) digester (Garching, Germany) was used for inoculating the thermophilic reactor. This approach has been proven suitable already in previous studies (e.g.[159]). Immediately after sampling, the sludge was flushed with N_2 for 15 min and stored in a tank under N_2 atmosphere for 60 min at 25°C. The sludge was sieved (100 µm stainless steel sieve) and the sieved sludge was flushed with N_2 for 30 min. Subsequently, 10.6 L of the sieved sludge were applied as inoculum and the experiment was started directly at thermophilic conditions (55±1°C) with a continuous hydrogen feed rate of 1.7 $m^3_{H_2}/(m^3_{\text{trickle bed}} \cdot d)$. Subsequent changes of the hydrogen feed rate throughout the entire experiment are listed in Table 4.1.

Table 4.1: Hydrogen gas feed rate, methane production rate and methane concentration in the product gas for the entire operational period.

Operational period	Hydrogen gas feed rate	Methane production rate	Methane concentration
[d]	[$m^3_{H_2}/(m^3_{trickle\ bed} \cdot d)$]	[$m^3_{CH_4}/(m^3_{trickle\ bed} \cdot d)$]	[%]
1 - 4	1.7	-	-
4 - 7	3.3	-	-
7 - 25	5.2	1.3 ± 0.2	91.8 ± 2.9
25 - 41	6.6	1.5 ± 0.1	71.4 ± 12.1
41 - 49	5.0	1.2 ± 0.1	72.7 ± 14.2
49 - 52	6.6	1.7 ± 0.0	99.1 ± 1.3
52 - 53	8.3	2.1 ± 0.0	95.9 ± 1.0
53 - 55	9.9	2.5 ± 0.1	95.5 ± 5.5
55 - 56	11.95	2.9 ± 0.0	95.9 ± 0.4
56 - 58	13.2	3.3 ± 0.0	95.4 ± 0.2
58 - 73	16.6	4.0 ± 0.2	83.7 ± 12.2
73 - 81	23.2	5.6 ± 0.1	86.1 ± 3.5
81 - 152	19.9	4.7 ± 0.7	87.6 ± 6.6
152 - 179	23.2	5.7 ± 0.1	90.1 ± 6.1
179 - 200	26.5	6.4 ± 1.0	93.7 ± 3.5
200 - 209	29.8	7.4 ± 0.0	95.5 ± 1.8
209 - 226	9.9	2.5 ± 0.2	98.2 ± 1.6
226 - 229	46.3	9.9 ± 1.6	95.6 ± 4.0
229 - 295	43.0	10.3 ± 1.4	89.5 ± 12.6
295 - 299	49.7	12.4 ± 0.1	98.7 ± 0.4
299 - 305	57.1	14.2 ± 0.2	98.3 ± 0.6
305 - 313	62.1	15.4 ± 0.0	98.5 ± 0.7

No nutrient and trace element addition and no pH control were applied initially. At day 39, continuous supplementation with nutrients and trace elements was started (Figure 4.2 - addition (I)) and continued for the remaining experimental period at flow rates of 50 mL/d to 800 mL/d, depending on the hydrogen feed rate. A mineral medium, adopted from[77], with the following composition was used (concentrations per liter): 7.3 g NH_4Cl, 9.0 g Na_2CO_3, 0.75 g EDTA, 0.3 g $MgCl_2 \cdot 6H_2O$, 0.75 g $FeCl_2 \cdot 4H_2O$, 1.5 mg $(NH_4)_6Mo_7O_{24} \cdot 2H_2O$, 0.1 mg $Na_2SeO_3 \cdot 5H_2O$, 9.0 mg $NiCl_2 \cdot 6H_2O$, 1.5 mg $CoCl_2 \cdot 6H_2O$. At day 47, a $Na_2S \cdot 9H_2O$ solution (0.5 M) was added to the trickling liquid to a final concentration of 0.3 mM for the first time (Figure 4.2 - addition (II)). From day 48 on, a Na2S · 9H2O solution (0.5 M) was applied continuously for the remaining experimental period at flow rates of 30 mL/d to 100 mL/d, depending on the hydrogen feed rate. At day 66, the pH value was carefully adjusted for the first time in the experiment by addition of NaOH (0.5 M) to achieve a pH of 7.0 (Figure 4.3 - addition (III)). A K_2HPO_4 buffer solution (1.0 M) was supplemented from day 71 on (Figure 4.3 - addition (IV)), for the remaining experimental period at flow rates of 60 mL/d to 100 mL/d, depending on the hydrogen feed rate.

4.2.3 Monitoring and experimental analysis

Online measurement equipment was installed for pH and temperature monitoring in the trickling liquid (Sensortechnik Meinsberg GmbH, Germany) as well as for temperature and pressure monitoring in the trickle bed (Endress und Hauser, Switzerland). The product gas was collected in

gas-tight bags (Tesseraux Spezialverpackungen GmbH, Germany) from day 7 to 34, and product gas composition was measured with a X-Stream Enhanced Gasanalyzer (Emerson Process Management GmbH & Co. OHG, Germany). CH_4 and CO_2 were measured with non-dispersive infrared (NDIR) sensors and H_2 with a thermal conductivity detector (TCD). From day 35 on, the Gasanalyzer was installed directly at the technical-scale system and the product gas composition was monitored and recorded continuously. Gasanalyzer and pH sensor were calibrated regularly according to manufacturer's instructions. Calibration gases (CH_4 > 99.5 mol%; CO_2 > 99.7 Vol.%; H_2 > 99.9 Vol.%) were obtained in gas bottles (Air Liquide Deutschland GmbH, Germany). Gas production was monitored with a drum-type gas counter (Ritter Apparatebau, Germany) along with temperature and pressure (Endress und Hauser, Switzerland) and translated to standard conditions (0°C; 105 Pa).

TS (total solids) and VS (volatile solids) were measured weekly according to standard methods[160]. The liquid effluent was collected and measured daily in a graduated cylinder. Samples for sulfide and trace element measurements were obtained directly from the trickling liquid. Dissolved sulfide concentrations were measured in a filtered sample (0.45 µm), with a photometric cuvette test (model LCK 053; Hach Lange GmbH, Germany). Samples for trace element measurements were prepared by an inverse aqua regia digestion (20 g sample in 10 mL HNO_3 (65%) and 30 mL HCl (32%) for 90 min at 180°C). The concentrations of trace elements were measured by flame atomic absorption spectrometry (AAS, Varian Spectrometer AA-240FS, Palo Alto, USA) according to the APHA Standard Method 3111. Limits of quantification (in µg/L) have been determined as follows: Ca 100; Co 50; Cu 50; Fe 100; K 20; Mg 10; Mn 50; Na 20; Ni 50 and Zn 20.

4.3 Results and discussion

The present study investigated the start-up and long-term microbial methanation performance of a mixed microbial biocenosis in a thermophilic anaerobic trickle bed reactor.

4.3.1 Reactor operation during start-up (day 1 - 50)

Figure 4.2 shows the development of the methane production, associated product gas quality, gas conversion, and pH value during the start-up (day 1 - 50). In order to identify limiting factors during this phase and to evaluate the nutrient and trace element reservoir capacity of the initial inoculum, no nutrient and trace element addition and no pH control were applied initially (day 0 - 39).

At day 7, stable methane concentrations above 90% at a rate of 1.3 $m^3_{CH_4}/(m^3_{\text{trickle bed}} \cdot d)$ were achieved (Table 4.1). Methane production rate remained at this level during the following 18 days, indicating rapid adaption of the mesophilic inoculum to thermophilic conditions as has also been observed in other anaerobic digestion processes (e.g.[159]). From day 25 until day 47, the gas conversion declined (Figure 4.2), which was shortly interrupted by a three-hour maintenance shutdown (day 34). Reasons that may have contributed at least partially to the observed decline of gas conversion are (i) lack of trace elements, (ii) mass transfer limitations, and (iii) an insufficient sulfur/sulfide supply. Trace element measurements in the trickle medium at day 38 (Table 4.2) revealed no deficit of trace elements. The concentration of critical elements (Co, Fe, Na, Ni, Zn)

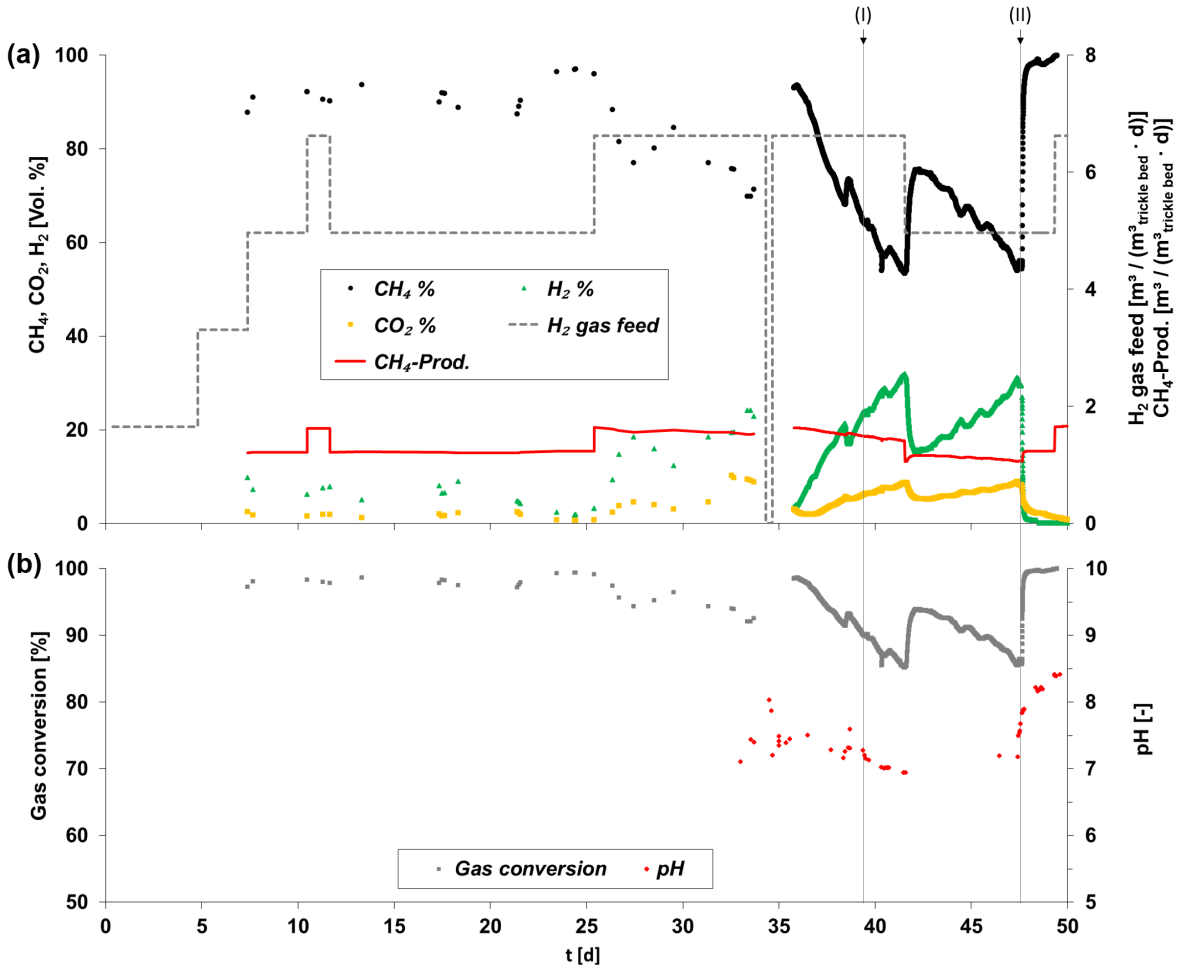

Figure 4.2: Development of (a) H_2 gas feed rate, methane production rate, product gas composition (CH_4, CO_2 and H_2) and (b) gas conversion and pH during operational days 1 - 50. (I) - begin of continuous trace element addition; (II) - begin of continuous sulfur addition.

were above levels that Lebuhn et al.[161] found to be limiting. In order to avoid a potential lack of trace elements during further operation, continuous supplementation with trace element stock solution started at day 39 (Figure 4.2 - addition (I)).

In order to rule out mass transfer limitations, the hydrogen feed rate was reduced to the previous level of 5.0 $m^3_{H_2}/(m^3_{\text{trickle bed}} \cdot d)$ at day 41. Methane concentration above 90% had already been achieved with these settings. However, the decline of gas conversion continued also after this measure.

At day 47, the sulfide concentration in the trickling liquid was measured for the first time in this experiment and was found to be below 0.02 mM (data not shown). Subsequently, a $Na_2S \cdot 9H_2O$ solution (0.5 M) was added (Figure 4.2 - addition (II)), in order to increase the sulfide concentration to 0.3 mM in the trickling liquid. While the hydrogen feed rate remained unchanged, methane concentration immediately recovered from 55% to 96% within six hours after sulfur addition.

The observed declining gas conversion was probably due to a sulfur/sulfide deficit that evolved after start-up. The role of sulfur for the metabolism of methanogenic archaea has already been

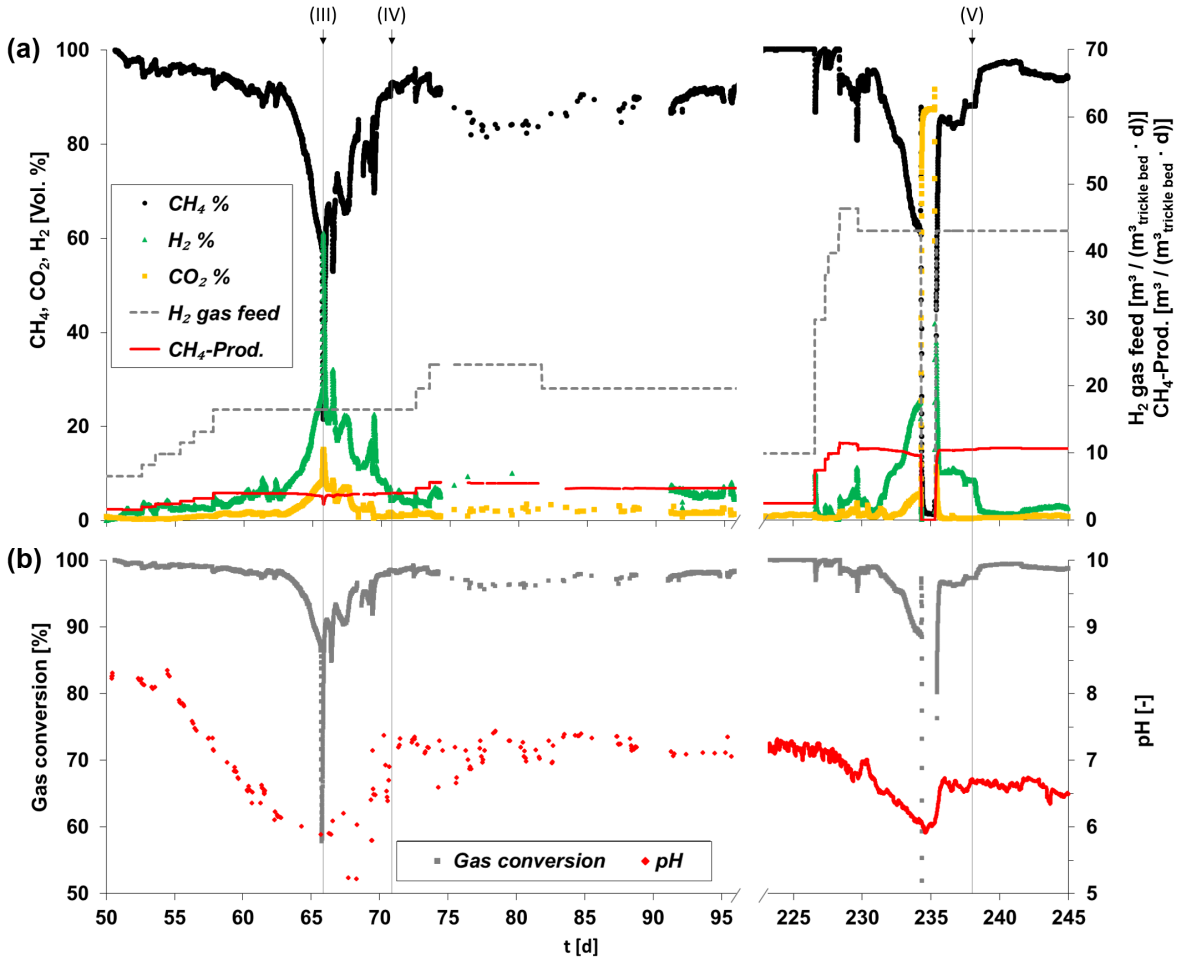

Figure 4.3: Development of (a) H_2 gas feed rate, methane production rate, product gas composition (CH_4, CO_2 and H_2) and (b) gas conversion and pH during operational days 50 - 95 and 225 - 245. (III) - manual pH adjustment; (IV) - begin of continuous pH buffer addition; (V) – adjustment of pH buffer and trace element addition.

described by Liu et al.[162]. The effect that was observed for the mixed thermophilic microbial biocenosis in this study is in accordance with findings of previous studies with pure thermophilic cultures. Rönnow and Gunnarsson[163] already showed increasing methane production and growth rates for *Methanothermobacter thermoautotrophicus* up to sulfide concentrations of 0.3 mM in the medium. Gerhard et al.[106] applied a constant sulfide concentration of 0.05 mM in the medium and observed limitation of growth and methane production for *Methanothermobacter thermoautotrophicus* after sulfide control was switched off. Results from Bernacchi et al.[69] showed a positive influence of sodium sulfide dilution rates on the performance of a pure culture (*Methanothermobacter marburgensis*). Savvas et al.[89], who operated a loop reactor with liquid recirculation but without any nutrient supply for 185 days, however, did not report limitations due to depletion of nutrients. This is in contrast to the findings of the current study. Possibly, the applied reactor design in this study, using a spraying nozzle close to the off-gas outlet to distribute the trickling liquid, might have led to increased loss of sulfide (as H_2S) in the off-gas. If biogas is

Table 4.2: Trace element concentrations measured in the trickling liquid at day 38 compared with typical compositions found by Lebuhn et al.[161]. Alarming concentrations in italics.

Element	This study [mg/kg$_{FM}$]	Trace element concentrations from Lebuhn et al.[161] [mg/kg$_{FM}$]
Ca	265.0	-
Co	0.17	*0.06* - 0.59
Cu	2.33	1.20 - 4.56
Fe	157	8.09 - 1919
K	115.0	-
Mg	56.0	-
Mn	1.6	1.66 - 157
Na	77.0	*10.0* - 295
Ni	4.0	*0.04* - 2.55
Zn	11.0	1.66 - 35.9

kg$_{FM}$: kg fresh matter

used as source of CO_2, the sulfide demand of the microbial community may be satisfied with the H_2S present in the biogas applied, which are typically in a range of 0 - 10,000 ppmv[20].

4.3.2 Process improvement and long-term operation (day 51 - day 313)

During the following experimental period (day 51 - 313), the reactor operation was optimized and the hydrogen feed rate was increased stepwise up to a maximum of 62.1 $m^3_{H_2}/(m^3_{\text{trickle bed}} \cdot d)$. With this setting a volumetric methane production rate of 15.4 $m^3_{CH_4}/(m^3_{\text{trickle bed}} \cdot d)$ with a corresponding methane concentration above 98% was achieved (Figure 4.4, Table 4.1). The capability to deal with fluctuating gas loads was also studied in this operational period, as this is crucial for the future application of biological methanation systems[153]. Declining pH values and decreasing gas conversion were observed after significant gas load increases during two periods (Figure 4.3, days 51 - 75 and days 225 - 245).

From day 50 until day 57, hydrogen feed rate was increased stepwise from 5.0 to 16.6 $m^3_{H_2}/(m^3_{\text{trickle bed}} \cdot d)$ (Figure 4.3a), followed by a slight decrease in gas conversion and a linear decline of the pH value starting at day 55 (Figure 4.3b). When pH value became less than 6.2, gas conversion declined sharply from 98% at day 63 to 85% at day 65. This finding is in accordance with results from Yang et al.[112] and Switzenbaum et al.[164], stating that pH values below 6.2 severely inhibit methanogenesis. Bassani et al.[56] also found reduced methanogenic activity at pH 6.0 compared to 7.0 and 8.0. From day 66 on, the gas conversion recovered after adjusting the pH value to 7.0 with NaOH (Figure 4.3 - addition (III)) and K_2HPO_4 buffer solution (Figure 4.3 - addition (IV)).

The mechanisms that may have contributed at least partially to the observed pH decline are (i) acidification due to initial dissolving of excess CO_2 after increasing the gas feed rate, (ii) reduced buffer capacity due to trickling medium dilution by increased metabolic water production and (iii) production of acetate via homoacetogenesis (Liu et al., 2016).

In order to reproduce the effect of declining pH values following significant increases of the hydrogen feed rate after a low load period, similar process conditions were applied at days

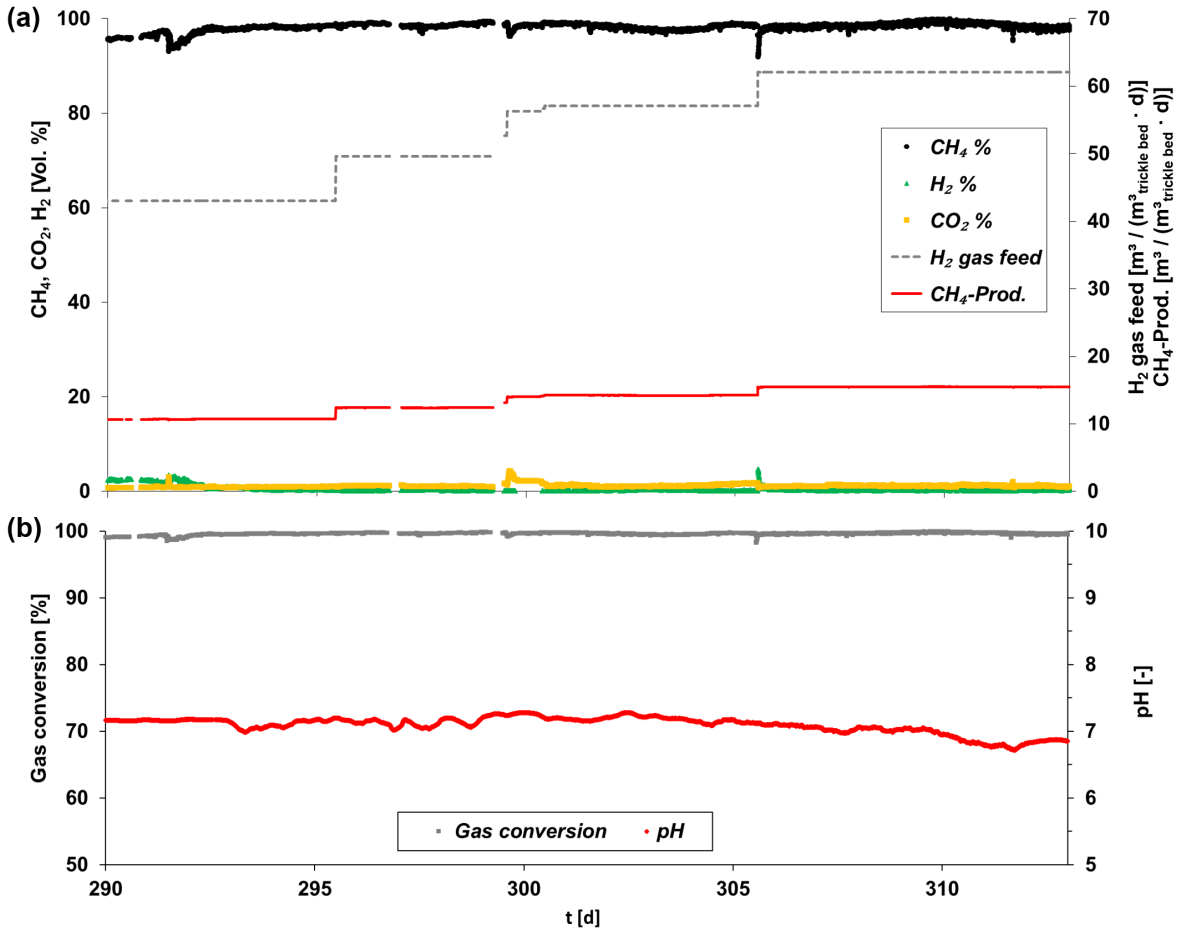

Figure 4.4: Development of (a) H_2 gas feed rate, methane production rate, product gas composition (CH_4, CO_2 and H_2) and (b) gas conversion and pH during operational days 290 - 313.

226-228 (Figure 4.3). Within this time period, the hydrogen feed rate was increased 4.6-fold from 9.9 $m^3_{H_2}/(m^3_{\text{trickle bed}} \cdot d)$ to 46.3 $m^3_{H_2}/(m^3_{\text{trickle bed}} \cdot d)$. In parallel, the addition of buffer, nutrient and trace element solutions was adjusted accordingly, based on the previous experience of reactor performance at a maximum hydrogen feed rate of 30.0 $m^3_{H_2}/(m^3_{\text{trickle bed}} \cdot d)$. Subsequently, a linear decline of pH and gas conversion was observed and could only temporarily be countervailed by reducing the hydrogen feed rate at day 229, but the decline continued at day 231. At a pH value below 6.3, the gas conversion decline rate changed sharply from 2.1%/d to 5.5%/d. This confirmed the observations already made at day 63.

As already mentioned, one reason for the pH decline might be acidification of the system due to dissolved excess CO_2. This hypothesis was tested by stopping the H_2 feed for 24 hours at day 234, while the CO_2 feed (data not shown) as well as the supply with buffer, nutrient and trace element solutions remained unchanged. Due to the lack of H_2, gas conversion stopped immediately and after two hours, the CO_2 concentration within the reactor increased above 85%. Since the pH value even increased during this 24-hour period from 6.0 to 6.4, acidification due to excess CO_2 can be ruled out. When the hydrogen feed was re-started, the gas conversion immediately achieved a level of

96.6%, and exceeded 99% after adapting buffer, nutrient and trace element supply. This adaption of supply rates turned out to be necessary, as no previous long-term experience at hydrogen feed rates above 30.0 $m^3_{H_2}/(m^3_{\text{trickle bed}} \cdot d)$ was available. The observed need of adapted medium compositions after significantly increased volumetric methane productivity is also in accordance with results from Seifert et al.[77].

Moreover, this finding indicates that declining pH values observed after significant increases of the hydrogen feed rate in the present study, are mainly caused by increasing trickling medium dilution due to metabolic water production, according to Eq. (4.1). In previous studies, the impact of liquid medium dilution has not been investigated in detail. Especially for trickle bed systems it is important to consider this effect, as the liquid volume (VLiquid) is significantly smaller compared to the methanation reaction volume (VTrickle bed). The present system has a $V_{\text{Trickle bed}}$ / V_{Liquid} ratio of 5.48, Burkhardt and Busch[80] and Rachbauer et al.[84] reported a ratio of 5.36 and 2.89, respectively. In contrast, in CSTR, fixed bed reactors or hollow-fiber membrane reactors, the methanation reaction volume and liquid volume are comparable (ratio of about 1:1). Therefore, at similar volumetric methane productivity, the liquid medium in trickle bed systems will be diluted more rapidly by the factor of $V_{\text{Trickle bed}}$ / V_{Liquid}, especially after significant gas load increases, e.g. during demand orientated reactor operation. Savvas et al.[86] operated a methanation reactor without nutrient dosage and pH control for 185 days. In contrast to findings in the present study, they observed a 76.4% reduction of mineral content, corresponding to a water production of 1.5-fold of their liquid reactor volume, but they found no limitations due to this medium dilution. A similar dilution of the trickling liquid due to water production and water addition along with buffer/nutrient/trace element supplementation was reached in the present trickle bed system already after 7 days at a hydrogen feed rate above 46.0 $m^3_{H_2}/(m^3_{\text{trickle bed}} \cdot d)$. This indicates that the effect of medium dilution, as observed in the present study, has important implications with regard to the required buffer, nutrient and trace element supply for future dynamic reactor operation. Significant gas load changes will require a very sensitive buffer, nutrient and trace element control especially for trickle bed systems, due to comparatively faster dilution after gas load increases. In previous studies of mesophilic trickle bed systems, buffer, nutrient and trace element media were reported to be occasionally substituted[84] or supplemented proportional to metabolic water production[113]. However, no gas load changes were evaluated in those studies. Potential toxic effects of trace elements have also to be considered when re-adjusting their concentrations. Therefore, the effect of different length of standby periods and reactor restart with different hydrogen feed rate increases needs to be further investigated. In addition, separating metabolically produced water from the trickling liquid may be beneficial to avoid dilution effects, increase biomass concentration (as discussed in section 3.3) and recover trace elements and nutrients. However, further research is required to identify benefits and challenges of potential technologies (e.g. membranes) in combination with microbial methanation systems.

Furthermore, the formation of acetate and possible other acids from H_2 and CO_2 via homoacetogenesis[34] may have contributed to the observed decline of the pH value. The significant increases of the gas feed rate might have led to locally H_2 overload, exceeding the conversion capacity of a relatively low concentration of hydrogenotrophic methanogens present after the previous low gas load period. If H_2 is available in excess at high partial pressure (0.96 bar), homoacetogens can convert up to 40% of H_2 under mesophilic conditions as shown by Liu et al.[67].

When investigating in-situ biogas upgrading with H_2 pulse additions, Agneessens et al.[43] also found increasing acetate formation at a high H_2:CO_2 ratio (10:1), however, along with a pH increase up to 8.4 due to limited availability of CO_2. In the present study, it can be assumed that CO_2 was not limiting in the considered period, due to the stoichiometric H_2:CO_2 feeding ratio of 4:1. H_2 overload of the hydrogenotrophic methanogens may thus have shifted the conversion of excess H_2 partially towards homoacetogenesis, contributing to the pH decrease. In order to prove this hypothesis, microbial population dynamics are currently investigated via molecular biological analyses (manuscript in preparation). Kougias et al.[82] observed a declining pH value along with volatile fatty acid accumulation (mainly acetate) after increased internal gas recirculation, indicating homoacetogenic acetate formation and inhibition of acetoclastic methanogenesis. In contrast, Rachbauer et al.[83] found no difference in the final product ratio of methane and acetate, when investigating the influence of low (0.75 bar) and high (1.50 bar) H_2 partial pressure at mesophilic conditions in batch cultures. Therefore, acetate formation and its influence especially during dynamic process operation with repetitive changes between low (standby) and high (restart) H_2 partial pressure require further investigation.

4.3.3 Potential and challenges of thermophilic anaerobic trickle bed systems

In order to identify potential and challenges of the studied system, it is compared to other biological methanation technologies that achieved methane concentrations in the range required for grid injection (>80 to 100% CH_4,[20]). Particularly in plug flow type reactors, the level of conversion in one reactor section determines partial pressures, gas volume, gas retention time (GRT), and thus the conversion, in the subsequent reactor section, due to a gas volume reduction according to Eq. (4.1). To consider these effects, a comparison should be based on the volumetric methane production rate, linked to the corresponding gas conversion or methane concentration[158]. In contrast, GRT is barely used as a reference value, as the actual GRT cannot be calculated from inlet and off-gas flow rates only.

The maximum methane production rate of 15.4 $m^3_{CH_4}/(m^3_{\text{trickle bed}} \cdot d)$ with 98% CH_4 (Figure 4.4, Table 4.1) in the present study exceeds the values observed in mesophilic trickle bed systems by Burkhardt et al.[95] (3.1 $m^3_{CH_4}/(m^3_{\text{trickle bed}} \cdot d)$ with 96% CH_4) and Rachbauer et al.[84]) (1.9 $m^3_{CH_4}/(m^3_{\text{trickle bed}} \cdot d)$ with 96% CH_4). This is generally in line with findings from previous studies that reported considerably higher methane production rates under thermophilic conditions[51,56,158].

The presented trickle bed system also performed better than a thermophilic hollow-fiber membrane reactor (Díaz et al.,[91]: 79% CH_4 at 9.6 $m^3_{CH_4}/(m^3 \cdot d)$) and a thermophilic fixed bed reactor (Alitalo et al.[92]: 75% CH_4 at 6.4 $m^3_{CH_4}/(m^3 \cdot d)$). This can be due to improved gas-liquid mass transfer in trickle bed reactors[99,102,103,115]. However, the highest methane production rates for a mixed culture reactor were reported by Savvas et al.[89] in a mesophilic biofilm plug flow reactor, achieving 52% CH_4 at 40.0 $m^3_{CH_4}/(m^3 \cdot d)$ and 93% CH_4 at 30.0 $m^3_{CH_4}/(m^3 \cdot d)$. The almost ideal plug flow conditions in their tube reactor (13 mm inner diameter) may have enhanced the gas-liquid mass transfer considerably. In the present study, plug flow conditions might not have been ideal because of a wider inner diameter (215 mm) of the pilot scale trickle bed reactor. This

can explain the lower methane production rate. At comparable methane concentrations, methane production rates achieved by Savvas et al.[89] were only exceeded with pure cultures in thermophilic reactors, e.g. in a CSTR (Peillex et al.,[74]: 96% CH_4 at 285.1 $m^3_{CH_4}/(m^3 \cdot d)$; Seifert et al.,[77]: 85% CH_4 at 137.2 $m^3_{CH_4}/(m^3 \cdot d)$). Martin et al.[72] achieved 85% CH_4 at 9.9 $m^3_{CH_4}/(m^3 \cdot d)$ in a thermophilic CSTR with pure cultures. However, with increasing gas feed rates, methane concentrations decreased to 22% CH_4 at 47.9 $m^3_{CH_4}/(m^3 \cdot d)$. Although vigorous mixing can clearly enhance gas-liquid mass transfer in CSTRs, the parasitic energy required for mixing increases with increasing reactor size[86]. With regard to upscaling of biological methanation technologies, this is an advantage of reactor systems requiring no additional mixing (e.g. trickle bed, fixed bed, and hollow-fiber membrane reactors).

Still, additional research is required for trickle bed reactors to identify the contribution of the biofilm community and the trickling liquid to the total gas conversion and their relevance for process stability. Burkhardt and Busch[80] observed a clear biofilm formation in a mesophilic trickle bed reactor. The biofilm also contributed primarily to the gas conversion in a mesophilic biofilm plug flow reactor studied by Savvas et al.[86] (approximately 4 $g_{VS,liquid}/L$ and approximately 33 $g_{VS,biofilm}/L$). In contrast, no macroscopic (visible) biofilm formation was observed in the thermophilic trickle bed reactor, even after 313 days of operation, while a biomass concentration of 7.0 g_{VS}/L accumulated in the trickling liquid. In comparison, Díaz et al.[91] obtained 9.6 $m^3_{CH_4}/(m^3 \cdot d)$ with 3.6 g_{VSS}/L in a thermophilic hollow-fiber membrane reactor. In the present study, the efficient methanation rate and the increased biomass concentration in the trickling liquid support the assumption that the major part of the gas was converted by hydrogenotrophic methanogenic archaea contained in the trickling liquid while passing the trickle bed. This can be relevant for future applications, as no or only a thin biofilm layer reduces the clogging potential. In consequence, carrier material with higher surface to volume ratios may be used to further enhance overall gas mass transfer and gas conversion rates. In return, this operation mode requires a relatively high biomass concentration in the trickling liquid. In contrast, Seifert et al.[77] showed that a CSTR, already limited by gas-liquid mass transfer, did not benefit from increased total solid concentrations of up to 36 g_{TS}/L. As the present trickle bed system achieved a gas conversion rate of $> 99\%$ at the maximum applied hydrogen feed rate, the system was probably not limited by gas-liquid mass transfer or by biomass concentration yet. As the hydrogen gas feed rate was not further increased during this period, the first limiting factor in the studied system cannot be deduced with certainty. Therefore, further research is required to identify possible maximum gas feed rates and mass transfer limitations of thermophilic anaerobic trickle bed reactors. In addition, the application of membrane techniques, separating metabolically produced water and avoiding wash out of biomass, trace elements and nutrients could further enhance the efficiency of this technology.

4.4 Conclusion

This study has shown the high potential of biological methanation using thermophilic anaerobic trickle bed reactors as a very efficient energy conversion and storage technology. The reactor required no mixing energy or introduction of pressurized gas and can easily compete with the

performance of other mixed culture methanation reactors. Control of pH and nutrient supply turned out to be crucial for stable operation, and was affected significantly by dilution due to metabolic water production, especially during demand-orientated operation. Considering practical applications, inoculation with digested sludge showed high adaptive capacity due to intrinsic biological diversity, however, without macroscopic biofilm formation.

Acknowledgements

The authors gratefully acknowledge the funding of this study by the Bavarian Ministry of Economic Affairs and Media, Energy and Technology (Grant BE/15/04).

5. Anaerobic thermophilic trickle bed reactor as a promising technology for flexible and demand-oriented H_2/CO_2 biomethanation

The capability to deal with fluctuating gas loads is crucial for the future application of ATTBR as a flexible and efficient energy conversion and long-term storage technology[153]. Extended standby periods could affect gas conversion performance, and a decreased gas conversion capacity due to a loss of activity or even decay of the microbial community[155], can be expected as the most severe effect of these standby periods. The following study (**Paper II**) tested **hypothesis #2**:

The standby strategy (temperature and duration) influences the time required to re-attain a stable CH_4 production rate (similar to previous levels) after standby periods.

In **Paper II** we identified critical operational parameters during various reactor standby settings and demonstrated the applicability of an ATTBR as a robust system with very good restart performance, which is suitable for demand-oriented operation within a dynamic energy system. Different combinations of standby period duration and temperature have revealed that the influence of the SP temperature on the restart performance greatly outweighs the standby period duration in the settings studied. A higher remaining biological gas conversion capacity was observed after standby periods at 25°C compared to 55°C, which can be attributed to the impact of significantly higher inactivation rates for thermophilic hydrogenotrophic methanogens at 55°C. Moreover, especially the repetitive effect of 55°C SPs was identified as a critical standby setting. In this respect, the **hypothesis #2 can be accepted**.

This chapter was published in a similar form with editorial changes as:

D. Strübing, A.B. Moeller, B. Mößnang, M. Lebuhn, J. E. Drewes, and K. Koch, "Anaerobic thermophilic trickle bed reactor as a promising technology for flexible and demand-oriented H_2/CO_2 biomethanation", *Applied Energy*, vol. 232, pp. 543–554, 2018.

Author contribution: D. Strübing (70%); A. B. Moeller (10%); B. Mößnang (5%); M. Lebuhn (5%); J. E. Drewes (5%); K. Koch (5%)

Graphical abstract

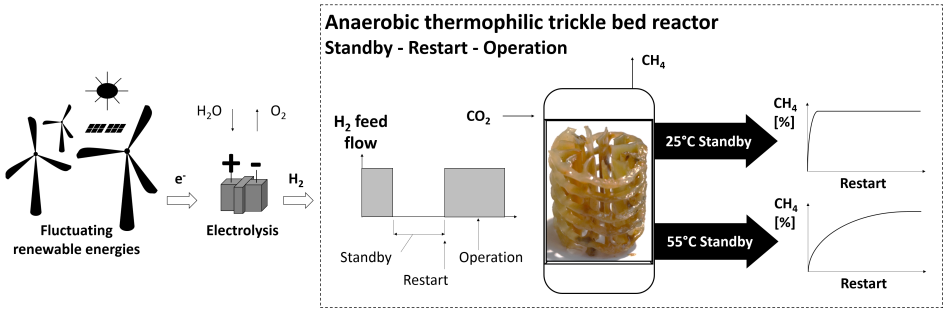

Abstract

Increasing energy production from variable renewable sources, especially wind and solar photovoltaic, requires measures to maintain a stable electricity grid that balances power production and demand. Flexible conversion of excess renewable energy into a storable substitute natural gas via H_2/CO_2 biomethanation may be a suitable approach for tackling this challenge. This study investigated the performance of an anaerobic thermophilic trickle bed reactor (ATTBR) during demand-oriented H_2/CO_2 biomethanation. Different combinations of standby periods (SPs) varying from 1 to 8 days and standby temperatures (25°C and 55°C) as well as their repetitive effect on the biological gas conversion performance were systematically evaluated using a standardized restart procedure. The results revealed that the influence of the SP temperature on the restart performance by far outweighed the length of SP investigated. While the investigated ATTBR represents a robust system with a very good restart performance after 25°C SPs, the repetitive effect of 55°C SPs was in particular identified as a critical standby setting that causes deterioration of the restart performance. This may be attributed to increased inactivation rates for thermophilic hydrogenotrophic methanogens at 55°C, which also influences volatile fatty acid transformation dynamics and leads to substantial propionate accumulation (3,000 mg/L) during 55°C SPs. For the application of ATTBR in dynamic energy conversion and storage scenarios, further research is required to reduce response times and enhance flexibility.

5.1 Introduction

The growing proportion of variable renewable energy sources (VRE), especially wind and solar photovoltaic, increases the challenges of balancing power production and demand[11]. In order to maintain the stability of the electricity grid, flexible energy conversion and long-term storage technologies are required[6,7]. One promising approach for enhancing VRE grid integration while reducing curtailment is the use of power-to-gas technologies. They provide a flexible conversion of excess VRE into a storable gas, which can subsequently be used on demand[12,13]. In a first

step, water electrolysis with excess VRE generates H_2[14], which can then be used as a fuel for transportation[15], as a feedstock for chemicals (e.g. acetate, polyhydroxybutyrate)[16], or can be stored in existing natural gas grids. However, the H_2 content in the gas grid is limited in the range of < 0.5 Vol.% (Sweden, The Netherlands) to < 6.0 Vol.% (France)[18], due to narrow H_2 tolerances of various devices in the natural gas infrastructure, such as piping, gas turbines or combined cycle plants[15,17]. Therefore, the subsequent conversion of H_2 together with CO_2 into high-quality substitute natural gas (second step of the power-to-gas process) according to Eq. 5.1 can generate a long-term energy storage compound, using the huge capacity of the existing natural gas grid infrastructure without injection restrictions[9].

$$4\ H_2 + CO_2 \rightarrow CH_4 + 2\ H_2O \tag{5.1}$$

Substitute natural gas can then be utilized in all natural gas facilities when needed, independent of time and space, or as a fuel in the form of compressed and liquefied natural gas[18,19]. Generation of high-quality substitute natural gas via biomethanation by hydrogenotrophic methanogenic archaea has the potential to become a flexible VRE conversion technology[31,37,38,158]. Due to their tolerance for impurities in the feed gas (e.g. H_2S)[29], hydrogenotrophic methanogenic archaea can use H_2 together with CO_2 emission streams (e.g. from wastewater treatment facilities, biogas plants or other industrial processes) to generate CH_4, reducing the requirements for upstream gas treatment.

Enhancement or isolation of hydrogenotrophic methanogenesis has been investigated in various reactor systems in in-situ and ex-situ biomethanation configurations[31]. Within in-situ biomethanation systems, H_2 is injected directly into an anaerobic digester in order to upgrade the produced biogas by converting a portion of the CO_2 into CH_4 and increase the volumetric methane production of the existing anaerobic digester volume[39,42,43,46,47]. However, accumulation of volatile fatty acids (VFA) resulting from an elevated H_2 partial pressure[42,64] as well as an increased pH due to bicarbonate removal[56] can impact the performance of acidogenesis, acetogenesis, and methanogenesis and thus limit the H_2 injection potential.

Ex-situ biomethanation systems aim at isolating hydrogenotrophic methanogenesis. This allows use of optimal operational conditions for hydrogenotrophic methanogenesis (e.g. pH, temperature, H_2 partial pressure, process design) that may be unfavorable for the upstream processes in conventional anaerobic digesters (hydrolysis, acidogenesis or acetogenesis)[158]. Several ex-situ biomethanation studies with pure[72,76,77] or mixed cultures[79–82,84,89] have shown that the isolated process achieves substantially higher gas conversion rates compared to the in-situ approach, and thus requires smaller reactor volumes.

Gas-liquid mass transfer was found to be the rate limiting step in various in-situ and ex-situ biomethanation systems and different reactor types, and H_2 introduction approaches have been studied with the purpose of overcoming these limitations[31,38]. In a previous study[90], an ex-situ anaerobic thermophilic trickle bed reactor (ATTBR) was shown to be a promising approach for reducing this mass transfer limitation. The studied ATTBR combined the high surface-area per reactor volume of a trickle bed reactor[99,120] with the substantially higher biological conversion activity observed under thermophilic compared to mesophilic conditions[32,56] and achieved comparably high methanation rates (up to 15.4 $m^3_{CH_4}/m^3/d$ with >98% CH_4) with a low parasitic

energy consumption[90].

Based on these results, this study further investigated the performance of an ATTBR with a focus on a flexible and demand-orientated operation. The importance of the flexible operation of microbial power-to-gas systems is emphasized e.g. by Van Dael et al.[23] if it is to be used to convert excess energy peaks from fluctuating VRE generation. The duration of these peaks will depend strongly on future VRE penetration scenarios as well as on the VRE mix, but specifying statements are controversial[135,136]. Thus, the duration of periods without excess VRE resulting in biomethanation standby as well as the required response times are presently not well defined. A study of German meteorological data by Hunecke et al.[137] revealed that maximum duration of periods without sufficient wind velocities and solar radiation for renewable power generation occurring between 2006 and 2016 was two weeks. Moreover, electricity pricing determines the feasibility of biomethanation technologies[23,138–140] and consequently influences potential standby period (SP) duration.

SPs require suitable standby strategies and also affect the ability to re-attain full methanation performance as quickly as possible after restart. Regarding the restart performance of the biomethanation process, it is hypothesized that standby settings influence the restart performance and the time required to re-attain a stable CH_4 production rate similar to previous levels. Savvas et al.[85] observed 80% recovery of substrate gas conversion (according to Eq. 1), within 17 and 24 hours subsequent to SPs of 13 and 45 days, respectively. Graf et al.[147] reported that restart after a 23-day SP was possible without problems using biomethanation lab-scale reactors. However, the authors did not report operational or process performance parameters.

To the authors' best knowledge, no study has thus far systematically investigated the impact of repetitive SP duration on biomethanation systems. Thus, this study aimed at evaluating different combinations of standby durations and temperatures with special focus on their repetitive effect on the biological gas conversion performance of an ATTBR during restart. The resulting implications for ATTBR application in future energy conversion and storage scenarios are evaluated and discussed based on the identified critical standby settings and possible limitations.

5.2 Material and methods

5.2.1 Trickle bed reactor setup

The experiments were performed in a gastight and thermally insulated technical-scale trickle bed reactor. While reactor design, dimensions and technical equipment of the trickle bed reactor have been previously described[90], the following operational parameters differ from the previous study. The trickling liquid was circulated at a trickling rate of 3 L/h. The reactor temperature was maintained throughout the experiment at 55±1°C, except for the 25°C standby periods as described in section 2.2.2. H_2 and CO_2 gas feed rates were controlled for each gas by means of mass flow controllers at a H_2/CO_2 ratio of 3.78. This ratio was determined experimentally during long-term operation and is in a similar range to previous studies[84,118]. Due to a continuous CO_2 loss with the excess trickling liquid (dissolved CO_2, biomass and volatile fatty acids; see carbon balance in section 3.3.1), a H_2/CO_2 ratio of 4.0 does not allow complete H_2 conversion.

Furthermore, trickling liquid distribution (saturated at 20 Vol.% CO_2 in the liquid reservoir) in the reactor headspace (containing > 96 Vol.% CH_4) led to an additional loss of CO_2 with the product gas in the current ATTBR configuration.

5.2.2 Operating, standby and restart conditions

Operating conditions

Anaerobic sludge originating from a mesophilic full-scale wastewater treatment plant digester (Garching, Germany) was used for inoculating the thermophilic reactor. Inoculation and start-up have already been described in detail[90].

During operational periods a mineral medium, adopted from Seifert et al.[77], with the following composition was supplemented at a flow rate of 300 mL/d (concentrations per liter): 7.3 g NH_4Cl, 9.0 g Na_2CO_3, 0.75 g EDTA, 0.3 g $MgCl_2{\cdot}6H_2O$, 0.75 g $FeCl_2{\cdot}4H_2O$, 1.5 mg $(NH_4)6Mo_7O_{24}{\cdot}2H_2O$, 0.1 mg $Na_2SeO_3{\cdot}5H_2O$, 9.0 mg $NiCl_2{\cdot}6H_2O$, 1.5 mg $CoCl_2{\cdot}6H_2O$. $Na_2S{\cdot}9H_2O$ solution (0.92 M) and K_2HPO_4 buffer solution (1.6 M) were supplemented continuously at a flow rate of 150 mL/d each.

Standby procedure

A simplified scheme of the experimental set-up with operational and standby periods, restart phases and the corresponding reactor temperatures is shown in Figure 5.1A. The standby period settings investigated in this study are listed in Table 5.1. Different SP durations were studied at two SP temperature levels (55°C and 25°C). Prior to each SP, 80 L of product gas was collected in a flexible gas bag. At the beginning of the SP, the gas supply was stopped completely, the connections for gas supply and liquid overflow were closed and the flexible gas bag was connected to the product gas outlet. The latter mode of operation prevented the formation of a vacuum in the reactor due to conversion of the remaining substrate gases (H_2, CO_2) as well as the gas volume reduction caused by cooling to 25°C.

For the 25°C SP, the thermostat was set to 25°C but no active cooling was applied and the cooling period ranged from 4 to 5 hours. The trickling pump was switched off during the first 24 hours of each standby but was operated for 4x15 min per day for the longer SP (beginning at the second day of $SP_{4d\text{-}25°C}$, $SP_{8d\text{-}25°C}$, $SP_{2d\text{-}55°C}$) to avoid desiccation of the trickle bed. The addition of mineral medium, Na_2S and K_2HPO_4 solutions was stopped throughout the SP. The experiments were repeated at least three times (triplicate/quadruplicate), depending on the SP setting and the obtained results (Table 5.1).

Standardized restart procedure

A standardized restart procedure was used to assess the effect of SP duration, based on product gas composition and the time required to re-attain CH_4 concentrations above 96% (Table 5.2). For the 25°C SP the thermostat was set back to 55°C 150 minutes prior to restart to ensure a similar restart temperature of 55°C for all experiments. Continuous trickling as well as the addition of mineral medium, Na_2S and K_2HPO_4 solutions were reinstated 30 minutes prior to restart at

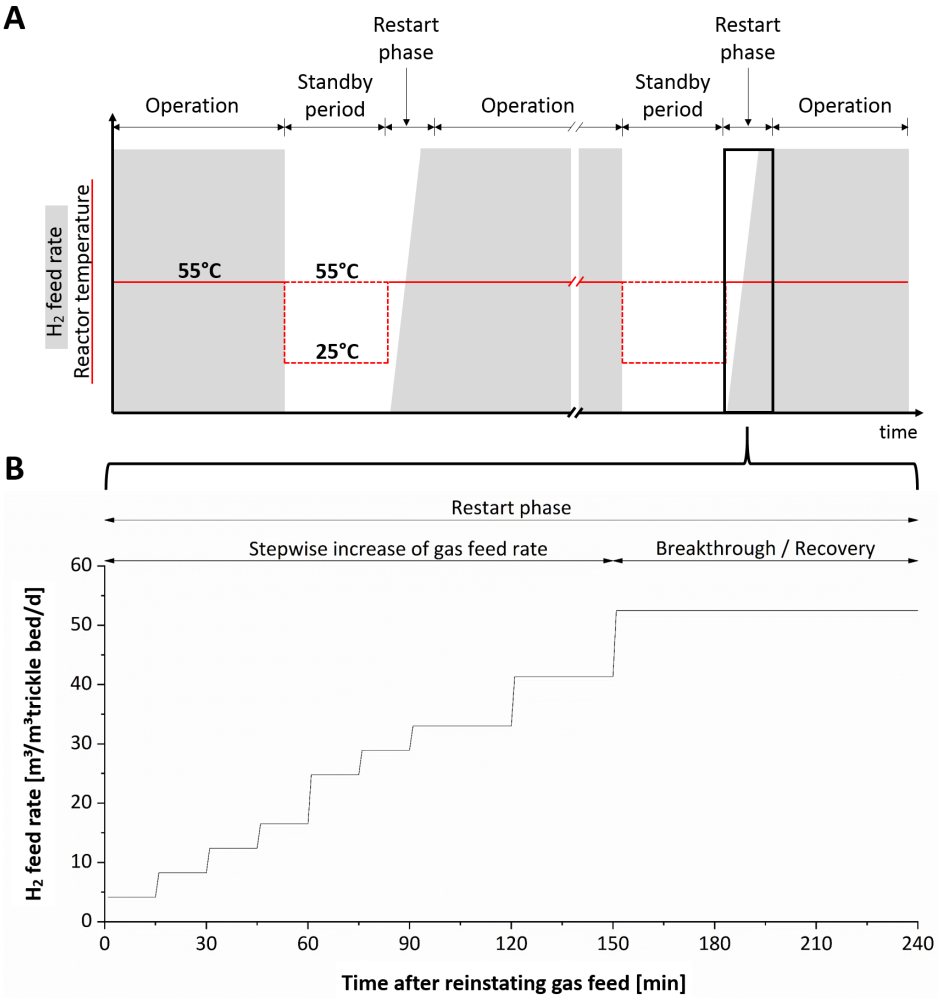

Figure 5.1: Simplified operational scheme (A), showing operational and standby periods, restart phase and the corresponding reactor temperatures as well as the detailed H_2 gas feed pattern (B) for the standardized restart procedure (CO_2 corresponds stoichiometrically to a ratio of H_2:CO_2 = 3.78:1)

previous flow rates. Immediately prior to the restart, the flexible gas bag was disconnected and connections for gas feed, product gas and liquid overflow were opened.

The H_2 gas feed pattern for the restart procedure is shown in Figure 5.1B. The gas feed rate was not immediately adjusted back to the reference level of 52.5 $m^3_{H_2}/m^3_{\text{trickle bed}}/d$, as this would probably have led to an immediate H_2 breakthrough during all tested settings. Instead, a stepwise increase of the gas feed rate was applied to identify different influences of the SP parameters on the restart performance. The reference gas feed rate was reached 150 minutes after restart. As shown in Figure 5.1B, the entire restart phase lasted 150 minutes (reaching of the reference gas feed rate) + 90 minutes (to monitor subsequent breakthrough/recovery). Except for the longer SPs ($SP_{4d\text{-}25°C}$ and $SP_{8d\text{-}25°C}$), an operational period of two to three times the standby period duration was maintained between SPs (Table 5.1) to allow the system to recover.

Table 5.1: Standby period settings.

SP Setting	Duration [h]	Temperature [°C]	Experimental runs [-]	Operational period between SP[1)] [d]
$SP_{1d\text{-}25°C}$	24	25	3	2 / 3
$SP_{4d\text{-}25°C}$	96	25	3	3 / 3
$SP_{8d\text{-}25°C}$	192	25	3	5 / 6
$SP_{1d\text{-}55°C}$	24	55	4	2 / 3 / 2
$SP_{2d\text{-}55°C}$	48	55	4	5 / 5 / 6

[1)] values indicate operational periods between 1st, 2nd, 3rd (and 4th) run

5.2.3 Monitoring and experimental analysis

Online monitoring equipment for pressure, temperature, product gas composition and flowrate of the reactor were identical to those previously described[90]. The volume of liquid effluent was collected and measured daily in a graduated cylinder. During standby periods, the trickling liquid was sampled every 24 hours. Total solids (TS) and volatile solids (VS) were measured according to[165]. Samples for measuring volatile fatty acids (VFA) and ammonium nitrogen (NH_4^+-N) were immediately filtered (0.45 µm). Dissolved NH_4^+-N was measured with a photometric cuvette test (NH_4^+-N: model LCK 302; Hach Lange GmbH, Germany). VFA were measured by ion chromatography (IC) (Model ICS-1000, ThermoFischer, Germany), equipped with an IonPac ICE-AS1 column (4mm) (ThermoFischer, Germany)[166]. A 0.75mM heptafluorobutyric acid solution was used as the eluent (0.16 mL/min) and tetrabutylammonium hydroxide (5mM) as the regenerant for the suppressor (Model AMMS-ICE 300, ThermoFischer, Germany).

5.3 Results and discussion

5.3.1 Reactor performance prior to standby experiments

The present study investigated the biological methanation performance of a mixed microbial biocenosis in an ATTBR during demand-oriented operation. Start-up and process optimization of the ATTBR have already been described in a previous study[90]. Prior to the standby experiments in the present study, the ATTBR was operated under stable conditions for 86 days at H_2 feed rates of 49.6 $m^3_{H_2}/m^3_{\text{trickle bed}}/d$ (for 48 days) and 52.5 $m^3_{H_2}/m^3_{\text{trickle bed}}/d$ during the last 38 days prior to the standby-restart experiments. The latter H_2 feed rate was identical to the maximum H_2 feed rate applied during all restart experiments (Figure 5.1B) and corresponds to 85% of the highest H_2 feed rate previously applied in this system[90]. The steady 86 d operational period was aimed at allowing the microbial community to adapt so that ATTBR operation below the biological gas conversion capacity during the following standby-restart experiments could be avoided. The observed mean CH_4, CO_2 and H_2 concentrations in the product gas were 97.5%, 1.7% and 0.8%, respectively (Table 5.2), at a methane production rate of 13.1 $m^3_{CH_4}/m^3_{\text{trickle bed}}/d$.

Table 5.2: Time periods required to re-attain $CH_4 > 96\%$ after reinstating gas feed (means of all experimental runs) as well as product gas composition, hydrogen conversion efficiency and methane production rate achieved between 230-240 min after reinstating gas feed (means and standard deviation of all experimental runs) and during the 86 day prior steady-state period (means and standard deviation).

SP Setting	Time period required to re-attain $CH_4 > 96\%$ [1] after reinstating gas feed [min]	Product gas composition between 230-240 min after reinstating gas feed			Hydrogen conversion efficiency [%]	Methane production rate [$m^3/m^3_{trickle\ bed}/d$]
		CH_4 [%]	CO_2 [%]	H_2 [%]		
$SP_{1d\text{-}25°C}$	186	97.1 ± 0.2	1.3 ± 0.1	1.6 ± 0.2	99.6 ± 0.1	13.1 ± 0.0
$SP_{4d\text{-}25°C}$	216	96.0 ± 1.3	2.5 ± 1.5	1.5 ± 0.4	99.4 ± 0.1	13.1 ± 0.0
$SP_{8d\text{-}25°C}$	271	94.9 ± 1.5	2.0 ± 0.1	3.1 ± 1.5	99.2 ± 0.4	13.0 ± 0.1
$SP_{1d\text{-}55°C}$	281	94.6 ± 3.4	1.7 ± 0.7	3.7 ± 2.7	99.0 ± 0.7	13.0 ± 0.1
$SP_{2d\text{-}55°C}$	742	72.8 ± 26.1	6.8 ± 5.7	20.4 ± 21.1	89.8 ± 13.4	11.8 ± 1.8
86 d prior steady-state period		97.5 ± 0.9	1.7 ± 0.6	0.8 ± 0.5	99.6 ± 0.1	13.1 ± 0.0

[1] Prerequisite for gas grid injection[18]

5.3.2 Dependency of restart performance on different standby period settings

Suitability of product gas composition as a comparison criterion

In order to evaluate the performance of the ATTBR after SP, a restart procedure with a standardized gas feed pattern (Figure 5.1B) was applied after each standby period. This allowed comparison of the impact of the SP based on the product gas composition during restart, which is the main criterion for subsequent gas grid injection[18]. In this respect, the methane concentration is a suitable parameter because due to the gas volume reduction during conversion (see 5.1), even small decreases in substrate gas conversion result in substantial changes in the product gas composition. For each individual standby-restart experiment, the CH_4, CO_2 and H_2 concentrations obtained during the restart phase (0 240 min; data acquisition every 2 min) were merged into one boxplot for each component (Figure 5.2).

While conversion and uptake of H_2 are almost solely dependent on mass transfer and microbiological conversion capacity, CO_2 concentrations are additionally influenced by solubility effects. H_2 concentrations below 1%, measured at the end of all SPs (Supplementary Material 1), indicated almost complete H_2 conversion, while at the same time, average CO_2 concentrations of 5.0% ($SP_{1d\text{-}25°C}$), 6.0% ($SP_{4d\text{-}25°C}$), 7.5% ($SP_{8d\text{-}25°C}$), 7.4% ($SP_{1d\text{-}55°C}$), and 12% ($SP_{2d\text{-}55°C}$) were observed (Supplementary Material 1). These elevated concentrations may partially result from a CO_2 release from the trickling liquid during SP. Compared to operation with a gas feed at 55°C, the almost complete substrate gas conversion during SP should have shifted the gas composition in the entire reactor towards CH_4 and thus should have decreased the gas-liquid solubility equilibrium of CO_2. While the pH value during the entire standby-restart experimental period (all SP experiments) was 7.0 ± 0.25 (means and standard deviation), slight increases in pH values were measured in the trickling medium within the first hours after the gas feed was ended (Supplementary Material 2). However, these pH changes showed only minor differences between the SP settings, while CO_2 concentrations at the end of the SP differed substantially, especially between $SP_{1d\text{-}55°C}$ and $SP_{2d\text{-}55°C}$. Thus, other processes, e.g. hydrolysis of decayed biomass as well

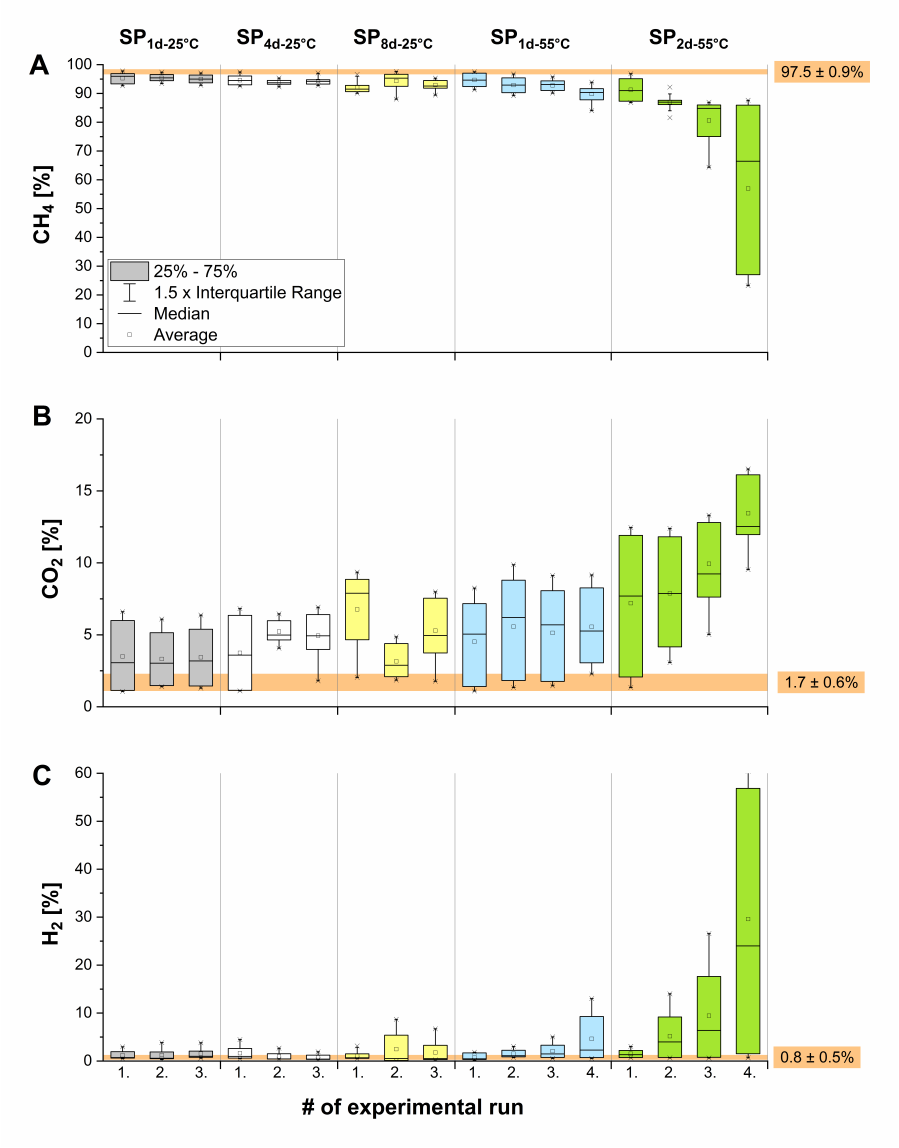

Figure 5.2: Compiled concentrations of CH_4 (A), CO_2 (B) and H_2 (C) during the restart phase for each individual restart experiment. Light orange areas represent the concentrations (means and standard deviation) during the steady-state period prior to the standby experiments.

as subsequent VFA formation and conversion to CH_4 and CO_2, might also have contributed to the observed CO_2 increase. Therefore, CO_2 concentrations alone do not allow drawing direct conclusions on microbiological performances during SP. As CH_4 in the product gas is consequently influenced by CO_2 solubility effects as well as conversion or breakthrough of both substrate gases, the observed H_2 concentration is considered as the main comparison criterion to evaluate the restart performance.

Development of product gas composition during standardized restart procedures

The application of the standardized restart procedure revealed (i) a decreasing performance with increasing SP durations for both investigated SP temperatures as well as (ii) a different restart performance with 25°C and 55°C settings after repetitive SPs.

$SP_{1d\text{-}25°C}$ / $SP_{4d\text{-}25°C}$ / $SP_{8d\text{-}25°C}$: After 25°C SPs, both effects were only slightly pronounced, although SP durations were increased eightfold from 1 to 8 days. During the restart phase, H_2 concentrations in all $SP_{1d\text{-}25°C}$ and $SP_{4d\text{-}25°C}$ experiments remained below 5%, while H_2 increased to a maximum of 8.7% in the 2nd $SP_{8d\text{-}25°C}$ run (Figure 5.2C). During this run, the trickling liquid was accidently contaminated with $\tilde{1}$ liter of Na_2S stock solution on the third standby day. Increased sulfide and/or H_2S levels may have reduced the bioavailability of trace elements (e.g. by sulfide-precipitation[167]) or inhibited methanogenic activity[168] and hence, could have led to slightly increased H_2 concentrations observed during restart (Figure 5.2C). Except for the 2nd $SP_{8d\text{-}25°C}$ run, no repetitive effect on the restart performance was found for all 25°C SP settings. The slight variations in CO_2 concentrations in the 2nd and 3rd $SP_{4d\text{-}25°C}$ run (Figure 5.2B) were due to an incorrect adjustment of the CO_2 gas supply between 120 and 240 minutes after restart. Stable CH_4 concentrations above 96% (criterion for gas grid injection in Austria, Germany and Switzerland[18] were achieved within 186, 216 and 271 minutes after reinstating gas feed in $SP_{1d\text{-}25°C}$ and $SP_{4d\text{-}25°C}$ and $SP_{8d\text{-}25°C}$ settings, respectively (Table 5.2).

In contrast to the 25°C results, a clear impact on the restart performance following 55°C SPs was immediately observed by doubling SP durations from 24 ($SP_{1d\text{-}55°C}$) to 48 hours ($SP_{2d\text{-}55°C}$). A loss of restart performance with an increasing number of experimental runs was revealed for both 55°C SP settings.

$SP_{1d\text{-}55°C}$: Loss of restart performance was less pronounced for the $SP_{1d\text{-}55°C}$ setting. While the first three $SP_{1d\text{-}55°C}$ runs achieved a similar performance to $SP_{1d\text{-}25°C}$ and $SP_{4d\text{-}25°C}$ (Figure 5.2), the last run led to a maximum H_2 breakthrough of 13% (4th $SP_{1d\text{-}55°C}$ run, Figure 5.2C). Surprisingly, overall $SP_{1d\text{-}55°C}$ restart performance results were comparable to $SP_{8d\text{-}25°C}$, based on product gas composition and the time periods required to re-attain $CH_4 > 96\%$ (Table 5.2), although the $SP_{8d\text{-}25°C}$ period was eight times longer than $SP_{1d\text{-}55°C}$.

$SP_{2d\text{-}55°C}$: A clear impairment of the restart performance with an increasing number of repetitions was found for $SP_{2d\text{-}55°C}$. While the 1st $SP_{2d\text{-}55°C}$ run showed comparable performance to the 25°C SP settings ($SP_{1d\text{-}25°C}$ and $SP_{4d\text{-}25°C}$), the following repetitions resulted in a non-linear (exponential) increase of the H_2 (median) concentrations and a maximum H_2 breakthrough of up to 60% in the 4th $SP_{2d\text{-}55°C}$ run (Figure 5.2C). For the 2nd to 4th $SP_{2d\text{-}55°C}$ run, the highest H_2 and CO_2 concentrations of all experiments were found throughout the entire restart phase, resulting in the lowest CH_4 concentration and methane production rate of all tested settings (Figure 5.2, Table 5.2). These findings confirm that the ATTBR is increasingly impaired with every $SP_{2d\text{-}55°C}$ standby, although each SP was interrupted by a 5-6 day operational period. Due to these results, SPs at 55°C were not extended beyond 48 hours.

Dependence of restart performance on standby temperature and duration

The findings outlined above clearly demonstrate that the influence of the SP temperature on the restart performance by far outweighs the SP duration at least for the settings studied. The higher remaining biological conversion capacity after SPs at 25°C compared to 55°C most likely indicates a better conservation and reactivation potential of the methanogenic population at the lower SP temperature. The lower reactivation after 55°C SPs may be attributed to the impact of higher inactivation rates for thermophilic hydrogenotrophic methanogens at 55°C than at 25°C, which agrees well with findings from a previous study[152]. Stams et al.[169] also reported relatively high inactivation rates of 0.48 d^{-1} for two thermophilic hydrogenotrophic *Methanothermobacter* strains. The authors observed that no reactivation of hydrogenotrophic methanogens was possible after as little as two weeks starvation at 55°C, indicating a dead culture.

Nevertheless, the effect of repetitive starvation needs to be considered as shown in the present study. H_2 concentrations in the 1st $SP_{2d\text{-}55°C}$ run were at a similar level as results from 25°C SPs ($SP_{1d\text{-}25°C}$ and $SP_{4d\text{-}25°C}$). Thus, the observed increased performance impairment with the $SP_{2d\text{-}55°C}$ repetition can be traced back to the repetitive starvation effect at 55°C. Here, even operational periods of 5 to 6 days between $SP_{2d\text{-}55°C}$ obviously did not allow for a sufficient recovery of the biological conversion capacity.

In contrast to 55°C, SPs at 25°C can be considered as better conservation/storage conditions. However, the low inactivation rates reported for mesophilic cultures (35-38°C), ranging between 0.004 and 0.034 d^{-1}[43,155,156], are probably not directly applicable for thermophilic hydrogenotrophic methanogens temporarily starving at 25°C. In the present study, gas conversion efficiencies of more than 99% were attained within 4.5 hours even after 8 days of starvation at 25°C. Savvas et al.[85] found gas conversion efficiency recovery of 80% (this corresponds to a CH_4 concentration in the product gas of 45%) in H_2/CO_2 methanation reactors, subsequent to starvation for 13 and 45 days at room temperature, within 17 and 24 hours, respectively. Repetitive starvation effects were not considered. However, these effects remained practically unobserved in the present study after 25°C SPs (Figure 5.2). Whether the different recovery times and levels between 8 days (this study) and 13 days[85] at room temperature were only due to the 5 days extended starvation period or also caused by different reactor settings cannot be indicated with certainty.

Longer starvation periods were investigated only for mixed anaerobic digestion populations. After two months starvation at room temperature (20-25°C), recoveries of specific (acetoclastic) methanogenic activity of 60 - 70% and 58 - 72% were observed for mesophilic[170] and thermophilic anaerobic sludge[171], respectively. Castro et al.[170] also reported a higher recovery of acetoclastic methanogens compared to the entire anaerobic population, indicating a potentially higher susceptibility to starvation of syntrophic bacteria and hydrogenotrophic methanogens compared to acetoclastic methanogens. This is supported by findings from Hao et al.[155] who reported that cell death may have contributed to reduced activity of mesophilic hydrogenotrophic and acetoclastic methanogens by 47±10% and 31±8% respectively, while the remaining fraction could be reactivated after a lag phase. These ratios might also be applied to thermophilic systems because Savvas et al.[85] found only slight differences for the recovery periods of mesophilic and thermophilic microorganisms after starvation. Nevertheless, further study is required to determine to what extent the overall inactivation rate of thermophilic hydrogenotrophic methanogens decreases with a lower

temperature.

5.3.3 Development of volatile fatty acids, and ammonium during standby and operational periods

VFA concentrations were measured throughout the experimental period to further identify mechanisms that cause process disturbance as indicated by formation of certain VFA[132,146].

Volatile fatty acid concentrations during the prior steady-state period

Acetate and propionate concentrations during the prior steady-state period (Table 5.3) were very similar to the concentrations of 600 mg/L and 1,400 mg/L reported by Savvas et al.[85] for comparable H_2 feed rates. In the present study, the elevated propionate concentrations can be attributed to a relatively high hydraulic retention time (5.9 d) combined with a low trickling rate, which may have caused enhanced decomposition of biomass. Although high acetate and propionate levels (6,000 mg/L and 7,400 mg/L) were found to be not inhibitory for *Methanothermobacter thermoautotrophicus* under thermophilic conditions[172], the high acetate, propionate and n-butyrate concentrations in the ATTBR (Table 5.3) as well as the elevated H_2 partial pressure could have further inhibited subsequent VFA turnover as has been shown previously[60,169,172,173]. In addition, as has already been described by Strübing et al.[90] the ATTBR configuration is characterized by a significantly smaller trickling liquid volume in relation to the reaction volume ($V_{\text{Trickle bed}}/V_{\text{Liquid}}$ = 5.5). Thus, at a similar acid formation per reaction volume (e.g. acetate via homoacetogenesis,[42]), higher acid concentrations would be measured in the ATTBR process liquid in comparison with other reactor systems with equal liquid and reaction volumes (e.g. CSTR, fixed bed reactors). However, the ATTBR carbon balance shows that only 1.3% of the carbon input is converted to VFA (Figure 5.3).

Table 5.3: VFA concentrations (means and standard deviation) during the 86 days prior to standby experiments (sampling every 72-96h) and the entire standby-restart experimental period (sampling every 24-48h).

		Prior steady-state period	Standby-restart experimental period	
			25°C SP	55°C SP
Acetate	mg/L	418 ± 180	1,240 ± 332	1,343 ± 309
Propionate	mg/L	1,874 ± 341	2,451 ± 269	2,607 ± 377
iso-Butyrate	mg/L	861 ± 337	802 ± 33 [1)]	712 ± 146
n-Butyrate	mg/L	128 ± 51	448 ± 107	291 ± 91
iso-Valerate	mg/L	n.a. [2)]	1,087 ± 273	1,124 ± 326
n-Valerate	mg/L	n.a. [2)]	76 ± 17	73 ± 14

[1)] Due to overlaying peaks in the chromatograms, iso-butyrate could not be determined in all $SP_{4d\text{-}25°C}$ and $SP_{8d\text{-}25°C}$ standby samples
[2)] Not analyzed

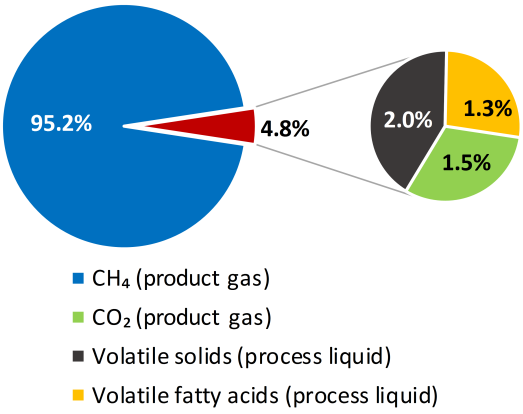

Figure 5.3: Carbon balance of the investigated ATTBR for the 86-day steady-state period. Percentage in relation to the overall carbon input. (Assumptions: H_2:CO_2 gas feed ratio: 3.78; product gas composition and VFA concentration according to Table 5.2 and Table 5.3; process liquid withdrawal: 1.83 L/d; VS: 9.2 g/L with $CH_{1.68}O_{0.39}N_{0.24}$[174])

Volatile fatty acid concentrations during the standby-restart experimental period

VFA means and standard deviations for the following standby-restart experimental period are shown in Table 5.3. Substantially higher levels, particularly of acetate, propionate and n-butyrate were found during this phase compared to the prior steady-state period, indicating a shift or disturbance of conversion pathways induced by the intermittent starvation phases[145,146]. The daily variation of acetate, propionate, n-butyrate and iso-valerate concentration (ΔVFA) are shown in Figure 5.4 for all 25°C and 55°C SPs. Due to the minor changes in all SP settings, n valerate was not further considered as an indicator for process disturbance (Table 5.3).

$SP_{1d\text{-}25°C}$ / $SP_{4d\text{-}25°C}$ / $SP_{8d\text{-}25°C}$: During the applied 25°C SPs, ΔVFA showed only minor changes and no obvious trend. The highest variations were found for iso-valerate with -80 and +90 mg/L/d during the 1st and 2nd $SP_{1d\text{-}25°C}$ runs, respectively. These results indicate only minimal process disturbance and are in line with the very good restart performance found after 25°C SPs.

Considerably higher variations of acetate, propionate and iso-valerate were observed during 55°C SPs, with a changing pattern throughout repetitive SPs for both settings. No clear trend was found in 55°C SPs for n-butyrate variations.

$SP_{1d\text{-}55°C}$: During $SP_{1d\text{-}55°C}$ runs, acetate and n-butyrate concentrations varied only slightly, while with every repetition, an increasing build up of propionate (up to +230 mg/L/d in run 4) and a slightly decreased iso-valerate turnover were found (Figure 5.4). This trend corresponds with the deteriorated H_2 conversion detected for $SP_{1d\text{-}55°C}$ repetitions (Figure 5.2C). As no trickling was applied during $SP_{1d\text{-}55°C}$, these observed VFA changes resulted mainly from transformation processes in the trickling liquid reservoir.

$SP_{2d\text{-}55°C}$: Compared to $SP_{1d\text{-}55°C}$, different VFA transformation patterns were found during $SP_{2d\text{-}55°C}$ experiments. A clear repetitive effect during the course of $SP_{2d\text{-}55°C}$ repetition is indicated by an overall decrease of VFA transformation processes, in particular propionate build up

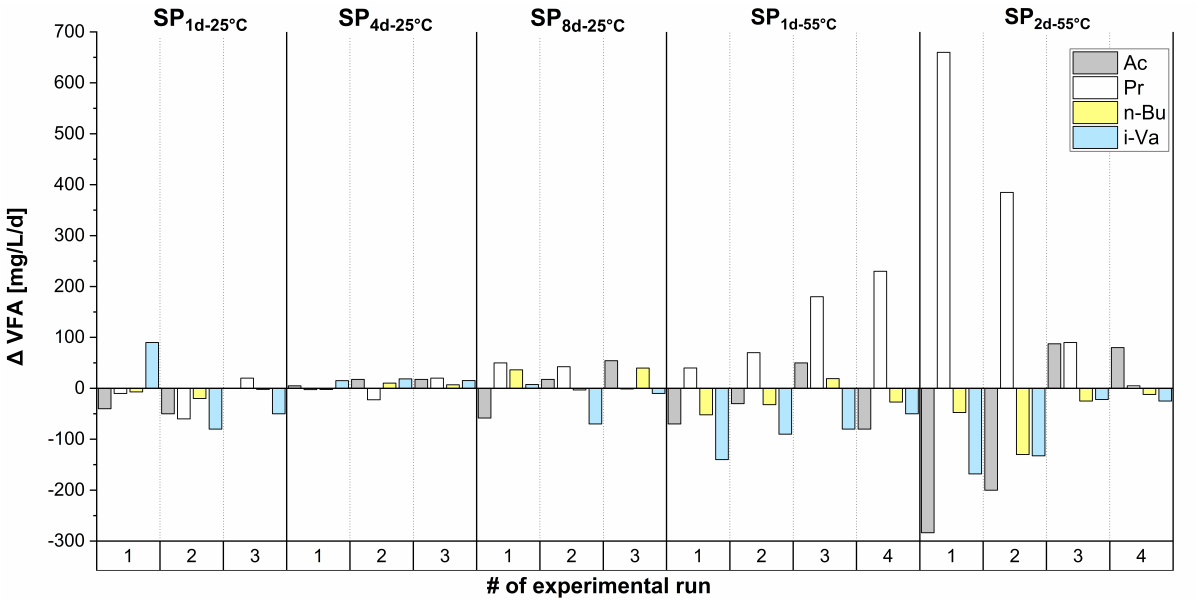

Figure 5.4: ΔVFA during each standby experiment (relative to the concentrations at the beginning of the SP). For $SP_{4d\ 25°C}$, $SP_{8d\text{-}25°C}$ and $SP_{2d\text{-}55°C}$ means for the entire SP are shown. (Ac = acetate; Pr = propionate; n-Bu = n-butyrate; i-Va = iso-valerate)

as well as acetate and iso-valerate turnover (Figure 5.4). The substantial acetate degradation, observed during the 1st and the 2nd $SP_{2d\text{-}55°C}$ run can probably be attributed to acetoclastic methanogenesis. However, syntrophic acetate oxidizing bacteria (SAOB), requiring a low H_2 partial pressure[175,176], may also have contributed. Furthermore conversion of iso-valerate and n-buyrate should only have been possible at the low H_2 partial pressures[177] during SPs. However, iso-valerate is reported as being degraded only to acetate and H_2[68,177,178], and might therefore be ruled out as a propionate source. The accumulated propionate can originate from cell decay and subsequent hydrolysis and acidogenesis processes. In addition, propionate formation from H_2 and (radioactively labeled) $^{14}CO_2$, [1-^{14}C]acetate or [2-^{14}C]acetate was reported by Conrad and Klose for an anaerobic biocenosis, colonizing washed rice roots[179]. Whether this mechanism could be present in the studied ATTBR, cannot be determined with certainty from the obtained data, meaning that the final conclusion about the dominating propionate formation mechanism remains open.

The variation of acetate, propionate, n-butyrate and iso-valerate concentrations (ΔVFA) are shown in Figure 5.5 for the operational periods, subsequent to each 25°C and 55°C SP. During the operating periods following the 1st and 2nd $SP_{2d\text{-}55°C}$ run, a substantial propionate turnover as well as an acetate build-up were found (Figure 5.5). This acetate build-up after restart can possibly be traced back to the parallel propionate conversion as well as to homoacetogenesis[42] and/or a lower SAOB activity due to the increased H_2 partial pressure and the delayed onset of hydrogenotrophic methanogenic activity.

However, VFA transformation activity decreased not only during the 3rd and 4th $SP_{2d\text{-}55°C}$ run (Figure 5.4) but also during the subsequent operational periods (Figure 5.5). These results imply that the ongoing SP repetition not only affected the restart performance, as described for $SP_{2d\text{-}55°C}$ settings above, but also had an increasingly negative impact on all VFA transformation processes

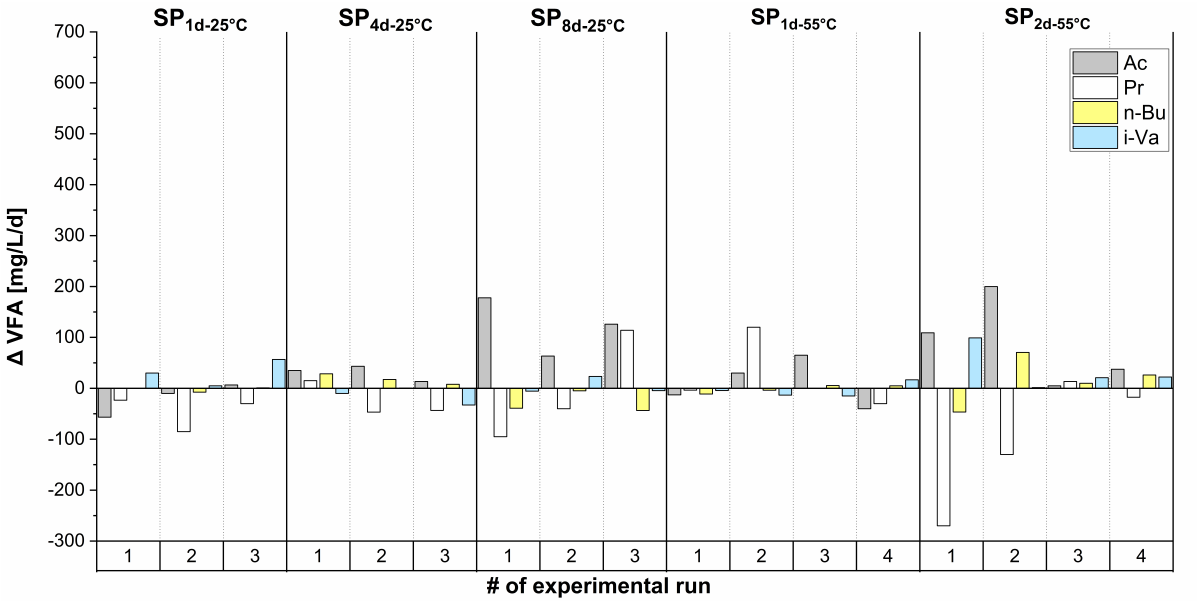

Figure 5.5: ΔVFA during operational periods subsequent to each standby experiment (relative to the concentrations at the end of the SP). (Ac = acetate; Pr = propionate; n-Bu = n-butyrate; i-Va = iso-valerate)

(acidogenesis and acetogenesis).

To further identify the main location of different VFA transformation processes (trickle bed or trickling liquid), the results in Figure 5.6B illustrate ΔVFA for each $SP_{2d\text{-}55°C}$, separately for the first (24h without trickling) and second days (24h with intermittent trickling for 4 x 15 min/d). Throughout day 1 of the first $SP_{2d\text{-}55°C}$ run, VFA varied only slightly, while the substantial changes (of acetate, propionate and iso-valerate) occurred during the following 24 hours. This day-1/ day-2 pattern was visible during the 1st to 3rd runs. Thus, the overall observed VFA variations during $SP_{2d\text{-}55°C}$ can mainly be attributed to the passage through the trickle bed indicating that substantial parts of the biomass, which are able to convert acetate and iso valerate, are immobilized in the trickle bed. Propionate formation also appeared to originate mainly from the trickle bed and was flushed into the liquid reservoir after reinstating the trickling. This assumption is further supported by the comparable day-1/ day-2 pattern for NH_4^+-N release (Figure 5.6A), which can be used as an indicator for decay processes[152], since NH_4^+-N was not added during the SPs.

Future studies might also consider C chain elongation as a potential conversion pathway as this has been reported previously, e.g. for ethanol production from carbon monoxide rich syngas[180] and for biochemical production in open culture systems[181]. Deeper insight might additionally be gained by suppling radioactively labeled CO_2 or alternatively spiking labeled acetate[176,179]. These investigations would require additional molecular biological analyses to identify the microbial groups involved.

In addition, the obtained results revealed that sampling the trickling liquid alone is not sufficient for quantifying inactivation and decay processes in the trickle bed. A different reactor setup with a separated trickle bed and liquid reservoir would be required for more detailed sampling and analysis of the VFA transformation processes.

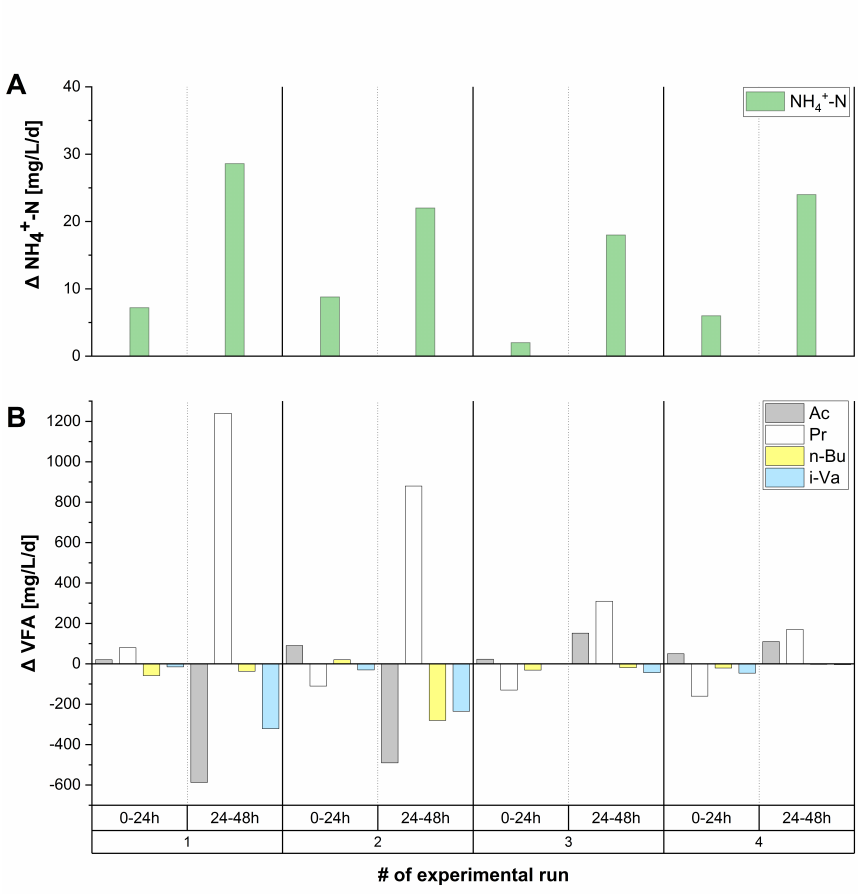

Figure 5.6: Daily ΔNH_4^+-N (A) and ΔVFA (B) (relative to the concentrations at the beginning of the SPs) for $SP_{2d\text{-}55°C}$ standby experiments, separated into 0-24h (no trickling) and 24-48h (trickling for 4 x 15 min/d). (Ac = acetate; Pr = propionate; n-Bu = n-butyrate; i-Va = iso-valerate) (Please note the different y-axis scaling of Figure 5.4 and Figure 5.6B

5.3.4 Implications for ATTBR operation within a dynamic energy system

Conversion efficiency

This study has demonstrated that an ATTBR does provide a flexible technology for conversion of excess VRE into storable methane. A comprehensive energy balance of an ATTBR system in combination with prior electrolysis, was beyond the scope of this study, but this topic has previously been discussed by Patterson et al.[182]. These authors analyzed a full-scale microbial power-to-gas system consisting of polymer electrolyte membrane electrolysis and a biomethanation loop-reactor (introduced by Savvas et al.[86]. They showed that 90% of the overall energy input was required for electrolysis and 10% for biomethanation and gas compression. However, it must be pointed out that 97% of the energy required for biomethanation was mixing energy for H_2 introduction.

In order to identify the specific conversion efficiency of the ATTBR, energy input and output were evaluated. The energy balance of the ATTBR is shown in Figure 5.7. While the ATTBR achieved a gas conversion efficiency of $>$ 99% (Table 5.2), energy conversion is generally limited to 83.2% due

to the lower heating values (LHV) for H_2 and CH_4 (3.00 kWh/$m^3_{H_2}$ and 9.97 kWh/$m^3_{CH_4}$ at STP). One major advantage of the ATTBR is that no reactor content mixing is required. The energy consumption of the trickling pump and the pump for liquid reservoir mixing (to avoid settlement of solids) were neglected due to very small flow rates. Thus, the required energy input for ATTBR reactor operation is mainly driven by the energy consumption for reactor heating. Although Schill et al.[174] observed substantial heat production during exothermic hydrogenotrophic methanogenesis, heat production has not been considered and quantified for the studied ATTBR system. The heat loss by conduction through reactor walls was therefore approximated according to Eq. (5.2)[182]:

$$q_s = U \cdot A_S \cdot DT \tag{5.2}$$

where q_s is the specific heat loss by conduction [kWh/$m^3_{trickle\ bed}$/d], U the heat transfer coefficient [W/m^2/°C], A_S the specific reactor wall surface area [m^2/m^3], and ΔT the temperature difference [K]. With U = 0.7 W/m^2/°C, A_S = 2.3 $m^2/m^3_{trickle\ bed}$ and ΔT = 45K, the resulting specific heat loss by conduction is 1.7 kWh/$m^3_{trickle\ bed}$/d, while the produced methane energy content is 130.6 kWh/$m^3_{trickle\ bed}$/d. The energy balance (Figure 5.7) shows that only 1.1% of the overall energy input is lost as parasitic consumption for reactor operation (heating), demonstrating high efficiency of the system.

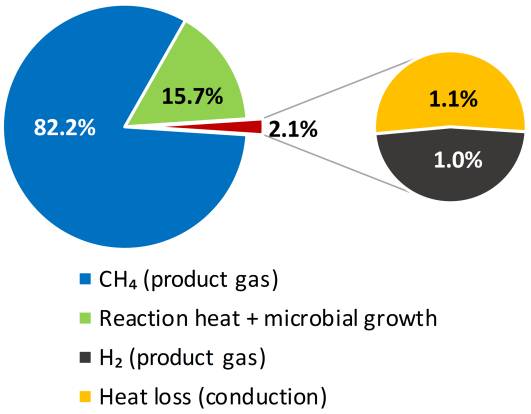

Figure 5.7: Energy balance of the studied ATTBR. Percentage in relation to the overall energy input. (Assumptions: gas conversion: 99%; H_2 feed rate: 52.5 $m^3_{H_2}/m^3_{trickle\ bed}$/d; LHV_{H_2}: 3.00 kWh/$m^3_{H_2}$; CH_4 production: 13.1 $m^3_{CH_4}/m^3_{trickle\ bed}$/d; LHV_{CH_4}: 9.97 kWh/$m^3_{CH_4}$

Improvement of standby and restart strategies

The obtained results are not limited to the studied ATTBR and may be applicable to other biomethanation reactor systems applying mixed microbial communities under thermophilic conditions. Suitable standby strategies are required that provide a compromise between the temperature for high performance operation, the impact of standby periods, and a rapid response during restart.

Electricity pricing influences the economic feasibility of power-to-gas technologies[138,139] and thus, also impacts potential standby durations. Furthermore, future VRE curtailment due to too high excess VRE generation can impact electricity pricing[141,142]. Joos and Staffell[143] showed that the curtailment of wind VRE and its compensation in Germany resulted in a loss of 3.35 TWh and a cost of €325.89 million (average price of €92.32/MWh) in 2016. Converting this amount of curtailed energy via power-to-gas and avoiding compensation would clearly enhance the feasibility of power-to-gas technologies. To evaluate potential standby periods, electricity prices from Germany/Austria in 2017 (15-min-spot-market-prices) were analyzed in accordance with McDonagh et al.[139], although, the effect of increasing electricity prices due to curtailment could not be considered in this evaluation. The derived distribution of continuous time periods below and above defined electricity price levels is shown by way of example in Figure 5.8 (mean and standard deviation in 2017: €34.50±17.69/MWh), only considering time periods longer than two hours. Based on a price limit, these periods would define operational (below price level) and standby (above price level) phases. An operational price limit of for instance €20/MWh would result in maximum standby and operational periods of 168 and 24 hours, respectively, with a total run time of 755 h/a. This would mean that an ATTBR would be idle more than 90% of the time. While this maximum standby duration has already been achieved by the studied ATTBR, it remains to be seen, whether the limited total run time would be sufficient to maintain a stable process. With regard to the stability of anaerobic microbial processes, research clearly shows that dynamic operation as well as changing substrate availability/starvation and temperature in anaerobic digestion systems cause disturbance or shifts from established towards more suitable conversion pathways[132,145,146]. Thus, operational strategies such as maintaining a minimal gas feed even at a high price may be more suitable for enduring high price or low excess VRE availability periods. Whether a reduction of the operational temperature to 25°C is still permissible at such low gas feed rates requires further investigation.

Furthermore, response times of an ATTBR within a dynamic energy system are critical for its applicability. The studied configuration represents a robust system with an excellent restart performance, achieving 99% conversion within 4.5 hours, even after standby of 8 days at 25°C. The chosen restart gas feed pattern in the present study was mainly aimed at visualizing differences between SP settings. According to the results from the first 90 minutes after restart (Supplementary Material 1) which showed only minor changes in the product gas composition, a faster increase in the gas feed rate would also have been possible and the full conversion performance could then even be re-attained within a shorter time period after restart. However, the lower standby temperature requires preheating, which prolongs the total response time. This is critical, particularly when the operation period cannot be predicted in advance. Whether the chosen gas feed pattern for the standardized restart procedure was fully representative for future applications is arguable. For restart or ramping scenarios, the gradients of excess power production from VRE sources, as presented in Huber et al.[144], must also be considered. These gradients will increase with the increasing proportion of wind and photovoltaic power in total power generation (α) as well as with the proportion of photovoltaic power in VRE generation (β). Depending on these parameters, maximum negative gradients (= excess energy) in 2014 for the EU28 were found to be 9.9% (1-hour gradient) and 33.4% (8-hour gradient) of the system peak load[3], but ranged from 10% (1-hour gradient, α=0.1, β=0.2) up to 200% (12-hour gradient, α=0.7, β=0.6) in a modelled

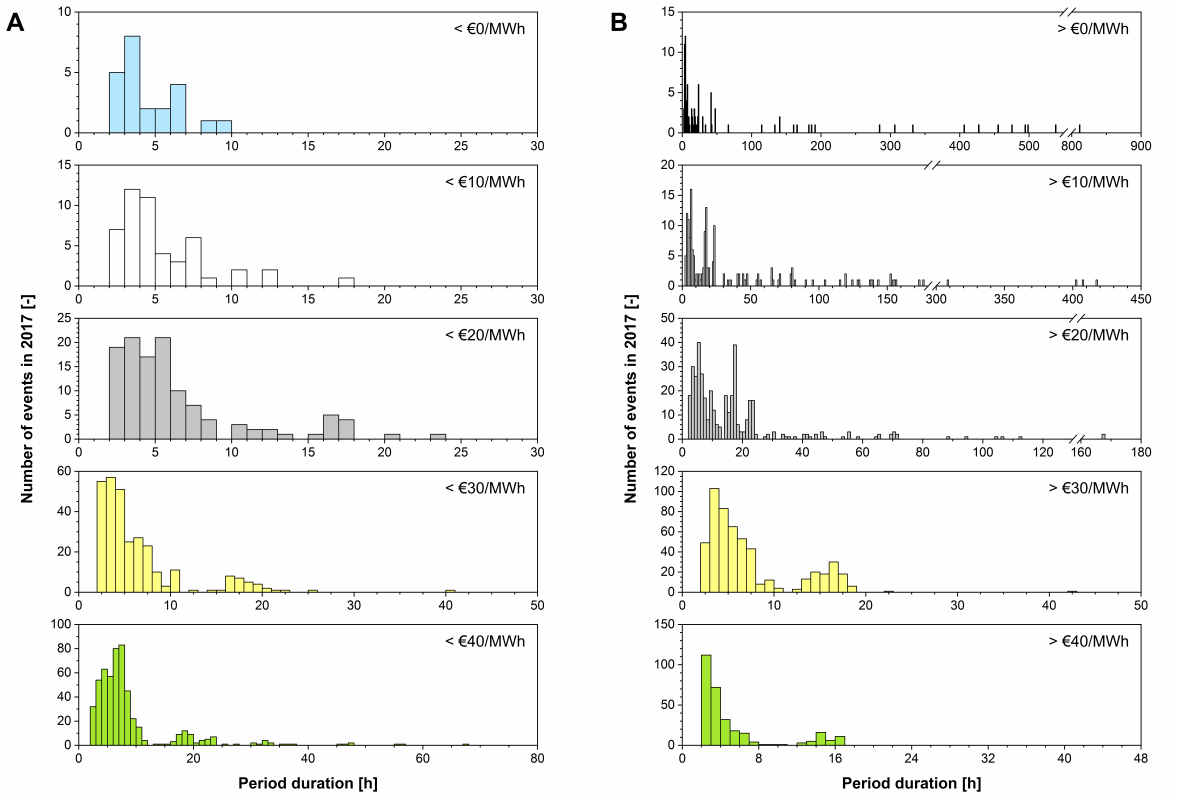

Figure 5.8: Continuous periods of German/Austrian electricity 15min-spot-market prices in 2017 below (A) or above (B) a certain price level. Only periods > 2 hours were evaluated (Data: https://www.exaa.at/download/history/DSHistory2017.xls)

scenario[144]. Although a 1-hour response time cannot be achieved by the ATTBR under optimum standby conditions (25°C), the ATTBR could be applied as a (negative) ramping reserve or supplemental (tertiary) reserve (according to the definition by Ela et al.[183] with non-instantaneous response times. Further improvement of the preheating period as well as identification of the fastest permissible restart gas feed pattern will hence be advantageous.

5.4 Conclusion

This study has demonstrated the applicability of an ATTBR as a robust system with very good restart performance, which is suitable for demand-oriented operation within a dynamic energy system. Different combinations of SP duration and temperature have revealed that the influence of the SP temperature on the restart performance greatly outweighs the SP duration in the settings studied. The higher remaining biological gas conversion capacity after SPs at 25°C compared to 55°C can be attributed to the impact of significantly higher inactivation rates for thermophilic hydrogenotrophic methanogens at 55°C, where especially the repetitive effect of 55°C SPs was identified as a critical standby setting. This effect also influences VFA dynamics and conversion pathways, leading to substantial propionate accumulation especially during 55°C SPs.

At 25°C standby settings, restart strategies that minimize the preheating period as well as shortening the restart gas feed pattern could further reduce response times and improve ATTBR flexibility. Alternatively, maintaining minimal gas feed rates even under economically unfavorable conditions, might be an alternative for enduring high price or low excess VRE availability periods. However, the optimum temperatures for these periods require further investigation.

Acknowledgements

The authors gratefully acknowledge the funding of this study by the Bavarian Ministry of Economic Affairs and Media, Energy and Technology (Grants: BE/15/04 and BE/18/04). We also thank Wolfgang Schröder for performing the VFA analysis.

6. Load change capability of anaerobic thermophilic trickle bed reactors for dynamic H_2/CO_2 biomethanation

The ability to re-attain full methanation capacity after restart is critical for ATTBR application[153]. The limitations of various restart strategies were studied by testing **hypothesis #3**:

ATTBRs have the capability for fast response, re-attaining full CH_4 production rate (at $c_{CH_4} > 96\%$) within 60 minutes after standby periods.

In Paper III we demonstrated the load change capability of an ATTBR while maintaining a high methane content. The application of full load (62.1 $m^3_{H_2}/m^3_{\text{trickle bed}}/d$) after 30-minutes operational breaks was possible almost immediately, while 24-hour interruptions required a 60-minutes stepwise load increase to reactivate the microbial community in the entire trickle bed. The actual gas conversion can be monitored and controlled using the ration of substrate and product gas, allowing suitable load increase strategies that ensure reactivation and avoid short-circuiting. In addition, the trickle bed gas phase provides a high quality gas buffer during the initial load increase phase. Still, even the best performing restart setting achieved only a methane concentration of 94.6±1.6% throughout the entire restart period. Therefore, **hypothesis #3 cannot be accepted**.

This chapter was published in a similar form with editorial changes as:

D. Strübing, A.B. Moeller, B. Mößnang, M. Lebuhn, J. E. Drewes, and K. Koch, "Load change capability of anaerobic thermophilic trickle bed reactors for dynamic H_2/CO_2 biomethanation", *Bioresource Technology*, vol. 289, Article No. 121735, 2019.

Author contribution: D. Strübing (70%); A. B. Moeller (10%); B. Mößnang (5%); M. Lebuhn (5%); J. E. Drewes (5%); K. Koch (5%)

Abstract

Increasing shares of energy production originating from fluctuating renewable sources require measures that are able to balance power production for a stable electricity grid. H_2/CO_2 biomethanation is a suitable approach to convert fluctuating excess renewable energy into the storable substitute natural gas. This study investigated the rapid load change capability of an anaerobic thermophilic trickle bed reactor while maintaining a high methane content. The return to full load (62.1 $m^3_{H_2}/m^3_{\text{trickle bed}}/d$) after a 30-minute operational off-cycle was possible almost immediately, while 24-hour interruptions required a 60-minute stepwise load increase. To accelerate this delayed microbial conversion activity, non-steady state substrate gas conversion can be controlled via substrate and product gas flow rates, allowing to reactivate the entire microbial community and produce high quality product gas. Reactor design might be further improved to avoid short-circuiting and use the entire trickle bed gas phase as high quality gas buffer during initial load increases.

6.1 Introduction

The increasing share of variable renewable energy sources (VRE), especially wind and photovoltaic, calls for highly flexible energy conversion and long-term storage strategies in order to balance power production and demand[9]. The application of power-to-methane technologies can provide flexible conversion of excess VRE into a storable gas product taking advantage of the huge storage capacity of the existing natural gas grid infrastructure[182]. Within the power-to-methane process, H_2 is generated via water electrolysis with excess VRE. From 6.1, H_2 and CO_2 are converted into methane, a high-quality substitute natural gas (SNG), providing opportunities for on-demand use within natural gas facilities or as a renewable fuel (e.g., liquefied and compressed natural gas)[9].

$$4\ H_2 + CO_2 \rightarrow CH_4 + 2\ H_2O \tag{6.1}$$

H_2/CO_2 biomethanation using hydrogenotrophic methanogenic archaea, is a promising approach for flexible SNG generation[31,36,38,50]. In contrast to the chemical-catalytic Sabatier process, hydrogenotrophic methanogenic archaea have a high tolerance for impurities in the substrate gas (SG), such as H_2S and NH_3[9], and can therefore directly use CO_2 emission streams (e.g. from biogas plants, wastewater treatment facilities or other industrial processes). Implementing H_2/CO_2 biomethanation within an ex-situ system allows optimized operational conditions and has been proven to result in high methane production rates employing various reactor systems (e.g.[36,72,74,77]). Still, H_2/CO_2 biomethanation reactors are facing conversion rate limitations due to low H_2 gas-liquid mass transfer rates[31,50]. Among different reactor types (e.g. CSTR, fixed bed reactors, hollow-fiber membrane reactors, bubble column reactors), trickle bed reactors were extensively investigated in order to overcome these mass transfer restrictions[54,81,84,90,113,117,118]. These reactors combine a high surface-area per reactor volume for gas-liquid mass transfer[120] with the benefits of immobilized hydrogenotrophic methanogenic archaea[81]. Anaerobic thermophilic trickle bed reactors (ATTBR) have already achieved comparably high methane production rates at grid injection quality along with low overall parasitic energy consumption[90,117].

Beside enhanced H_2 gas-liquid mass transfer, the ability for flexible conversion of VRE into high quality SNG is an essential criteria for the application of H_2/CO_2 biomethanation systems[23]. In a recent study on standby settings during flexible operation of an ATTBR[117], the upshift from standby to full load was very gentle (> 150 minutes). In comparison, upstream electrolysis technologies, providing H_2 for biomethanation, can respond to VRE availability within seconds to minutes[9]. Rapid load change capability is thus critical for highly efficient H_2/CO_2 biomethanation. In the present study, the capability of a H_2/CO_2 biomethanation reactor to achieve the fastest possible load change has been investigated for the first time. Therefore, an ATTBR was operated alternately between standby and operation for a period of 100 days, applying the optimum standby settings obtained in a previous study[117]. SG conversion efficiency and product gas (PG) quality were evaluated after a rapid return (within 0-60 minutes) to the nominal operating capacity previously achieved for this system (62.1 $m^3_{H_2}/m^3$trickle bed/d)[90]. Consequently, operational control strategies are proposed in order to maintain PG qualities suitable for grid injection (> 95%)[184] also in periods with dynamic operation.

6.2 Material and methods

6.2.1 Trickle bed reactor setup

The experiments were performed in a technical-scale ATTBR with a trickle bed volume of 58.1 L. Design, dimensions, technical equipment, installed online monitoring equipment for pressure, pH, temperature, PG composition and flowrate as well as the reactor start-up have been described previously[90,117]. Compared to these previous studies, the following settings differed in the current study. The process liquid reservoir had a volume of 3.0 L. The SG (H_2/CO_2 ratio: 3.78, cf. Strübing et al.[117]) was introduced above the trickle bed to achieve concurrent gas flow parallel to the process liquid trickling flow. During the operational periods studied, digester supernatant from a mesophilic full-scale wastewater treatment plant digester (31,000 PE Wastewater Treatment Plant Garching, Germany) was supplied as a substitute mineral medium at a rate of 3.0 L/d. To ensure sufficient trace element concentrations, 10 mL of a trace element solution (200×trace element solution as described by Taubner and Rittmann[128]) were added to 990 mL digester supernatant. In addition, $Na_2S{\cdot}9H_2O$ solution (0.92 M) was supplemented continuously as source of the essential nutrient sulfur into the trickling circuit at a flow rate of 150 mL/d.

6.2.2 Standby and restart procedure

Two types of load change experiments (LCE) were performed subsequent to gas feed breaks or standby periods (SPs). In order to evaluate the load change capability after "hot standby" (HSB[184]) the gas feed was terminated for 30 minutes and afterwards ramped up immediately (within 15 seconds) from 0 to 62.1 $m^3_{H_2}/m^3_{\text{trickle bed}}/d$. Load change capability was further investigated subsequent to 24-hour SPs at 25°C, applying five different restart gas feed pattern to re-attain full gas load within 0 to 60 minutes (Table 6.1). A simplified scheme of the corresponding standby/restart procedures along with a detailed description is given in Figure 6.1. The experiments were repeated two to three times in order to reveal adaptation phenomena, and an operational

recovery period of at least two times the SP duration was maintained between SPs. Acetate in the trickling liquid was determined as described in Strübing et al.[117].

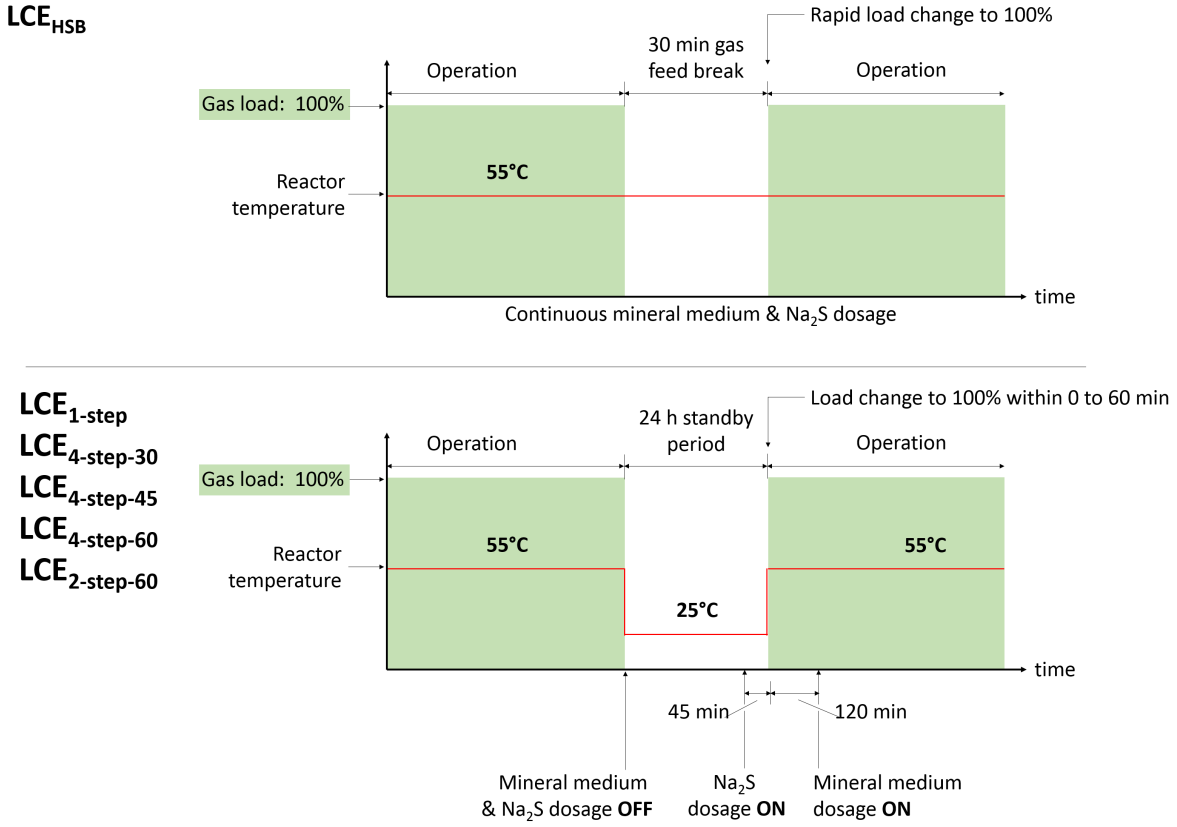

Figure 6.1: Simplified scheme of the standby and restart procedure for the different load change experiments (LCE). For the detailed load change pattern, applied after reinstating gas fed in the different settings, refer to Table 6.1. After terminating the gas feed, a standardized procedure was applied for all experiments to avoid vacuum formation due to conversion of remaining substrate gases[117]. In order to evaluate the load change capability during hot standby (LCE_{HSB}), the gas feed was terminated for 30 minutes and afterwards ramped up immediately (within 15 seconds) from 0 to 62.1 $m^3_{H_2}/m^3_{trickle\ bed}/d$. During 30-minute gas feed breaks, the reactor temperature was maintained at 55±1°C and the trickling pump as well as mineral medium and Na_2S supply remained in operation. Load change capability subsequent to 24-hour SPs at 25°C was investigated by applying five different restart gas feed pattern to re-attain full gas load within 0 to 60 minutes (Table 6.1). Active cooling was applied in order to achieve a standby temperature of 25°C (cf. Strübing et al.[117]) within 30 to 45 minutes. Throughout the SPs, the trickling pump was operated continuously, while neither mineral medium nor Na_2S solution were supplied. The preheating procedure before reinstating the gas feed has been described previously[117]. Na_2S solution was added 45 minutes prior to restart. Mineral medium was supplied only 120 minutes after restart, enabling to determine unbiased pH and acetate values in the trickling liquid reservoir.

6.2.3 Monitoring and experimental analysis

According to Martin et al.[72], the substrate gas conversion efficiency X_{SG} [%] was calculated based on the flow rates of SG Q_{SG} [$m^3/m^3_{trickle\ bed}/d$] and PG Q_{PG} [$m^3/m^3_{trickle\ bed}/d$], and the H_2 content of the SG $c_{H_2,SG}$ [%]:

Table 6.1: Gas feed break conditions, gas load pattern as well as the lowest product gas quality achieved within the first 120 minutes after reinstating gas feed.

Setting	Exp. Runs	Gas feed break Temp.	Duration	Load change pattern to approach nominal operating capacity (62.1 $m^3_{H_2}/m^3_{\text{trickle bed}}/d$)	Restart duration[1)]	CH_4 minimum[2)]	CO_2 maximum[2)]	H_2 maximum[2)]
LCE_{HSB}	2	55°C	24 h	Immediate increase 0 → 100%	0 min	94.3 ± 0.6%	1.9 ± 0.1%	4.8 ± 0.6%
$LCE_{1\text{-step}}$	3	25°C	24 h	Immediate increase 0 → 100%	0 min	72.7 ± 9.2%	5.9 ± 1.4%	21.3 ± 7.9%
$LCE_{4\text{-step-}30}$	3	25°C	24 h	25% (10 min) → 50% (10 min) → 75% (10 min) → 100%	30 min	89.0 ± 6.4%	3.9 ± 1.1%	7.2 ± 5.5%
$LCE_{4\text{-step-}45}$	3	25°C	24 h	25% (5 min) → 50% (5 min) → 75% (35 min) → 100%	45 min	87.3 ± 3.6%	3.3 ± 0.7%	9.5 ± 3.0%
$LCE_{4\text{-step-}60}$	3	25°C	24 h	25% (5 min) → 50% (20 min) → 75% (35 min) → 100%	60 min	94.6 ± 1.6%	2.3 ± 0.3%	3.4 ± 1.3%
$LCE_{2\text{-step-}60}$	2	25°C	24 h	50% (60 min) → 100%	60 min	88.5 ± 3.5%	2.9 ± 0.9%	8.6 ± 2.5%

[1)]Time to return to nominal operating capacity; [2)]Not all minimum/maximum values appeared in parallel; LCE: Load change experiment

$$X_{\text{SG}} = \frac{(Q_{\text{SG}} - Q_{\text{PG}}) \cdot 10,000}{Q_{\text{SG}} \cdot c_{\text{H}_2,\text{SG}}} \tag{6.2}$$

6.3 Results and discussion

LCE were performed in an ATTBR over a 100-day operational period. Steady-state gas conversion (X_{SG}) above 99% resulted in a methane production rate of 15.5±0.1 $m^3_{CH_4}/m^3_{\text{trickle bed}}/d$ and a PG composition of 98.1±2.1% CH_4, 0.9±0.5% CO_2 and 1.1±1.5% H_2 (values excluding load change phases). As not all LCE re-attained a gas conversion above 99% within 120 minutes, a X_{SG} of 98% was used for comparison of the different settings.

6.3.1 Load change capability

Hot standby LCEs were performed by increasing the gas feed immediately from 0 to 62.1 $m^3_{H_2}/m^3_{\text{trickle bed}}/d$ (= 100% gas load) after a 30-minute gas feed break at 55°C (LCE_{HSB}, Table 6.1). X_{SG} above 98% was re-attained after 26±1 minutes (Figure 6.2a). The H_2 maximum values (4.8±0.6%) were reached 37 minutes after the load change, while CH_4 dropped to 94.3±0.6% (Table 6.1) at the same time. In contrast, the CO_2 concentration increased slightly during the first 15 minutes but decreased afterwards to a minimum of 0.8±0.0% (Figure 6.2b). The initial CO_2 increase may have been partially caused by liquid-to-gas CO_2 release during the gas feed break[117], resulting in a pH increase in the trickling liquid reservoir from 8.0 to 8.1 during the first 30 minutes after restart. The delayed pH response can be explained by a lagged and attenuated response of pH monitoring in the trickling liquid reservoir, compared to the actual conversion in the trickle bed. While the released CO_2 partially left the system with the PG after restart, re-balancing the $CO_{2\ (gas)}/CO_{2\ (liq.)}/HCO_3^{-}{}_{(liq.)}$ equilibrium may have led to locally reduced CO_2 availability for H_2 conversion, resulting in the observed CO_2 and H_2 concentration pattern. In comparison, limiting effects on hydrogenotrophic conversion during in-situ biomethanation have already been observed for CO_2 head space concentrations below 12% by Agneessens et al.[43].

Compared to LCE_{HSB}, the immediate load change from 0 to 100% after 24-hour SPs at 25°C ($LCE_{1\text{-step}}$) resulted in the lowest PG quality of all studied settings (Figure 6.2d, Table 6.1). X_{SG} above 98% was re-attained after 65±3 minutes, which was substantially more slowly compared to

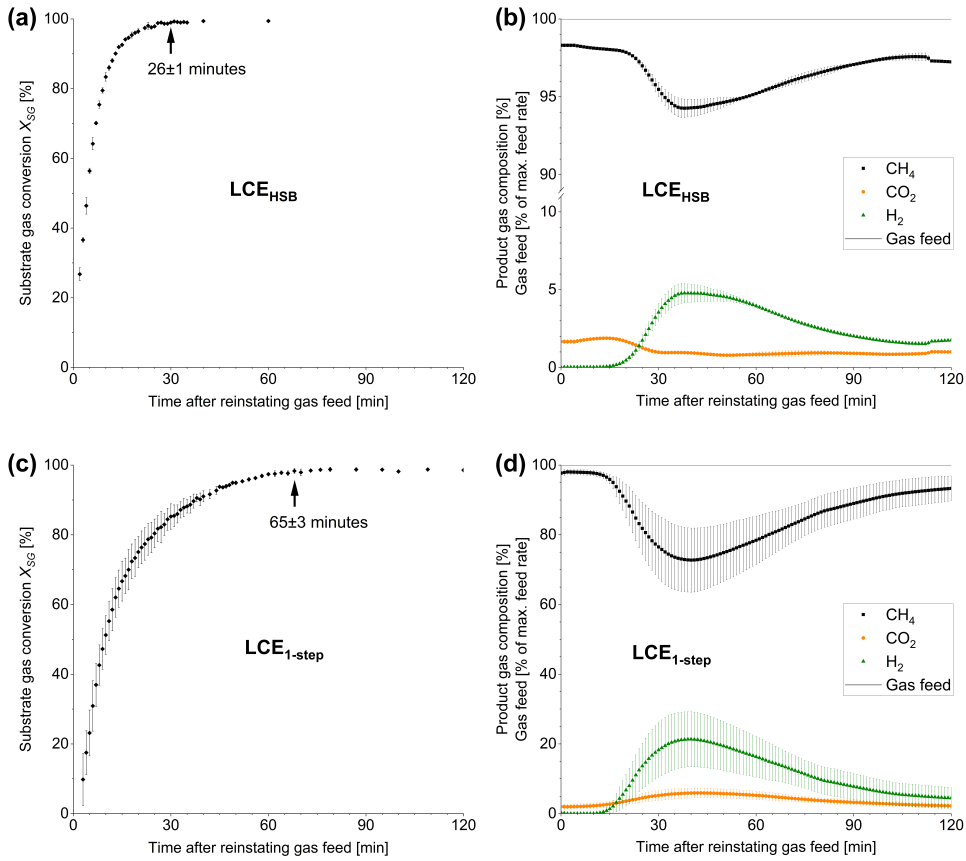

Figure 6.2: Substrate gas conversion efficiency (means ± standard deviation) and product gas composition (CH_4, CO_2, H_2: means ± standard deviation), respectively, after reinstating the gas feed: (a) and (b): LCE_{HSB} experiments (n=2); (c) and (d): $LCE_{1\text{-step}}$ experiments (n=3). For the detailed load change pattern refer to Table 6.1. Arrows in substrate gas conversion plots indicate a conversion level of $> 98\%$ (LCE: Load change experiment)

LCE_{HSB} (Figure 6.2a, c). In contrast to LCE_{HSB}, the observed breakthrough of H_2 and CO_2 in $LCE_{1\text{-step}}$ occurred almost stoichiometric proportional (Figure 6.2d), along with a temporary decrease of the trickling liquid pH from 7.7±0.1 to 7.4±0.1 for about 90 minutes. This decrease may have been partially caused by CO_2 accumulation in the trickling liquid due to the initially reduced conversion efficiency (microbial delay), which superimposed the effect of liquid-to-gas CO_2 release as observed in LCE_{HSB}. Furthermore, an increase of the acetate concentration in the trickling liquid from 154±28 mg/L to 352±37 mg/L within the first 15 minutes after restart indicates homoacetogenic acetate formation due to H_2 overload[42], which may have additionally contributed to the pH decrease. Still, this initial microbial delay appeared to be only a temporal effect, most probable induced by the low standby temperature[132,170]. From the time intervals to re-attain $X_{SG} > 98\%$ in LCE_{HSB} (26±1 minutes) and $LCE_{1\text{-step}}$ (65±3 minutes), an additional microbial delay due to the 24-hour SP (25°C) of approximately 39 minutes may be estimated.

Assuming full SG conversion during gas feed breaks/SPs[117] and ideal plug-flow conditions[184], the entire trickle bed gas volume (48 L, Strübing et al.[90]) can be considered as high quality PG buffer

against SG breakthrough. However, during the immediate load change settings the breakthrough of H_2 and CO_2 ($LCE_{1\text{-step}}$) or mainly H_2 (LCE_{HSB}) was already observed when only 33 L ($LCE_{1\text{-step}}$) and 24 L (LCE_{HSB}) of PG had left the reactor. This indicates short-circuiting through the trickle bed during the initial rapid load increase, probably induced by insufficient distribution of SG above the trickle bed or by locally clogged sections. Temperature differences between the gas in the reactor and incoming SG may have amplified this effect. Breakthrough as a result of density differences (lighter SG) can probably be neglected due to the top-to bottom gas flow direction. While short-circuiting effected the observed PG quality, its impact on X_{SG} cannot be deduced with certainty due to different SG distribution within the trickle bed.

Compared to $LCE_{1\text{-step}}$, the extension of the restart phase by four-step load change patterns, reaching 100% load within 30 minutes ($LCE_{4\text{-step-30}}$) and 45 minutes ($LCE_{4\text{-step-45}}$) generally led to an improved PG quality (Table 6.1). The total gas load during the first 30 minutes after restart was 25% higher for $LCE_{4\text{-step-45}}$ compared to $LCE_{4\text{-step-30}}$, but it was balanced again after 45 minutes between the two settings (Table 6.1). Despite the later return to full load, $LCE_{4\text{-step-45}}$ resulted in an earlier SG breakthrough (Figure 6.3a, c) and slightly worse PG quality (Table 6.1). These results show that especially during the first 30 to 45 minutes, the initially reduced microbial conversion capacity and the trickle bed PG buffer limit the permissible total gas load, and full load cannot be re-attained within 45 minutes with the aspired PG quality.

Beside microbial delay, an additional spatial reactivation effect along the gas flow path was observed by comparing the return to full load after 60 minutes in $LCE_{4\text{-step-60}}$ and $LCE_{2\text{-step-60}}$. The four-step pattern ($LCE_{4\text{-step-60}}$) resulted in PG qualities even comparable to LCE_{HSB} (Figure 6.3b, Table 6.1). In contrast, $LCE_{2\text{-step-60}}$ allowed 60 minutes of adaption at 50% gas load (Table 6.1). Conversion above 98% was re-attained after 33±1 minutes and CH_4 and H_2 concentrations within the first 60 minutes remained at 98.2±0.3% and 0.9±0.2%, respectively (Figure 6.3d). However, despite a 20% reduced total gas load compared to $LCE_{4\text{-step-60}}$ within the first 60 minutes, $LCE_{2\text{-step-60}}$ resulted in a lower PG quality after the load change to 100% (Figure 6.3b,d, Table 6.1). This indicates that probably the major part of the SG was already converted upstream, due to the lower total gas load within the first 60 minutes in $LCE_{2\text{-step-60}}$, as compared to $LCE_{4\text{-step-60}}$. Consequently, downstream parts of the microbial trickle bed community were exposed to less H_2/CO_2 and thus not well prepared to convert full load after 60 minutes. This is generally in line with results from Dupnock and Deshusses (2017), who observed 88% of the totally achieved conversion in a trickle bed already after 50% of the reactor volume, as conversion rates decrease considerably along the reaction path due to their dependence on the partial pressure of SG.

6.3.2 Implications for dynamic operation while maintaining grid injection qualities

The results of this study reveal the capability of the investigated ATTBR to return to 100% load almost immediately after short operational interruptions (LCE_{HSB}), while 60 minutes were required subsequent to 24-hour SPs ($LCE_{4\text{-step-60}}$). Although the latter result is considerably faster compared to a previous study (186 minutes, Strübing et al.[117]), the ATTBR did not achieve response times of seconds to minutes as provided by electrolysis units[9].

The present study revealed the following aspects that require further improvement in order to

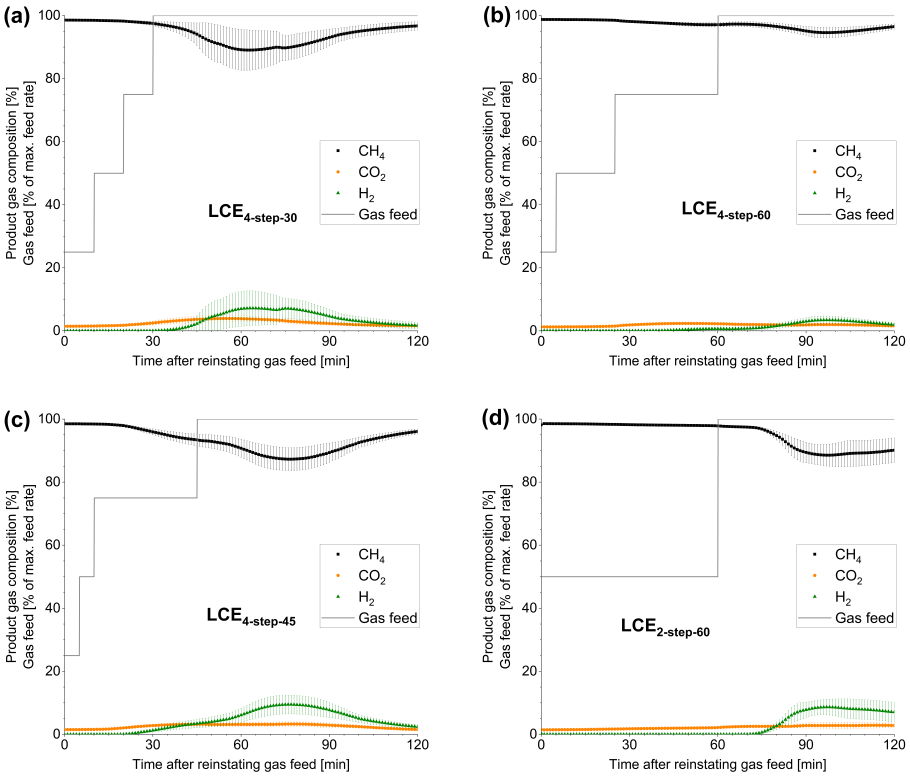

Figure 6.3: Product gas composition (CH_4, CO_2, H_2: means ± standard deviation) after reinstating the gas feed: (a) $LCE_{4\text{-step-}30}$ experiments (n=3); (b): $LCE_{4\text{-step-}60}$ experiments (n=3); (c): $LCE_{4\text{-step-}45}$ experiments (n=3); (d): $LCE_{2\text{-step-}60}$ experiments (n=2). For the detailed load change pattern refer to Table 6.1. (LCE: Load change experiment)

achieve optimum X_{SG} and grid injection qualities: i) delayed microbial conversion activity, ii) sufficient microbial reactivation along the gas flow path and iii) short-circuit flow through the trickle bed.

i): Suitable standby strategies[117] could already reduce the extent of delayed microbial conversion activities that have been observed in biomethanation systems[81,85]. In order to further adapt the load increase strategy to delayed microbial conversion, monitoring the current gas conversion efficiency can be applied, using Q_{SG} and Q_{PG} as monitoring parameters. Due to the volume reduction of SG during conversion (Eq.6.1), Q_{SG} and Q_{PG} allow direct calculation of the actual gas conversion within the reactor also in a non-steady state (Eq.6.2). This allows operating any biomethanation system at a desired gas conversion efficiency (e.g. $X_{SG} > 98\%$) by adjusting the SG feed. Due to different gas hold-up properties of various reactor types[184], PG quality monitoring may respond delayed to load changes and thus, should only be applied as a secondary control parameter.

ii): In order to reactivate the entire microbial community, biomethanation reactors with intense backmixing, such as CSTR or bubble column reactors[9,184]), equally distribute SG immediately after restart, independent of the actual load level. In contrast, sufficient SG exposure of an immobilized microbial community (trickle bed reactor, fixed bed reactor) can easily result in SG breakthrough (cf. $LCE_{1\text{-step}}$). A suitable approach for the latter systems may be the combination of an initial full

load pulse, which is stopped just before SG breakthrough (as observed in $LCE_{1\text{-step}}$), and subsequent controlled operation at the desired gas conversion level (as described above).

iii) Further optimization of the ATTBR reactor design (e.g. gas introduction and distribution, gas pre-heating) is required in order to improve plug-flow conditions and overcome the observed short-circuiting through the trickle bed. This would allow using the entire PG buffer, which is theoretically available in the ATTBR trickle bed volume during load increases. Due to the high gas hold-up and plug-flow conditions[120,184], the ATTBR releases PG first, while SG is either converted or leaves the trickle bed considerably delayed. In contrast, reactor types with a liquid reaction volume (e.g. CSTR or bubble column reactors) release unconverted SG earlier due to a substantially lower gas hold-up and backmixing effects[184].

In order to further improve the load increase after SPs, pressurized operation of biomethanation reactors[72,77,118] generally allows to feed SG without releasing PG until a desired reactor pressure is re-attained. Due to the large gas hold-up, especially trickle bed reactors might further benefit from this operational mode due to additionally generated gas feed capacity.

6.4 Conclusion

This study demonstrated the load change capability of an ATTBR while maintaining a high methane content. The application of full load (62.1 $m^3_{H_2}/m^3_{\text{trickle bed}}/d$) after 30-minute operational breaks was possible almost immediately, while 24-hour interruptions required a 60-minute stepwise load increase. To accelerate this delayed microbial conversion activity, the actual gas conversion can be controlled by monitoring Q_{SG} and Q_{PG}, ensuring reactivation of the entire microbial community and high quality PG. Reactor design might be further improved to avoid short-circuiting and use the entire trickle bed gas phase as high quality gas buffer during the initial load increase.

Acknowledgements

The authors gratefully acknowledge the funding of this study by the Bavarian Ministry of Economic Affairs, Regional Development and Technology (Grant: BE/18/04).

7. Overall discussion and future research needs - Implications and constraints for application and upscaling of ATTBR for H_2/CO_2 biomethanation

Along with a rising availability of fluctuating renewable energy sources, the increasing research interest in BM technologies demonstrates their potential to become a flexible PtG technology that converts excess VRE into high-quality SNG and uses the huge capacity of the existing natural gas grid infrastructure[31,36–38]. Various BM concepts have been studied to overcome H_2 gas-liquid mass transfer limitations, while achieving the highest methane production rates with H_2 introduction by energy-intensive stirring in CSTR[50].

This study was initiated to develop and test an alternative and efficient reactor concept with low H_2 gas-liquid mass transfer restrictions and simultaneously low parasitic energy consumption, suitable for flexible on-demand BM. ATTBR were identified as a potentially suitable reactor concept and two detailed research objectives were derived to explore their capability for efficient BM. Three hypotheses (cf. Chapter 3) were developed and tested by a series of experiments with results being presented in Chapters 4-6.

The first research objective aimed at proofing the ATTBR concept by combining the possible mass-transfer advantages of trickle bed systems with the potential enhancement of biological conversion of CO_2 and H_2 to CH_4 at thermophilic conditions. An ATTBR at technical-scale was set up, inoculated with sewage sludge from a local wastewater treatment plant digester and operated at 55°C at ambient pressure for more than 300 days (cf. Chapter 4).

Besides proving the suitability of the ATTBR concept, its capability for flexible and demand-oriented H_2/CO_2 BM is crucial for the future application. In order to apply ATTBR in any energy conversion and storage scenario, different combinations of standby and restart strategies need to be evaluated. The impact of SP durations and temperatures on the restart performance was investigated within the established ATTBR technical-scale set-up and operational constraints and suitable strategies to manage SPs were identified (cf. Chapter 5).

Based on the obtained knowledge regarding an optimized standby management, the ability to re-attain full methanation capacity as fast as possible after restart was further studied. The constraints of various restart strategies as well as approaches for improvement were revealed using the ATTBR technical-scale set-up (cf. Chapter 6).

The ATTBR provides a large surface area for a potential biofilm establishment. The influence of decoupling hydraulic retention time (HRT) and solid retention time (SRT) on biofilm formation processes during biofilm based reactor start-up was studied using a lab-scale set-up that was established at the Aarhus University (DK) and investigated in a joint study (cf. Appendix A).

Based on these results, a preliminary assessment on the applicability of the ATTBR concept for flexible and demand-oriented H_2/CO_2 BM is provided in the following sections, additionally

addressing current knowledge gaps and future research needs. Therefore, the nexus of i) dynamic operational requirements, ii) process stability, as well as iii) by-product formation and the resulting opportunities and constraints for dynamic process control are being comprehensively discussed. Subsequently, perspectives and challenges for the integration into future energy systems are discoursed and finally, alternative ATTBR application opportunities beside PtG are evaluated.

7.1 General applicability of the ATTBR concept

The **general applicability** of the ATTBR concept for BM was investigated in a technical-scale system. In the resulting long-term experiments (**Paper I**, **Paper II** and **Paper III**), the promising combination of mass transfer advantages of trickle bed reactors with the enhancement of BM rates at thermophilic conditions has been demonstrated. Based on the comparison of volumetric methane production rates, linked to the corresponding gas conversion or methane concentration[36,184], the ATTBR can compete with the performance of other mixed culture BM reactors. As hypothesized, the achieved methane production rate of 15.4 $m^3_{CH_4}/(m^3 \cdot d)$ with 98% CH_4 (**Paper I**) exceeded not only the performance of mesophilic trickle bed systems (Table 2.2), but also the performance comparison rate of 12.3 $m^3_{CH_4}/(m^3 \cdot d)$ (cf. section 3.1). Thus, **hypothesis #1 can be accepted**. This result is in accordance with findings from previous studies, reporting considerably higher methane production rates under thermophilic conditions[36,51,56,98]. The ATTBR also exceeded performance levels of various thermophilic reactor types, e.g. hollow-fiber membrane reactor (79% CH_4 at 9.6 $m^3_{CH_4}/(m^3 \cdot d)$)[91] or fixed bed reactor (75% CH_4 at 6.4 $m^3_{CH_4}/(m^3 \cdot d)$)[92] (cf. Table 2.2). This indicates a potential advantage due to an improved gas-liquid mass transfer in trickle bed reactors[99,102,103,115] and could thus further support the significance of the desired reactor concept.

Plug-flow conditions: Considering mixed culture BM reactors, presently, the highest methane production rates were reported by Savvas et al. (30.0 $m^3_{CH_4}/(m^3 \cdot d)$ at 93% CH_4)[89] in a mesophilic biofilm tube reactor, providing almost ideal plug-flow conditions by an inner diameter of only 13 mm and a length of 7 meter. In contrast, ATTBR plug-flow conditions may not be ideal because of a wider inner diameter (215 mm in the present study). This assumption is backed by short-circuit flows that were observed following rapid load increase experiments (**Paper III**). Design measures to improve the ATTBR regarding plug-flow (e.g. optimized substrate gas distribution, gas pre-heating, height-to-diameter ratio) require further investigations and experimental verification.

Energy consumption: At methane concentrations $> 75\%$, methane production rates achieved by Savvas et al.[89] were only exceeded with pure cultures in thermophilic CSTR (cf. Table 2.2). Although vigorous mixing can clearly enhance gas-liquid mass transfer in CSTRs, the parasitic energy required for mixing increases with increasing reactor size, requiring approximately 10% of the overall energy input into the methanation step[89,182]. In parallel, the conversion efficiency of the methanation step is limited to at most 83.2% based on LHV (3.00 $kWh/m^3_{H_2}$ and 9.97 $kWh/m^3_{CH_4}$ at STP). With regard to upscaling of biological methanation technologies, reactor systems requiring no additional mixing (e.g. trickle bed, fixed bed, and partially hollow-fiber membrane reactors)[50,54,92,113] are in advantage. The studied ATTBR required no mixing energy or

introduction of pressurized gas and thus provides a set-up with low parasitic energy consumption. Furthermore, the energy consumption for trickling and liquid reservoir mixing can be neglected due to very small flow rates. Based on the overall energy input into the methanation step, the heat loss (conduction) of the ATTBR has been determined to approximately 1.1% (1.7 $kWh/m^3_{trickle\ bed} \cdot d$), while approximately 15.7% went into microbial growth and reaction heat (**Paper II**). Still, the latter could not be quantified in the studied technical-scale ATTBR as it would require a calorimetric reactor set-up. In such a set-up, Schill et al.[174] observed a considerable heat generation during highly exothermic growth of Methanothermobacter thermoautotrophicus (391 $kWh/(m^3 \cdot d)$ at 576 $m^3_{H_2}/(m^3 \cdot d)$). The heat generation is caused by a substantial decrease of entropy due to an inevitable mole reduction during hydrogenotrophic methanogenesis (cf. Eq. 2.1). This is contrary to the complex anaerobic degradation processes of organic matter where entropy increases[185]. Hence, a certain heat dissipation is even required to maintain a sufficiently negative Gibbs free energy as driving force for hydrogenotrophic methanogenesis[70,174]. Considering these results, it can be assumed that in an appropriately insulated ATTBR reactor set-up, the reaction heat generated can at least compensate the calculated heat loss. Depending on the maximum volumetric methane production, heat might even be recovered from the methanation reactor.

7.2 By-product formation

7.2.1 Process liquid composition

Besides reactor design, various studies revealed that process liquid composition, especially macronutrient (N, S, P) and trace element concentrations, plays a key role for the efficiency of hydrogenotrophic methanogenic archaea's metabolism[161,167,186–188]. Among macronutrients, particularly sulfur is essential for their metabolism[162]. A dropping conversion performance of the mixed microbial biocenosis due to a sulfur deficit during ATTBR start-up (**Paper I**) was in accordance with results from previous studies with pure thermophilic strains (*Methanothermobacter thermoautotrophicus, Methanothermobacter marburgensis*)[69,106,163]. Sulfur supply (by Na_2S) must therefore be considered a sensitive operational parameter, with a narrow range between bioavailability and toxicity due to immediate dissociation to HS^- and S_2^- and formation of inhibiting H_2S[70]. If biogas is used as CO_2 source, the sulfide demand of the microbial community may be supplied with the H_2S present in the biogas (up to 10,000 ppmv)[20] in future applications[189].

Beside macronutrients, the availability of trace elements impacts the productivity and growth of hydrogenotrophic methanogenic archaea, as they are required for the formation of coenzymes and membrane-bound enzymes complexes[64] and as catalyzers or cofactors for the electron transport[186]. Nickel, iron, cobalt and molybdenum are among the essential trace elements for metabolism and growth of hydrogenotrophic methanogenic archaea and their optimum concentrations are discussed in various studies[128,167,186,190].

7.2.2 ATTBR-specific effect of by-product formation

The importance of optimal nutrient and trace element concentrations increases when the formation of by-products during H_2/CO_2 BM is taken into account. According to Eq. 2.1, hydrogenotrophic

methanogenesis produces two moles of H_2O together with each mole of CH_4 produced (1.6 $L_{H_2O}/m^3_{CH_4}$). This "metabolic water production" leads to a continuous dilution of the process liquid if no corrective operative measures are taken[70].

While in previous studies, this liquid medium dilution has not been investigated in detail, the experiments performed at the technical-scale ATTBR revealed an amplified effect especially in trickle bed systems (**Paper I**). Here, the methanation reaction volume ($V_{Reaction}$) is uncoupled from the process liquid volume (V_{Liquid}), and the latter is significantly smaller (Figure 7.1). While the investigated ATTBR was operated at $V_{Reaction}$ / V_{Liquid} ratios between 5.5 (**Paper I**, **Paper II**) and 19.4 (**Paper III**), other trickle bed BM studies reported ratios in the range of 1.0 (Porté et al.[54]) to 8.7 (Ullrich et al.[118]). In contrast, methanation reaction volume and liquid volume are similar in CSTR, fixed bed reactors or hollow-fiber membrane reactors (ratio of about 1:1). As metabolic water production occurs proportional to the volumetric methane productivity, the liquid medium in trickle bed systems is thus diluted more rapidly by the factor of $V_{Reaction}$ / V_{Liquid} at similar gas feed rates and conversion efficiencies (**Paper I**). This needs to be considered when operational strategies are developed.

Thereby, metabolic water production not only affects a sufficient nutrient availability, but also the process liquid buffer capacity (**Paper I**). Thus, the system becomes more sensitive to e.g. formation of acids or a changing $CO_{2(g)}/CO_{2(l)}/HCO_3^-{}_{(l)}$ equilibrium and hence, the buffering capacity that affects the pH and consequently the process performance (cf. section 2.3.1).

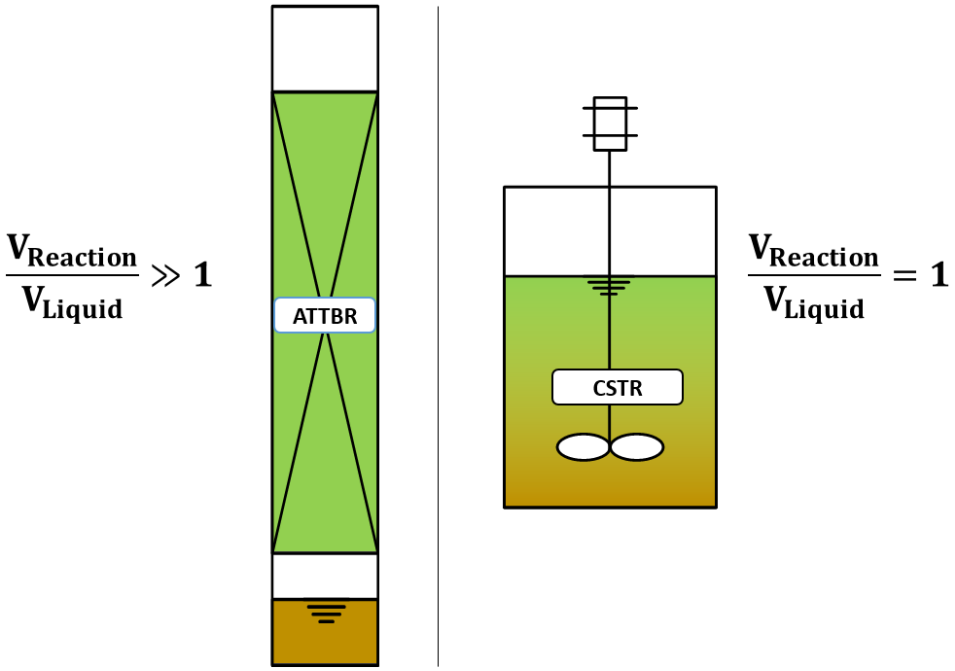

Figure 7.1: Comparison of reaction-to-liquid-volume ratio in an ATTBR and a CSTR.

7.2.3 Medium supply strategies

Independent of the reactor design, all BM systems face the challenge to maintain sufficient nutrient and trace element concentrations for an efficient process by supplying medium and/or withdrawing process liquid. CSTR were the most studied reactors for BM, mainly operated as continuously fed chemostat and dilution rates in the range of 0.005 h^{-1} to 0.4 h^{-1} were reported[36,70,108]. Bernacchi et al.[70] have shown that already at a dilution rate of 0.05 h^{-1}, the medium feed contributed to 82% of the totally withdrawn process liquid (0.061 h^{-1}; 841 $m^3_{H_2}/(m^3 \cdot d)$; 80% gas conversion efficiency). However, applying this dilution rate requires a daily medium supply of 1.2-fold V_{Liquid} and generates a liquid waste stream of 1.46-fold V_{Liquid}. Regarding biomass washout, which is inevitable at high dilution rates in systems with planktonic biomass, it has been demonstrated that even at dilution rates of 0.4 h^{-1} these reactors were still gas-liquid mass transfer limited[191]. For comparability (e.g. to CSTR) ATTBR dilution rates have to be divided by the ratio $V_{Reaction}$ / V_{Liquid}. Based on the reactor design, the studied technical-scale ATTBR would theoretically allow high dilution rates as described above. With the trickling rate of 3 L/h (**Paper II**, **Paper III**), an ATTBR dilution rate above 0.051 h^{-1} would allow even an operation without liquid recirculation. However, due to experimental liquid handling restrictions, the highest liquid ATTBR dilution rate, applied in **Paper III**, was 0.003 h^{-1}.

As high dilution rates have been shown to minimize the effect of metabolic water production and allow direct application of process media with the target nutrient and trace element concentrations, they can be generally assumed as suitable for all BM systems. However, buffer volumes as well as suitable handling strategies for the large liquid waste streams are required. Contrary, application of low dilution rates increases the sensitivity for an exact liquid media composition. Substantially higher nutrient and trace element concentrations must be supplied to compensate metabolic water production, which may results in solubility and/or precipitation issues, especially with a parallel sulfur supply[167]. The minimum permissible dilution rate is thus system dependent and needs to be determined for each case. Dilution rate also plays a substantial role for the biofilm formation in fixed or trickle bed reactors (**Paper IV**) which is further discussed in section 7.4.

In contrast to the dilution effect of metabolic water production outlined above, Savvas et al. demonstrated the possibility of nutrient recycling in closed-loop-reactors[85,86]. The authors operated four different loop reactors (mesophilic and thermophilic) with liquid recirculation without any nutrient supply for 185 days. Despite a 1.5-fold dilution of their liquid reactor volume, they reported no limitations. As a similar process liquid dilution was attained in the ATTBR after 7 days (**Paper I**), the operational period in the study reported by Savvas et al. may have not been long enough to experience any limitation yet. Furthermore, several other promising attempts to establish BM set-ups with an alternative nutrient/trace element supply have been made, e.g. applying locally available centrate or digestate[53,54,79,82](**Paper III**) or integrating a nutrient source into a fixed bed[92]. However, these approaches are limited to mixed culture BM systems as no axenic reactor operation can be ensured.

Independent of the operational advantages or constraints of different medium dilution rates, all BM systems generate a least a liquid waste stream equivalent to their metabolic water production. This stream could either be re-fed as trace element supplementation[187,192] into an anaerobic digester, which may already be available as CO_2 source on site. Alternatively, membrane

technologies represent a suitable and well-studied option to extract the metabolic water only, while keeping the nutrients in the system[70].

7.2.4 Membrane technologies

Separating only metabolically produced water by membrane based approaches would allow retaining biomass in the BM system and reducing the required nutrient supply by re-feeding the concentrated streams as medium into the BM reactor. A schematic overview of the proposed integration of membrane technologies into BM operation is given in Figure 7.2.

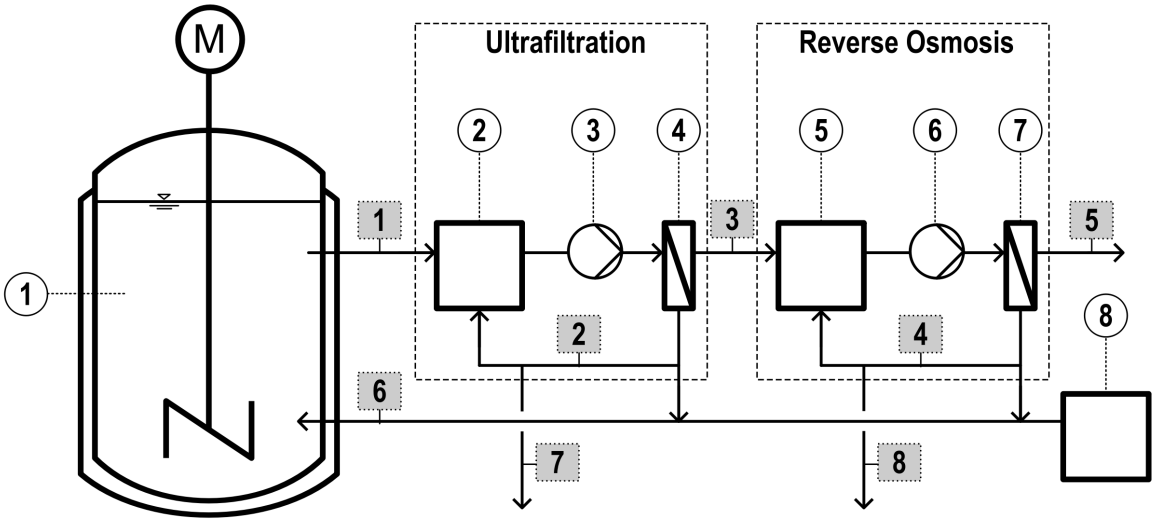

Figure 7.2: Schematic overview of the proposed integration of membrane technologies into BM operation. **Technical equipment (white circles)**: (1) BM reactor; (2) (cooled) buffer tank for process liquid + ultrafiltration (UF) concentrate; (3) UF feed pump; (4) UF membrane module; (5) buffer tank for UF permeate + reverse osmosis (RO) concentrate; (6) RO feed pump; (7) RO membrane module; (8), buffer tank for replacement medium (optional). **Liquid streams (grey squares):** (1) excess BM process liquid; (2) UF concentrate (high biomass content, reactor's nutrient and trace elements content); (3) UF permeate (no biomass, reactor's nutrient and trace elements content); (4) RO concentrate (no biomass, high nutrient and trace elements content); (5) RO permeate (pure H_2O); (6) medium re-feed to reactor; (7) UF brine; (8) RO brine.

The selection of suitable membrane technologies should aim for the generation of three different liquid streams containing i) a high biomass concentration (stream 2), ii) a high nutrient and trace element concentration (but no biomass; stream 4), and iii) pure water (stream 5). The quantities of the respective streams depend on the capability of the BM reactor to handle a high biomass content.

Thus, the impact of increasing the biomass content compared to operation with a continuous fresh medium supply has to be evaluated in a first step. Potential positive effects of a high biomass content on BM conversion rates have been reported in previous studies[33,77,89]. However, high biomass retention may also cause an imbalance between biomass decay and gas feed dependent biomass growth. Regarding these processes, this reactor state is comparable to a previously studied starvation mode (**Paper II**) that can results in elevated decay (especially under thermophilic conditions[152,169]) and in subsequent hydrolysis and acid formation (particularly in mixed cultures,

cf. section 7.2.5). In contrast, dead biomass is not expected to cause subsequent conversion processes in axenic pure culture systems with hydrogenotrophic methanogenic archaea only.

To achieve the aspired high biomass content, the application of tubular membrane modules is proposed, using either microfiltration (pore size: 0.08 - 2.0 µm) or ultrafiltration (UF) (pore size: 0.005 - 0.2 µm) membranes[193,194]. In particular tubular modules show good cleaning performance in process liquids with a high biomass content or clogging potential. As they are manufactured as a monolithic unit, consisting of one or more channels[193,195], high velocity cross-flow operation is typical for this module type. The advantage of this operating mode is a continuous separation of the solid (fouling) cake from the membrane surface, due to high shear forces induced by the feed stream that flows tangentially to the membrane surface. In cross flow mode, potentially UF allow operation with an even higher biomass content than microfiltration. Due to the smaller pore size of UF membranes, fewer particles tend to penetrate the pores and cause irreversible clogging/blocking, but directly form a reversible solid "cake layer" that can be removed more easily with the high shear forces in cross-flow operation[196]. With regard to biofouling, the UF operating temperature is critical. Due to increased amounts of biopolymer clusters, extracellular polymeric substances and soluble microbial products, 5 to 10 times higher filter resistance was reported for anaerobic membrane reactors (microfiltration) operated at thermophilic conditions compared to mesophilic conditions[197]. Particularly the UF modules should thus be fed from an external, cooled buffer tank as indicated in Figure 7.2. This reduces microbial decay processes[169] and biologically induced fouling layer formation within the membrane modules[196], but also minimizes the general interference between UF and BM reactor (e.g. heat removal, mixing).

In order to retain macronutrients and trace elements from the obtained UF permeate (stream 3), the subsequent application of reverse osmosis (RO) is required. RO is the most selective membrane technology (molecular weight cut-off usually $>$ 100 Dalton) that typically uses spiral wound membranes operated in cross flow mode[198]. RO is primarily applied to retain single or double charged ions (e.g. Cl^-, Na^+, $Ca_2{}^+$, $Mg_2{}^+$), e.g. during desalination[199]. Although RO clogging through biological colonization on the membrane surface can substantially be reduced by UF pretreatment, chemical cleaning is still required to reduce fouling and scaling due to soluble microbial products and chemical precipitates, respectvely[193,196]. RO operational parameters such as permeate flux or recovery rate mainly define the energetic and economic feasibility of a membrane treatment train applied together with a BM reactor. As the hydraulic pressure in RO must exceed the osmotic pressure to achieve permeate flow, maintaining low concentration gradients of target components throughout the RO module is preferable[196,198]. However, the optimum energetic and economic operating point has to be determined for each membrane treatment step individually, varying cross-flow and recovery rates to optimize the transmembrane flux.

The obtained UF and RO concentrate streams can then be fed back to the BM reactor (optionally together with fresh medium) or are partially disposed as brine streams to avoid accumulation of salts, precipitates (e.g. sulfur-metal complexes) and non-degradable organic matter (cf. Figure 7.2). The pure water (stream 5) could potentially be used for electrolytic H_2 generation (cf. section 2.1). At 100% conversion efficicency of the electrolysis and methanation steps, 50% of the introduced water for electrolysis could theoretically be recovered as metabolic water (neglecting water loss through vapor). At this time, no scientific study investigated the suitability and operational limits of UF and RO for BM process liquid treatment as well as quality limitations for

potential re-introduction for electrolysis. Hence, intensive research is required to reveal optimum operation strategies. Nevertheless, it has to be noted that the operational complexity of a BM system increases substantially with the application of the proposed membrane treatment approach, which needs to be considered in each individual case.

7.2.5 VFA transformation processes

Supplying H_2 to a mixed microbial biocenosis in *ex-situ* BM reactors can result in various undesirable VFA transformation processes, among which reductive homoacetogenesis (Eq. 2.9) is the most commonly reported one[84,85]. In **Paper II**, VFA concentration measurements were used to further identify process disturbances indicated by VFA formation[132,146]. Although the ATTBR carbon balance showed that only 1.3% of the carbon input is converted to VFA (**Paper II**), unexpectedly high acetate, propionate, iso-butyrate and n-butyrate concentrations were observed even during steady-state operation (418±180 mg/L, 1874±341 mg/L, 861±337 mg/L and 128±51 mg/L, respectively). These concentrations have been attributed to enhanced biomass decay, followed by hydrolysis and acidogenesis processes, which may have been induced by a relatively high hydraulic retention time in the process liquid reservoir (5.9 d) combined with a low trickling rate. A subsequent VFA turnover could have been inhibited by product inhibition (acetate, propionate or H_2) as has been shown previously[60,169,172,173]. Measures to avoid biomass decay in the process liquid reservoir might be high dilution rates or supply of substrate gas into the process liquid reservoir. However, as these measures may also interfere with a desired biomass immobilization, they are discussed in section 7.4.

In addition, the unfavorable $V_{Reaction}$ / V_{Liquid} ratio in the ATTBR described above can amplify the impact of VFA transformation processes, especially when they occur in $V_{Reaction}$ (e.g. reductive homoacetogenesis). Beside biomass decay, observations during dynamic ATTBR operation indicate additional transformation processes such as acetoclastic methanogenesis, syntrophic acetate oxidation[175,176] or potential propionate formation from H_2 and CO_2[179]. However, whether the latter mechanism was present in the studied ATTBR could not be determined with certainty from the obtained data. Deeper insight might additionally be gained by suppling radioactively labeled CO_2 or alternatively spiking labeled acetate[176,179]. These investigations would also require additional molecular biological analyses to identify the microbial groups involved.

Finally, it must be noted that undesirable VFA formation has not been reported for pure culture BM systems due to their axenic operation.

7.3 Process stability and control during dynamic operation

As outlined in section 2.3.2, fluctuating VRE availability requires dynamic operation of H_2/CO_2 BM systems. Their corresponding operational states were defined in a recent study by Thema et al.[184] and are summarized in Table 7.1. The results of dynamic ATTBR operational experiments are discussed based on these definitions.

Table 7.1: Definition of operational states of H_2/CO_2 BM systems (according to Thema et al.[184])

Operating state	Definition
Nominal operation	Operation at nominal capacity.
Partial load operation	Percentage of nominal operation.
Intermittent operation	Gas load follows VRE availability. H_2/CO_2 BM is directly coupled to electrolytic H_2 generation. State is defined by load change frequency and order of magnitude.
Hot standby	Short operational breaks. Quick return to previous operation state. Temperature and pressure in nominal operation mode.
Cold standby	Extended operational break (no time period defined).
Shut down	No operation (except for plant safety, e.g. gas/fire detection).

The applicability of the ATTBR technical-scale set-up as a robust system that is suitable for demand-oriented operation within a dynamic energy system has been demonstrated in **Paper II** (cold standby) and **Paper III** (hot standby and intermittent operation). The impact of different combinations of SP durations and temperatures on the restart performance was investigated in **Paper II**. As hypothesized, the standby strategy, defined by temperature and duration, affected the time required to re-attain a stable CH_4 production rate at the pre-standby level and thus, **hypothesis #2 can be accepted**. The results published in **Paper II** showed a strong influence of the SP temperature on the restart performance, beginning already after 24-hour operational breaks. A higher remaining biological gas conversion capability was observed after SPs at 25°C compared to 55°C, as significantly higher decay rates prevail at thermophilic conditions compared to mesophilic systems (decay rates: 55°C: 0.48 d^{-1}, 38°C: 0.034 d^{-1})[152,155,156]. Moreover, especially repetition of SPs at 55°C caused impairment of reactor performance as a consequence of standby operation. The impact of temperature greatly outweighed the impact of extended SP duration in the settings studied and only a minimal impairment of restart performance was observed even after 8 days of cold standby. It can be assumed that these observations are not dependent on the investigated ATTBR set-up and are thus applicable to other thermophilic BM reactor systems, too.

These experiments revealed the requirement for an appropriate temperature management during "extended" SPs. The maximum permissible hot standby duration has not been determined in detail yet. However, already repetitive 24-hour hot SPs resulted in a deteriorating biological gas conversion capability (**Paper II**). Hence, frequent changes between "hot" operation and extended cold SPs may be required. In this context, a possible advantage of the ATTBR are the gases filling the reaction volume (=trickle bed). Due to their significantly lower specific heat capacity compared to water filled reaction volumes[200], less energy or time is required to preheat or cool down, respectively. This would increase the flexibility of the ATTBR system. As discussed in section 7.1, heat generation due to the exothermic reaction may require cooling during operation, if a quick return to lower temperatures is desired. External heating might then only be necessary during periods without sufficient gas conversion for heat generation (e.g. initial load increase phases or partial load operation). When applying water or oil as heat transfer medium (reactor with water jacket), cooling to ambient temperature and heating to process temperature might be possible with less effort compared to electric heating mats/jackets, which do not allow process heat recovery.

The capability for the fastest possible return to full methanation capacity after restart was studied in **Paper III**. The results revealed the capability to return to 100% load almost immediately after a hot standby, while a 60-minute adaption phase was required subsequent to 24-hour cold SPs. Although the latter result is considerably faster compared to **Paper II** (> 186 minutes), **hypothesis #3 can not be accepted** as the aspired product gas quality (c_{CH_4} > 96%) could not be maintained continuously while returning to full load within 60 minutes ($c_{CH_4,achieved}$: 94.6±1.6%). The major operational challenges identified were the inevitable delayed microbial conversion activity as well as an insufficient microbial reactivation along the gas flow path. Due to a very gentle restart pattern in **Paper II**, the delayed microbial conversion activity was not identified beforehand. It can be mainly attributed to the reduced reactor temperature during cold standby and its duration may expand with extended cold SPs. However, the precise dependency of these two parameters requires further investigations. It has been demonstrated that microbial reactivation along the gas flow path, subsequent to cold standby, is necessary particularly in plug-flow-like BM systems (e.g. ATTBR) with immobilized biomass (**Paper III**). A comparable, but not so pronounced spatial inactivation may also be expected during partial load operation. Hence, these two operational modes require specific gas load patterns to ensure complete spatial reactivation to re-attain or maintain the activity of the entire immobilized biomass. These patterns should include an initial or frequent full load pulses to expose the entire reactor bed to substrate gases, combined with controlled gas supply to maintain an aspired gas conversion level **Paper III**.

The large gas hold-up of an ATTBR compared to CSTR, bubble column reactors or hollow-fiber membrane reactors[184] offers further possibilities to increase ATTBR flexibility. Assuming plug-flow-like conditions, the gas phase provides a high quality product gas buffer during load increase phases. In addition, operation at elevated reactor pressure may increase flexibility throughout hot or cold SPs. The pressurized gas phase allows to compensate gas volume reduction after terminating the gas feed and/or cool down for cold standby. During restart, the reactor gas phase can be slowly re-pressurized by heating and reinstating the gas feed, while avoiding the release of product gas during the initial microbial lag phase.

However, along with plug-flow-like behavior, temporally varying H_2/CO_2 ratios can occur in the trickle bed throughout dynamic gas feed operation. Results from **Paper II** and **Paper III** indicated liquid-to-gas CO_2 release during gas feed breaks or partial load operation, which required re-balancing of the $CO_{2(gas)}/CO_{2(liq.)}/HCO_3^-{}_{(liq.)}$ equilibrium throughout subsequent gas feed increases. This may have led to locally disadvantageous H_2/CO_2 ratios for parts of the microbial trickle bed community that are acclimatized to elevated CO_2 concentrations. A limiting effect on hydrogenotrophic conversion has already been observed for CO_2 gas phase concentrations below 12% during *in-situ* BM[43]. Pressurized reactor operation, as proposed above, may further amplify limiting effects. Hence, the underlying mechanisms require further investigations in order to develop appropriate gas feed strategies. As has been shown in **Paper II** and **Paper III** also the pH was affected by local CO_2 release or solution processes. pH can be controlled by buffer media supply as applied in various studies[77,108,128,167]. Alternatively, Savvas et al.[86] proposed pH control solely by CO_2 supply in a closed loop-reactor. However, this reactor was fully mixed without spatial concentration profiles, which limits the transferability of these results to an ATTBR. Further peripheral processes, such as nutrient / trace element addition as well as (optional) membrane separation technologies require operation along with dynamic feed conditions. Both processes are

linked (cf. Figure 7.2) and should be operated proportional to the volumetric methane production rate that defines metabolic water production.

7.4 Immobilized vs. planktonic biomass

Paper I revealed the need for additional research to identify the respective contribution of biofilm community and planktonic biomass to the total gas conversion and their relevance for process stability. Previous studies observed biofilm formation in mesophilic trickle bed[80] and biofilm plug-flow reactors[89] as well as in a thermophilic trickle bed reactor[54]. In contrast, no macroscopic (visible) biofilm formation was observed in the ATTBR, even after 313 days of operation, while a biomass concentration of 7.0 g_{VS}/L was detected in the process liquid (**Paper I**). The latter result can be attributed to the high HRT of 6-7 days. Considering growth rates of far below 24 hours for thermophilic hydrogenotrophic methanogenic archaea[36], this HRT did likely not allow sufficient decoupling from SRT to enforce biofilm formation.

In this context, the ATTBR set-up generally allows two different operational approaches regarding its active microbial community: i) immobilization of the desired hydrogenotrophic methanogenic archaea as biofilm or ii) increasing the planktonic hydrogenotrophic methanogenic archaea content.

7.4.1 Immobilization of hydrogenotrophic methanogenic archaea

Low HRT was identified as a significant process parameter for determining the formation of an active methanogenic biofilm in a mixed-culture *ex-situ* BM system with carriers continuously covered by liquid (**Paper IV**). Biofilm activity was clearly enhanced at 18 hours HRT due to wash-out of competing planktonic species, which hindered proliferation of biofilm biomass at long HRT. Reducing liquid HRT or wetting frequency is suggested as important operational parameters for enhancing biofilm formation to reduce competing hydrogenotrophic activity in the liquid competing with the biofilm and proliferation of active methanogenic biofilms. This is in line with results from Zheng et al.[127], who reported that a low HRT was essential for biofilm formation in hyper-thermophilic upflow biofilm reactors for mixed culture biohydrogen production. Still, although low HRT led to faster biofilm formation, they observed lower production rates at too low HRT due to increased washout of high yielding biomass. Thus, a careful selection of HRT is required to derive the optimum operating point for start-up of biofilm based systems. In contrast to low HRT, high hydrodynamic shear forces cannot be applied as a driving force for immobilization in trickle bed system, as high trickling rates (inducing high hydrodynamic shear forces) would negatively impact the gas-liquid mass transfer[113].

Operation with immobilized biomass, originating from a mixed culture inoculum, further allows the establishment of a diverse microbial community profile along the gas flow path, due to adaption to plug-flow conditions. Whether this is entirely beneficial also for dynamic operation with changing longitudinal substrate gas concentration profiles needs further investigations.

In contrast, the immobilization of a single hydrogenotrophic methanogenic archaea strain has not been investigated yet. Trickle bed systems for syngas fermentation (cf. section 7.6.2) were operated

with a defined triculture, however, the authors did not report on specific contributions of immobilized cultures to the overall conversion[114,201].

In the ATTBR set-up, operation with low planktonic biomass can easily be achieved using the proposed membrane technologies for process liquid treatment (Figure 7.2). The UF concentrate/brine stream contains a high planktonic biomass concentration that can be fully discharged. This operational mode would also avoid biomass decay in the process liquid that was observed in **Paper II**. Alternatively, a "one-way-through" trickling regime, using non-recycled (fresh) process liquid at the lowest possible trickling rate can generate high selective pressures for immobilization, while avoiding energy intensive membrane treatment. However, it requires additional investigations, whether a sufficient nutrient and trace element supply can be guaranteed or if too high nutrient and trace element concentrations may even result in metabolic limitations.

7.4.2 High concentration of planktonic hydrogenotrophic methanogenic archaea

The efficient methanation rate and the increased planktonic biomass concentration shown in **Paper I**, support the assumption that initially the major part of the gas was converted by planktonic hydrogenotrophic methanogenic archaea when passing the trickle bed. Regarding biomass contribution, this operational mode (high planktonic biomass concentration) may reduce the clogging potential, allowing to use carrier material with higher surface to volume ratios (**Paper I**) to further enhance overall gas-liquid mass transfer and gas conversion rates. The high planktonic biomass concentration required, can easily be maintained with the proposed membrane treatment (Figure 7.2) by recycling the entire UF concentrate. However, this operational mode may result in biomass decay in the process liquid reservoir and subsequent VFA formation as outlined above. A supplementation of substrate gas feed into the process liquid reservoir would exploit additional reaction volume while maintaining a higher level of microbial activity and avoiding biomass decay. A potentially required adaption to longitudinal gas concentration profiles, as discussed for immobilized biomass, needs further investigation to verify the suitability of high planktonic biomass. Furthermore, single hydrogenotrophic methanogenic archaea strains could be easily used in this operational mode as no immobilization is required.

7.5 Integration of *ex-situ* BM reactors

As outlined in Chapter 2, PtG aims at converting excess VRE in storable gases. While the function and integration of electrolysis as first step is undisputed, there are two main concepts to integrate *ex-situ* BM reactors (e.g. ATTBR) into a PtG system. Figure 7.3 illustrates these integration approaches, based on CO_2 emission sources such as biogas or wastewater treatment plants as well as industrial processes (cf. section 2.3.2)[9,31,38,50,182].

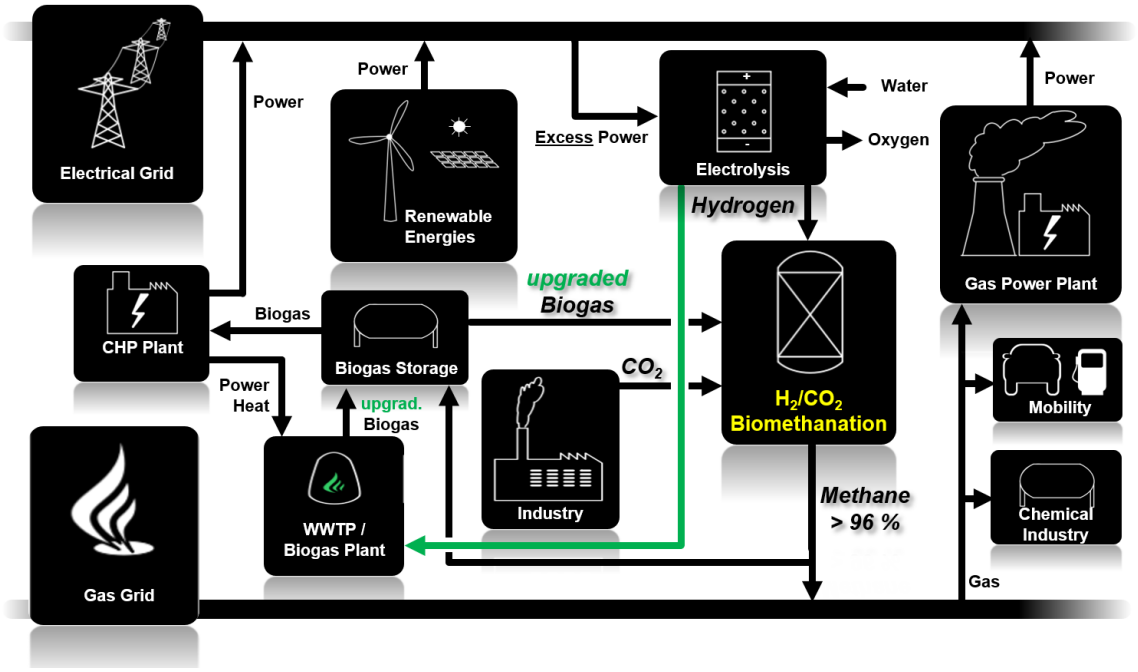

Figure 7.3: Simplified scheme for the integration of the H_2/CO_2 BM process as an energy conversion and storage approach (PtG) that couples electrical grid (excess power) and natural gas grid (storage capacity and utilization). The green pathway represents an optional addition of *in-situ* BM (=Hybrid process[31])

7.5.1 Stand-alone *ex-situ* BM

Stand-alone *ex-situ* BM reactors receive the entire H_2 generated exclusively. Optimum gas-liquid mass transfer with the highest possible H_2 partial pressure would be achieved when feeding only H_2 and CO_2 into this reactor (as investigated in **Papers I**, **II** and **III**). However, this mode results in additional capital and operational expenditures (CAPEX and OPEX) for upgrading technologies to separate CO_2 streams (e.g. amine scrubbing or membrane cascade separation)[23,138,140,182,202]. As a result, H_2/CO_2 BM would lose one of the major operational advantages compared to catalytic methanation with its very high purity requirements for the CO_2 source (cf. section 2.1). Alternatively, untreated biogas is fed directly into the *ex-situ* BM reactor along with H_2. As a consequence, the inert CH_4 content in the biogas (50-70%)[31] will reduce the H_2 partial pressure in the substrate gas to levels between 66% and 54%, while the total feed stream increases by 20% to 47% (compared to "H_2/CO_2-only" at a similar H_2 feed rate). This will affect gas-liquid mass transfer[151] and as a result, a larger reaction volume is required.

Due to its plug-flow conditions, the required reaction volume can be estimated from an ATTBR (fed with H_2/CO_2-only, assumption: H_2:CO_2 = 4:1 at 80 $L_{H_2,feed}/h$). At the longitudinal position within such an ATTBR, where a gas composition with e.g. 31.8% CH_4 is reached (=70% substrate gas conversion, Table 7.2), the remaining reaction volume (V_{Remain}) is required to convert the residual 30% of substrate gas (= 24 L_{H_2}/h). To convert a gas stream containing the initial H_2 feed rate of 80 L_{H_2}/h and 31.8% CH_4, V_{Remain} can be extrapolated resulting in a required reaction volume of 3.3 x V_{Remain}. Similar estimations are possible for every CH_4 content. However, this

Table 7.2: Composition of CO_2 source (biogas), substrate gas stream and resulting ATTBR conversion states

Biogas (CO_2 source)	$CH_{4,biogas}$ [%]	50.0	60.0	70.0
	$CO_{2,biogas}$ [%]	50.0	40.0	30.0
Substrate gas	$CH_{4,substrate\ gas}$ [%]	16.7	23.1	31.8
	$CO_{2,substrate\ gas}$ [%]	16.7	15.4	13.6
	$H_{2,substrate\ gas}$ [%]	66.7	61.5	54.5
	Increase of total feed stream [%]	20	30	47
ATTBR	Gas conversion equivalent (with pure H_2/CO_2 feed) to achieve CH_4 content of substrate gas [%]	50	60	70
	V_{Remain} [L]	To be determined		
	Required reaction volume as multiples of V_{Remain} [-]	2.0	2.5	3.3

estimation requires the determination of detailed longitudinal gas composition profiles.

In order to reduce the necessary ATTBR reaction volume for direct biogas usage without pre-treatment, biogas addition can be split up to multiple ports in a single ATTBR (at different reactor heights) or in-between a cascade of ATTBR. Thus, locally higher H_2 partial pressures and lower gas flow rates and consequently, enhanced gas-liquid mass transfer could be generated in comparison with the addition of the entire CO_2 source (biogas) at the reactor gas inlet. However, this mode requires additional monitoring equipment and a more complex control approach, especially during dynamic operation with changing feed rates.

The economic feasibility and extent of possible pre-treatment vs. construction of larger reaction volumes and multiple port biogas injection has to be determined for each application individually.

7.5.2 Hybrid BM systems

A further compromise may be the combination of *in-situ* and *ex-situ* biogas upgrading in a hybrid BM system as proposed by Angelidaki et al.[31]. In a first step, *in-situ* upgrading would allow valorizing the existing infrastructure by retrofitting BM technologies to existing biogas plants (green H_2 path in Figure 7.3). Consequently, the reactor size of a second (*ex-situ*) BM reactor can be reduced. For this approach, the possible process disturbance to anaerobic digesters through *in-situ* H_2 addition needs to be considered (cf. section 2.3.1).

As described in section 7.5.1, the required *ex-situ* reactor size increases with increasing methane content in the substrate gas. The maximum achievable synergetic effect of a hybrid system depends on a compromise between the *in-situ* H_2 injection limit as well as on CAPEX and economic feasibility of the resulting *ex-situ* reactor size.

As described in section 7.5.1, the required *ex-situ* reactor size increases with increasing methane content in the substrate gas. The maximum achievable synergetic effect of a hybrid system depends on a compromise between the *in-situ* H_2 injection limit as well as on CAPEX and economic feasibility of the resulting *ex-situ* reactor size.

7.5.3 Economic constraints

The BM reactor technology, the integration concept as well as the process efficiency define the required reactor size, and thus directly affect the methanation step CAPEX. While a techno-economic analysis is beyond the scope of this thesis, several other parameters, which effect the economic feasibility of the overall PtG process chain, are summarized below. Up to now, only three studies evaluated BM technology within a techno-economic analysis[23,182,203]. Therefore, also publications investigating catalytic methanation were considered, particularly regarding their evaluation of electrolysis CAPEX and OPEX.

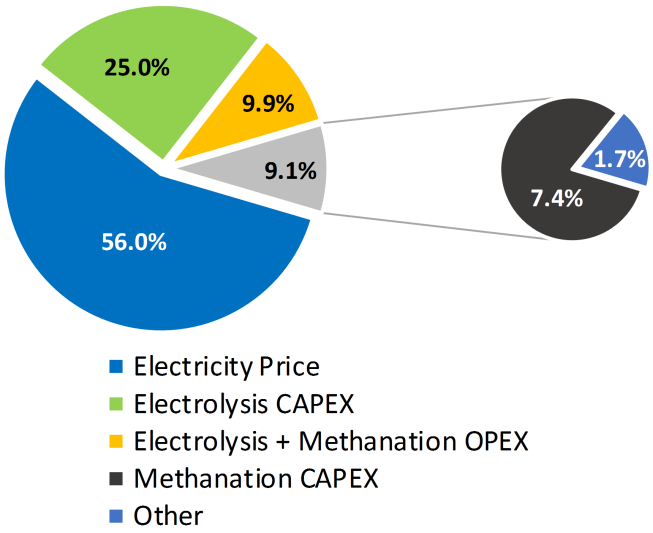

Figure 7.4: Exemplary contribution of CAPEX and OPEX parameters to the resulting LCOE (Percentage values from McDonagh et al.[139]). A comparable CAPEX range (14-20% of total CAPEX) can be assumed for the Methanation step[139,182])

In all studies, the electricity price had the highest impact with approximately 56% of the levelized cost of energy (LCOE)[139] (Figure 7.4) or 73% of the total OPEX[182], depending on the studied case. Particularly in Germany, the current surcharge for electricity from renewable energy sources (Renewable Energy Sources Act - EEG 2017)[204] increases the negative effect of this factor. For the conversion of electricity directly from a renewable source into H_2, EEG surcharge would not apply, however these plant specific boundary conditions can be considered as fairly rare. In contrast, using the electricity grid as an intermediate route (as illustrated in Figure 7.3) results in additional EEG surcharge of approximately 67.90 €/MWhel in 2018[205]. This corresponds to 41% of the total electricity price (for industries with a yearly demand of 0.16 to 20GW: 164.20 €/MWhel, excl. electricity tax)[205]. EEG discount (surcharge reduced from 67.90 €/MWhel to 1.10 €/MWhel) for energy intensive industries (e.g. cement, steel or paper industry) apply above a yearly demand of 20 GW. Hence, in order to strengthen the implementation of PtG technologies, regulatory actions are clearly needed to make discounts, as granted for energy intensive industries, also applicable for PtG technologies or even consider complete tax waiving for technologies that serve the stability of the grid. Additional parameters with an economic influence are: i) electrolysis CAPEX (PEM

electrolysis: approx. 25% of LCOE[139] or 80-85% of total CAPEX[139,182]), ii) electrolysis and methanation OPEX (excluding electricity price: 9.9% of LCOE[139] or 27% of total OPEX[182]), and iii) methanation CAPEX (7.4% of LCOE[139] or 14-20% of total CAPEX[139,182]) (Figure 7.4). Furthermore, the desired target selling price for the produced SNG[206], the operational hours per year (studied between 6,500h/a[139] and 8760h/a[138,182]) as well as the amortization period and interest rates influence the economic feasibility. However, the respective order of the parameters depends strongly on the application investigated.

As electricity pricing has the major contributor to LCOE, the overall energy conversion efficiency of the entire process chain is crucial. In this context, Power-to-SNG systems are most sensitive to the electrolysis efficiency[182,206]. PEM technologies (most flexible electrolysis technology) can provide an electrical efficiency of 62-82%[17,22] and further improvement is expected (cf. section 2.1)[9]. The conversion efficiency of the methanation step is limited to 83.2% of the H_2 energy input (cf. Chapter 2) and further reduced by a parasitic energy consumption of approximately 1% (Paper II) to 10%[86] (cf. section 7.1). Hence, an overall efficiency of 40% up to 67%[9,139] of the PtG process chain is realistic for future applications, while these values do not consider the conversion back to electricity (e.g. with combined cycle power plant), liquefied fuels or other products. By improving the volumetric BM efficiency (defined by $m^3_{CH_4}/(m^3 \cdot d)$ and c_{CH_4}), the BM CAPEX can be further reduced. However, its impact on the overall LCOE or CAPEX is limited. Future BM research effort should thus also be directed towards BM process (and side process) resilience, especially during flexible operation. With higher flexibility also operating hours increase as shorter periods with sufficiently low electricity prices can also be used, which substantially improves OPEX and LCOE[23,139]. Furthermore, optimization of operational strategies (e.g. media supply, metabolic water deduction) and peripheral equipment (e.g. membrane systems, compressor, heat exchanger, pumps) would reduce BM CAPEX and OPEX[13].

7.6 Application of ATTBR for alternative processes

Beside the application for H_2/CO_2 BM, ATTBR might provide a reactor set-up for products from other gaseous substrates or may be used for alternative methanation routes.

7.6.1 Chemical product formation from gaseous substrates

A common utilization of gaseous substrates through a bio-catalytic route is the fermentation of synthesis gas (syngas) to obtain various biofuels and products such as methane, ethanol, butanol or acetic acid[102,180,207–216]. Historically, syngas was derived via coal gasification[99] and was used as a major buiding block for fuel and chemical production[115,217]. During the last decades the focus changed towards syngas generation from non-food biomass feedstock via gasification[102,212]. The latter process thermally cracks the lignocellulosic structure of biomass into the main syngas compounds CO, H_2 and CO_2 and minor amounts of CH_4 and trace gases, using fluidized bed gasification as the most suitable technology for large scale syngas production[212,217]. However, depending on the feedstock, syngas composition can vary substantially.

Subsequently, syngas can be converted into fuels/products either chemical-catalytically

Table 7.3: Selected biochemical syngas fermentation reactions

Process	Reaction	#
Water gas-shift reaction	$CO + H_2O \rightarrow CO_2 + H_2$	(7.1)
Methane formation	$CO + 3\ H_2 \rightarrow CH_4 + H_2O$	(7.2)
Ethanol formation	$6\ CO + 3\ H_2O \rightarrow C_2H_5OH + 4\ CO_2$	(7.3)
	$2\ CO_2 + 6\ H_2 \rightarrow C_2H_5OH + 2\ H_2O$	(7.4)
Acetate formation	$4\ CO + 5\ H_2O \rightarrow CH_3COOH + 2\ CO_2$	(7.5)
	$2\ CO_2 + 4\ H_2 \rightarrow CH_3COOH + 2\ H_2O$	(7.6)
Butanol formation	$12\ CO + 5\ H_2O \rightarrow C_4H_9OH + 8\ CO_2$	(7.7)
	$4\ CO_2 + 12\ H_2 \rightarrow C_4H_9OH + 7\ H_2O$	(7.8)

(Fischer-Tropsch process) or bio-catalytically via syngas fermentation (SGF)[212]. Similar to chemical-catalytic methanation, the Fischer-Tropsch process is very sensitive to feed stream impurities (e.g. H_2S, CO_2 or carbonyl sulfide)[218] and requires pre-treatment. Furthermore, the applied catalysts are very selective and require a narrow range of syngas compositions. In contrast, SGF has no pre-treatment requirements due to robust microbial strains or communities. Applying a mixed microbial community even allows to flexibly convert a wide range of syngas compositions into various products[212,218] such as methane, ethanol, acetate or butanol (Table 7.3). SGF is operated at different operational ranges (especially pH) than BM and detailed statements regarding process operation can be found in various review studies[208,219,220], but are outside the scope of this thesis.

Using gaseous substrates, SGF faces the challenge of an adequate reactor design for efficient gas-liquid mass transfer (H_2 concentration between 5 and 35%)[220] as outlined in section 2.3.2. As trickle bed reactors are among the intensively investigated reactor systems for SGF[99,102,103,114,115,221], ATTBR could provide a promising set-up for this application. However, especially CO conversion reactions are highly exothermic[219] and thus, require a sophisticated temperature management, particularly when applying changing syngas compositions for various products.

Integration of SGF into a dynamically operation ATTBR might generate additional synergetic effects. Adding hydrogen from electrolysis into a syngas converting ATTBR, could avoid the need for the water-gas shift reaction and reduce additional H_2 storage. In times without VRE, the ATTBR can be operated with syngas and biogas only to increase the ATTBR full load hours.

7.6.2 Direct electron supply to BM systems (Electromethanogenesis)

Within the past decade, increasing research interest is directed towards the promising biocatalytic electromethanogenesis process (BEM)[222–227]. BEM uses direct electron supply into a digester or BM system applying electric current between an anode and a cathode, skipping the electrolysis step used for PtG[224,228]. According to Blasco-Gómez et al.[225], methane production at a biocathode aiming for BEM can take place directly and/or indirectly via three main pathways: i) direct BEM: Electromethanogens recieve electrons directly from the biocathode and use HCO_3^- and H^+ from liquid phase; ii) indirect BEM: H_2 production at the biocathode and subsequent conversion by

hydrogenotrophic methanogenic archaea, and iii) indirect BEM: acetate or formate production at the biocathode and subsequent conversion by acetoclastic or hydrogenotrophic methanogenic archaea.

However, all BEM systems require an electric current between cathode and anode and consequently a conductive medium as well as a separation of cathode and anode, (usually) via a membrane. Transferring these requirements towards application within an ATTBR results in a very challenging reactor design. The present reactor packing, providing a high surface-to-volume-ratio for gas-liquid mass transfer, would lose this advantage when being placed into a liquid phase required for electric current conduction. Hence, although gas-liquid mass transfer is one major challenge in BEM systems[225], the ATTBR is clearly not suitable for this application.

7.7 Conclusion

The investigations performed within the framework of this thesis demonstrated the capability of the developed ATTBR set-up for efficient and dynamic BM. The ATTBR concept proved its competitiveness with other mixed microbial culture systems, although it could be applied to pure cultures as well, which can achieve an even higher performance as indicated in the literature. In order to prove and improve the general feasibility for ATTBR scale-up and implementation into the changing energy sector, the major research needs and questions derived throughout the previous sections are summarized below.

The plug-flow reactor design needs further optimization to minimize short-circuiting, but avoiding operational or maintenance restrictions through additional installations (cf. section 7.1). Determination of longitudinal conversion profiles during dynamic operation (cf. section 7.3) and a parallel development of a process model to predict the dynamic performance can further support reactor design improvement.

The suitability of UF/RO systems for BM process liquid treatment to recycle trace elements and retain biomass (cf. section 7.2.4) has to be evaluated, aiming for stable BM performance as well as for long-term membrane operation. To reveal the influence on ATTBR-OPEX, UF/RO operation need to be compared with a "high medium exchange strategy" (cf. section 7.2.3: no biomass and trace element recovery), e.g. regarding consumables, generated liquid waste streams as well as for energy consumption in relation to the overall energy output of the BM process. As membrane systems are also used to maintain high planktonic biomass concentrations, high performance strains (pure culture) might benefit from the surface area provided by the trickle bed carriers for enhanced mass transfer (cf. section 7.4.2).

For the economic feasibility of an *ex-situ* integration approach, it needs to be evaluated, whether increasing the CO_2 content by biogas pre-treatment (CAPEX + OPEX) might generate sufficient ATTBR-CAPEX savings due to a reduced $V_{Reacion\text{-}ATTBR}$ (cf. section 7.5.1). Finally, for hybrid systems, the tradeoff between *in-situ* H_2 injection limits and *ex-situ* performance (CH_4 concentration in substrate gas) has to be identified as a selection parameter (cf. section 7.5.2).

Appendix A

Stick or leave – pushing methanogens to biofilm formation for ex situ biomethanation

Previous studies have shown pronounced variation in colonization and activity of methanogenic biofilms in biofilm-based methanation reactors. Effects of operational conditions on biofilm dynamics remain largely uncharacterized but may increase reactor potentials further. This study elucidated the effect of hydraulic retention time (HRT) on methanogenic biofilm activity and composition during reactor start-up. HRT was identified as a significant process parameter for determining the formation of an active methanogenic biofilm in a mixed-culture ex-situ BM system with carriers continuously covered by liquid. Biofilm activity was clearly enhanced at 18 hours HRT due to wash-out of competing planktonic species, which hindered proliferation of biofilm biomass at long HRT (10 to 20 days). Reducing liquid HRT or wetting frequency is suggested as important operational parameters for enhancing biofilm formation to reduce competing hydrogenotrophic activity in the liquid overlaying the biofilm and proliferation of active methanogenic biofilms.

This chapter was published in a similar form with editorial changes as:

M. B. Jensen, D. Strübing, N. de Jonge, J. L. Nielsen, L. D. M. Ottosen, K. Koch, M. V. W. Kofoed, "Stick or leave – pushing methanogens to biofilm formation for *ex-situ* biomethanation", *Bioresource Technology*, vol. 291, Article No. 121784, 2019.

Author contribution: M. B. Jensen (60%), D. Strübing (10%); N. de Jonge (5%); J. L. Nielsen (5%); L. D. M. Ottosen (5%); K. Koch (5%); M. V. W. Kofoed (10%)

Graphical abstract

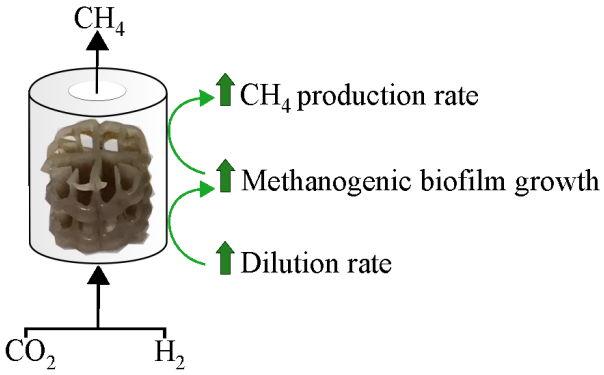

Abstract

Biomethanation exploits the ability of methanogenic archaea to convert CO_2 and renewable H_2 from electrolysis to biomethane. Biofilm reactors are promising for biomethanation scale-up due to high CH_4 productivity and low energy input for H_2 gas-liquid mass transfer. Effects of operational conditions on biofilm dynamics remain largely uncharacterized but may increase reactor potentials further. This study investigated the effect of hydraulic retention time (HRT) on methanogenic biofilm activity and composition. Commercial carriers floating in liquid were exposed to H_2/CO_2 for 87 days with the liquid phase being subject to either 18 hours, 10 days, or 20 days HRT. Methanogenic biofilms were dominated by hydrogenotrophic methanogens, but biofilm CH_4 productivity was enhanced at 18 hours HRT due to wash-out of competing planktonic species, which otherwise hampered proliferation of biofilm biomass at long HRT. It is suggested that high-rate biofilm reactors can increase methanogenic biofilm activity by minimizing the liquid's H_2 exposure.

A.1 Introduction

Substitution of fossil-based natural gas with renewable biomethane (CH_4) is critical for a successful transition to a 100% renewable energy system due to its versatile application across all energy sectors[229]. Biomethane currently comprises around 4% of the gas consumption in Europe and is mainly produced from upgraded biogas through removal of biogas-CO_2[230]. Significant efforts are being made to advance biological methanation (biomethanation) from lab to demonstration scale, as it has potential of becoming a low-cost, robust and flexible process for biomethane production from CO_2 waste streams and (renewable) electricity-derived H_2[231]. Biomethanation reactions are catalyzed by methanogenic archaea enriched from anaerobic digesters[32]. Recent progress in biomethanation has been covered in several reviews[31,38,232]. Enhancing the supply of H_2 to the methanogenic archaea in a cost-effective manner has been identified as a key challenge for biomethanation scale-up[46].

Methanogenic biofilm reactors are among the most frequently studied reactor designs for solving the challenge of H_2 mass transfer due to its high gas-liquid mass transfer potential and low energy consumption. The latter was estimated to constitute only about 1% of the H_2 energy input in a trickle bed reactor[117] A critical factor in developing a high-performing and robust biofilm reactor is the build-up and maintenance of an active methanogenic biofilm. A robust biofilm will (1) increase the methanogenic surface density and thus H_2 flux compared to methanogens in suspensions[233]; (2) exhibit increased resilience to chemical inhibitors compared to their planktonic counterparts[234]; (3) not risk dilution by the metabolic water production from methanogenesis.

Previous studies on mixed-culture biomethanation biofilm reactors focus on continuous high-rate production of CH_4-rich gases that comply with natural gas grid standards, but process performances vary widely, e.g. 1.5 $NL_{CH_4} \cdot L^{-1} \cdot d^{-1}$ (98% CH_4) in a mesophilic trickle bed reactor[113] and 30 $NL_{CH_4} \cdot L^{-1} \cdot d^{-1}$ (93% CH_4) in a mesophilic plug flow reactor[89]. While these studies have shown the immediate potential of biofilm reactors, there has been limited focus on how operational conditions affect the formation and activity of methanogenic biofilms from mixed cultures. As an example, a macroscopic biofilm, containing 10% methanogens by the end of experiment, was formed after two weeks of operation in the study by Savvas et al.[89], while no macroscopic biofilm was observed after more than 300 days of operation in a thermophilic trickle bed reactor producing 15.4 $NL_{CH_4} \cdot L^{-1} \cdot d^{-1}$ (98% CH_4)[90]. A thorough understanding of methanogenic biofilm formation in response to reactor operation has the potential to facilitate a substantial progress of the biofilm reactor technology.

Studies in anaerobic and aerobic systems have identified biofilm dynamics to be influenced by several factors like shear stress[235], temperature and nutrient availability[236], type of carrier material[237] and hydraulic retention time (HRT)[238,239]. The present study focuses on the influence of liquid HRT on methanogenic biofilm formation, as this is a universal parameter, which has received limited attention in previous biomethanation biofilm studies. Previous biofilm studies either do not specify liquid handling, or indicate limited or no exchange of reactor liquid equivalent to long HRT conditions[54,90,92]. Biofilm formation has been studied in other systems like wastewater-based aerobic airlift reactors, where biofilm proliferation was limited when HRT exceeded microbial doubling times[238,239]. Similarly, short HRTs (below 24 hours) have been used to support biofilm formation in mesophilic anaerobic fixed-bed reactors for digesting organic material[237,240].

The aim of study was to investigate the impact of liquid HRT on methanogenic biofilm formation and activity on commercial polyethylene carriers in a continuous mesophilic *ex-situ* biomethanation system. Studied HRTs were 18 hours (R_{18h}), 10 days (R_{10d}), and 20 days (R_{20d}). R_{18h} was hence operated with a HRT in the range of mesophilic methanogenic doubling times[40], while HRTs of R_{10d} and R_{20d} reflected conditions with limited medium renewal, as deployed in several biomethanation biofilm studies. The study was conducted with excess H_2 and CO_2 to promote biofilm formation and did thus not focus on obtaining effluent gas with high CH_4 purity (natural gas grid quality), which is otherwise important to *ex-situ* biomethanation. It was hypothesized that (1) biofilm formation and activity increased in R_{18h} due to the increased wash-out of competing planktonic hydrogenotrophic species and (2) that the expected wash-out of slow growing microorganisms in R_{18h} would induce changes in the microbial community compared to those of R_{10d} and R_{20d}. The effect of HRT on biofilm formation was evaluated with biological material from two different sludge-based digesters to test the universality of our findings.

A.2 Material and methods

A.2.1 Experimental conditions

Inoculation and experimental setup

Sludge from a mesophilic, sludge-based anaerobic digester operated at 25 days HRT and 37°C (Marselisborg wastewater treatment plant (WWTP), Denmark) was used as inoculum. The sludge was sieved over a 0.8 mm mesh to remove particles and incubated 15 days at 37°C to lower the content of organic carbon prior to experiment and thereby limit heterotrophic growth advantages and CH_4 production from organic material. Prior to inoculation of the experimental lab reactors, total solids (TS), volatile solids (VS), and pH of the sludge amounted to 1.71%, 0.87%, and 8.18, respectively. Six 1.4 L reactors were inoculated with 400 mL sludge along with 75 Hel-X carriers characterized by a specific surface area of 859 m^2/m^3 (HXF12KLL; Christian Stöhr GmbH & Co.KG, Germany). The carriers replaced less than 4 mL of liquid when submerged but occupied 0.21 L without liquid. Headspace volume was approximately 1 L. The density difference caused the carriers to float on top of the liquid keeping them well in contact with substrate gases in headspace. Reactor temperatures of 37°C (liquid) and 36°C (headspace) were sustained in two shaking water baths (18L; VWR, Denmark) operated at 38 ± 0.2°C and shaking speed 110 /min. The six reactor headspaces were connected in series to enable a continuous flow of H_2 and CO_2 in all reactors (Figure A.1). H_2 and CO_2 were supplied from gas cylinders (Air Liquide Denmark) in a reaction stoichiometric 4:1 ratio at 1.92 $NL_{H_2} \cdot h^{-1}$ and 0.48 $NL_{CO_2} \cdot h^{-1}$. Gas flow rates were controlled with mass flow controllers (Brooks Instruments, USA).

Continuous operation mode

After an initial inoculation period of 24 hours, the reactors were operated at different liquid HRTs in duplicates: 18 hours (R_{18h}), 10 days (R_{10d}), and 20 days (R_{20d}) (Table 1). To avoid that reactor performance was biased by the position in the serial connection, each of the duplicate reactors was placed in different water baths in series with reactors of different HRT (Figure A.1). To minimize variations in headspace gas composition among reactors, gas feed flows were gradually increased to 4.32 $NL_{H_2} \cdot h^{-1}$ and 1.08 $NL_{CO_2} \cdot h^{-1}$ as microbial activities increased, resulting in a constant input of H_2 and CO_2 which by far exceeded the reactors' combined conversion rates. A constant non-limiting availability of gaseous substrates in all reactors was confirmed by periodic compositional analyses of the gas exiting the last reactor in series, which was characterized by 75.7 ± 1.8% H_2, 19.3% ± 0.8% CO_2, and 5.0 ± 2.4% CH_4 throughout the experimental period, with no linkage between reactor position and activity when comparing duplicate reactors.

The influent medium used to maintain HRT was reject water from the anaerobic sludge dewatering process at Marselisborg WWTP. This medium was chosen, because of its potential application as a low-cost nutrient source with a limited content of solids and degradable VS. The influent medium contained 0.3% TS, 0.05% VS with pH 7.9. NH_4^+-N concentration was 898 ± 54 $mg \cdot L^{-1}$ in the 6-month period prior to sampling (data provided by Marselisborg WWTP). The HRT of R_{18h} was maintained using an IPC tubing pump (Ismatec, Germany) that exchanged 50

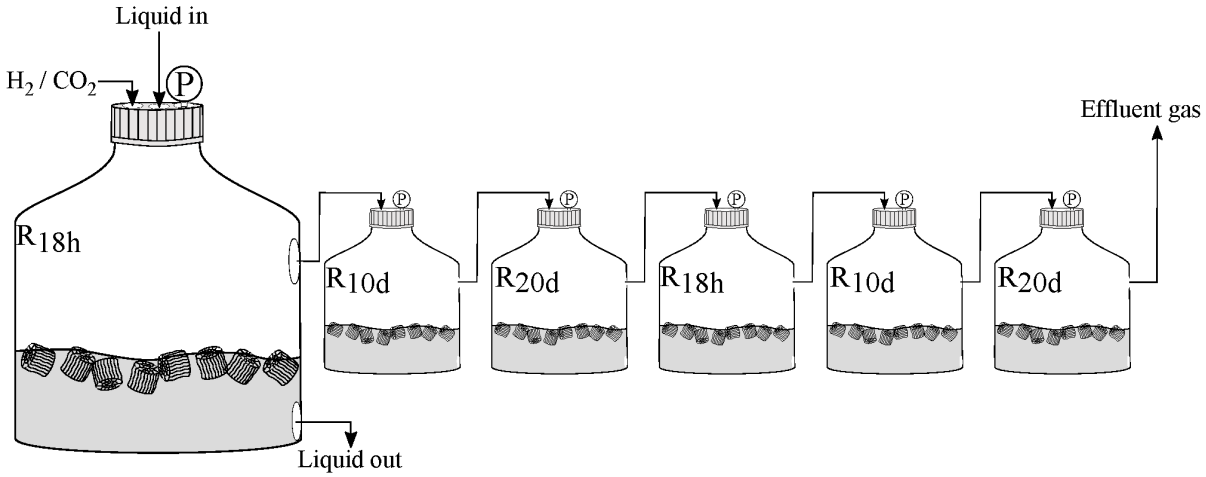

Figure A.1: Schematic overview of the experimental setup during operation. The first reactor is magnified for illustration purposes. H_2 and CO_2 was fed continuously to reactor headspaces connected in series, while carriers floated at the gas-liquid interface. Reactor sequence is indicated with R_{18h}, R_{10d}, and R_{20d} being 18 hours, 10 days, and 20 days HRT, respectively. Liquid was added through the top of the reactor and withdrawn at the bottom according to the specified HRT. Reactors were equipped with pressure sensors (P), valves (not shown), and sampling ports (not shown) for measurements of reaction-induced pressure drop rates and gas sampling. Reactors were placed in shaken water baths to mix and keep temperature at 37°C (not shown).

Table A.1: Experimental conditions. Reactors were operated in duplicates. Experiments with different sludge materials (Marselisborg, Denmark / Garching, Germany) were conducted in separate runs.

	Main study			Replicate study	
Reactor	R_{18h}	R_{10d}	R_{20d}	$R_{18h\text{-}Ge}$	$R_{20d\text{-}Ge}$
HRT	18 hours	10 days	20 days	18 hours	20 days
Sludge source	Marselisborg WWTP (Denmark)			Garching WWTP (Germany)	
Duration of experiment	87 days			45 days	

mL of the reactor volume with 2.25 h interval. HRTs of R_{10d} (40 mL · d^{-1}) and R_{20d} (20 mL · d^{-1}) were maintained manually with maximum interval between feedings being 3 days. The reactors were operated for 87 days.

Biological replicate

An additional experimental trial served to investigate if the source of inoculum and influent medium affected biofilm development and activity (Table B.2). Inoculum (2.28% TS, 1.25% VS, pH 8.0) and influent (0.2% TS, 0.02% VS, pH 8.4, 1,100 ± 527 mg NH_4^+-N · L^{-1}) were sourced from the digester at Garching WWTP (Germany) operated at 40 °C and 30 days HRT. This study was conducted in a similar manner as the above, except that each reactor contained 90 Hel-X carriers and the study was terminated at day 45 (Table 1). HRT 18h ($R_{18h\text{-}Ge}$) and 20d ($R_{20d\text{-}Ge}$) conditions were evaluated.

A.2.2 Activity test

CH_4 production and H_2 uptake rates were periodically determined in batch activity trials. Prior to these activity trials, the gas feed was increased to 12 $NL_{H_2} \cdot h^{-1}$ and 3 $NL_{CO_2} \cdot h^{-1}$ to minimize variations in headspace gas composition further. This was done until a steady gas composition with low CH_4 concentrations (<1.5%) was measured from the last reactor in series. To evaluate total reactor performance, i.e. the combined activity of carrier-based and suspended microorganisms as depicted in Figure A.1, the gas feed was disconnected and individual reactor inlet and outlet valves closed, resulting in reaction-induced pressure drop due to microbial consumption of H_2 and CO_2. CH_4 production and H_2 uptake rates were evaluated from headspace pressure (continuous logging) and gas composition measured after 30 to 120 min depending on the rate of the pressure drop. Pressure drop rates were evaluated at pressures above 900 mbar where the linear pressure profiles indicated that biological rates were independent of the H_2 mass transfer rate (zero-order kinetics). Liquid samples for volatile fatty acids (VFA) analysis were collected following these experiments and stored at -20°C prior to analysis.

To evaluate the carrier (biofilm) activity only, conditioned reactor liquids were completely removed from reactors and stored at room temperature. Carriers were washed in 500 mL reject water at increased shaking speed (120 min^{-1}) to remove conditioned liquid remaining on the carriers and biomass deposits from reactor walls. Washing liquids were discarded, leaving the reactors containing carriers only. Reactors were flushed with H_2 and CO_2, and carrier activities were evaluated on basis of pressure drop and mass balances as described above. Conditioned liquids were reintroduced to the reactors following carrier activity trials, and the system was restored to normal operation with continuous H_2/CO_2 feed.

A.2.3 Analytical methods

H_2, CH_4, and CO_2 concentrations were analyzed using GC-TCD (GC-2014, Shimadzu, Japan) with separate detection pathways for (i) H_2 and (ii) CO_2 and CH_4. H_2 was analyzed from a ShinCarbon ST Packed Column (Restek, USA) using argon as carrier gas. CO_2 and CH_4 were analyzed from a Porapak Q column (Agilent Technologies, USA) using helium as carrier gas. VFAs were analyzed by GC-FID (System 7890A, Agilent Technologies, USA) using a HP-INNOWAX column (Agilent Technologies, USA) with helium as carrier gas. TS and VS were analyzed according to standard procedures (APHA, 2017). Reactor pH was measured manually in the conditioned liquid upon withdrawal during activity tests (section 8.2.2). pH amounted to 7.6 ± 0.1 in all reactors throughout the experiment.

A.2.4 Calculations

Rates

H_2 consumption and CH_4 production rates in units of $NL \cdot L_{reactor}^{-1} \cdot h^{-1}$ (for total reactor performance), and $NL \cdot L_{carrier}^{-1} \cdot h^{-1}$ (for carrier activity only) were determined from:

$$r_{H_2} = \Delta P_{H_2} \cdot V_{hs} \cdot T_{stp} \,/\, (T_{exp} \cdot P_{stp} \cdot \Delta t \cdot V) \tag{A.1}$$

$$r_{CH_4} = \Delta P_{CH_4} \cdot V_{hs} \cdot T_{stp} \,/\, (T_{exp} \cdot P_{stp} \cdot \Delta t \cdot V) \tag{A.2}$$

where ΔP_X (bar) is difference in partial pressures of H_2 and CH_4 from start to end of an activity experiment, V_{hs} (approx. 1.0 L) is reactor headspace volume, T_{stp} and P_{stp} are standard condition temperature (273 K) and pressure (1 bar), respectively, T_{exp} is the headspace temperature (309 K), Δt (h) is the duration of the activity experiment (using zero-order rates as described in section 8.2.2), and V is the working volume (total reactor activity: 0.4 $L_{reactor}$; carrier activity: 0.21 $L_{carrier}$ (Marselisborg) or 0.25 $L_{carrier}$ (Garching).

H_2 and CH_4 rates for carrier trials of R_{10d} and R_{20d} and all trials in $R_{18h\text{-}Ge}$ and $R_{20d\text{-}Ge}$ were estimated from pressure drop rates only, by assuming stoichiometric CH_4 production (4:1:1 H_2:CO_2:CH_4) in accordance with the method of Agneessens et al.[43]. Hence, calculations are similar to the above (r_{H_2}), except that the pressure drop was assumed to be completely caused by H_2 conversion into CH_4.

H_2 mass balances

H_2 can either be consumed via hydrogenotrophic methanogensis:

$$4\ H_2 + CO_2 \rightarrow CH_4 + 2\ H_2O \tag{A.3}$$

or homoacetogenesis:

$$4\ H_2 + 2\ CO_2 \rightarrow CH_3COOH + 2\ H_2O \tag{A.4}$$

Acetate can further be converted by acetoclastic methanogens:

$$CH_3COOH \rightarrow CH_4 + CO_2 \tag{A.5}$$

Acetate accumulation from heterotrophic metabolism was neglected as the influent medium only contained limited amounts of organic substrates (0.02 - 0.05% VS) and 3 ± 7 mg acetate · L^{-1}, with no other VFAs detected. VFA accumulation from biomass decay processes was also neglected. Acetate accumulation was therefore assumed to be a result of the imbalance between homoacetogenic and methanogenic activities. H_2 equivalents accumulated as acetate in the conditioned liquid was estimated according to the above stoichiometry:

$$Y_{H_2,Ac} = F_l \,/\, c_{Ac} \,/\, 4 \,/\, r_{n,H_2} \tag{A.6}$$

where F_l (L · h^{-1}) is liquid flow rate, c_{Ac} (mole · L^{-1}) is acetate concentration, and r_{n,H_2} is the molar H_2 consumption rate (mole · h^{-1}).

CH_4 yields from consumed H_2 were calculated as:

$$Y_{CH_4} = r_{CH_4} \,/\, 4 /\, r_{H_2} \tag{A.7}$$

A.2.5 DNA extraction and amplicon sequencing

Total DNA was extracted from the biofilm using half a carrier, and from 500 µL homogenized liquid from the inoculum, influent and reactor with FastDNA Spin Kit for Soil (MP Biomedicals). Carrier samples were analyzed in biological duplicates, while liquid samples were analyzed without replication. Extracts were quantified using Qubit dsDNA Broad Range Assay Kit and a Qubit 3.0 fluorometer (Thermo Fisher Scientific). Extracts were normalized to 5 ng/µL prior to amplification. The relative microbial composition of liquid and biofilm samples were determined from amplicon sequencing of the V4 region of the 16S rRNA gene. 10 ng of genomic DNA was amplified using the V4 primer set 515F GTGCCAGCMGCCGCGGTAA and 806R GGACTACHVGGGTWTCTAAT[241] in a total reaction volume of 25 µL (containing 2 mU Platinum Taq DNA Polymerase, 1x Platinum High Fidelity buffer (Thermo Fisher Scientific), 400 nM of each dNTP, 1.5 mM $MgSO_4$, and 400 nM of each primer fused with Illumina adaptors) in duplicates. Amplicons were validated using Qubit dsDNA High Sensitivity Assay Kit (Thermo Fisher Scientific), and TapeStation 2200 using D1000 ScreenTapes (Agilent), and subsequently purified using Ampure XP bead protocol (Beckmann Coulter) with a bead:sample ratio of 0.8. Barcoding was performed in accordance with Nextera XT barcode protocol (Illumina). Libraries were pooled in equimolar concentrations and sequenced on a MiSeq platform (Illumina) using MiSeq reagent kit v3 (2 x 300 PE), and a 20% PhiX spike-in.

A.2.6 Data processing and analysis

Raw sequencing reads were subjected to quality control using Trimmomatic v0.32[242], and merged using FLASH v1.2.7[243]. The reads were screened for PhiX contamination and formatted for use with the UPARSE pipeline[244]. Removal of chimeric sequences and clustering into Operational Taxonomic Units (OTUs) was performed using USEARCH7. Taxonomy was assigned using the RDP algorithm implemented in QIIME[245] with the SILVA database release S132 as reference[246]. Analyses of the sequencing data was performed in R version 3.5.2 (https://cran.r-project.org/) via RStudio version 1.1.463 (https://www.rstudio.com/) using the ampvis2 package[247]. Microbial diversities were described using the number of identified OTUs and Chao1 index, while visualizing the 20 most abundant microbial genera with heatmaps. The number of high-quality reads per sample varied between 24,797 and 43,504. Rarefaction curves showed that the sequencing depth sufficiently covered species richness in all samples.

A.2.7 Data availability

The obtained raw sequencing reads have been deposited in the European Nucleotide Archive (ENA) under project accession number PRJEB33152.

A.3 Results and discussion

A.3.1 Methanogenic biofilm activity increases at short HRT

Methanogenic biofilm activity clearly increased in R_{18h} compared to R_{10d} and R_{20d}, where CH_4 production mainly occurred in the liquid phase (Figure A.2). The majority of consumed H_2 was converted to CH_4 in all reactors (Figure A.3), revealing a selective proliferation of methanogenic communities as seen in previous studies[89,233]. After 87 days of operation, carrier-based CH_4 productivity amounted to 0.15 ± 0.01 $NL_{CH_4} \cdot L_{carrier}^{-1} \cdot h^{-1}$ in R_{18h}, 0.028 ± 0.012 $NL_{CH_4} \cdot L_{carrier}^{-1} \cdot h^{-1}$ in R_{10d}, and 0.012 ± 0.003 $NL_{CH_4} \cdot L_{carrier}^{-1} \cdot h^{-1}$ in R_{20d} (Figure A.2), corresponding to 5.4 and 12.5 times higher production rate in R_{18h} compared to R_{10d} and R_{20d}, respectively. 92.2 ± 5.3% of the H_2 consumed by the biofilm in R_{18h} was converted into CH_4 from day 22 and onwards (Figure A.3). Due to their low metabolic rates, biofilm activity from carriers of R_{10d} and R_{20d} (Figure A.2) were estimated based on the observed pressure drop rates and theoretical reaction stoichiometry (4:1:1 H_2:CO_2:CH_4), hereby assuming that all H_2 was converted to CH_4 by the biofilms. The validity of these estimates is evidenced by the high relative abundance of hydrogenotrophic methanogens in the biofilms (Figure A.4), and the observation that 93.5 ± 5.1% (R_{10d}) and 93.3 ± 4.3% (R_{20d}) of the consumed H_2 was converted to CH_4 when evaluating the activity of the total reactor content (Figure A.3). The lower biofilm activities at long HRT conditions reduced overall CH_4 production rates of the total reactor contents (biofilm + reactor liquid), which on average amounted to 0.061 ± 0.011 $NL_{CH_4} \cdot L_{reactor}^{-1} \cdot h^{-1}$ (52% of R_{18h}) and 0.072 ± 0.016 $NL_{CH_4} \cdot L_{reactor}^{-1} \cdot h^{-1}$ (62% of R_{18h}) in R_{10d} and R_{20d}, respectively, compared to 0.12 ± 0.01 $NL_{CH_4} \cdot L_{reactor}^{-1} \cdot h^{-1}$ in R_{18h} (Figure A.2). The individual experimental trials with digestate from both Marselisborg and Garching digesters showed that the effect of HRT was independent of the source of biological material. The development in biofilm and total reactor activities thus followed similar increase in CH_4 production rates within the first 45 days after reactor start-up for R_{18h} and $R_{18h\text{-}Ge}$, and for R_{20d} and $R_{20d\text{-}Ge}$, respectively (Figure A.2).

Methanogenic biofilm activity in R_{18h} was found to be sensitive to excessive feeding of the influent medium (occurring prior to measurements at day 41 and day 52) which resulted in a transient decrease in biofilm CH_4 production rates (Figure A.2). The total reactor performance remained unaffected, indicating that planktonic organisms benefitted from biofilm disturbances (Figure A.2). The biofilm restored its CH_4 production within the following measurements, suggesting that the inhibition was reversible. The excessive feeding incident increased the liquid level in R_{18h}, which impaired reactor mixing and most likely decreased H_2 mass transfer to the biofilm due to increased thickness of the liquid layer that covered the carrier. The reduced H_2 flux would result in a decrease in cell-specific metabolic activity of the methanogens. The (partial) biofilm starvation lasted 1-2 days until liquid levels were reestablished immediately prior to the measurements at day 41 and 52. Although methanogenic communities have previously been shown to recover from starvation within hours after H_2 has been reintroduced[85,117], there would not have been sufficient time for the methanogens to resume full activity during activity trials. The excessive feeding events also diluted the conditioned reactor medium with new influent medium and hereby skewed the balance between homoacetogenesis and methanogenesis, as acetate accumulation in the liquid increased from 1,414 ± 202 mg $\cdot L^{-1}$ at day 31 (pre-perturbations) to 2,149 ± 295 mg $\cdot L^{-1}$

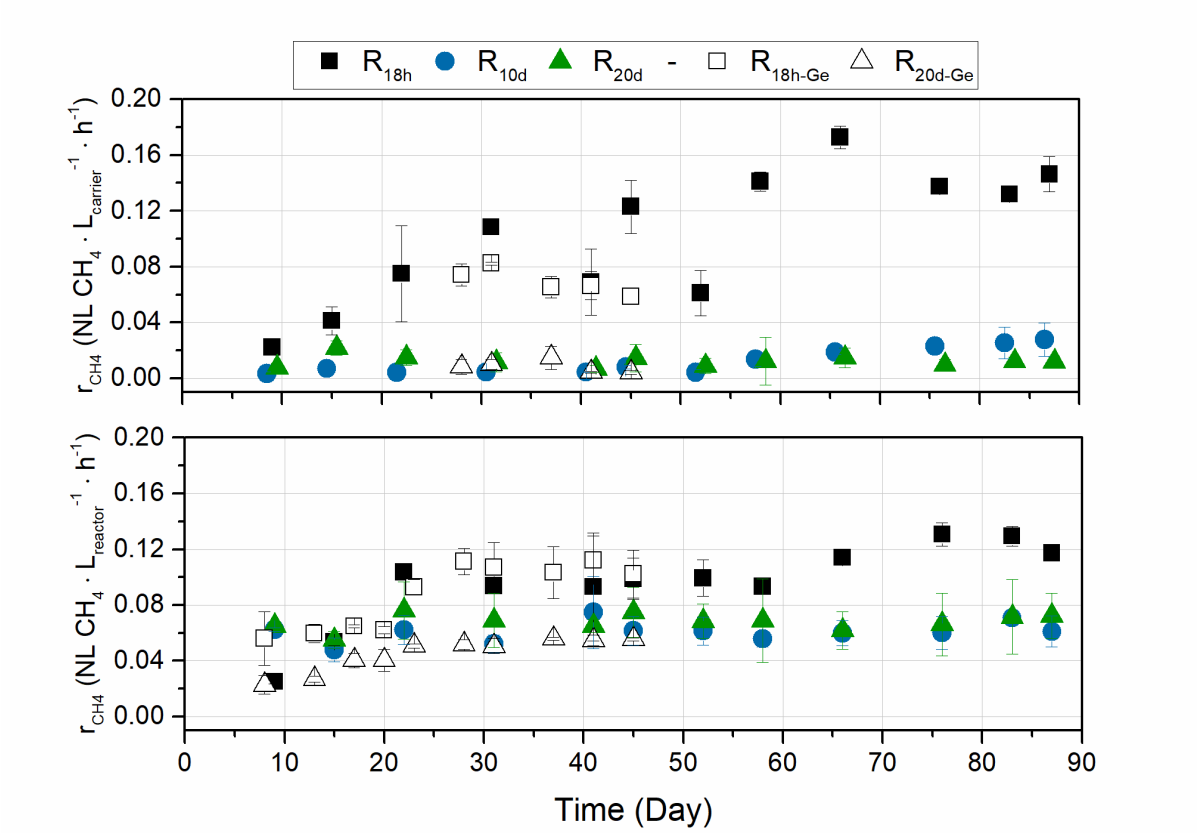

Figure A.2: CH_4 production rates (rCH_4) from carriers (top) and from total reactor content (conditioned liquid and carriers combined) (bottom). Carrier-rates were estimated based on pressure drop rates and stoichiometric CH_4 production (4:1:1 H_2:CO_2:CH_4) except in the case of R_{18h}, where rates were calculated based on mass balances. Rates from total reactor content were estimated in $R_{18h\text{-}Ge}$ and $R_{20d\text{-}Ge}$, but calculated from mass balances in R_{18h}, R_{10d}, and R_{20d}.

and 1,820 ± 1031 mg · L^{-1} at day 45 and 58, respectively (post-perturbation) (Figure A.3). These findings underline the need for further studies on methanogenic biofilm responses to different process perturbations (such as operational incidents), which may occur during biomethanation.

A.3.2 Acetate accumulation increases at short HRT

CH_4 production from H_2 either occurs by hydrogenotrophic methanogenesis, or homoacetogenic acetate production followed by acetoclastic methanogenesis[42]. Acetate accumulation is common during startup of mixed-culture *in-situ* and *ex-situ* biomethanation reactors, where H_2 addition initially stimulates homoacetogenic activity compared to methanogenic activity[42,67,83]. Homoacetogenesis was also considered to be the dominant source of acetate in this study, whereas acetate from organic material was thought to be negligible due to the low VS content (0.05%) in the influent medium. Acetate production was not evaluated during carrier activity trials, but its accumulation was evident in the conditioned liquid of R_{18h}, where it comprised a significant part of the consumed H_2 based on total reactor mass balances (Figure A.3). For R_{18h}, acetate accumulation in the reactor liquid balanced 63 ± 8% (2,366 ± 977 mg · L^{-1}) and 45 ± 1% (2,376 ±

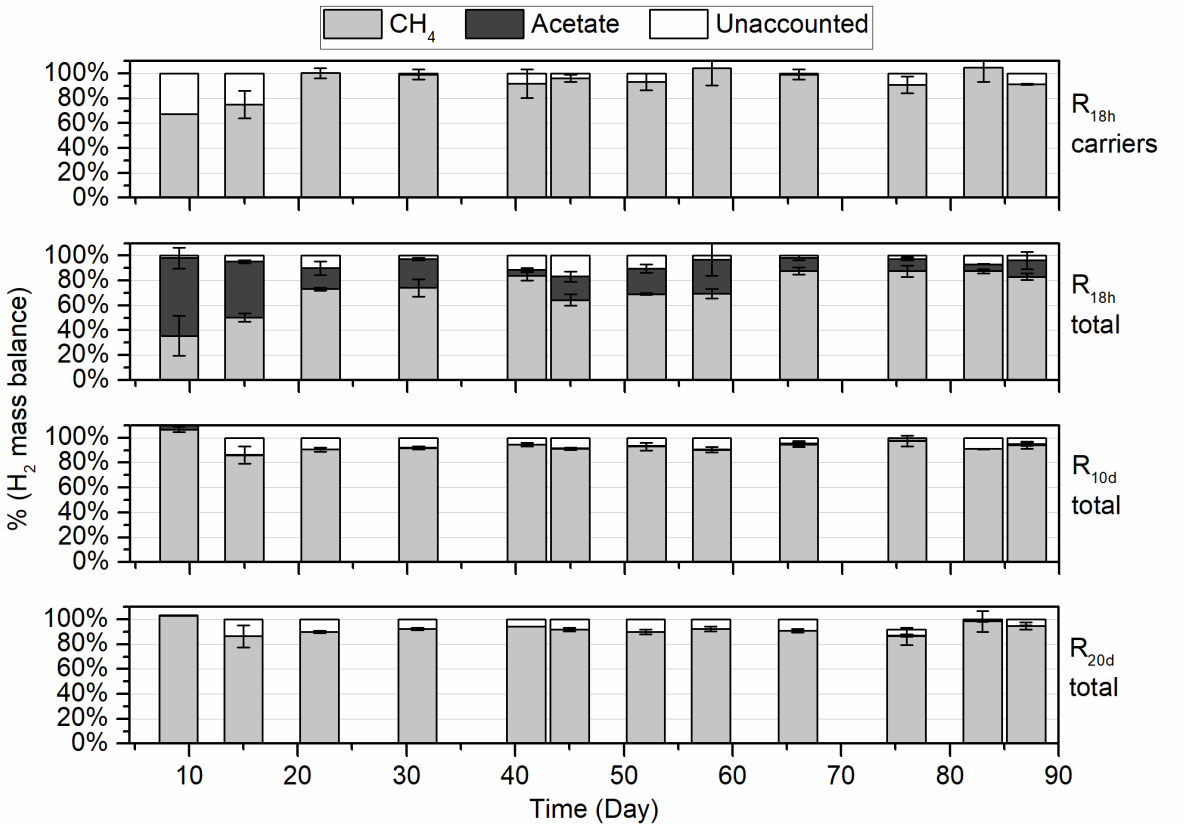

Figure A.3: H_2 mass balances for R_{18h} carrier activity (upper panel) and total reactor activities (biofilm and reactor liquid) of R_{18h}, R_{10d}, and R_{20d}. 'Unaccounted' likely comprised the H_2 fraction assimilated into biomass. Acetate was not measured during carrier activity trials in R_{18h}.

272 mg · L^{-1}) of consumed H_2 at day 9 and 15, respectively, but had declined to 13 ± 7% (866 ± 400 mg · L^{-1}) at day 87 (Figure A.3). CH_4 yields increased accordingly from 36 ± 16% (day 9) to 83 ± 2% (day 87). For R_{10d} and R_{20d}, acetate accumulation corresponded to less than 1% of consumed H_2 throughout the experimental period with average concentrations of 211 ± 319 and 217 ± 362 mg · L^{-1}, respectively (Figure A.3). Hydrogenotrophic methanogenesis was found to gradually outcompete homoacetogenesis at long HRT conditions during *in-situ* biomethanation[42], but the increasing conversion of H_2 to CH_4 in R_{18h} may also reflect increased acetate conversion by acetoclastic methanogens. The microbial profiles confirmed that hydrogenotrophic methanogenesis dominated in all reactors, but acetate was still indicated to be an important intermediate in the conversion of H_2 to CH_4, especially in R_{18h}.

A.3.3 Microbial communities

HRT conditions determine growth of methanogenic biofilms

Methanogenic biofilms formed in all reactors regardless of HRT and source of biological material (Figure A.4). The microbial diversity decreased in both biofilm and liquid samples compared to influent and inoculum media, reflecting a shift in substrates from complex organic molecules to H_2

and CO_2 (Figure A.5). The adapted communities were characterized by complex microbiomes containing hundreds of species with estimated species richness (Chao1) of 360 – 600 in biofilm samples.

The matured biofilms (day 87) of R_{18h}, R_{10d}, and R_{20d} were all dominated by hydrogenotrophic methanogens with species affiliating *Methanobacterium* (14.1% - 20.8% relative abundance) and *Methanobrevibacter* (14.9% - 37.9% relative abundance) being highly abundant (Figure A.4). Both genera are part of the *Methanobacteriaceae* family[248] and these species are commonly dominating biomethanation reactors, both *in-situ*[43,249] and *ex-situ*[54,83,89]. The fact that methanogenic biofilm communities with similar compositions developed regardless of HRT shows that the limited biofilm activity at long HRT was not due to discrimination against microorganisms able to colonize the surface. The predominant production of CH_4 from suspended hydrogenotrophic methanogens in R_{10d} and R_{20d} consequently suggests that H_2 consumption by suspended hydrogenotrophic species in the liquid overlaying the carriers reduces H_2 supply to the biofilm and thereby limits its proliferation, which negatively influences overall biofilm activity (Figure A.2). This effect is more pronounced at long HRT, where liquid biomass accumulates to a larger extend. Similar findings were reported from a wastewater-based airlift reactor, where biofilm biomass increased with decreasing HRT due to wash-out of competing planktonic species[239]. Visual inspections of the carrier materials showed only macroscopic biofilm formation in R_{18h}, which supported the liquid layer's negative influence on biofilm growth at longer HRT. Microscale studies of (non-adapted) mesophilic anaerobic slurry accordingly found that high hydrogenotrophic activity restricted the H_2 diffusion layer to less than 0.5 mm until complete conversion[250]. Even a thin overlaying suspension of active microorganism can therefore reduce H_2 supply to the biofilm significantly.

Increased relevance of acetoclastic methanogenesis at short HRT

HRT affects the importance of acetoclastic methanogenesis. In all reactors, *Sporomusa* sp. constituted a potential source of acetate from H_2 and CO_2, which could be converted to CH_4 by the acetoclastic *Methanosaeta* (Figure A.4). In R_{18h}, acetoclastic *Methanosaeta* comprised 12.2% of the biofilm community compared to 1.3% in both R_{10d} and R_{20d} (Figure A.4). The differences in relative abundance of *Methanosaeta* at short and long HRT comply with the differences in relative abundance of *Sporomusa* and acetate accumulation levels (section 8.3.2), which were both highest in R_{18h}. *Sporomusa* sp. thus comprised 52.4% of the planktonic community and 4.8% of the biofilm community of R_{18h} at day 87 and 28% of the biofilm community in $R_{18h\text{-}Ge}$ at day 45 (Figure A.4). The genus *Sporomusa* harbors known homoacetogens e.g. used for acetate production in microbial electrosynthesis systems[251]. One of the four identified *Sporomusa* OTUs could indeed be assigned to the homoacetogenic *Sporomusa sphaeroides* DSM 2875[252].

The most abundant *Methanosaeta* sequences could be affiliated with *Methanosaeta harundinacea 6Ac*, which has a doubling time of 33 hours in synthetic medium containing 20 mM (1,160 $mg \cdot L^{-1}$) acetate[253]. A doubling time of 33 hours suggests that *M. harundinacea 6Ac* would only be able to survive as part of a biofilm community at a HRT of 18 hours – a fact which was supported by high relative abundance of *Methanosaeta* in the biofilm of R_{18h} (12.2%) and only low relative abundance in the liquid (0.5%) (Figure A.4). Shorter doubling times of 1.8 and 3.1 hours reported for different strains of *Sporomusa*[252] thus facilitate acetate production and accumulation

in R_{18h}. The produced acetate enables proliferation and biofilm formation of the slower growing *Methanosaeta*, supporting the increase in relative production of CH_4 in R_{18h} following inoculation (Figure A.3). The apparent growth advantage of *Sporomusa* reduces in favor of hydrogenotrophic methanogens at long HRT, with high abundance of hydrogenotrophic methanogens ($> 65\%$) in R_{10d} and R_{20d} compared to *Sporomusa* ($< 7\%$) (Figure A.4).

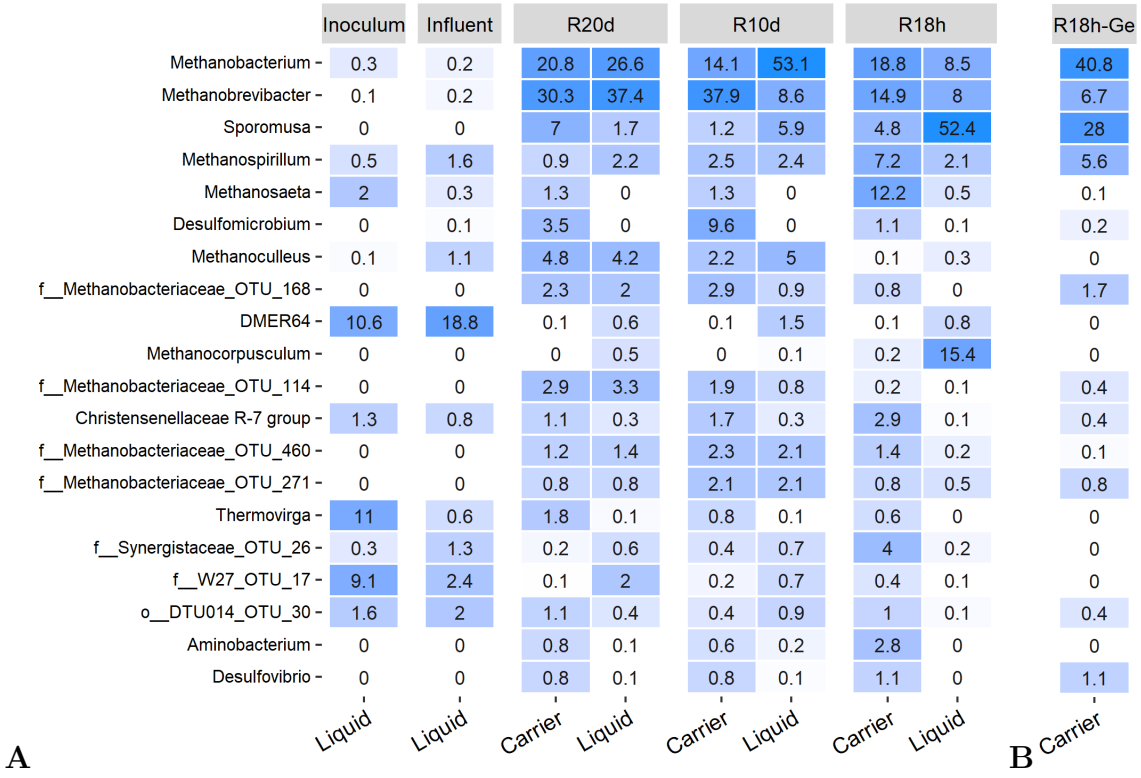

Figure A.4: Heatmap of the 20 most dominant microbial groups presented at genus level. Numbers are averaged on duplicate reactors. (A) Biofilm and liquid sample compositions from reactors with Marselisborg sludge. (B) Biofilm composition from reactor operated at 18 hours HRT using Garching sludge.

A high relative abundance of *Methanosaeta* sp. in the biofilm as observed in R_{18h} (Figure A.4) is uncharacteristic to methanogenic biofilm reactors, but has previously been reported in a high-rate biomethanation reactor with high acetate concentrations during the start-up period ($> 2{,}000$ mg $\cdot$ L^{-1})[89]. These authors do not specify the liquid HRT or size of liquid holding vessel but indicate a high degree of recirculation of a synthetic medium. The current study implies that keeping the duration of liquid H_2 exposure short leads to an increase in relative fitness of homoacetogens and thereby acetoclastic methanogenesis, but the influence of other operational parameters on the balance between these microbial groups needs further investigation.

Methanogenic biofilm formation seemingly requires a phenotypic trait

Research in methanogenic biofilm formation related to biomethanation is scarce, leaving the microbial prerequisites largely uncharacterized. The results from this study indicate that methanogens require specific phenotypic traits in order to form biofilms. The biofilm communities

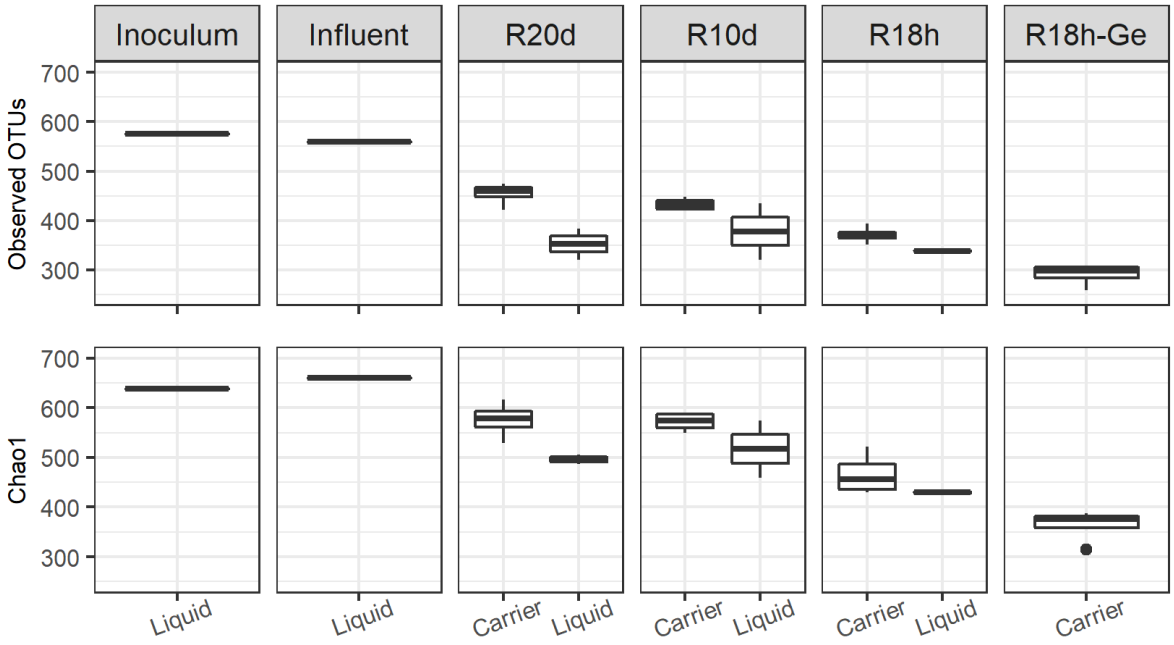

Figure A.5: Alpha diversity. Number of observed OTUs in all samples (A) and Chao1 index (B) as an estimate of true sample richness. $R_{18h\text{-}Ge}$ was operated with Garching digester sludge, which was not analyzed in this study.

were thus highly abundant in methanogenic OTUs, which have previously been associated with biofilm or granule formation (Figure A.4). The most abundant genera across all samples were *Methanobacterium* and *Methanobrevibacter*, which have been found highly abundant in biofilm on cathodes[254], and in granules in upflow anaerobic sludge blanket reactors[255]. Sequences affiliating with *Methanobrevibacter arboriphilus* (DSM 1125), a species which harbors 50 genes important for adhesion[256], were highly abundant in all samples. The identified acetoclastic *Methanosaeta* sp. (1.3% - 12.2% of biofilm communities, Figure A.4) has also been proposed as an important player in anaerobic granule formation[255]. Conversely, *Methanocorpusculum* sp. showed limited ability to form biofilm, as it comprised only 0.2% of the biofilm community in R_{18h}, although its relative abundance in the liquid amounted to 15.4% (Figure A.4). This suggests that species within this genus are not able to produce the necessary extracellular molecules needed to participate in the biofilm community. A previous study accordingly found *Methanocorpusculum* in low abundance in biofilms of an anaerobic fixed bed reactor[257]. However, reported doubling times of 5 - 10 hours enable their growth in the liquid of R_{18h}[258]. These results indicate that the ability to form biofilm is limited to selected genera, irrespective of other operational and controlling factors employed to stimulate biofilm formation in methanogenic biofilm reactors. Optimizing operational conditions of biofilm reactors with respect to the growth of biofilm-forming methanogenic genera may therefore further enhance their colonization and activity.

A.3.4 Implications for high-rate biofilm reactors

Ullrich and Lemmer[119] reported that substrate conversion decreased following carrier wetting in a trickle bed biomethanation reactor due to increased H_2 gas-liquid mass transfer resistance. The present results suggest that biofilm proliferation and thus metabolic capacity is not only restricted by the liquid's physical diffusion barrier, but also by microbial H_2 consumption in the trickling liquid. Carriers were constantly covered by a thin liquid layer in the present experimental setup. The experimental conditions thus resemble constant carrier wetting in a trickle bed reactor while controlling the HRT of the liquid. The HRTs of R_{10d} and R_{20d} mimic conditions in high-rate biofilm reactors where the trickling liquid is retained for a long time in the reactor and therefore repeatedly exposed to H_2 as it is being recirculated over the carrier material. Increased exposure of reactor liquid to H_2 was clearly shown to favor growth of suspended organisms and in turn limit biofilm activity and proliferation by reducing the biofilm's H_2 supply. To reduce the growth of suspended organisms and in this way favor biofilm growth, the liquid's H_2 exposure time must be limited. In high-rate biomethanation biofilm reactors, liquid H_2 exposure can be controlled by adjusting liquid HRT or frequency of the H_2 exposure (i.e. sprinkling frequency). Longer HRTs can therefore be accepted if liquid sprinkling rates over the carriers can be reduced. Dedicated studies investigating the relation between HRT and sprinkling regimes with respect to methanogenic biofilm activity are consequently needed to optimize operation of trickle bed reactors.

The presence of both homoacetogens and acetoclastic methanogens at short HRT indicated that acetate constituted an important intermediate in the conversion of H_2 to CH_4. Accumulated acetate will however constitute a potential loss because acetate can be washed out with the trickling liquid before it is converted to CH_4. Homoacetogens readily take up H_2 and will dominate at the early phase of H_2 addition but acetate accumulation decreases at longer incubation times with H_2 due to methanogenic adaption. Further studies are needed to elucidate how to repress opportunistic homoacetogens while still limiting the trickling liquid's exposure to H_2 for maximum biofilm performance.

A.4 Conclusion

The present study identified HRT as a significant process parameter determining the formation of an active methanogenic biofilm in a mixed-culture *ex-situ* biomethanation system with carriers continuously covered by liquid. Hydrogenotrophic methanogenic species dominated all conditions, but homoacetogenic acetate production increased at short HRT with increased selection of biofilm-forming acetoclastic *Methanosaeta* as a consequence. Reducing liquid HRT or wetting frequency is suggested as important operational parameters for enhancing biofilm formation in biomethanation reactors by limiting the activity of competing hydrogenotrophic species in the liquid overlaying the biofilm.

Acknowledgements

This study was funded by Innovation Fund Denmark (4106-00017B Electrogas), the Danish Council for Strategic Research under the project Nomigas (grant number: 1305-00018B), and through research project "APPLAUSE: Apple - Aarhus University - Sustainable Energy". The authors would also like to express their gratitude to Augustinus Fonden, Knud Højgaards Fond, Oticon Fonden, and the Graduate School of Science and Technology at Aarhus University for financially supporting the stay of MBJ at the Technical University of Munich.

Appendix B

B.1 Peer-reviewed publications

Paper I / Chapter 4
D. Strübing, B. Huber, M. Lebuhn, J. E. Drewes, and K. Koch (2017). "High performance biological methanation in a thermophilic anaerobic trickle bed reactor", *Bioresource Technology*, vol. 245, pp. 1176–1183.

Paper II / Chapter 5
D. Strübing, A.B. Moeller, B. Mößnang, M. Lebuhn, J. E. Drewes, and K. Koch (2018). "Anaerobic thermophilic trickle bed reactor as a promising technology for flexible and demand-oriented H_2/CO_2 biomethanation", *Applied Energy*, vol. 232, pp. 543–554.

Paper III / Chapter 6
D. Strübing, A.B. Moeller, B. Mößnang, M. Lebuhn, J. E. Drewes, and K. Koch (2019). "Load change capability of anaerobic thermophilic trickle bed reactors for dynamic H_2/CO_2 biomethanation", *Bioresource Technology*, vol. 289, Article No. 121735.

Paper IV / Chapter 8 - Appendix A
M. B. Jensen, **D. Strübing**, N. de Jonge, J. L. Nielsen, L. D. M. Ottosen, K. Koch, and M. V. W. Kofoed, (2019). "Stick or leave – pushing methanogens to biofilm formation for ex situ biomethanation", *Bioresource Technology*, vol. 291, Article No. 121784.

B.2 Conference presentations and poster

D. Strübing, J. E. Drewes, and K. Koch (2016). Biologische Methanisierung in Rieselbettreaktoren, 44. Abwassertechnisches Seminar der TU München, Ismaning, Germany, 2016-07-14 (Presentation).

D. Strübing, B. Huber, M. Lebuhn, J. E. Drewes, and K. Koch (2016). "Biologische Methanisierung in Rieselbettreaktoren durch Mischbiozönosen unter thermophilen Bedingungen", OTTI Fachforum "Biologische Methanisierung", Regensburg, Germany,2016-10-25 (Presentation).

D. Strübing, B. Huber, M. Lebuhn, J. E. Drewes, and K. Koch (2017). "Microbial methanation of H_2/CO_2 in anaerobic trickle bed reactors - A study of microbial biocenoses and nutrient supply strategies under thermophilic conditions", International Conference "Progress in Biogas IV", Stuttgart, Germany. 2017-03-09 (Presentation).

M. Lebuhn, **D. Strübing**, B. Huber, J. E. Drewes, and K. Koch (2017). "MikMeth processes for microbial methanation", 3rd International Conference on Biogas Microbiology (ICBM-3),

Wageningen, The Netherlands, 2017-05-03 (Poster).

D. Strübing, B. Huber, M. Lebuhn, J. E. Drewes, and K. Koch (2017). "Conversion and storage of renewable energy via microbial methanation of H_2/CO_2 in thermophilic anaerobic trickle bed reactors", 4^{th} Water Research Conference: The Role of Water Technology Innovation in the Blue Economy, Waterloo, Canada, 2017-09-12 (Presentation).

D. Strübing, B. Huber, M. Lebuhn, J. E. Drewes, and K. Koch (2017). "Microbial methanation of H_2/CO_2 in thermophilic anaerobic trickle bed reactors by a mixed microbial biocenosis", 15^{th} IWA World Conference on Anaerobic Digestion, Bejing, China, 2017-10-19 (Poster).

M. Lebuhn, **D. Strübing**, B. Huber, J. E. Drewes, and K. Koch (2017). "Thermophile Biologische Methanisierung im MikMeth-Prozess", KTBL/FNR Kongress „Biogas in der Landwirtschaft – Stand und Perspektiven", Bayreuth, Germany, 2017-09-27 (Presentation).

D. Strübing, A.B. Moeller, B. Mößnang, M. Lebuhn, J. E. Drewes, and K. Koch (2018). "Demand-oriented H_2 biomethanation in an anaerobic thermophilic trickle bed reactor", 4^{th} Biogas Science Conference - International Conference on Anaerobic Digestion, Torino, Italy, 2018-09-17 (Presentation)

K. Koch, **D. Strübing**, B. Mößnang, M. Lebuhn, and J. E. Drewes (2019)."Betriebserfahrungen mit der BHM im Rieselbettverfahren unter thermophilen Bedingungen", Biogas Infotage 2019, Ulm, Germany, 2019-01-30 (Presentation)

K. Koch, **D. Strübing**, A.B. Moeller, B. Mößnang, M. Lebuhn, and J. E. Drewes (2019). "Anaerobic thermophilic trickle bed reactor as a promising technology for flexible and demand-oriented H_2/CO_2 biomethanation", 16^{th} IWA World Conference on Anaerobic Digestion, Delft, The Netherlands, 2019-06-25 (Presentation)

B.3 Supplementary material - Paper II

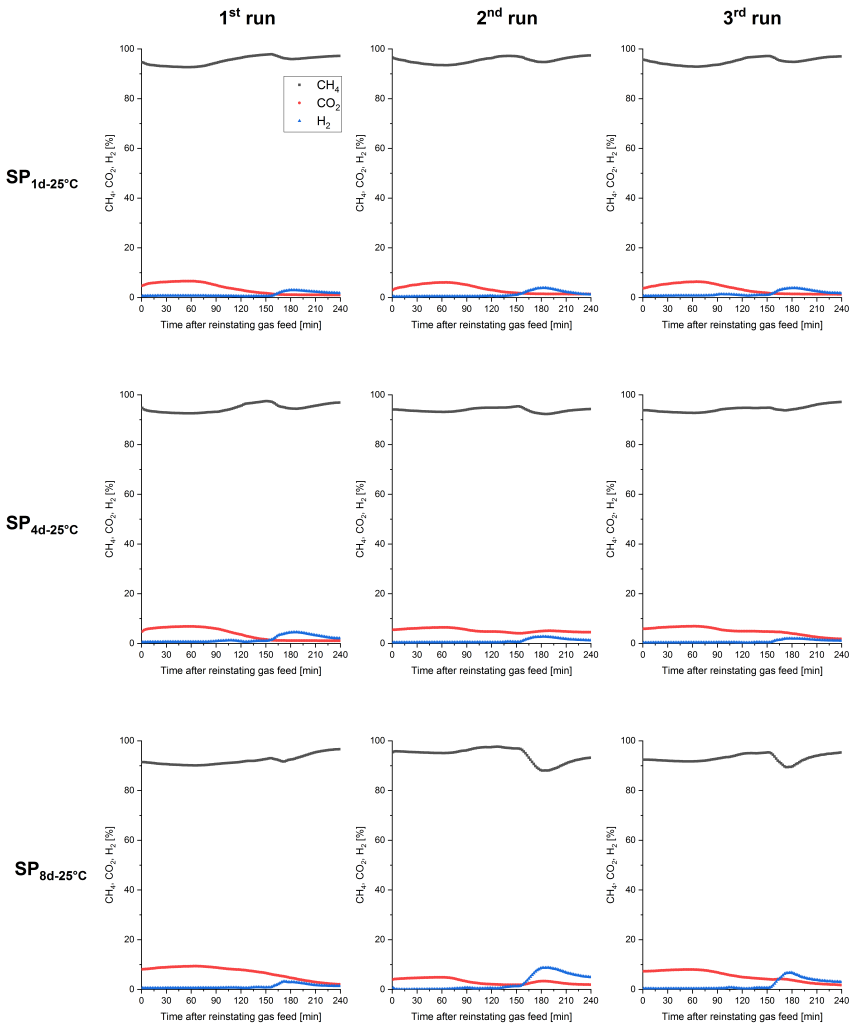

Figure B.1: Time course of CH_4, CO_2 and H_2 during the restart phase for all $SP_{1d\text{-}25°C}$, $SP_{4d\text{-}25°C}$ and $SP_{8d\text{-}25°C}$ experiments.

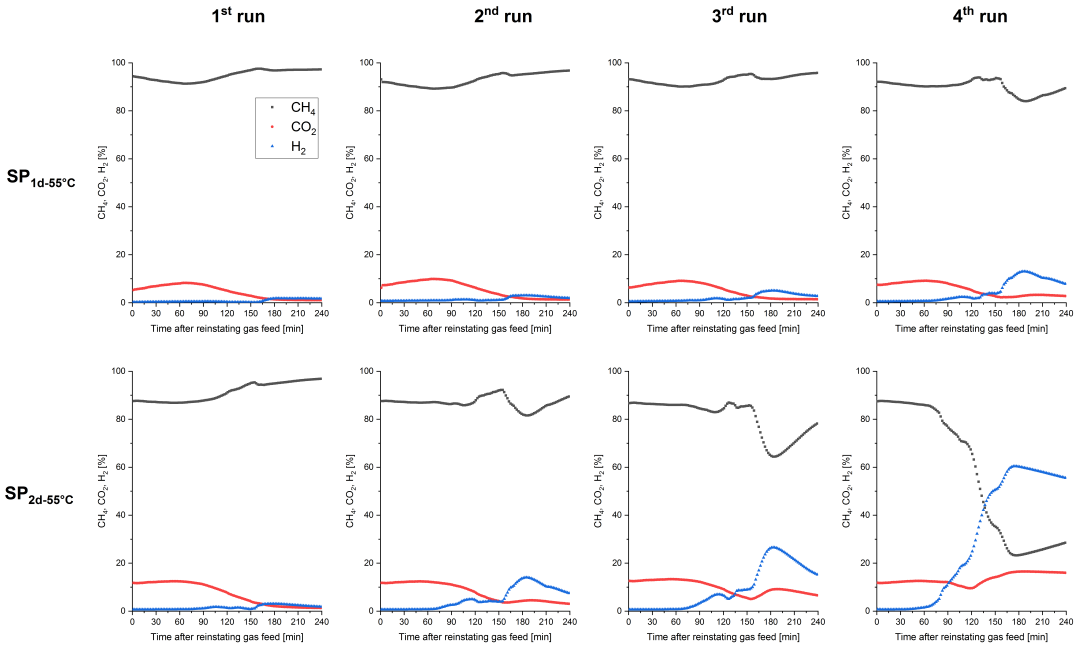

Figure B.2: Time course of CH_4, CO_2 and H_2 during the restart phase for all $SP_{1d\text{-}55°C}$ and $SP_{2d\text{-}55°C}$ experiments.

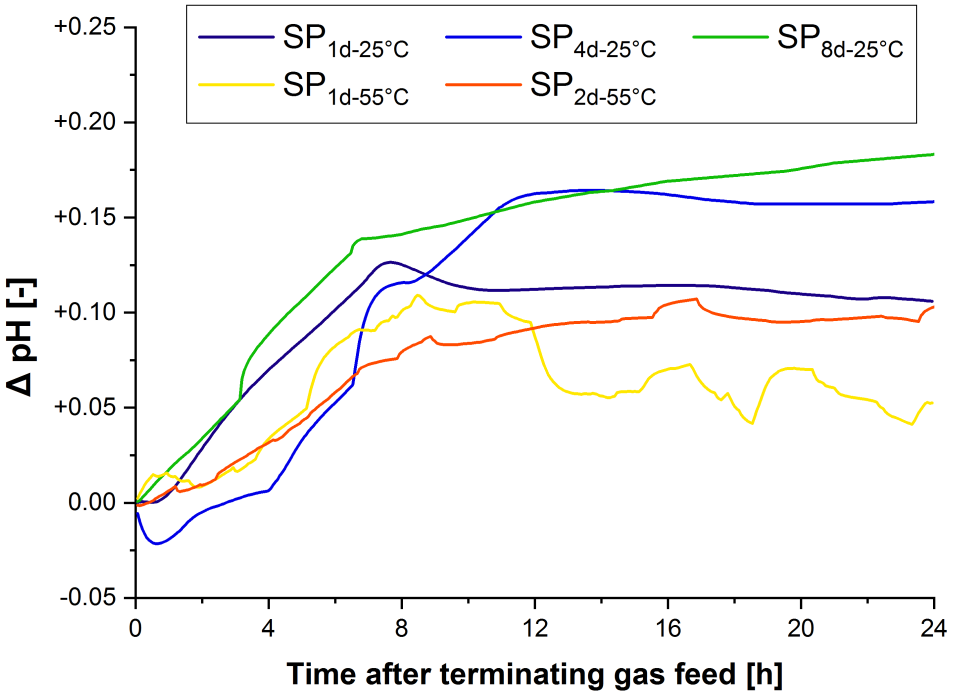

Figure B.3: Time course of Δ pH (averaged for each SP setting) during the first 24 hours of standby periods.

B.4 Supplementary material - Paper III

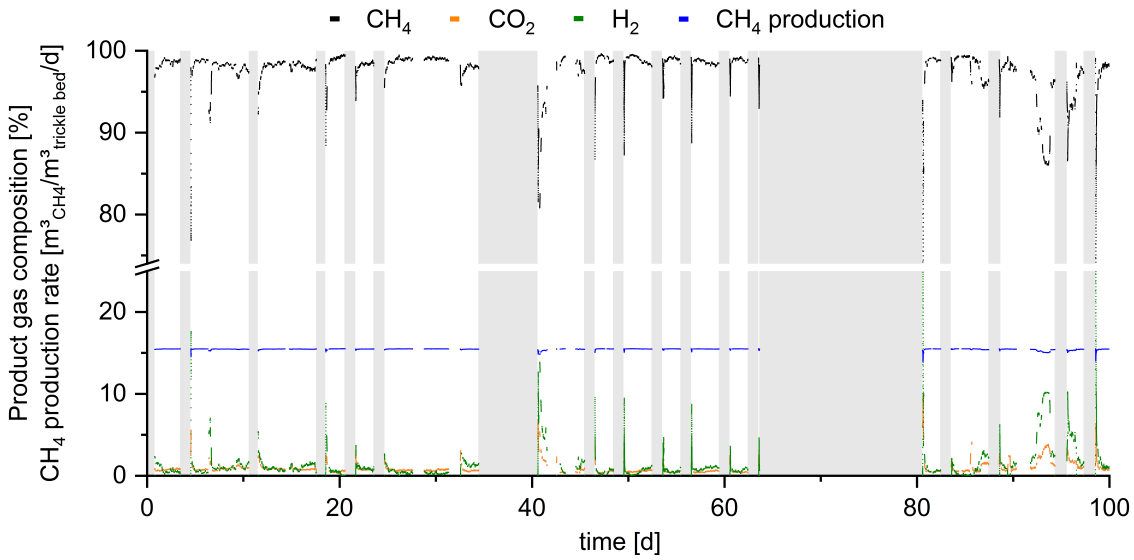

Figure B.4: Product gas composition (CH_4, CO_2, H_2) and methane production rate during the entire experimental period. Grey areas indicate standby periods.

Table B.1: Average composition of mineral medium and ATTBR process liquid throughout the entire experimental period. The process liquid was sampled at the beginning of each SP as well as after reinstating the gas feed (after: 0 minutes, 15 minutes, 30 minutes, 60 minutes, 120 minutes). Acetate, total solids (TS), volatile solids (VS) and ammonium (NH_4^+-N) concentrations were determined as described in Strübing et al.[117]. Total and dissolved chemical oxygen demand (COD) from raw (homogenized) and filtered (0.45 µm) samples, respectively, were determined with photometric cuvette test models LCK 114 and LCK 014 (Hach Lange GmbH, Germany).

	Mineral medium	ATTBR process liquid
Total COD [mg/L]	827 ± 175	8,321 ± 2454
Soluble COD [mg/L]	380 ± 54	4,487 ± 1212
NH_4^+-N [mg/L]	1,251 ± 215	242 ± 110
Total solids [g/L]	1.29 ± 0.17	7.52 ± 2.14
Volatile solids [g/L]	0.50 ± 0.10	4.75 ± 1.58

B.5 Supplementary material - Paper IV

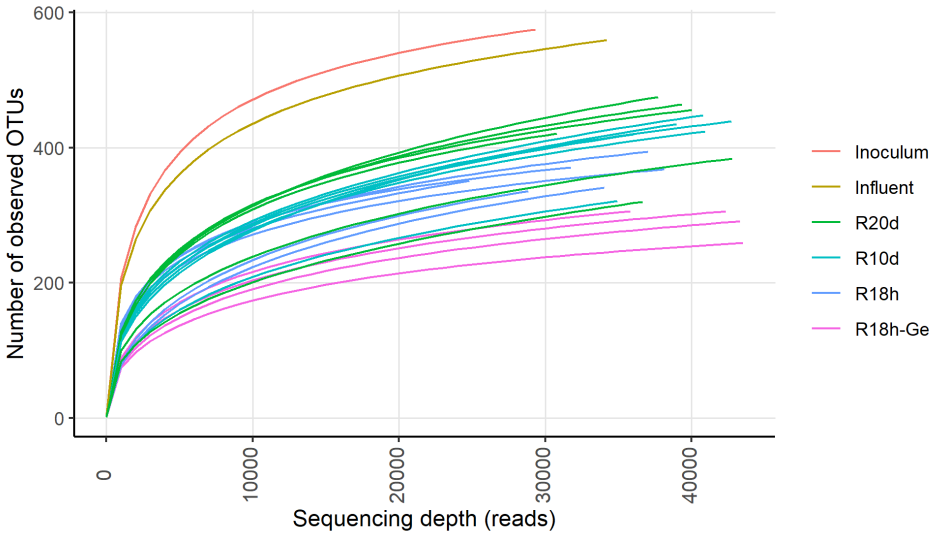

Figure B.5: Rarefaction curves.

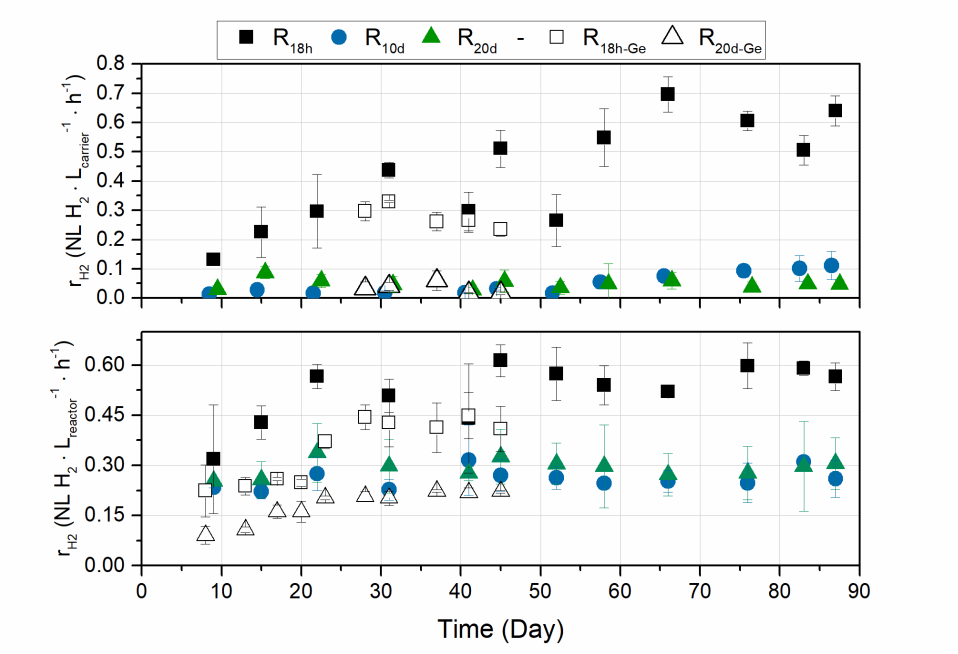

Figure B.6: H_2 conversion rates in R_{18h}, R_{10d}, and R_{20d}. H_2 consumption rates from carriers (top) and from total reactor content (conditioned liquid and carriers combined) (bottom). Carrier-rates (top) were estimated based on pressure drop rates and stoichiometric CH_4 production (4:1:1 H_2:CO_2:CH_4) except in the case of R_{18h}, where rates were calculated based on mass balances. Rates from total reactor content (bottom) were estimated in $R_{18h\text{-}Ge}$ and $R_{20d\text{-}Ge}$, but calculated from mass balances in R_{18h}, R_{10d}, and R_{20d}.

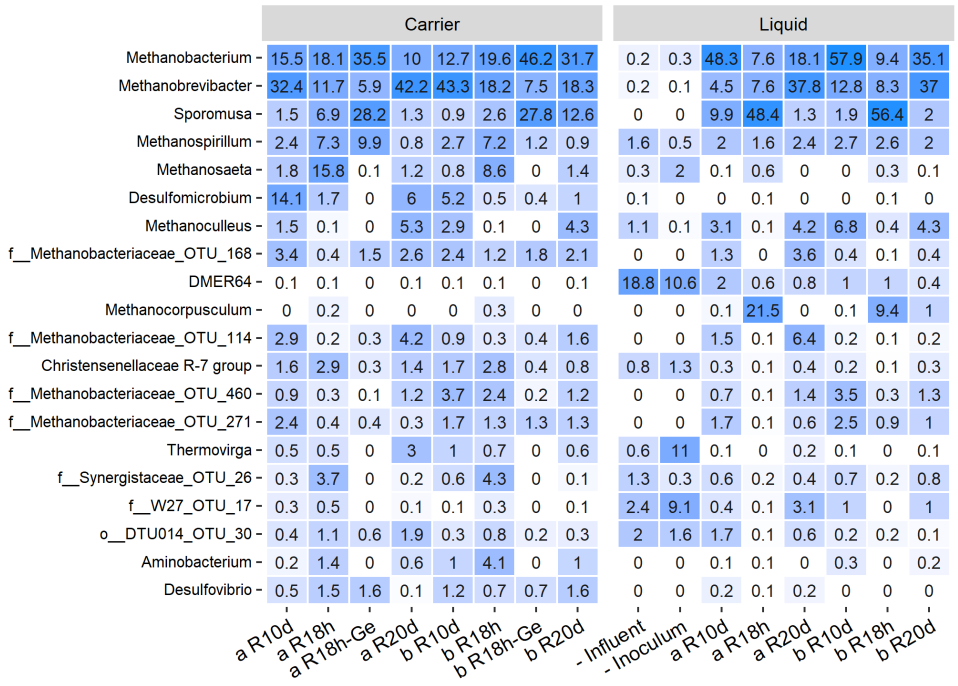

Figure B.7: Heatmap of the 20 most dominant species, presented at genus level for each sample. x-axis is shown by Reactor ID and applied HRT.

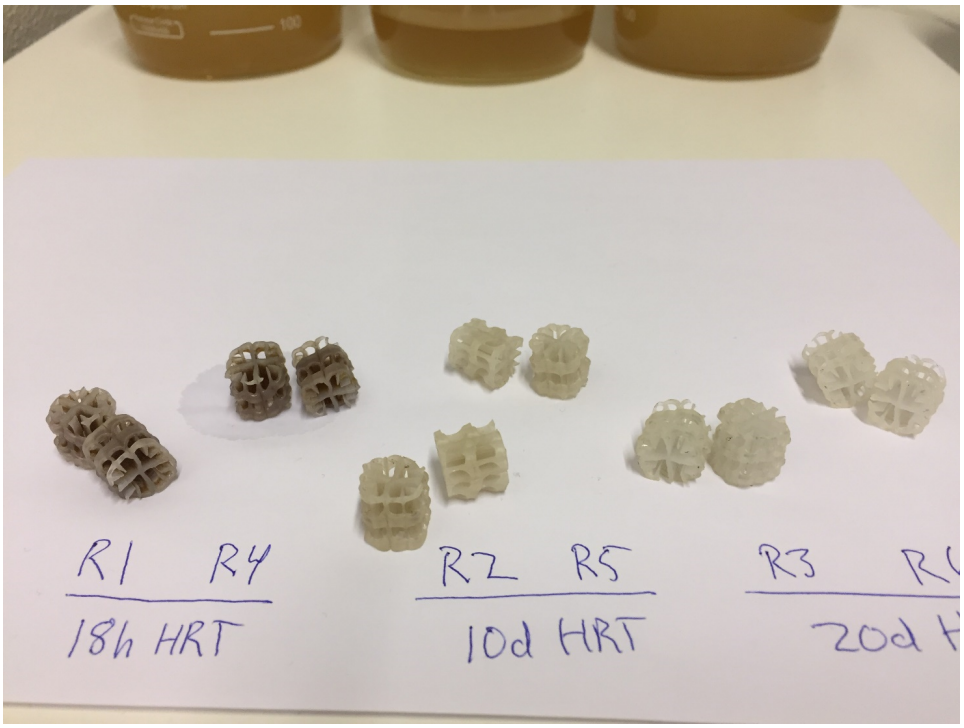

Figure B.8: Carrier appearance by day 87.

Table B.2: Data from ex situ biomethanation biofilm studies with biofilm reactors based on mixed culture inoculum. Reported CH_4 concentrations in effluent gas is given along with methane production rate (MPR). N.A. = Not Available from information provided.

Reactor	MPR ($NL \cdot L^{-1} \cdot d^{-1}$)	Biofilm	Liquid HRT (days)	Liquid recirculation ($L \cdot L^{-1} \cdot d^{-1}$)	T (°C)	Reference
Trickle bed	38 (44 % CH_4)	27% *Euryarchaeota*	N.A.	65 (constant supply)	35	Dupnock and Deshusses,[81]
PFR	30 (93 % CH_4)	10% *methanogens*	N.A.	19.2 (constant supply)	37	Savvas et al.,[89]
Trickle bed	15.4 (98.5 % CH_4)	-	7.4 [1]	4.1 (constant supply)	55	Strübing et al.,[90]
Trickle bed	6.35 (90 % CH_4)	-	No exchange	0.08 (intermittent supply)	54	Alitalo et al.,[92]
Trickle bed	5.6 (95 % CH_4)	-	No exchange	1.1 (intermittent supply)	40 (4 barg)	Ullrich and Lemmer,[119]
Trickle bed	1.9 (95 % CH_4)	-	N.A.	62 (constant supply)	37	(Rachbauer et al.,[84]
Trickle bed	1.7 (95 % CH_4)	30% *archaea*	175 [2]	0.05 (intermittent supply)	54	(Porté et al.,[54]
Trickle bed	1.5 (98% CH_4)	-	N.A.	3.3 (constant supply)	37	Burkhardt et al.,[113]

[1] Estimated from media exchange rate of 100 mL $\cdot$ d^{-1} and metabolic water production at given MPR

[2] Estimated from liquid sample volume and sampling frequency

References

1. European Comission. Energy Roadmap 2050. *Communication from the Commission to the European Parliament, the Council, the European Economic and Social Committee and the Committee of the Regions, Brussels* (2012).
2. Eurostat. Renewable energy statistics 2018. *Statistics explained* (2018).
3. Buttler, A., Dinkel, F., Franz, S. & Spliethoff, H. Variability of wind and solar power – An assessment of the current situation in the European Union based on the year 2014. *Energy* **106,** 147–161 (2016).
4. Heide, D., Greiner, M., von Bremen, L. & Hoffmann, C. Reduced storage and balancing needs in a fully renewable European power system with excess wind and solar power generation. *Renewable Energy* **36,** 2515–2523 (2011).
5. Heide, D., von Bremen, L., Greiner, M., Hoffmann, C., Speckmann, M. & Bofinger, S. Seasonal optimal mix of wind and solar power in a future, highly renewable Europe. *Renewable Energy* **35,** 2483–2489 (2010).
6. Denholm, P. & Hand, M. Grid flexibility and storage required to achieve very high penetration of variable renewable electricity. *Energy Policy* **39,** 1817–1830 (2011).
7. De Sisternes, F. J., Jenkins, J. D. & Botterud, A. The value of energy storage in decarbonizing the electricity sector. *Applied Energy* **175,** 368–379 (2016).
8. Evans, A., Strezov, V. & Evans, T. J. Assessment of utility energy storage options for increased renewable energy penetration. *Renewable and Sustainable Energy Reviews* **16,** 4141–4147 (2012).
9. Götz, M., Lefebvre, J., Mörs, F., Koch, A. M., Graf, F., Bajohr, S., Reimert, R. & Kolb, T. Renewable Power-to-Gas: A technological and economic review. *Renewable Energy* **85,** 1371–1390 (2016).
10. Newton, J. *Power-to-Gas and Methanation - Pathways to a 'Hydrogen Economy'* London, 2014-03-12.
11. Solomon, A. A., Kammen, D. M. & Callaway, D. The role of large-scale energy storage design and dispatch in the power grid: A study of very high grid penetration of variable renewable resources. *Applied Energy* **134,** 75–89 (2014).
12. Guandalini, G., Campanari, S. & Romano, M. C. Power-to-gas plants and gas turbines for improved wind energy dispatchability: Energy and economic assessment. *Applied Energy* **147,** 117–130 (2015).
13. Parra, D., Zhang, X., Bauer, C. & Patel, M. K. An integrated techno-economic and life cycle environmental assessment of power-to-gas systems. *Applied Energy* **193,** 440–454 (2017).
14. Zhang, X., Bauer, C., Mutel, C. L. & Volkart, K. Life Cycle Assessment of Power-to-Gas: Approaches, system variations and their environmental implications. *Applied Energy* **190,** 326–338 (2017).
15. Schiebahn, S., Grube, T., Robinius, M., Tietze, V., Kumar, B. & Stolten, D. Power to gas: Technological overview, systems analysis and economic assessment for a case study in Germany. *International Journal of Hydrogen Energy* **40,** 4285–4294 (2015).
16. Al Rowaihi, I. S., Kick, B., Grötzinger, S. W., Burger, C., Karan, R., Weuster-Botz, D., Eppinger, J. & Arold, S. T. A two-stage biological gas to liquid transfer process to convert carbon dioxide into bioplastic. *Bioresource Technology Reports* **1,** 61–68 (2018).

17. Gahleitner, G. Hydrogen from renewable electricity: An international review of power-to-gas pilot plants for stationary applications. *International Journal of Hydrogen Energy* **38,** 2039–2061 (2013).

18. Ullah Khan, I., Hafiz Dzarfan Othman, M., Hashim, H., Matsuura, T., Ismail, A. F., Rezaei-DashtArzhandi, M. & Wan Azelee, I. Biogas as a renewable energy fuel – A review of biogas upgrading, utilisation and storage. *Energy Conversion and Management* **150,** 277–294 (2017).

19. Meylan, F. D., Moreau, V. & Erkman, S. Material constraints related to storage of future European renewable electricity surpluses with CO_2 methanation. *Energy Policy* **94,** 366–376 (2016).

20. Muñoz, R., Meier, L., Diaz, I. & Jeison, D. A review on the state-of-the-art of physical/chemical and biological technologies for biogas upgrading. *Reviews in Environmental Science and Bio/Technology* **14,** 727–759 (2015).

21. Genovese, J., Harg, K., Paster, M. & Turner, J. *Current (2009) State-of-the-Art Hydrogen Production Cost Estimate Using Water Electrolysis: Independent Review: Published for the U.S. Department of Energy Hydrogen Program* (ed National Renewable Energy Lab.) Golden, Colorado, USA, 2009.

22. Carmo, M., Fritz, D. L., Mergel, J. & Stolten, D. A comprehensive review on PEM water electrolysis. *International Journal of Hydrogen Energy* **38,** 4901–4934 (2013).

23. van Dael, M., Kreps, S., Virag, A., Kessels, K., Remans, K., Thomas, D. & de Wilde, F. Techno-economic assessment of a microbial power-to-gas plant – Case study in Belgium. *Applied Energy* **215,** 416–425 (2018).

24. Ghaib, K. & Ben-Fares, F.-Z. Power-to-Methane: A state-of-the-art review. *Renewable and Sustainable Energy Reviews* **81,** 433–446 (2018).

25. Rönsch, S., Schneider, J., Matthischke, S., Schlüter, M., Götz, M., Lefebvre, J., Prabhakaran, P. & Bajohr, S. Review on methanation – From fundamentals to current projects. *Fuel* **166,** 276–296 (2016).

26. Kopyscinski, J., Schildhauer, T. J. & Biollaz, S. M. Production of synthetic natural gas (SNG) from coal and dry biomass – A technology review from 1950 to 2009. *Fuel* **89,** 1763–1783 (2010).

27. Schaaf, T., Grünig, J., Schuster, M. R., Rothenfluh, T. & Orth, A. Methanation of CO_2 - storage of renewable energy in a gas distribution system. *Energy, Sustainability and Society* **4,** 342 (2014).

28. Mills, G. A. & Steffgen, F. W. Catalytic Methanation. *Catalysis Reviews* **8,** 159–210 (1974).

29. Seifert, A. H., Rittmann, S. K.-M., Bernacchi, S. & Herwig, C. Method for assessing the impact of emission gasses on physiology and productivity in biological methanogenesis. *Bioresource Technology* **136,** 747–751 (2013).

30. Bartholomew, C. H. Mechanisms of catalyst deactivation. *Applied Catalysis A: General* **212,** 17–60 (2001).

31. Angelidaki, I., Treu, L., Tsapekos, P., Luo, G., Campanaro, S., Wenzel, H. & Kougias, P. G. Biogas upgrading and utilization: Current status and perspectives. *Biotechnology Advances* **36,** 452–466 (2018).

32. Luo, G. & Angelidaki, I. Integrated biogas upgrading and hydrogen utilization in an anaerobic reactor containing enriched hydrogenotrophic methanogenic culture. *Biotechnology and Bioengineering* **109,** 2729–2736 (2012).

33. Wise, D. L., Cooney, C. L. & Augenstein, D. C. Biomethanation: Anaerobic fermentation of CO2, H2 and CO to methane. *Biotechnology and Bioengineering,* 1153–1172 (1978).

34. Schink, B. Energetics of syntrophic cooperation in methanogenic degradation. *Microbiology and Molecular Biology Reviews* **61,** 262–280 (1997).

35. Weiland, P. Biogas production: Current state and perspectives. *Applied Microbiology and Biotechnology* **85,** 849–860 (2010).

36. Rittmann, S. K.-M. in *Biogas Science and Technology* 117–135 (Springer, 2015).

37. Bailera, M., Lisbona, P., Romeo, L. M. & Espatolero, S. Power to Gas projects review: Lab, pilot and demo plants for storing renewable energy and CO_2. *Renewable and Sustainable Energy Reviews* **69,** 292–312 (2017).

38. Zabranska, J. & Pokorna, D. Bioconversion of carbon dioxide to methane using hydrogen and hydrogenotrophic methanogens. *Biotechnology Advances* **36,** 707–720 (2017).

39. Sahota, S., Shah, G., Ghosh, P., Kapoor, R., Sengupta, S., Singh, P., Vijay, V., Sahay, A., Vijay, V. K. & Thakur, I. S. Review of trends in biogas upgradation technologies and future perspectives. *Bioresource Technology Reports* **1,** 79–88 (2018).

40. Demirel, B. & Scherer, P. The roles of acetotrophic and hydrogenotrophic methanogens during anaerobic conversion of biomass to methane: a review. *Reviews in Environmental Science and Bio/Technology* **7,** 173–190 (2008).

41. Angelidaki, I., Karakashev, D., Batstone, D. J., Plugge, C. M. & Stams, A. J. M. Biomethanation and its potential. *Methods in enzymology* **494,** 327–351 (2011).

42. Agneessens, L. M., Ottosen, L. D. M., Andersen, M., Berg Olesen, C., Feilberg, A. & Kofoed, M. V. W. Parameters affecting acetate concentrations during in-situ biological hydrogen methanation. *Bioresource Technology* **258,** 33–40 (2018).

43. Agneessens, L. M., Ottosen, L. D. M., Voigt, N. V., Nielsen, J. L., de Jonge, N., Fischer, C. H. & Kofoed, M. V. W. In-situ biogas upgrading with pulse H_2 additions: The relevance of methanogen adaption and inorganic carbon level. *Bioresource Technology* **233,** 256–263 (2017).

44. Bassani, I., Kougias, P. G. & Angelidaki, I. In-situ biogas upgrading in thermophilic granular UASB reactor: key factors affecting the hydrogen mass transfer rate. *Bioresource Technology* **221,** 485–491 (2016).

45. Fontana, A., Kougias, P. G., Treu, L., Kovalovszki, A., Valle, G., Cappa, F., Morelli, L., Angelidaki, I. & Campanaro, S. Microbial activity response to hydrogen injection in thermophilic anaerobic digesters revealed by genome-centric metatranscriptomics. *Microbiome* **6,** 194 (2018).

46. Jensen, M. B., Kofoed, M. V. W., Fischer, K., Voigt, N. V., Agneessens, L. M., Batstone, D. J. & Ottosen, L. D. M. Venturi-type injection system as a potential H_2 mass transfer technology for full-scale in situ biomethanation. *Applied Energy* **222,** 840–846 (2018).

47. Lovato, G., Alvarado-Morales, M., Kovalovszki, A., Peprah, M., Kougias, P. G., Rodrigues, J. A. D. & Angelidaki, I. In-situ biogas upgrading process: Modeling and simulations aspects. *Bioresource Technology* **245,** 332–341 (2017).

48. Luo, G. & Angelidaki, I. Co-digestion of manure and whey for in situ biogas upgrading by the addition of H(2): Process performance and microbial insights. *Applied Microbiology and Biotechnology* **97,** 1373–1381 (2013).

49. Luo, G. & Angelidaki, I. Hollow fiber membrane based H_2 diffusion for efficient in situ biogas upgrading in an anaerobic reactor. *Applied Microbiology and Biotechnology* **97,** 3739–3744 (2013).

50. Lecker, B., Illi, L., Lemmer, A. & Oechsner, H. Biological hydrogen methanation - A Review. *Bioresource Technology* **245,** 1220–1228 (2017).

51. Guiot, S. R., Cimpoia, R. & Carayon, G. Potential of wastewater-treating anaerobic granules for biomethanation of synthesis gas. *Environmental Science & Technology* **45,** 2006–2012 (2011).

52. Sander, R. Compilation of Henry's law constants (version 4.0) for water as solvent. *Atmospheric Chemistry & Physics* **15** (2015).

53. Corbellini, V., Kougias, P. G., Treu, L., Bassani, I., Malpei, F. & Angelidaki, I. Hybrid biogas upgrading in a two-stage thermophilic reactor. *Energy Conversion and Management* **168,** 1–10 (2018).

54. Porté, H., Kougias, P. G., Alfaro, N., Treu, L., Campanaro, S. & Angelidaki, I. Process performance and microbial community structure in thermophilic trickling biofilter reactors for biogas upgrading. *Science of The Total Environment* **655,** 529–538 (2018).

55. O'Flaherty, V., Mahony, T., O'Kennedy, R. & Colleran, E. Effect of pH on growth kinetics and sulphide toxicity thresholds of a range of methanogenic, syntrophic and sulphate-reducing bacteria. *Process Biochemistry* **33,** 555–569 (1998).

56. Bassani, I., Kougias, P. G., Treu, L. & Angelidaki, I. Biogas upgrading via hydrogenotrophic methanogenesis in two-stage continuous stirred tank reactors at mesophilic and thermophilic conditions. *Environmental Science & Technology* **49,** 12585–12593 (2015).

57. Yenigün, O. & Demirel, B. Ammonia inhibition in anaerobic digestion: A review. *Process Biochemistry* **48,** 901–911 (2013).

58. Deublein, D. & Steinhauser, A. *Biogas from Waste and Renewable Resources: An Introduction* 4th ed. (John Wiley & Sons, Hoboken, 2011).

59. Schmidt, J. E. & Ahring, B. K. Effects of hydrogen and formate on the degradation of propionate and butyrate in thermophilic granules from an upflow anaerobic sludge blanket reactor. *Applied and Environmental Microbiology* **59,** 2546–2551 (1993).

60. Ahring, B. K. & Westermann, P. Product Inhibition of Butyrate Metabolism by Acetate and Hydrogen in a Thermophilic Coculture. *Applied and Environmental Microbiology* **54,** 2393–2397 (1988).

61. Ahring, B. K. & Westermann, P. Kinetics of butyrate, acetate, and hydrogen metabolism in a thermophilic, anaerobic, butyrate-degrading triculture. *Applied and Environmental Microbiology* **53,** 434–439 (1987).

62. Flotats, X., Ahring, B. K. & Angelidaki, I. Parameter Identification of Thermophilic Anaerobic Degradation of Valerate. *Applied Biochemistry and Biotechnology* **109,** 47–62 (2003).

63. Ahring, B. K., Sandberg, M. & Angelidaki, I. Volatile fatty acids as indicators of process imbalance in anaerobic digestors. *Applied Microbiology and Biotechnology* **43,** 559–565 (1995).

64. Liu, Y. & Whitman, W. B. Metabolic, phylogenetic, and ecological diversity of the methanogenic archaea. *Annals of the New York Academy of Sciences* **1125,** 171–189 (2008).

65. Pind, P. F., Angelidaki, I. & Ahring, B. K. Dynamics of the anaerobic process: Effects of volatile fatty acids. *Biotechnology and Bioengineering* **82,** 791–801 (2003).

66. Kotsyurbenko, O. R. Trophic interactions in the methanogenic microbial community of low-temperature terrestrial ecosystems. *FEMS microbiology ecology* **53,** 3–13 (2005).

67. Liu, R., Hao, X. & Wei, J. Function of homoacetogenesis on the heterotrophic methane production with exogenous H_2/CO_2 involved. *Chemical Engineering Journal* **284,** 1196–1203 (2016).

68. Batstone, D. J., Pind, P. F. & Angelidaki, I. Kinetics of thermophilic, anaerobic oxidation of straight and branched chain butyrate and valerate. *Biotechnology and Bioengineering* **84,** 195–204 (2003).

69. Bernacchi, S., Rittmann, S. K.-M., Seifert, A., Krajete, A. & Herwig, C. Experimental methods for screening parameters influencing the growth to product yield ($Y_{(x/CH4)}$) of a biological methane production (BMP) process performed with Methanothermobacter marburgensis. *AIMS Bioengineering* **1,** 72–86 (2014).

70. Bernacchi, S., Weissgram, M., Wukovits, W. & Herwig, C. Process efficiency simulation for key process parameters in biological methanogenesis. *AIMS Bioengineering* **1,** 53–71 (2014).

71. Fardeau, M.-L., Peillex, J.-P. & Belaich, J.-P. Energetics of the growth of Methanobacterium thermoautotrophicum and Methanococcus thermolithotrophicus on ammonium chloride and dinitrogen. *Archives of Microbiology* **148,** 128–131 (1987).

72. Martin, M. R., Fornero, J. J., Stark, R., Mets, L. & Angenent, L. T. A single-culture bioprocess of *Methanothermobacter thermautotrophicus* to upgrade digester biogas by CO_2-to-CH_4 conversion with H_2. *Archaea* **2013,** 1–11 (2013).

73. Mauerhofer, L.-M., Reischl, B., Schmider, T., Schupp, B., Nagy, K., Pappenreiter, P., Zwirtmayr, S., Schuster, B., Bernacchi, S., Seifert, A. H., Paulik, C. & Rittmann, S. K.-M. R. Physiology and methane productivity of Methanobacterium thermaggregans. *Applied Microbiology and Biotechnology* (2018).

74. Peillex, J.-P., Fardeau, M.-L. & Belaich, J.-P. Growth of Methanobacterium thermoautotrophicum on H_2-CO_2: High CH_4 Productivities in Continuous Culture. *Biomass* **21,** 315–321 (1990).

75. Peillex, J.-P., Fardeau, M.-L., Boussand, R., Navarro, J.-M. & Belaich, J.-P. Growth of Methanococcus thermolithotrophicus in batch and continuous culture on H_2 and CO_2: influence of agitation. *Applied Microbiology and Biotechnology* **29,** 560–564 (1988).

76. Rittmann, S. K.-M., Seifert, A. H. & Bernacchi, S. Kinetics, multivariate statistical modelling, and physiology of CO_2 -based biological methane production. *Applied Energy* **216,** 751–760 (2018).

77. Seifert, A. H., Rittmann, S. K.-M. & Herwig, C. Analysis of process related factors to increase volumetric productivity and quality of biomethane with *Methanothermobacter marburgensis*. *Applied Energy* **132,** 155–162 (2014).

78. Alfaro, N., Fdz-Polanco, M., Fdz-Polanco, F. & Díaz, I. Evaluation of process performance, energy consumption and microbiota characterization in a ceramic membrane bioreactor for ex-situ biomethanation of H_2 and CO_2. *Bioresource Technology* **258,** 142–150 (2018).

79. Bassani, I., Kougias, P. G., Treu, L., Porté, H., Campanaro, S. & Angelidaki, I. Optimization of hydrogen dispersion in thermophilic up-flow reactors for ex situ biogas upgrading. *Bioresource Technology* **234,** 310–319 (2017).

80. Burkhardt, M. & Busch, G. Methanation of hydrogen and carbon dioxide. *Applied Energy* **111,** 74–79 (2013).

81. Dupnock, T. L. & Deshusses, M. A. High-Performance Biogas Upgrading Using a Biotrickling Filter and Hydrogenotrophic Methanogens. *Applied Biochemistry and Biotechnology* **183,** 488–502 (2017).

82. Kougias, P. G., Treu, L., Benavente, D. P., Boe, K., Campanaro, S. & Angelidaki, I. Ex-situ biogas upgrading and enhancement in different reactor systems. *Bioresource Technology* **225,** 429–437 (2017).

83. Rachbauer, L., Beyer, R., Bochmann, G. & Fuchs, W. Characteristics of adapted hydrogenotrophic community during biomethanation. *Science of The Total Environment* **595,** 912–919 (2017).

84. Rachbauer, L., Voitl, G., Bochmann, G. & Fuchs, W. Biological biogas upgrading capacity of a hydrogenotrophic community in a trickle-bed reactor. *Applied Energy* **180,** 483–490 (2016).

85. Savvas, S., Donnelly, J., Patterson, T., Chong, Z. S. & Esteves, S. R. Methanogenic capacity and robustness of hydrogenotrophic cultures based on closed nutrient recycling via microbial catabolism: Impact of temperature and microbial attachment. *Bioresource Technology* **257,** 164–171 (2018).

86. Savvas, S., Donnelly, J., Patterson, T. P., Dinsdale, R. & Esteves, S. R. Closed nutrient recycling via microbial catabolism in an eco-engineered self regenerating mixed anaerobic microbiome for hydrogenotrophic methanogenesis. *Bioresource Technology* **227,** 93–101 (2017).

87. Voelklein, M. A., Rusmanis, D. & Murphy, J. D. Biological methanation: Strategies for in-situ and ex-situ upgrading in anaerobic digestion. *Applied Energy* **235,** 1061–1071 (2019).

88. Kleerebezem, R. & van Loosdrecht, M. C. M. Mixed culture biotechnology for bioenergy production. *Current Opinion in Biotechnology* **18,** 207–212 (2007).

89. Savvas, S., Donnelly, J., Patterson, T., Chong, Z. S. & Esteves, S. R. Biological methanation of CO_2 in a novel biofilm plug-flow reactor: A high rate and low parasitic energy process. *Applied Energy* **202,** 238–247 (2017).

90. Strübing, D., Huber, B., Lebuhn, M., Drewes, J. E. & Koch, K. High performance biological methanation in a thermophilic anaerobic trickle bed reactor. *Bioresource Technology* **245,** 1176–1183 (2017).

91. Díaz, I., Pérez, C., Alfaro, N. & Fdz-Polanco, F. A feasibility study on the bioconversion of CO_2 and H_2 to biomethane by gas sparging through polymeric membranes. *Bioresource Technology* **185,** 246–253 (2015).

92. Alitalo, A., Niskanen, M. & Aura, E. Biocatalytic methanation of hydrogen and carbon dioxide in a fixed bed bioreactor. *Bioresource Technology* **196,** 600–605 (2015).

93. Ju, D.-H., Shin, J.-H., Lee, H.-K., Kong, S.-H., Kim, J.-I. & Sang, B.-I. Effects of pH conditions on the biological conversion of carbon dioxide to methane in a hollow-fiber membrane biofilm reactor (Hf–MBfR). *Desalination* **234,** 409–415 (2008).

94. Kim, S., Choi, K. & Chung, J. Reduction in carbon dioxide and production of methane by biological reaction in the electronics industry. *International Journal of Hydrogen Energy* **38,** 3488–3496 (2013).

95. Burkhardt, M., Jordan, I., Heinrich, S., Behrens, J., Ziesche, A., Tietze, M. & Busch, G. *Long term and demand-orientated biocatalytic synthesis of highly concentrated methane in a trickle bed reactor and scale up* Stuttgart, Germany. ISBN: 978-3-940706-09-6, 2017-03-09.

96. Lee, J. C., Kim, J. H., Chang, W. S. & Pak, D. Biological conversion of CO_2 to CH_4 using hydrogenotrophic methanogen in a fixed bed reactor. *Journal of Chemical Technology & Biotechnology* **87,** 844–847 (2012).

97. Wang, W., Xie, L., Luo, G., Zhou, Q. & Angelidaki, I. Performance and microbial community analysis of the anaerobic reactor with coke oven gas biomethanation and in situ biogas upgrading. *Bioresource Technology* **146,** 234–239 (2013).

98. Guneratnam, A. J., Ahern, E., FitzGerald, J. A., Jackson, S. A., Xia, A., Dobson, A. D. W. & Murphy, J. D. Study of the performance of a thermophilic biological methanation system. *Bioresource Technology* **225,** 308–315 (2017).

99. Bredwell, M. D., Srivastava, P. & Worden, R. M. Reactor Design Issues for Synthesis-Gas Fermentations. *Biotechnology Progress* **15,** 834–844 (1999).

100. Kulkarni, A. A. & Joshi, J. B. Bubble Formation and Bubble Rise Velocity in Gas−Liquid Systems: A Review. *Industrial & Engineering Chemistry Research* **44,** 5873–5931 (2005).

101. Kraakman, N. J. R., Rocha-Rios, J. & van Loosdrecht, M. C. M. Review of mass transfer aspects for biological gas treatment. *Applied Microbiology and Biotechnology* **91,** 873–886 (2011).

102. Munasinghe, P. C. & Khanal, S. K. Biomass-derived syngas fermentation into biofuels: opportunities and challenges. *Bioresource Technology* **101,** 5013–5022 (2010).

103. Orgill, J. J., Atiyeh, H. K., Devarapalli, M., Phillips, J. R., Lewis, R. S. & Huhnke, R. L. A comparison of mass transfer coefficients between trickle-bed, hollow fiber membrane and stirred tank reactors. *Bioresource Technology* **133,** 340–346 (2013).

104. Ako, O. Y., Kitamura, Y., Intabon, K. & Satake, T. Steady state characteristics of acclimated hydrogenotrophic methanogens on inorganic substrate in continuous chemostat reactors. *Bioresource Technology* **99,** 6305–6310 (2008).

105. Fardeau, M.-L. & Belaich, J.-P. Energetics of the growth of Methanococcus thermolithotrophicus. *Archives of Microbiology* **144,** 381–385 (1986).

106. Gerhard, E., Butsch, B. M., Marison, I. W. & von Stockar, U. Improved growth and methane production conditions for Methanobacterium thermoautotrophicum. *Applied Microbiology and Biotechnology* **40,** 432–437 (1993).

107. De Poorter, L. M. I., Geerts, W. J. & Keltjens, J. T. Coupling of Methanothermobacter thermautotrophicus methane formation and growth in fed-batch and continuous cultures under different H2 gassing regimens. *Applied and Environmental Microbiology* **73,** 740–749 (2007).

108. Rittmann, S. K.-M., Seifert, A. & Herwig, C. Quantitative analysis of media dilution rate effects on Methanothermobacter marburgensis grown in continuous culture on H_2 and CO_2. *Biomass and Bioenergy* **36,** 293–301 (2012).

109. Schill, N. A., van Gulik, W. M., Voisard, D. & von Stockar, U. Continuous cultures limited by a gaseous substrate: Development of a simple, unstructured mathematical model and experimental verification with Methanobacterium thermoautotrophicum. *Biotechnology and Bioengineering* **51,** 645–658 (1996).

110. Schill, N. & von Stockar, U. Thermodynamic analysis of Methanobacterium thermoautotrophicum. *Thermochimica acta* **251,** 71–77 (1995).

111. Munasinghe, P. C. & Khanal, S. K. Syngas fermentation to biofuel: Evaluation of carbon monoxide mass transfer and analytical modeling using a composite hollow fiber (CHF) membrane bioreactor. *Bioresource Technology* **122,** 130–136 (2012).

112. Yang, Y., Zhang, Z. Y., Lu, J. & Maekawa, T. Continuous methane fermentation and the production of vitamin B12 in a fixed-bed reactor packed with loofah. *Bioresource Technology* **92,** 285–290 (2004).

113. Burkhardt, M., Koschack, T. & Busch, G. Biocatalytic methanation of hydrogen and carbon dioxide in an anaerobic three-phase system. *Bioresource Technology* **178,** 330–333 (2015).

114. Kimmel, D. E., Klasson, K. T., Clausen, E. C. & Gaddy, J. L. Performance of trickle-bed bioreactors for converting synthesis gas to methane. *Applied Biochemistry and Biotechnology* **28/29,** 457–469 (1991).

115. Klasson, K. T., Ackerson, M. D., Clausen, E. C. & Gaddy, J. L. Bioreactors for synthesis gas fermentations. *Resources, Conservation and Recycling* **5,** 145–165 (1991).

116. Strübing, D., Moeller, A. B., Mößnang, B., Lebuhn, M., Drewes, J. E. & Koch, K. Load change capability of an anaerobic thermophilic trickle bed reactor for dynamic H_2/CO_2 biomethanation. *Bioresource Technology,* 121735 (2019).

117. Strübing, D., Moeller, A. B., Mößnang, B., Lebuhn, M., Drewes, J. E. & Koch, K. Anaerobic thermophilic trickle bed reactor as a promising technology for flexible and demand-oriented H2/CO2 biomethanation. *Applied Energy* **232,** 543–554 (2018).

118. Ullrich, T., Lindner, J., Bär, K., Mörs, F., Graf, F. & Lemmer, A. Influence of operating pressure on the biological hydrogen methanation in trickle-bed reactors. *Bioresource Technology* **247,** 7–13 (2017).

119. Ullrich, T. & Lemmer, A. Performance enhancement of biological methanation with trickle bed reactors by liquid flow modulation. *GCB Bioenergy* (2018).

120. Andrews, G. F. & Noah, K. S. Design of Gas–Treatment Bioreactors. *Biotechnology Progress* **11,** 498–509 (1995).

121. Montalvo, S., Guerrero, L., Borja, R., Sánchez, E., Milán, Z., Cortés, I. & La Angeles de la Rubia, M. Application of natural zeolites in anaerobic digestion processes: A review. *Applied Clay Science* **58,** 125–133 (2012).

122. Escudié, R., Cresson, R., Delgenès, J.-P. & Bernet, N. Control of start-up and operation of anaerobic biofilm reactors: An overview of 15 years of research. *Water Research* **45,** 1–10 (2011).

123. Hulshoff Pol, L. W., de Castro Lopes, S. I., Lettinga, G. & Lens, P. N. L. Anaerobic sludge granulation. *Water Research* **38,** 1376–1389 (2004).

124. Lauwers, A. M., Heinen, W., Gorris, L. G. M. & van der Drift, C. Early stages in biofilm development in methanogenic fluidized-bed reactors. *Applied Microbiology and Biotechnology* **33,** 352–358 (1990).

125. Liu, Y., Xu, H.-L., Yang, S.-F. & Tay, J.-H. Mechanisms and models for anaerobic granulation in upflow anaerobic sludge blanket reactor. *Water Research* **37,** 661–673 (2003).

126. Liu, Y. & Tay, J.-H. The essential role of hydrodynamic shear force in the formation of biofilm and granular sludge. *Water Research* **36,** 1653–1665 (2002).

127. Zheng, H., Zeng, R. J. & Angelidaki, I. Biohydrogen production from glucose in upflow biofilm reactors with plastic carriers under extreme thermophilic conditions (70°C). *Biotechnology and Bioengineering* **100,** 1034–1038 (2008).

128. Taubner, R.-S. & Rittmann, S. K.-M. Method for Indirect Quantification of CH_4 Production via H_2O Production Using Hydrogenotrophic Methanogens. *Frontiers in Microbiology* **7** (2016).

129. Levén, L., Eriksson, A. R. B. & Schnürer, A. Effect of process temperature on bacterial and archaeal communities in two methanogenic bioreactors treating organic household waste. *FEMS microbiology ecology* **59,** 683–693 (2007).

130. Ahring, B. K., Ibrahim, A. A. & Mladenovska, Z. Effect of temperature increase from 55 to 65°C on performance and microbial population dynamics of an anaerobic reactor treating cattle manure. *Water Research* **35,** 2446–2452 (2001).

131. Pender, S., Toomey, M., Carton, M., Eardly, D., Patching, J. W., Colleran, E. & O'Flaherty, V. Long-term effects of operating temperature and sulphate addition on the methanogenic community structure of anaerobic hybrid reactors. *Water Research* **38,** 619–630 (2004).

132. Regueiro, L., Carballa, M. & Lema, J. M. Outlining microbial community dynamics during temperature drop and subsequent recovery period in anaerobic co-digestion systems. *Journal of Biotechnology* **192 Pt A,** 179–186 (2014).

133. van Lier, J. B., Martin, J. L. S. & Lettinga, G. Effect of temperature on the anaerobic thermophilic conversion of volatile fatty acids by dispersed and granular sludge. *Water Research* **30,** 199–207 (1996).

134. van Lier, J. B., Hulsbeek, J., Stams, A. J. & Lettinga, G. Temperature susceptibility of thermophilic methanogenic sludge: Implications for reactor start-up and operation. *Bioresource Technology* **43,** 227–235 (1993).

135. Blanco, H. & Faaij, A. A review at the role of storage in energy systems with a focus on Power to Gas and long-term storage. *Renewable and Sustainable Energy Reviews* **81,** 1049–1086 (2018).

136. Walker, S. B., Mukherjee, U., Fowler, M. & Elkamel, A. Benchmarking and selection of Power-to-Gas utilizing electrolytic hydrogen as an energy storage alternative. *International Journal of Hydrogen Energy* **41,** 7717–7731 (2016).

137. Huneke, F., Linkenheil, C. P. & Niggemeier, M.-L. *Kalte Dunkelflaute: Robustheit des Stromsystems bei Extremwetter* (ed Energy Brainpool GmbH & Co. KG, Berlin) Berlin, 12.05.2017.

138. Collet, P., Flottes, E., Favre, A., Raynal, L., Pierre, H., Capela, S. & Peregrina, C. Techno-economic and Life Cycle Assessment of methane production via biogas upgrading and power to gas technology. *Applied Energy* **192,** 282–295 (2017).

139. McDonagh, S., O'Shea, R., Wall, D. M., Deane, J. P. & Murphy, J. D. Modelling of a power-to-gas system to predict the levelised cost of energy of an advanced renewable gaseous transport fuel. *Applied Energy* **215,** 444–456 (2018).

140. Vo, T. T., Wall, D. M., Ring, D., Rajendran, K. & Murphy, J. D. Techno-economic analysis of biogas upgrading via amine scrubber, carbon capture and ex-situ methanation. *Applied Energy* **212,** 1191–1202 (2018).

141. Klinge Jacobsen, H. & Schröder, S. T. Curtailment of renewable generation: Economic optimality and incentives. *Energy Policy* **49,** 663–675 (2012).

142. Schill, W.-P. Residual load, renewable surplus generation and storage requirements in Germany. *Energy Policy* **73,** 65–79 (2014).

143. Joos, M. & Staffell, I. Short-term integration costs of variable renewable energy: Wind curtailment and balancing in Britain and Germany. *Renewable and Sustainable Energy Reviews* **86,** 45–65 (2018).

144. Huber, M., Dimkova, D. & Hamacher, T. Integration of wind and solar power in Europe: Assessment of flexibility requirements. *Energy* **69,** 236–246 (2014).

145. Hwang, K., Song, M., Kim, W., Kim, N. & Hwang, S. Effects of prolonged starvation on methanogenic population dynamics in anaerobic digestion of swine wastewater. *Bioresource Technology* **101,** S2–6 (2010).

146. De Jonge, N., Moset, V., Møller, H. B. & Nielsen, J. L. Microbial population dynamics in continuous anaerobic digester systems during start up, stable conditions and recovery after starvation. *Bioresource Technology* **232,** 313–320 (2017).

147. Graf, F., Götz, M., Henel, M., Schaaf, T. & Tichler, R. *Technoökonomische Studie von Power-to-Gas-Konzepten* 2014.

148. Napp, T. A., Gambhir, A., Hills, T. P., Florin, N. & Fennell, P. A review of the technologies, economics and policy instruments for decarbonising energy-intensive manufacturing industries. *Renewable and Sustainable Energy Reviews* **30,** 616–640 (2014).

149. Jürgensen, L., Ehimen, E. A., Born, J. & Holm-Nielsen, J. B. Utilization of surplus electricity from wind power for dynamic biogas upgrading: Northern Germany case study. *Biomass and Bioenergy* **66,** 126–132 (2014).

150. Deremince, B., Königsberger, S. *European Biogas Association - Statistical report 2017* (ed European Biogas Association) Brussels, Belgium, 2017.

151. Dupnock, T. L. & Deshusses, M. A. Detailed Investigations of Dissolved Hydrogen and Hydrogen Mass Transfer in a Biotrickling Filter for Upgrading Biogas // Detailed investigations of dissolved hydrogen and hydrogen mass transfer in a biotrickling filter for upgrading biogas. *Bioresource Technology* **290,** 121780 (2019).

152. Siegrist, H., Vogt, D., Garcia-Heras, J. L. & Gujer, W. Mathematical Model for Meso- and Thermophilic Anaerobic Sewage Sludge Digestion. *Environmental Science & Technology* **36,** 1113–1123 (2002).

153. Jentsch, M., Trost, T. & Sterner, M. Optimal use of power-to-gas energy storage systems in an 85% renewable energy scenario. *Energy Procedia* **46,** 254–261 (2014).

154. Heard, B. P., Brook, B. W., Wigley, T. & Bradshaw, C. Burden of proof: A comprehensive review of the feasibility of 100% renewable-electricity systems. *Renewable and Sustainable Energy Reviews* **76,** 1122–1133 (2017).

155. Hao, X., Cai, Z., Fu, K. & Zhao, D. Distinguishing activity decay and cell death from bacterial decay for two types of methanogens. *Water Research* **46,** 1251–1259 (2012).

156. Maillacheruvu, K. Y. & Parkin, G. F. Kinetics of growth, substrate utilization and sulfide toxicity for propionate, acetate, and hydrogen utilizers in anaerobic systems. *Water Environment Research* **68,** 1099–1106 (1996).

157. Ulleberg, Ø., Nakken, T. & Eté, A. The wind/hydrogen demonstration system at Utsira in Norway: Evaluation of system performance using operational data and updated hydrogen energy system modeling tools. *International Journal of Hydrogen Energy* **35,** 1841–1852 (2010).

158. Rittmann, S. K.-M., Seifert, A. & Herwig, C. Essential prerequisites for successful bioprocess development of biological CH_4 production from CO_2 and H_2. *Critical Reviews in Biotechnology* **35,** 141–151 (2015).

159. Ortega, L., Barrington, S. & Guiot, S. R. Thermophilic adaptation of a mesophilic anaerobic sludge for food waste treatment. *Journal of Environmental Management* **88,** 517–525 (2008).

160. APHA, AWWA & WPCF. Standard methods for the examination of water and wastewater. *American Public Health Association (APHA): Washington, DC, USA* (2005).

161. Lebuhn, M., Munk, B. & Effenberger, M. Agricultural biogas production in Germany-from practice to microbiology basics. *Energy, Sustainability and Society* **4,** 1–21 (2014).

162. Liu, Y., Beer, L. L. & Whitman, W. B. Methanogens: a window into ancient sulfur metabolism. *Trends in Microbiology* **20,** 251–258 (2012).

163. Rönnow, P. H. & Gunnarsson, L. Å. H. Sulfide-dependent methane production and growth of a thermophilic methanogenic bacterium. *Applied and Environmental Microbiology* **42,** 580–584 (1981).

164. Switzenbaum, M. S., Giraldo-Gomez, E. & Hickey, R. F. Monitoring of the anaerobic methane fermentation process. *Enzyme and Microbial Technology* **12,** 722–730 (1990).

165. APHA, AWWA & WPCF. *Standard methods for the examination of water and wastewater* 23rd edition (American Public Health Association, Washington, D.C., 2017).

166. Heidrich, E. S., Edwards, S. R., Dolfing, J., Cotterill, S. E. & Curtis, T. P. Performance of a pilot scale microbial electrolysis cell fed on domestic wastewater at ambient temperatures for a 12 month period. *Bioresource Technology* **173,** 87–95 (2014).

167. Azim, A. A., Pruckner, C., Kolar, P., Taubner, R.-S., Fino, D., Saracco, G., Sousa, F. L. & Simon, K.-M. R. The physiology of trace elements in biological methane production. *Bioresource Technology* **241,** 775–786 (2017).

168. Visser, A., Nozhevnikova, A. N. & Lettinga, G. Sulphide inhibition of methanogenic activity at various pH levels at 55°C. *Journal of Chemical Technology & Biotechnology* **57,** 9–13 (1993).

169. Stams, A. J. M., Grolle, K. C. F., Frijters, C. T. M. & van Lier, J. B. Enrichment of thermophilic propionate-oxidizing bacteria in syntrophy with *Methanobacterium thermoautotrophicum* or *Methanobacterium thermoformicicum*. *Applied and Environmental Microbiology* **58,** 346–352 (1992).

170. Castro, H., Queirolo, M., Quevedo, M. & Muxi, L. Preservation methods for the storage of anaerobic sludges. *Biotechnology Letters* **24,** 329–333 (2002).

171. Li, J., Zicari, S. M., Cui, Z. & Zhang, R. Processing anaerobic sludge for extended storage as anaerobic digester inoculum. *Bioresource Technology* **166,** 201–210 (2014).

172. van Lier, J. B., Grolle, K. C., Frijters, C. T., Stams, A. J. & Lettinga, G. Effects of acetate, propionate, and butyrate on the thermophilic anaerobic degradation of propionate by methanogenic sludge and defined cultures. *Applied and Environmental Microbiology* **59,** 1003–1011 (1993).

173. Fukuzaki, S., Nishio, N., Shobayashi, M. & Nagai, S. Inhibition of the fermentation of propionate to methane by hydrogen, acetate, and propionate. *Applied and Environmental Microbiology* **56,** 719–723 (1990).

174. Schill, N. A., Liu, J. S. & von Stockar, U. Thermodynamic analysis of growth of Methanobacterium thermoautotrophicum. *Biotechnology and Bioengineering* **64,** 74–81 (1999).

175. Westerholm, M., Moestedt, J. & Schnürer, A. Biogas production through syntrophic acetate oxidation and deliberate operating strategies for improved digester performance. *Applied Energy* **179,** 124–135 (2016).

176. Gehring, T., Niedermayr, A., Berzio, S., Immenhauser, A., Wichern, M. & Lübken, M. Determination of the fractions of syntrophically oxidized acetate in a mesophilic methanogenic reactor through an ^{12}C and ^{13}C isotope-based kinetic model. *Water Research* **102,** 362–373 (2016).

177. Stieb, M. & Schink, B. Anaerobic degradation of isovalerate by a defined methanogenic coculture. *Archives of Microbiology* **144,** 291–295 (1986).

178. Wang, Q., Kuninobu, M., Ogawa, H. I. & Kato, Y. Degradation of volatile fatty acids in highly efficient anaerobic digestion. *Biomass and Bioenergy* **16,** 407–416 (1999).

179. Conrad, R. & Klose, M. Anaerobic conversion of carbon dioxide to methane, acetate and propionate on washed rice roots. *FEMS microbiology ecology* **30,** 147–155 (1999).

180. Richter, H., Molitor, B., Wei, H., Chen, W., Aristilde, L. & Angenent, L. T. Ethanol production in syngas-fermenting *Clostridium ljungdahlii* is controlled by thermodynamics rather than by enzyme expression. *Energy and Environmental Science* **9,** 2392–2399 (2016).

181. Angenent, L. T., Richter, H., Buckel, W., Spirito, C. M., Steinbusch, K. J. J., Plugge, C. M., Strik, D. P. B. T. B., Grootscholten, T. I. M., Buisman, C. J. N. & Hamelers, H. V. M. Chain Elongation with Reactor Microbiomes: Open-Culture Biotechnology To Produce Biochemicals. *Environmental Science & Technology* **50,** 2796–2810 (2016).

182. Patterson, T., Savvas, S., Chong, A., Law, I., Dinsdale, R. & Esteves, S. Integration of Power to Methane in a waste water treatment plant - A feasibility study. *Bioresource Technology* **245,** 1049–1057 (2017).

183. Ela, E., Kirby, B., Lannoye, E., Milligan, M., Flynn, D., Zavadil, B. & O'Malley, M. Evolution of operating reserve determination in wind power integration studies. *IEEE Transactions on Sustainable Energy* **3,** 1–8 (2012).

184. Thema, M., Weidlich, T., Hörl, M., Bellack, A., Mörs, F., Hackl, F., Kohlmayer, M., Gleich, J., Stabenau, C., Trabold, T., Neubert, M., Ortloff, F., Brotsack, R., Schmack, D., Huber, H., Hafenbradl, D., Karl, J. & Sterner, M. Biological CO_2-Methanation: An Approach to Standardization. *Energies* **12,** 1670 (2019).

185. Roels, J. A. Thermodynamics of growth. *Basic biotechnology,* 57–74 (1987).

186. Glass, J. B. & Orphan, V. J. Trace metal requirements for microbial enzymes involved in the production and consumption of methane and nitrous oxide. *Frontiers in Microbiology* **3,** 61 (2012).

187. Hendriks, A. T. W. M., van Lier, J. B. & de Kreuk, M. K. Growth media in anaerobic fermentative processes: The underestimated potential of thermophilic fermentation and anaerobic digestion. *Biotechnology Advances* (2017).

188. Rönnow, P. H. & Gunnarsson, L. Å. H. Response of growth and methane production to limiting amounts of sulfide and ammonia in two thermophilic methanogenic bacteria. *FEMS Microbiology Letters* **14,** 311–315 (1982).

189. Strevett, K. A., Vieth, R. F. & Grasso, D. Chemo-autotrophic biogas purification for methane enrichment: mechanism and kinetics. *Chemical Engineering Journal Biochemical Engineering Journal* **58,** 71–79 (1995).

190. Demirel, B. & Scherer, P. Trace element requirements of agricultural biogas digesters during biological conversion of renewable biomass to methane. *Biomass and Bioenergy* **35,** 992–998 (2011).

191. Nishimura, N., Kitaura, S., Mimura, A. & Takahara, Y. Cultivation of Thermophilic Methanogen KN-15 on H2-CO2 under Pressurized Conditions. *Journal of Fermentation and Bioengineering* **73,** 477–480 (1992).

192. Romero-Güiza, M. S., Vila, J., Mata-Alvarez, J., Chimenos, J. M. & Astals, S. The role of additives on anaerobic digestion: A review. *Renewable and Sustainable Energy Reviews* **58,** 1486–1499 (2016).

193. Hoslett, J., Massara, T. M., Malamis, S., Ahmad, D., van den Boogaert, I., Katsou, E., Ahmad, B., Ghazal, H., Simons, S., Wrobel, L. & Jouhara, H. Surface water filtration using granular media and membranes: A review. *The Science of the total environment* **639,** 1268–1282 (2018).

194. Pavez, J., Cabrera, F., Azócar, L., Torres, A. & Jeison, D. Ultrafiltration of non-axenic microalgae cultures: Energetic requirements and filtration performance. *Algal Research* **10,** 121–127 (2015).

195. Hashisho, J. & El-Fadel, M. Membrane bioreactor technology for leachate treatment at solid waste landfills. *Reviews in Environmental Science and Bio/Technology* **15,** 441–463 (2016).

196. Skouteris, G., Hermosilla, D., López, P., Negro, C. & Blanco, Á. Anaerobic membrane bioreactors for wastewater treatment: A review. *Chemical Engineering Journal* **198-199,** 138–148 (2012).

197. Lin, H. J., Xie, K., Mahendran, B., Bagley, D. M., Leung, K. T., Liss, S. N. & Liao, B. Q. Sludge properties and their effects on membrane fouling in submerged anaerobic membrane bioreactors (SAnMBRs). *Water Research* **43,** 3827–3837 (2009).

198. Metcalf, E. & Eddy, M. Wastewater engineering: treatment and Resource recovery. *McGraw-Hill Education, New York* (2014).

199. Judd, S. *The MBR book: Principles and applications of membrane bioreactors for water and wastewater treatment* (Elsevier, 2010).

200. Wagman, D. D., Evans, W. H., Parker, V. B., Schumm, R. H. & Halow, I. *The NBS tables of chemical thermodynamic properties. Selected values for inorganic and C1 and C2 organic substances in SI units* 1982.

201. Klasson, K. T., Cowger, J. P., Ko, C. W., Vega, J. L., Clausen, E. C. & Gaddy, J. L. Methane production from synthesis gas using a mixed culture of R. rubrum, M. barkeri, and M. formicicum. *Applied Biochemistry and Biotechnology* **24,** 317–328 (1990).

202. Budzianowski, W. M., Wylock, C. E. & Marciniak, P. A. Power requirements of biogas upgrading by water scrubbing and biomethane compression: Comparative analysis of various plant configurations. *Energy Conversion and Management* **141,** 2–19 (2017).

203. Vo, T. Q. T. *A technical, economic and environmental analysis of renewable gas produced from power to gas systems* PhD Thesis (University College Cork, Cork, Ireland, 2018).

204. Deutscher Bundestag. *Erneuerbare-Energien-Gesetz vom 21. Juli 2014 (BGBl. I S. 1066), das zuletzt durch Artikel 5 des Gesetzes vom 13. Mai 2019 (BGBl. I S. 706) geändert worden ist: EEG 2017* 2014.

205. BDEW Bundesverband der Energie- und Wasserwirtschaft e. V. *BDEW-Strompreisanalyse Januar 2019: Haushalte und Industrie* (ed BDEW Bundesverband der Energie- und Wasserwirtschaft e. V.) 2019.

206. Pääkkönen, A., Tolvanen, H. & Rintala, J. Techno-economic analysis of a power to biogas system operated based on fluctuating electricity price. *Renewable Energy* **117,** 166–174 (2018).

207. Acharya, B., Dutta, A. & Basu, P. Ethanol production by syngas fermentation in a continuous stirred tank bioreactor using Clostridium ljungdahlii. *Biofuels* **85,** 1–17 (2017).

208. Acharya, B., Roy, P. & Dutta, A. Review of syngas fermentation processes for bioethanol. *Biofuels* **5,** 551–564 (2015).

209. Daniell, J., Köpke, M. & Simpson, S. Commercial Biomass Syngas Fermentation. *Energies* **5,** 5372–5417 (2012).

210. Diender, M., Uhl, P. S., Bitter, J. H., Stams, A. J. M. & Sousa, D. Z. High Rate Biomethanation of Carbon Monoxide-Rich Gases via a Thermophilic Synthetic Coculture. *ACS Sustainable Chemistry & Engineering* **6,** 2169–2176 (2018).

211. Dürre, P. Butanol formation from gaseous substrates. *FEMS Microbiology Letters* **363** (2016).

212. Mohammadi, M., Najafpour, G. D., Younesi, H., Lahijani, P., Uzir, M. H. & Mohamed, A. R. Bioconversion of synthesis gas to second generation biofuels: A review. *Renewable and Sustainable Energy Reviews* **15,** 4255–4273 (2011).

213. Omar, B., El-Gammal, M., Abou-Shanab, R., Fotidis, I. A., Angelidaki, I. & Zhang, Y. Biogas upgrading and biochemical production from gas fermentation: Impact of microbial community and gas composition. *Bioresource Technology* **286,** 121413 (2019).

214. Omar, B., Abou-Shanab, R., El-Gammal, M., Fotidis, I. A., Kougias, P. G., Zhang, Y. & Angelidaki, I. Simultaneous biogas upgrading and biochemicals production using anaerobic bacterial mixed cultures. *Water Research* **142,** 86–95 (2018).

215. Richter, H., Molitor, B., Diender, M., Sousa, D. Z. & Angenent, L. T. A Narrow pH Range Supports Butanol, Hexanol, and Octanol Production from Syngas in a Continuous Co-culture of Clostridium ljungdahlii and Clostridium kluyveri with In-Line Product Extraction. *Frontiers in Microbiology* **7,** 1773 (2016).

216. Richter, H., Martin, M. & Angenent, L. A Two-Stage Continuous Fermentation System for Conversion of Syngas into Ethanol. *Energies* **6,** 3987–4000 (2013).

217. Klasson, K. T., Elmore, B. B., Vega, J. L., Ackerson, M. D., Clausen, E. C. & Gaddy, J. L. Biological production of liquid and gaseous fuels from synthesis gas. *Applied Biochemistry and Biotechnology* **24,** 857–873 (1990).

218. Griffin, D. W. & Schultz, M. A. Fuel and chemical products from biomass syngas: A comparison of gas fermentation to thermochemical conversion routes. *Environmental Progress & Sustainable Energy* **31,** 219–224 (2012).

219. Grimalt-Alemany, A., Skiadas, I. V. & Gavala, H. N. Syngas biomethanation: State-of-the-art review and perspectives. *Biofuels, Bioproducts and Biorefining* **12,** 139–158 (2018).

220. Slivka, R. M., Chinn, M. S. & Grunden, A. M. Gasification and synthesis gas fermentation: An alternative route to biofuel production. *Biofuels* **2,** 405–419 (2014).

221. Asimakopoulos, K., Gavala, H. N. & Skiadas, I. V. Biomethanation of Syngas by Enriched Mixed Anaerobic Consortia in Trickle Bed Reactors. *Waste and Biomass Valorization* **364,** 3067LP (2019).

222. Baek, G., Kim, J., Lee, S. & Lee, C. Development of biocathode during repeated cycles of bioelectrochemical conversion of carbon dioxide to methane. *Bioresource Technology* (2017).

223. Bajracharya, S., Vanbroekhoven, K., Buisman, C. J. N., Pant, D. & Strik, D. P. B. T. B. Application of gas diffusion biocathode in microbial electrosynthesis from carbon dioxide. *Environmental science and pollution research international* **23,** 22292–22308 (2016).

224. Barua, S. & Dhar, B. R. Advances towards understanding and engineering direct interspecies electron transfer in anaerobic digestion. *Bioresource Technology* **244,** 698–707 (2017).

225. Blasco-Gómez, R., Batlle-Vilanova, P., Villano, M., Balaguer, M. D., Colprim, J. & Puig, S. On the Edge of Research and Technological Application: A Critical Review of Electromethanogenesis. *International journal of molecular sciences* **18** (2017).

226. Fu, Q., Kuramochi, Y., Fukushima, N., Maeda, H., Sato, K. & Kobayashi, H. Bioelectrochemical analyses of the development of a thermophilic biocathode catalyzing electromethanogenesis. *Environmental Science & Technology* **49,** 1225–1232 (2015).

227. Geppert, F., Liu, D., van Eerten-Jansen, M., Weidner, E., Buisman, C. & Ter Heijne, A. Bioelectrochemical Power-to-Gas: State of the Art and Future Perspectives. *Trends in biotechnology* **34,** 879–894 (2016).

228. Cheng, S., Xing, D., Call, D. F. & Logan, B. E. Direct Biological Conversion of Electrical Current into Methane by Electromethanogenesis. *Environmental Science & Technology* **43,** 3953–3958 (2009).

229. EIA. *International Energy Outlook 2017* 2017.

230. Wall, D. M., Dumont, M. & Murphy, J. D. *Green Gas: Facilitating a Future Green Gas Grid Through the Production of Renewable Gas* (IEA Bioenergy, 2018).

231. Benjaminsson, G., Benjaminsson, J. & Rudberg, R. B. *Power-to-Gas: A technical review* (Svenskt gastekniskt center, 2013).

232. Aryal, N., Kvist, T., Ammam, F., Pant, D. & Ottosen, L. D. M. An overview of microbial biogas enrichment. *Bioresource Technology* (2018).

233. Maegaard, K., Garcia-Robledo, E., Kofoed, M. V. W., Agneessens, L. M., de Jonge, N., Nielsen, J. L., Ottosen, L. D. M., Nielsen, L. P. & Revsbech, N. P. Biogas upgrading with hydrogenotrophic methanogenic biofilms. *Bioresource Technology* **287,** 121422 (2019).

234. Hori, K. & Matsumoto, S. Bacterial adhesion: From mechanism to control. *Biochemical Engineering Journal* **48,** 424–434 (2010).

235. van Loosdrecht, M. C. M., Eikelboom, D., Gjaltema, A., Mulder, A., Tijhuis, L. & Heijnen, J. J. Biofilm structures. *Water Science and Technology* **32,** 35–43 (1995).

236. Veiga, M. C., Jain, M. K., Wu, W., Hollingsworth, R. I. & Zeikus, J. G. Composition and role of extracellular polymers in methanogenic granules. *Applied and Environmental Microbiology* **63,** 403–407 (1997).

237. Habouzit, F., Hamelin, J., Santa-Catalina, G., Steyer, J.-P. & Bernet, N. Biofilm development during the start-up period of anaerobic biofilm reactors: The biofilm Archaea community is highly dependent on the support material. *Microbial biotechnology* **7,** 257–264 (2014).

238. Heijnen, J. J., van Loosdrecht, M. C., Mulder, A. & Tijhuis, L. Formation of biofilms in a biofilm air-lift suspension reactor. *Water science and technology : a journal of the International Association on Water Pollution Research* **26,** 647–654 (1992).

239. Tijhuis, L., van Loosdrecht, M. C. & Heijnen, J. J. Formation and growth of heterotrophic aerobic biofilms on small suspended particles in airlift reactors. *Biotechnology and Bioengineering* **44,** 595–608 (1994).

240. Cresson, R., Escudié, R., Steyer, J.-P., Delgenès, J.-P. & Bernet, N. Competition between planktonic and fixed microorganisms during the start-up of methanogenic biofilm reactors. *Water Research* **42,** 792–800 (2008).

241. Caporaso, J. G., Lauber, C. L., Walters, W. A., Berg-Lyons, D., Lozupone, C. A., Turnbaugh, P. J., Fierer, N. & Knight, R. Global patterns of 16S rRNA diversity at a depth of millions of sequences per sample. *Proceedings of the national academy of sciences* **108,** 4516–4522 (2011).

242. Bolger, A. M., Lohse, M. & Usadel, B. Trimmomatic: A flexible trimmer for Illumina sequence data. *Bioinformatics (Oxford, England)* **30,** 2114–2120 (2014).

243. Magoč, T. & Salzberg, S. L. FLASH: Fast length adjustment of short reads to improve genome assemblies. *Bioinformatics (Oxford, England)* **27,** 2957–2963 (2011).

244. Edgar, R. C. UPARSE: Highly accurate OTU sequences from microbial amplicon reads. *Nature methods* **10,** 996 (2013).

245. Caporaso, J. G., Kuczynski, J., Stombaugh, J., Bittinger, K., Bushman, F. D., Costello, E. K., Fierer, N., Pena, A. G., Goodrich, J. K. & Gordon, J. I. QIIME allows analysis of high-throughput community sequencing data. *Nature methods* **7,** 335 (2010).

246. Quast, C., Pruesse, E., Yilmaz, P., Gerken, J., Schweer, T., Yarza, P., Peplies, J. & Glöckner, F. O. The SILVA ribosomal RNA gene database project: Improved data processing and web-based tools. *Nucleic acids research* **41,** D590–D596 (2012).

247. Andersen, K. S., Kirkegaard, R. H., Karst, S. M. & Albertsen, M. ampvis2: An R package to analyse and visualise 16S rRNA amplicon data. *BioRxiv,* 299537 (2018).

248. Oren, A. The Family Methanopyraceae. *The Prokaryotes: Other Major Lineages of Bacteria and The Archaea,* 247–252 (2014).

249. Mulat, D. G., Mosbæk, F., Ward, A. J., Polag, D., Greule, M., Keppler, F., Nielsen, J. L. & Feilberg, A. Exogenous addition of H_2 for an in situ biogas upgrading through biological reduction of carbon dioxide into methane. *Waste management (New York, N.Y.)* **68,** 146–156 (2017).

250. Garcia-Robledo, E., Ottosen, L. D. M., Voigt, N. V., Kofoed, M. W. & Revsbech, N. P. Micro-scale H_2-CO_2 Dynamics in a Hydrogenotrophic Methanogenic Membrane Reactor. *Frontiers in Microbiology* **7,** 1276 (2016).

251. Aryal, N., Tremblay, P.-L., Lizak, D. M. & Zhang, T. Performance of different Sporomusa species for the microbial electrosynthesis of acetate from carbon dioxide. *Bioresource Technology* **233,** 184–190 (2017).

252. Möller, B., Oßmer, R., Howard, B. H., Gottschalk, G. & Hippe, H. Sporomusa, a new genus of gram-negative anaerobic bacteria including Sporomusa sphaeroides spec. nov. and Sporomusa ovata spec. nov. *Archives of Microbiology* **139,** 388–396 (1984).

253. Ma, K., Liu, X. & Dong, X. Methanosaeta harundinacea sp. nov., a novel acetate-scavenging methanogen isolated from a UASB reactor. *International journal of systematic and evolutionary microbiology* **56,** 127–131 (2006).

254. Siegert, M., Yates, M. D., Spormann, A. M. & Logan, B. E. Methanobacterium dominates biocathodic archaeal communities in methanogenic microbial electrolysis cells. *ACS Sustainable Chemistry & Engineering* **3,** 1668–1676 (2015).

255. Schmidt, J. E. & Ahring, B. K. Granular sludge formation in upflow anaerobic sludge blanket (UASB) reactors. *Biotechnology and Bioengineering* **49,** 229–246 (1996).

256. Poehlein, A., Daniel, R. & Seedorf, H. The draft genome of the non-host-associated methanobrevibacter arboriphilus strain dh1 encodes a large repertoire of adhesin-like proteins. *Archaea* **2017** (2017).

257. Zellner, G., Diekmann, H., Austermann–Haun, U., Baumgarten, G. & Seyfried, C.-.-.-F. Biofilm formation on polypropylene during start–up of anaerobic fixed–bed reactors. *Biofouling* **6,** 345–361 (1993).

258. Oren, A. The Family Methanocorpusculaceae. *The Prokaryotes: Other Major Lineages of Bacteria and The Archaea,* 225–230 (2014).